FRICTION EQUATION FOR UNIFORM FLOW IN CHANNELS OF LARGE RELATIVE ROUGHNESS

Edwin Lillie, B.Sc (Eng.) in Civil Engineering
University of Cape Town

A thesis submitted in partial fulfilment of the requirements for the degree of Master of Science in Engineering

Department of Civil Engineering

September 1989.

DECLARATION OF CANDIDATE

I, EDWIN LILLIE, hereby declare that this thesis is my own work and that it has not been submitted for a degree to another university.

Signed by candidate

Signature Removed

E. LILLIE

September 1989.

SYNOPSIS

This thesis is an experimental investigation of the roughness problem in open channel flow. A literature review is given on the previous research done on friction factors. It is done in chronological order, so that the historical development of the friction equation can be seen. Most researchers have developed an equation for turbulent flow over a large relative roughness of the form :

$$\frac{1}{\sqrt{f}} = A + B\log\frac{R}{k}$$

(where A is a constant and B is equal to a factor of the reciprocal of von Karman's constant).

Experiments were conducted in a flume 0,310 m by 6 m. Two sizes of hemispheres at different concentrations were used to determine the effect of roughness geometry on the friction factor. All test runs were done under uniform turbulent flow conditions and the relative roughness ranged from 0,065 to 1 ($0{,}065 < k/_R < 1$). The resistance to flow was considered to be caused by form drag on the roughness elements only as the viscous forces were considered to be negligible during the test runs as the wall Reynolds numbers were always greater than 60. $\left[\frac{\rho V_* k}{\mu} > 60\right]$.

The roughness height (k) was shown not to be sufficient to predict the friction factor for large relative roughness. The constant A was found to be a function of roughness concentration and B was a function of $\left[L_s/T_s\right]$. The friction equation for large relative roughness in the fully developed turbulent zone is:

$$\boxed{\frac{1}{\sqrt{f}} = \left\{0{,}67 + \frac{0{,}04}{\left[\frac{k^2}{L_s T_s}\right]}\right\} + 2\left[\frac{T_s}{L_s}\right]^{0{,}25} \log\frac{R'}{k}}.$$

ACKNOWLEDGEMENTS

The author wishes to thank the following:

Professor F.A. Kilner, Head of the Department of Civil Engineering, University of Cape Town, thesis supervisor, for his guidance and encouragement over the past two years.

The Council for Scientific and Industrial Research for the award of a post-graduate bursary which made this research possible.

Mr A. Wilson, undergraduate student, for his help with the building of the experimental apparatus.

The technical staff of the Civil Engineering Workshop, Mr E.N. von Guerard, Mr G. Bertuzzi, Mr R.G. Edge and Mr D.J. Botha for the help and advice given in building the experimental apparatus.

Mr J.H. George, Mr N. Hassan, Mr A. Siko and Mr J.J. Williams of the Department of Civil Engineering, University of Cape Town, for assistance given in the laboratory.

Mrs V.H. Atkinson for the efficient typing of this thesis.

TABLE OF CONTENTS

			Page
Declaration			i
Synopsis			ii
Acknowledgements			iii
Table of Contents			iv
List of figures			vii
List of tables			x
List of photographic plates			xi
Nomenclature			xii
1.	Introduction		1.1
2.	Literature Review		2.1
	2.1	Introduction	2.1
	2.2	H. Schlichting	2.2
	2.3	C.F. Colebrook and C.M. White	2.6
	2.4	L.F. Moody	2.11
	2.5	R.W. Powell	2.14
	2.6	A.R. Robinson and M.L. Albertson	2.18
	2.7	M.C. Boyer	2.22
	2.8	H.M. Morris	2.25
	2.9	W.W. Sayre and M.L. Albertson	2.30
	2.10	A.G. Mirajgaoker and K.L.N. Charlu	2.34
	2.11	M. Bayazit	2.38
	2.12	J.C. Bathurst	2.41
	2.13	S.M. Thompson and P.L. Campbell	2.45
	2.14	D.I. Bray	2.48
	2.15	R. Pyle and P. Novak	2.51
	2.16	J.C. Bathurst, R.Li and D.B. Simons	2.56
	2.17	J.P. Pansegrouw	2.59
	2.18	A.B. Shahalam and A.R. Mansour	2.61
3.	Theoretical Analysis		3.1
	3.1	Development of uniform flow formulae	3.1
		3.1.1 The Chézy formula	3.3
		3.1.2 The Manning formula	3.4
	3.2	Roughness Description	3.6
	3.3	Dimensional Analysis	3.7
	3.4	Velocity distribution	3.9
	3.5	Theoretical bottom location	3.10

3.6 Types of rough surface flow 3.10

3.6.1 Isolated-roughness flow 3.11

3.6.2 Wake-interference flow 3.12

3.6.3 Quazi-smooth flow 3.12

3.7 Von Karman's constant 3.12

4. Experimental Apparatus 4.1

4.1 Initial assumptions 4.1

4.2 Equipment used 4.4

4.2.1 Flume 4.4

4.2.2 Gauges 4.6

4.2.3 Brass plates 4.6

4.2.4 Hemi-spheres 4.11

5. Experimental Procedure 5.1

5.1 Setting the slope 5.2

5.2 Obtaining uniform flow 5.3

5.3 The velocity distribution 5.4

5.4 The roughness patterns tested 5.5

6. Analysis of Experimental Results 6.1

6.1 Introduction 6.1

6.2 Calculation of parameters in worksheet 6.1

6.2.1 Geometric mean 6.1

6.2.2 Hydraulic radius 6.1

6.2.3 Flow parameter 6.1

6.2.4 Friction coefficients 6.2

6.2.5 Equivalent roughness size 6.3

6.2.6 Dimensionless numbers 6.3

6.3 Relationships between friction factor f and relative roughness 6.4

6.4 Relationships between Manning's n and relative roughness 6.9

7. Conclusions 7.1

List of references R.1

Bibliography Biblio 1

Appendices

A.	Open channel flow formulae	A.1
B.	Friction factors for large scale roughness	B.1
C.	Dimensional Analysis	C.1
D.	Integration of the velocity distribution over the flow depth	D.1
E.	Worksheet calculations	E.1
F.	$1/\sqrt{f}$ versus Log (R'/k)	F.1
G.	Examinations written by the author to complete the requirements of the degree	G.1

LIST OF FIGURES

		Page
2.1	Roughness patterns tested	2.2
2.2	General arrangement of test pattern	2.6
2.3	Roughness patterns tested	2.6
2.4	Transition Law	2.8
2.5	f versus R_e	2.9
2.6	f versus R_e	2.9
2.7	"Moody diagram"	2.12
2.8	Friction factor versus relative roughness	2.12
2.9	Spacing and size of roughness tested	2.14
2.10	Chézy c versus R_e (with transisiton)	2.16
2.11	Chézy c versus R (without transition)	2.16
2.12	Experimental equipment	2.18
2.13	Forces producing flow	2.18
2.14	Chézy c versus relative roughness	2.20
2.15	Chézy c versus Reynolds number	2.21
2.16	Manning coefficient versus relative roughness	2.23
2.17	Relation between Manning coefficient and the velocity distribution	2.24
2.18	Velocity-distribution curves	2.26
2.19	Resistance function versus wall Reynolds number	2.29
2.20	Experimental equipment	2.30
2.21	Chézy c versus relative roughness	2.33
2.22	Chézy c versus relative roughness	2.33
2.23	Roughness patterns tested	2.34
2.24	Resistance function versus relative roughness	2.35
2.25	Resistance function versus roughness density	2.36
2.26	Resistance function versus relative roughness	2.36
2.27	Friction factor versus relative roughness	2.39
2.28	Friction factor versus relative roughness	2.39
2.29	Velocity profiles at different values of relative roughness	2.39
2.30	Cross sections of river Tees at test sites	2.41
2.31	Relationship between roughness concentration and relative roughness	2.43
2.32	Ratio of f and channel geometry versus relative roughness	2.43

2.33	Ratio of f and channel geomety versus relative roughness	2.43
2.34	Tekapo B power station discharging 100 m^3/s	2.45
2.35	Friction factor versus relative roughness	2.47
2.36	Histogram of percent deviation	2.49
2.37	Roughness patterns tested	2.51
2.38	Friction factor versus relative roughness (before datum correction)	2.53
2.39	Constant of turbulence versus concentration	2.54
2.40	Friction factor versus relative roughness (after datum correction)	2.54
2.41	Effective roughness height versus concentration	2.55
2.42	Definition diagram for relative roughness area	2.56
2.43	Comparison between observed and calculated f	2.58
2.44	Friction factor versus relative roughness	2.62
2.45	Comparison of observed to calculated n values	2.63
2.46	Relationship between the velocity ratio and Manning's n	2.64
3.1	f versus Re (for open channel flow)	3.2
3.2	Derivation of the Chézy formula	3.4
3.3	Log f versus Log R/k_s	3.5
3.4	Three types of rough-surface flow	3.11
4.1	Roughness geometry	4.2
4.2	General layout of flume and recirculating system	4.4
4.3	Position of pitot cylinder	4.8
4.4	Pattern of holes in brass plate	
5.1	Worksheet	5.2
5.2	Setting the slope	5.3
5.3	Uniform flow	5.4
5.4	Cross section of Pitot cylinder	5.5
5.5	Test pattern 1	5.5
5.6	Test pattern 2	5.6
5.7	Test pattern 3	5.6
5.8	Test pattern 4	5.7
5.9	Test pattern 5	5.7
5.10	Test pattern 6	5.8
5.11	Test pattern 7	5.8
5.12	Test pattern 8	5.9
5.13	Test pattern 9	5.9
5.14	Test pattern 10	5.10

5.15	Test pattern 11	5.10
5.16	Test pattern 12	5.11
5.17	Test pattern 12b	5.11
6.1	$1/\sqrt{f}$ versus Log (R'/k)	6.5
6.2	log f versus Log (R'/k)	6.5
6.3	A versus concentration (Hemispheres)	6.8
6.4	A versus concentration (Hemispheres and Boulders)	6.8
6.5	Von Karman's constant versus concentration	6.10
6.6	B versus concentration (before correction)	6.10
6.7	B versus concentration (Hemispheres)	6.11
6.8	B versus concentration (Hemispheres and Boulders)	6.11
6.9	Calculated versus observed friction factors	6.12
6.10	Manning's n versus relative roughness	6.12

LIST OF TABLES

		Page
2.1	Data on test plates	2.5
2.2	Summary of experimental results	2.6
2.3	Table of results	2.17
2.4	Field data on flow resistance	2.46
2.5	Summary of results	2.49
2.6	Roughness heights corresponding to measured Manning coefficients	2.60
2.7	Field data	2.61
2.8	Summary of friction equations	2.62
6.1	A and B values related to roughness geometry	6.7
6.2	A and B values related to roughness geometry	6.7

LIST OF PHOTOGRAPHIC PLATES

		Page
1.1	Example of uniform flow over large relative roughness	1.2
1.2	Example of uniform flow over large relative roughness	1.2
4.1	Van Gysen, test pattern 12	4.3
4.2	Van Gysen, test pattern 12b	4.3
4.3	Flume and gauges	4.5
4.4	Inlet valve and tank	4.5
4.5	Jacking device and outlet gate	4.7
4.6	Adjustable outlet gate	4.8
4.7	Micrometre point gauge	4.8
4.8	Pitot cylinder	4.8
4.9	Brass plate with tapped holes	4.10
4.10	Brass plate covered with rubber	4.10
4.11	Wooden mould for Ø 50 mm hemispheres	4.12
4.12	Wooden mould for Ø 25 mm hemispheres	4.12
4.13	Test pattern I	4.13
4.14	Test pattern II	4.13

NOMENCLATURE

Symbol	Description	Dimension
A	constant in the friction equation	-
A_B	plan area of a roughness element	L^2
A_c	cross sectional area of conduit	L^2
A_F	cross sectional area of a roughness element	L^2
B	coefficient in friction equation	-
C	Chézy coefficient	$L^{\frac{1}{2}}\ T^{-1}$
C_D	drag coefficient	-
C_o	roughness concentration	-
d	pipe diameter	L
D	diameter of boulder	L
D_F	profile drag on a roughness element	L
D_X	the size of the median axis in a sample of sediment that is bigger than or equal to X% of the median axes of the sample	L
f	Darcy-Weisbach friction factor	-
F_r	Froude number	-
g	gravitational constant	$L\ T^{-2}$
k	absolute roughness height	L
k_s	equivalent roughness height	L
L	length of conduit	L
L_m	mixing length	L
L_s	longitudinal spacing between roughness elements	L
p	wetted perimeter	L
n	Manning's coefficient	$T\ L^{-1/3}$
Q	flow discharge rate	$L^3\ T^{-1}$
r	radius of pipe	L
R	hydraulic radius	L
R_e	Reynolds number	-
R_{ew}	wall Reynolds number	-
S	slope	-
T_s	transverse spacing between roughness elements	L
V	the velocity at a distance y from the bottom	$L\ T^{-1}$

$\bar{V}$	the mean velocity	$L\ T^{-1}$
V_*	the shear velocity	$L\ T^{-1}$
W	widths of channel	L
X	ratio of the velocities measured at 0,2 and 0,8 of the depth	-
y	distance from the boundary	L
y_n	depth of flow under unfirom flow conditions	L
y_o	distance from the boundary where the velocity equation goes to zero	L

GREEK SYMBOLS

α	constant of proportionality	-
β	function of channel shape	-
γ	specific weight of water	$M\ L^{-2}\ T^{-2}$
$\bar{\epsilon}$	measures the effect of free surface and corners	-
κ	Von Karman's universal constant	-
μ	dynamic viscosity	$M\ L^{-1}\ T^{-1}$
ν	kinematic viscosity	$L^{2}\ T^{-1}$
ζ	parameter describing roughness density	L^{-2}
ρ	density of water	$M\ L^{-3}$
σ	function describing roughness element shape	-
τ	shear stress	$M\ L^{-1}\ T^{-2}$
τ_o	shear stress at the boundary	$M\ L^{-1}\ T^{-2}$
$\phi(...)$	function of (....)	-
	parameter describing roughness geometry	L
ϕ	gradient of the velocity distribution in the wall zone	-

Log	Logarithm to the base 10
Ln	natural logarithm, to the base e

CHAPTER 1

INTRODUCTION

Although the conveyance of water in open channels is one of the earliest of engineering achievements, many of the phenomena involved in the flow of water in open channels are only partially understood. One of the most basic of these is the effect of boundary roughness on the discharge formulas in present use, the resistance coefficient (Chezy c or Manning n), is considered to be a constant for a particular type of rough boundary. However it has been shown to vary considerably as the depth of flow varies in many investigations.

The importance of precise knowledge of the roughness characteristics increases as the ratio of the conduit size to the roughness size decreases. For small values of the ratio i.e. for small conduits and/or large roughness values the knowledge of all the roughness parameters is important in order to predict the resistance coefficient accurately. To describe the roughness type completely one has to consider its height, concentration, configuration and shape.

The objectives of this thesis are :

(a) to study the available literature on large relative roughness and make use of the relevant research already available on the subject ;

(b) to test different roughness patterns in a systematic way. These tests would be conducted in a 0,3 by 6 m flume available in the University of Cape Town Civil Engineering laboratory ;

(c) to analyze the results obtained and develop a friction equation which can predict the friction coefficient accurately from the roughness description ;

(d) to make conclusions from the experimental results thus obtained.

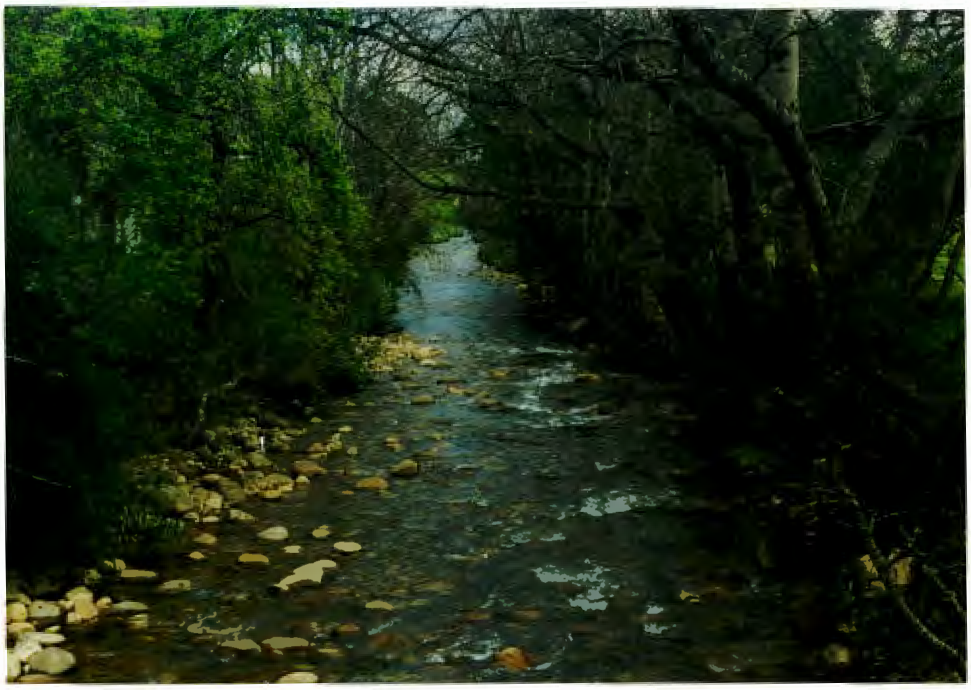

plate 1.1 : example of uniform flow over large relative roughness (downstream view)

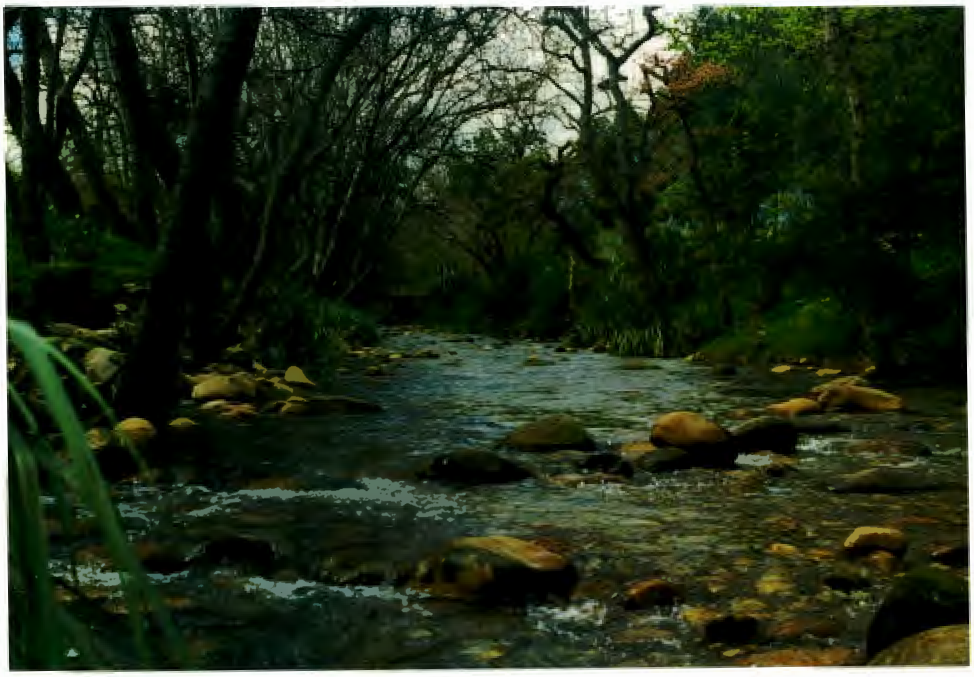

plate 1.2 : example of uniform flow over large relative roughness (upsteam view)

CHAPTER 2

LITERATURE REVIEW

2.1 Introduction

This literature review is based on literature obtained from journals dating from 1937 to 1988. Research on large scale roughness derived mainly from the United States and the United Kingdom, but work has also been carried out in the following countries: Canada, Germany, India, Jordan, New Zealand, South Africa and Turkey.

The literature is dealt with in chronological order, so that the historical development of the research carried out on large scale roughness may be traced through its development. Each article is reviewed in a systematic way, extracting from each the experimental equipment and procedure used, the theoretical analysis done, the results obtained and the conclusions reached.

There is an historical conflict in the choice of the friction factor, f, USA practice mainly used

$$S = \frac{f\bar{V}^2}{2gd} \quad \text{(the energy line slope for pipe flow)}$$

whereas UK practice favoured f such that

$$S = \frac{2f\bar{V}^2}{gd} \quad \left(\text{from} \quad \tau_o = f\,\frac{1}{2}\,\rho\,\bar{V}^2\right)$$

(throughout this thesis U.S.A. practice has been used).

2.2			
	Author	:	H Schlichting [1]
	Title	:	An Experimental Investigation of the Roughness problem
	Date	:	November 1937
	Place	:	Kaiser Wilhelm Institute, Gottingen, Germany.

2.2.1 Experimental Equipment

The experiments were done in a 64 by 1,7 metre flume. The flume was converted into a closed conduit by a test plate which was fitted to the top of the flume, which was removable. The velocity distribution was measured using a Pitot tube. Different roughness patterns were soldered onto the test plate and five types of roughness element were tested at several different concentrations. (See Figure 2.1).

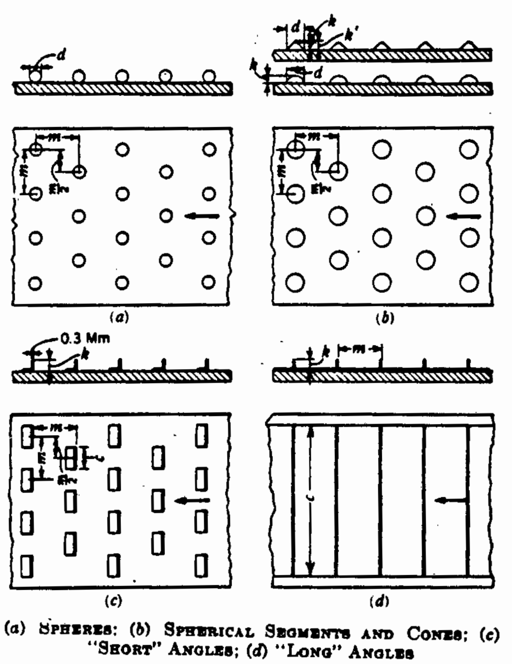

(a) Spheres; (b) Spherical Segments and Cones; (c) "Short" Angles; (d) "Long" Angles

Figure 2.1 : Roughness Patterns tested.

2.2.2 Theoretical analysis

(a) The velocity distribution for a smooth pipe was found by J Nikuradse to be:

$$\frac{V}{V_*} = 5,5 + 5,75 \log \frac{yV_*}{\nu} .$$

This was found to be valid even for very high Reynolds numbers, where

V	is the velocity at distance y from the wall
V_*	is the shear velocity $= \sqrt{\frac{\tau_o}{\rho}}$
ν	is the kinematic viscosity.
τ_o	is the shear stress at the boundary.

The resistance law for smooth pipes is obtained by integrating the velocity distribution

$$\frac{1}{\sqrt{f}} = 2 \log \left[\frac{R_e}{\sqrt{f}} \right] - 0{,}8 \qquad (2.1)$$

f being the Darcy-Weisbach friction factor and R_e the Reynolds number.

(b) The velocity distribution for a rough pipe in fully developed turbulent flow is:

$$\frac{V}{V_*} = A + 5{,}75 \log \frac{y}{k}$$

$$A = \phi \left[\frac{V_* k}{\nu} \right] \quad \text{as} \quad \frac{V_* R}{\nu} = \left[\frac{R}{k} \frac{V_* k}{\nu} \right]$$

k being the absolute roughness.

The resistance law for a rough wall is

$$\frac{1}{\sqrt{f}} = 2 \log \frac{R}{k} + a \qquad (2.2)$$

where R is the hydraulic radius

Nikuradse found from his results.

$$\frac{1}{\sqrt{f}} = 2 \log \frac{R}{k_s} + 1,74 \qquad (2.3)$$

k_s is the equivalent roughness, which is a multiple of k . This suggests k does not suffice in order to calculate the friction factor. Hence there is a necessity to study other roughness characteristics (e.g. roughness concentration and shape).

2.2.3 Results

The velocity distribution was plotted on a log scale and was found to consist of two straight lines. Plotting $^1/\sqrt{f}$ against log $^R/k$, the following relationship was verified:

$$\frac{1}{\sqrt{f}} = 2 \log \frac{R}{k} + a \quad .$$

Assuming Nikuradse friction eqtn. (2.3) is correct. It is important to calculate k_s , and a dimensionless ratio is introduced α, $\alpha = {}^{ks}/k$. A summary of the roughness types used and their characteristic α values can be seen in Tables 2.1 and 2.2 respectively

2.2.4 Conclusions

All the velocity profiles agree closely with

$$\frac{V}{V_*} = 8,48 + 5,75 \log \frac{y}{k_s} \quad ,$$

α can be determined from Tables 2.1 and 2.2 (for different roughness concentrations and shapes). These tables are based on experimental data. The friction factor may be calculated from

$$\frac{1}{\sqrt{f}} = 1,74 + 2 \log \frac{R}{k_s} \quad .$$

Type of roughness	Plate No.	d, in centimeters	m, in centimeters	$\frac{m}{d}$	k, in centimeters	c or k', in centimeters	b, in centimeters	$\frac{F_r}{F}$	$\frac{F_1}{F}$
Spheres:	XII	0.41	4	9.75	0.41	....	3.99	0.00785	0.992
	XII(a)*	1.0	10	10	1.0	....	*	0.00785	0.992
	III	0.41	2	4.88	0.41	....	3.99	0.0314	0.969
	I	0.41	1	2.44	0.41	....	3.96	0.126	0.874
	II	0.41	0.6	1.46	0.41	....	3.88	0.349	0.651
	V	0.41	†	†	0.41	....	3.68	0.907	0.093
	VI	0.21	1	4.86	0.21	....	3.99	0.0314	0.969
	IV	0.21	0.5	2.43	0.21	....	3.97	0.126	0.874
Spherical segments:	XIII	0.8	4	5	0.26	....	3.99	0.0087	0.969
	XIV	0.8	3	3.75	0.26	....	3.99	0.0155	0.944
	XV	0.8	2	2.5	0.26	....	3.98	0.0348	0.874
	XIX	0.8	†	†	0.26	....	3.85	0.251	0.093
Cones:	XXIII	0.8	4	5	0.375	0.425	3.99	0.0106	0.969
	XXIV	0.8	3	3.75	0.375	0.425	3.98	0.0189	0.944
	XXV	0.8	2	2.5	0.375	0.425	3.95	0.0425	0.874
"Short" angles:	XVI	....	4	....	0.30	0.8	4.0	0.0151	0.998
	XVIII	....	3	....	0.30	0.8	4.0	0.0269	0.996
	XVII	....	2	....	0.30	0.8	3.99	0.0605	0.994
"Long" angles:	XX	....	6	....	0.32	17	3.90	0.0538	0.995
	XXI	....	4	....	0.31	17	3.96	0.0776	0.992
	XXII	....	2	....	0.30	17	3.96	0.152	0.985

* Measured only in large wind tunnel. † Elements packed together as closely as possible.

Table 2.1 : Data on test plates

Plate No.	$\frac{v_{er}}{V}$	A	k_s, in centimeters	$\frac{k_s}{k} = \alpha$	Plate No.	$\frac{v_{er}}{V}$	A	k_s, in centimeters	$\frac{k_s}{k} = \alpha$
Sphere Roughness: $k = 0.41$ cm					Cone Roughness: $k = 0.375$ cm				
XII	0.0689	12.2	0.093	0.227	XXIII	0.0652	13.1	0.059	0.159
III	0.0881	8.92	0.344	0.838	XXIV	0.0754	10.6	0.104	0.437
I	0.120	5.68	1.26	3.07	XXV	0.0894	8.49	0.374	0.996
II	0.131	5.15	1.56	3.81					
V	0.0854	9.65	0.257	0.626					
Sphere Roughness: $k = 0.21$ cm					"Short Angle" Roughness: $k = 0.30$ cm				
VI	0.0779	8.98	0.172	0.819	XVI	0.0356	8.56	0.291	0.965
IV	0.106	5.27	0.759	3.61	XVIII	0.101	6.67	0.618	2.05
					XVII	0.124	4.53	1.47	4.86
Spherical Segment Roughness: $k = 0.26$ cm					"Long Angle" Roughness: $k = 0.323$ cm				
XIII	0.0590	13.8	0.031	0.118	XX	0.137	4.17	1.81	5.61
XIV	0.0631	12.7	0.049	0.186	XXI	0.167	2.28	3.70	11.9
XV	0.0763	9.89	0.149	0.571	XXII	0.179	2.33	3.56	11.75
XIX	0.0909	7.64	0.365	1.40					

Table 2.2 : Summary of experimental results

2.3

Authors:	C.F. Colebrook and C.M. White [2,3]
Titles:	Experiments with Fluid Friction in Roughened Pipes and Turbulent Flow in pipes, with particular reference to the Transition between the smooth and rough pipe laws.
Date:	1937 - 1939.
Place:	Imperial College, London, U.K.

2.3.1 Experimental equipment

The experiments were conducted in a pipe of diameter 53,5 mm and length of 6 m . The pipe was split longitudinally in order to expose the inner surface to which sand grains were fixed by bituminous paint. (See Figure 2.2).

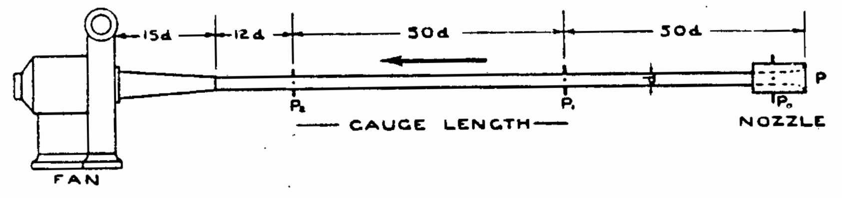

Figure 2.2 : General arrangement of test pipe

Experiments were conducted using air. Six different types of roughness were formed from a combination of two sand sizes, 0,035 cm and 0,35 cm diameters. (See Figure 2.3).

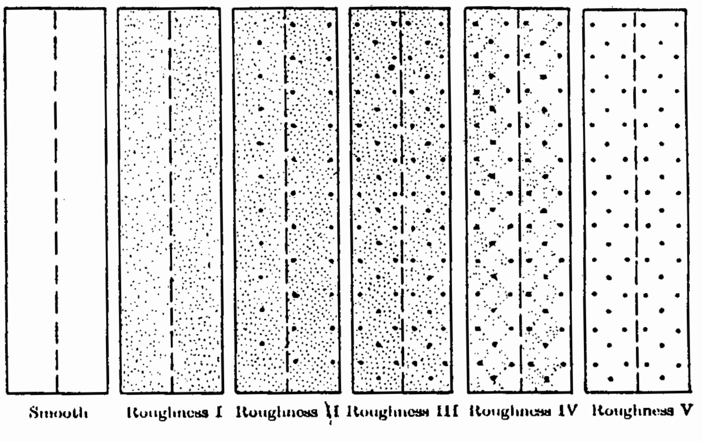

Figure 2.3 : Roughness patterns tested

2.3.2 Theoretical Analysis

The velocity gradient in the turbulent zone is

$$\frac{dV}{dy} = \sqrt{\frac{\tau_o}{\rho}}\,\frac{2,5}{y} \quad ,$$

by integrating the equation, the velocity distribution is obtained in the form

$$V = 5,76\sqrt{\frac{\tau_o}{\rho}}\ \log\frac{y}{y_o} \quad .$$

As V=0 at $y = y_o$, the hydraulic wall may be regarded as being displaced inwards by y_o from the actual wall.

The mean velocity is numerically equal to the local velocity at y = 0,113d , d being the diameter of the pipe

$$\bar{V} = 5,76\sqrt{\frac{\tau_o}{\rho}}\ \log\frac{0,113d}{y_o} \quad .$$

This equation may be regarded as applicable to all types of turbulent flow in pipes. The shift of the hydraulic wall y_o depends on

(a) the roughness at the wall k

(b) the shear stress at the boundary τ_o

(c) the kinematic viscosity of the fluid $\nu = \mu/\rho$.

Experimentally it has been observed that if $\rho\frac{V_* k}{\mu} > 60$ then the resistance-coefficient, f, is independent of the viscosity of the fluid. By dimensional reasoning the shift y_o can only be proportional to k, and Nikuradse determined experimentally that

$$y_o = \frac{k}{33} \quad .$$

The resistance-law for rough pipes becomes

$$\frac{1}{\sqrt{f}} = 2 \log 3{,}7 \frac{d}{k} \tag{2.4}$$

In the case of smooth pipe $\left\{ \frac{\rho V_* k}{\mu} < 3 \right\}$ from Nikuradse :

$$y_o = \frac{1}{10} \frac{\mu}{\rho V_*} .$$

The resistance-law for smooth pipes becomes

$$\frac{1}{\sqrt{f}} = 2 \log R_e \frac{\sqrt{f}}{2{,}51} \tag{2.5}$$

By combining the smooth and rough pipe resistance-laws a transition formula is produced

$$\frac{1}{\sqrt{f}} = - 2 \log \left\{ \frac{k}{3{,}7d} + \frac{2{,}51}{R_e \sqrt{f}} \right\} . \tag{2.6}$$

The comparison of the transition formula with experimental results is shown in Figure 2.4.

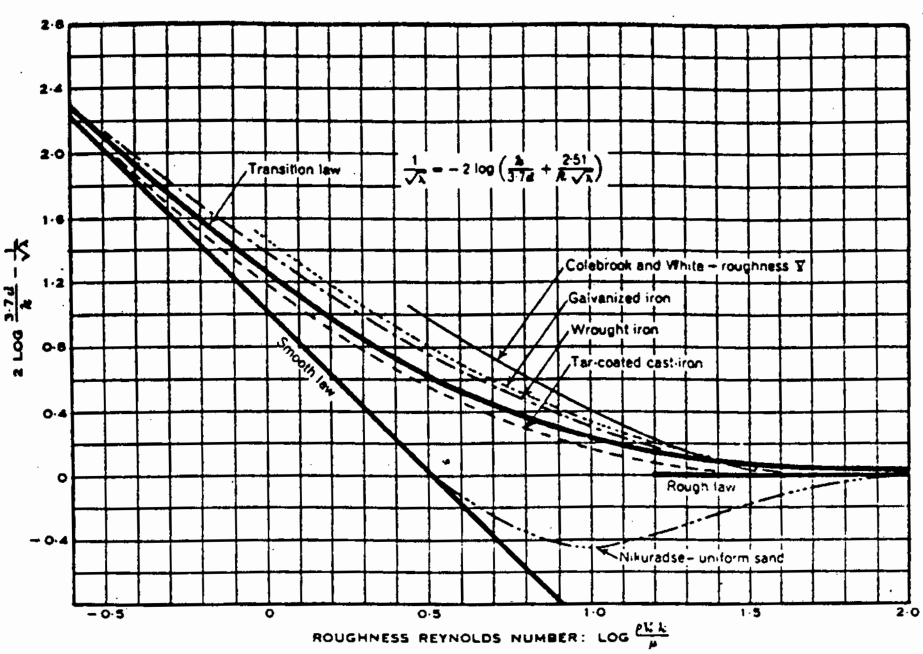

Figure 2.4

2.3.3 Results

For each type of roughness, the value of k_s was determined, being calculated from

$$\frac{\tau_o}{\rho \bar{V}^2} = \frac{1}{8} \left[2 \log \frac{3,7d}{k_s} \right]^{-2}$$

at values of $\rho \; V_* \frac{k}{\mu} > 150$ (fully developed turbulent flow)

Figures 2.5 and 2.6 show how f varies with increasing Reynolds number and for different roughness types:

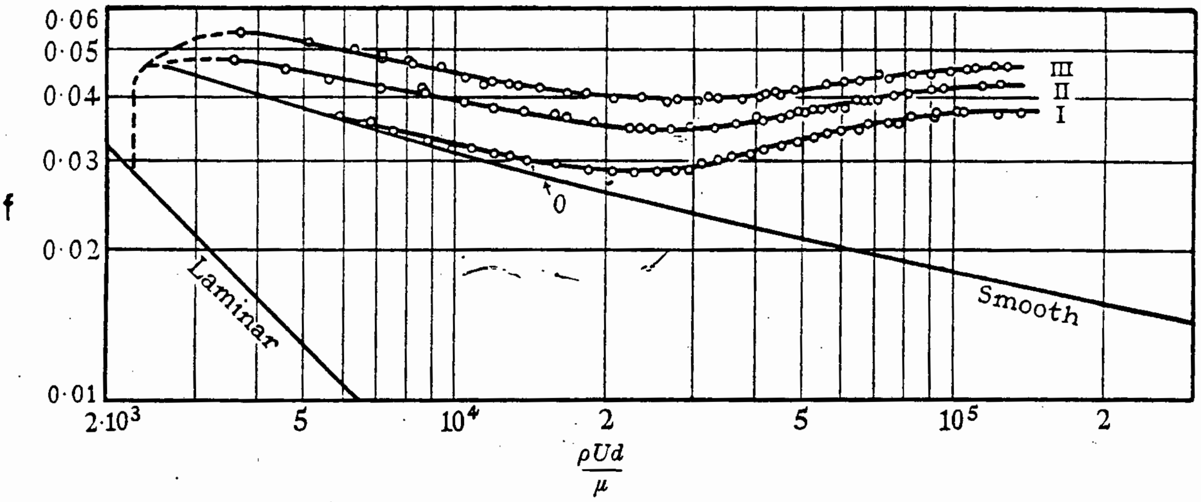

Figure 2.5

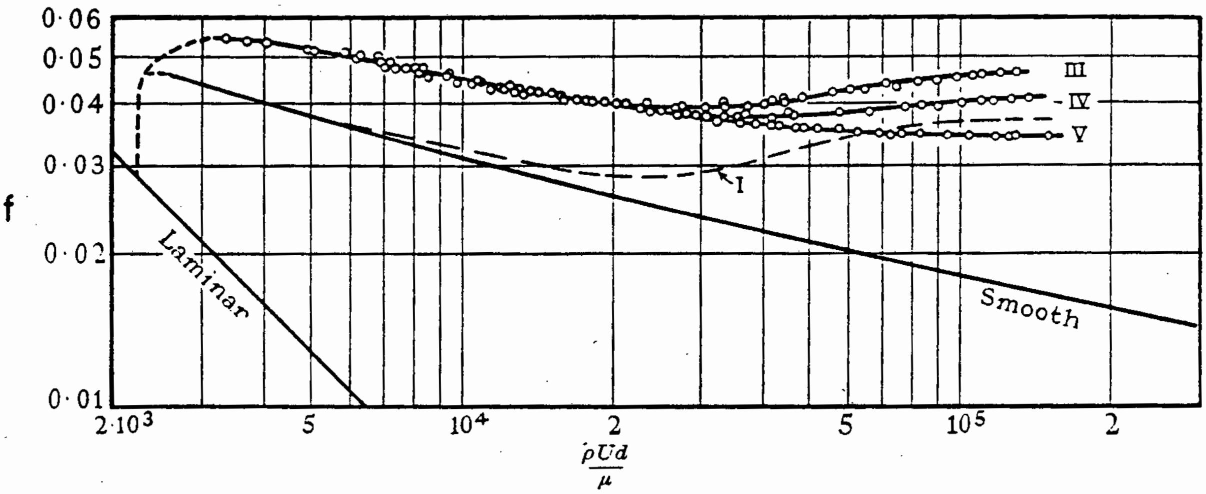

Figure 2.6

$2 \log \frac{3,7d}{k_s} - \frac{1}{\sqrt{f}}$ was seen to tend to zero as the Reynolds number increased.

2.3.4 Conclusions

The transition formula is valid for a wide range of Reynolds numbers as it accounts for the combined effects of both viscous and form drag. At values of

$$\frac{\rho V_* k}{\mu} > 60$$

viscous drag becomes negligible as form drag predominates, thus making the friction coefficient f dependent on relative roughness only in the zone of fully developed roughness, where

$$\frac{1}{\sqrt{f}} = 2 \log 3,7d/k_s \quad \text{at large } R_e \text{ values.}$$

2.4		
Author	:	L.F. MOODY [4]
Title	:	Friction factors for pipe flow
Date	:	1944
Place	:	Princeton, New Jersey, U.S.A.

2.4.1 Theoretical Analysis

Moody developed a graphical solution for determining the friction coefficient f, in the expression

$$h_f = f \frac{L}{d} \frac{V^2}{2g}$$

where h_f is the head loss due to friction and L is the length of pipe.

In order to draw the graph of f against Reynolds number with respect to relative roughness (see Figure 2.7), the following theories were used :

(a) Laminar flow: $f = 64/R_e$ (Hagen-Poiseuille Law).

(The flow is independent of roughness.)

(b) Turbulent flow:

$$\frac{1}{\sqrt{f}} = 2 \log \left[\frac{k/d}{3{,}7} + \frac{2{,}51}{R_e \sqrt{f}} \right]$$

(the Colebrook-White transition formula).

For fully developed roughness, the situation to the right of the dashed line in Figure 2.7 , f becomes independent of R_e. Therefore it is possible to draw a graph for this region of f versus pipe diameter with respect to type of pipe or roughness size. (See Figure 2.8).

Two other graphs were also presented, one to determine the Reynolds number from the pipe diameter and the velocity (for water at 60°F), the other to determine the kinematic viscosity from the type of fluid used and the temperature.

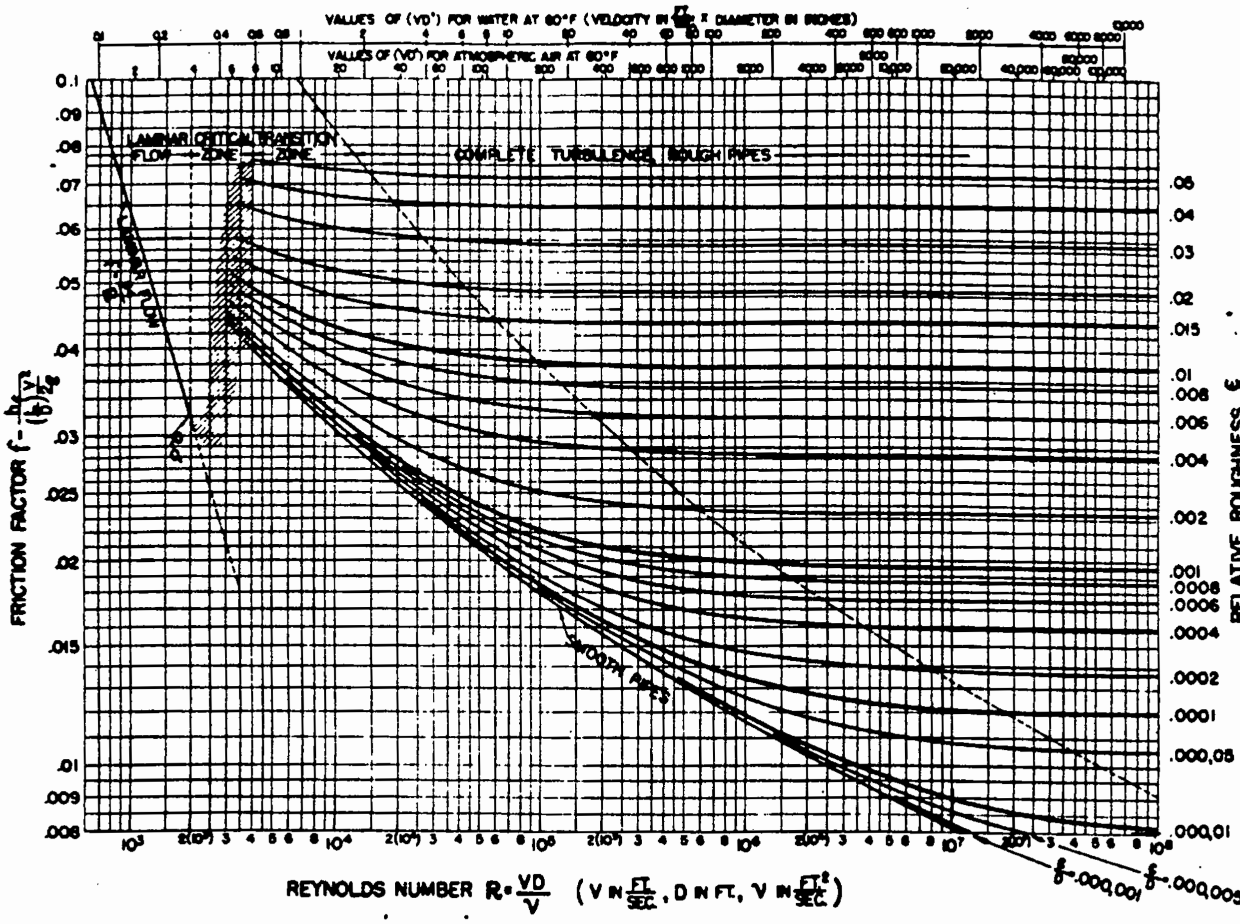

Figure 2.7 : "Moody diagram"

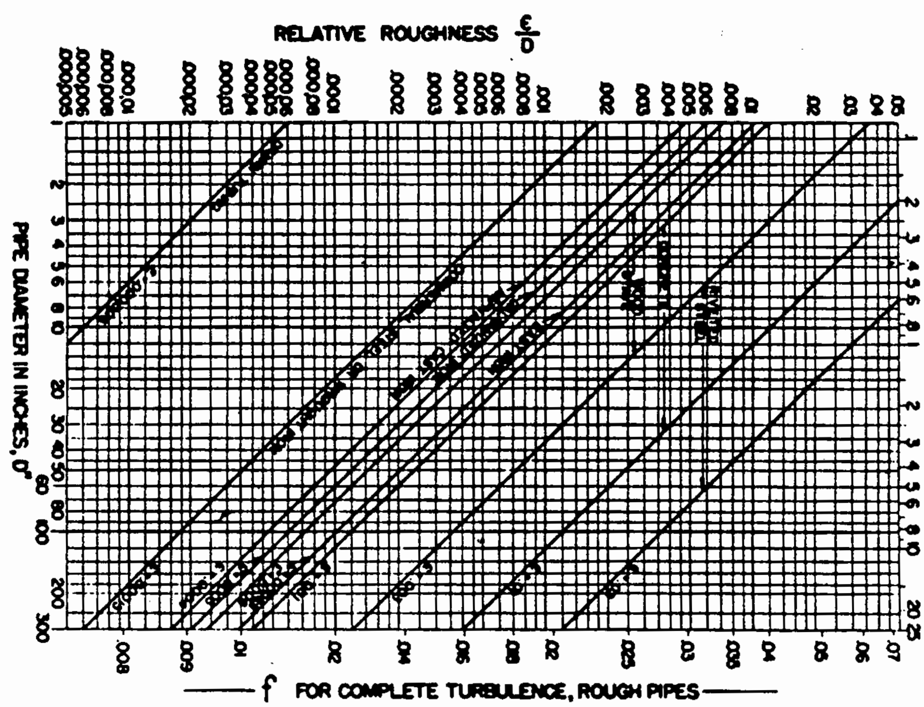

Figure 2.8 : Friction factor versus relative roughness

The pipe friction factors can be applied to open channel flow by using $f = {}^{8g}/C^2$ and $d = 4R$, using the Chezy formula $\bar{V} = C\sqrt{RS}$, S being the channel slope. The author expressed caution in doing this as Chezy coefficients have been derived principally from wide shallow channels of large cross sectional area and rough bottoms, far from circular in shape and involving a free surface. The presence of a free surface introduces surface waves and disturbances, which linked to the Froude number.

2.4.2 Conclusions

Figures 2.7 and 2.8 introduced a simple and accurate means of estimating the friction factors for commercial pipes. The graphical solution for the friction factor in open channels is complicated by the fact that the relative roughness does not remain constant for a particular channel, as the depth changes, thus not lending itself to the same type of solution as pipe flow.

2.5		
Author :	R.W. POWELL [5,6]
Title :	Flow in a Channel of Definite Roughness and Resistance to flow in Rough Channels
Date :	1946, 1950
Place :	Institute of Hydraulic Research, Iowa, U.S.A.

2.5.1 Experimental equipment

The flume used was 50 feet long by 8 inches wide and 7 inches deep. The definite wall roughness was provided by square steel strips which extended down the sides and across the bottom so as to act as cleats or battens. The batten spacing used can be seen in Figure 2.9 . Two batten sizes were used 1/4 inches square and 1/8 inches square.

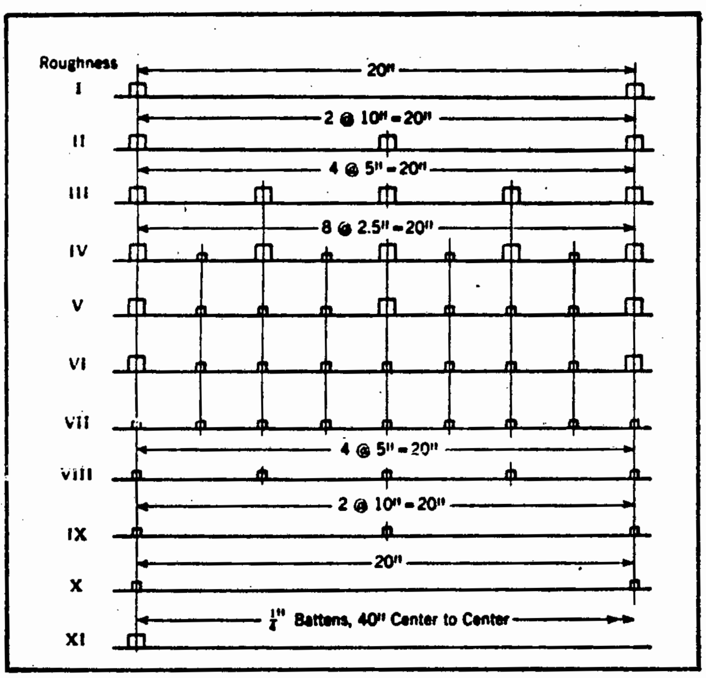

Figure 2.9 : Spacing and size of roughness tested

The flow rate was measured with a diaphragm orifice making use of manometers. A control gate was used at the end of the flume to ensure uniform flow. The depth was measured using hook gauges.

2.5.2 Theoretical analysis

Keulegan's formula for rough channel flow is

$$\frac{\bar{V}}{V_*} = 6,25 + 5,75 \log \left[\frac{R}{k} \right]$$

as $$\frac{\bar{V}}{V_*} = \frac{C}{\sqrt{g}}$$

giving $$\frac{C}{\sqrt{g}} = 6,25 + 5,75 \log \left[\frac{R}{k} \right] ,$$

but this is based entirely on experiments from pipes, thus neglects the effect of the free surface and of the angles, between the walls and the bottom of the channel.

Keulegan's more fundamental formula is

$$\frac{\bar{V}}{V_*} = a_r - b + b \cdot \mathrm{Ln} \left[\frac{R}{k} \right] + b\,\beta - \bar{\epsilon}\,\frac{\bar{V}}{V_*} ,$$

where a_r is a function of the roughness geometry, b is 2,50 , (the reciprocal of Von Kármán's universal constant) β is a function of the shape of the cross-section, and $\bar{\epsilon}$ measures the effect of the free surface and the corners.

$$\frac{C}{\sqrt{g}} (1 + \bar{\epsilon}) = 0,32J + 2,5\,\beta + 5,75 \log \left[\frac{R}{k} \right] ,$$

where $J = \sqrt{g}\,(a_r - 2,5)$.

Assuming $\bar{\epsilon} = - 0,208$ (the same value as for smooth channels) thia gives $\dfrac{C}{\sqrt{g}} = 0{,}40J + 3{,}16\,\beta + 7{,}26\,\log\left[\dfrac{R}{k}\right]$.

Making $\log k = \log k_s + \dfrac{0{,}4J}{7{,}26}$,

$$\therefore \quad \frac{C}{\sqrt{g}} = 3{,}16\,\beta_k + 7{,}26\,\log\frac{R}{k_s} ,$$

where k_s represents Nikuradse's equivalent roughness size. By changing the coefficient 7,26 to 7,40 , it is possible to drop the shape correction factor (3,16 β).

$$\frac{C}{\sqrt{g}} = 7{,}40\,\log\left[\frac{R}{k_s}\right] . \qquad (2.7)$$

In order to make this formula applicable to the transition zone, between smooth and rough laws.

$$\frac{C}{\sqrt{g}} = -\,7{,}40\,\log\left[\frac{C}{R_e} + \frac{k_s}{R}\right] \qquad (2.8)$$

(which is analogous to the Colebrook-White formula). A graphical representation of this formula can be seen in Figures 2.10 and 2.11, the latter being without transition. Both these graphs can be seen as a development of the Moody diagrams for pipe flow to be applied to free surface flow.

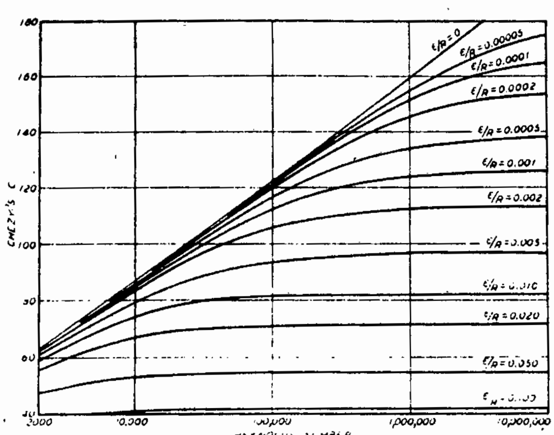

Figure 2.10

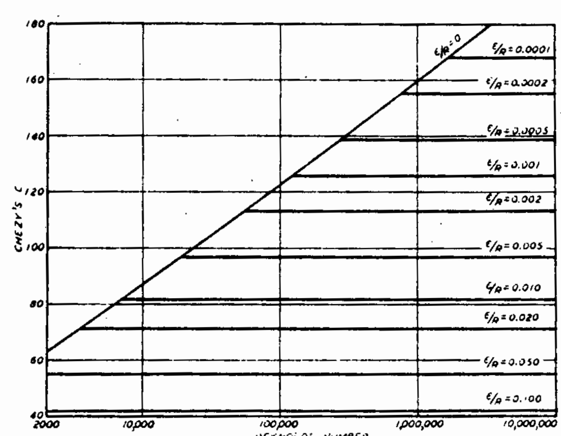

Figure 2.11

2.5.3 Results

The author displayed a table of results for each roughness type tested. Comparing the observed "C" to the calculated "C" for each run, Table 2.3 is an example of the tables given.

Run*	y (ft)	R (ft)	V (ft per sec)	S ×10⁴	Observed C	F	t (degrees Centigrade)	R ×10⁻⁴	c_s	Computed C	Discrepancy −	Discrepancy +
(k) Roughness VIII (Fig. 3); Discrepancies by Eq. 17												
37-1	0.083	0.067	0.264	4.6	45.8	0.16	21.2	0.640	1.4	45.6	0.2	....
37-2	0.130	0.094	0.278	3.4	49.2	0.14	21.2	0.992	1.0	52.0	....	2.8
37-3	0.181	0.118	0.422	4.8	56.0	0.18	21.3	1.89	2.3	56.4	....	0.4
37-4	0.257	0.146	0.543	5.6	59.9	0.19	21.3	3.02	2.6	60.4	....	0.5
37-5	0.322	0.165	0.628	6.8	59.2	0.20	21.4	3.95	2.7	62.6	....	3.4
37-6	0.388	0.181	0.724	7.6	61.7	0.20	21.4	4.99	2.7	64.2	....	2.5
32-1	0.097	0.076	0.561	20.8	44.8	0.32	21.1	1.60	1.5	47.8	....	3.0
32-2	0.133	0.096	0.706	20.0	51.0	0.34	21.1	2.55	1.9	52.3	....	1.3
32-3	0.202	0.127	0.926	20.2	57.9	0.36	21.3	4.46	2.4	57.7	0.2	....
32-4	0.245	0.142	0.962	20.5	56.3	0.34	21.8	5.26	2.6	58.9	....	2.6
32-5	0.320	0.165	1.14	20.1	62.7	0.36	21.9	7.25	2.7	62.6	0.1	....
15-1	0.372	0.178	2.41	78	64.8	0.70	25.7	18.1	2.7	63.9	0.9	....
12-1	0.111	0.084	2.60	312	50.8	1.37	27.0	9.43	1.7	49.8	1.0	....
12-2	0.151	0.105	3.20	311	56.1	1.45	27.1	14.5	2.1	54.1	2.0	....
12-3	0.195	0.124	3.72	310	60.0	1.49	27.1	20.0	2.3	57.2	2.8	....
12-4	0.246	0.143	4.12	312	61.7	1.46	27.2	25.6	2.6	60.0	1.7	....
12-5	0.321	0.165	4.55	311	63.4	1.41	27.2	32.7	2.7	62.6	0.8	....

Table 2.3 : Table of results

2.5.4 Conclusions

The formula $C/\sqrt{g} = -7{,}40 \log \left\{ \frac{C}{R_e} + \frac{k_s}{R} \right\}$ was shown to give accurate estimation for the resistance to flow in open channels and is believed to be an improvement on Manning's "n" . The constant 7,40 needs more extensive tests as does a list of values for k_s for different roughness geometries.

2.6

Authors:	A.R. Robinson and M.L. Albertson [7]
Title :	Artificial Roughness standard for open channels
Date :	December 1952
Place :	Colorado Agriculture and Mechanical College, Fort Collins, Colorado, U.S.A.

2.6.1 Experimental equipment

An adjustable slope wooden flume of 14feet long by 9 inches wide and 10,5 inches deep was used. A weir box was used to measure discharge. The artificial roughness was in the form of small sheet metal angles 0,5 and 1 inch high. (Figure 2.12).

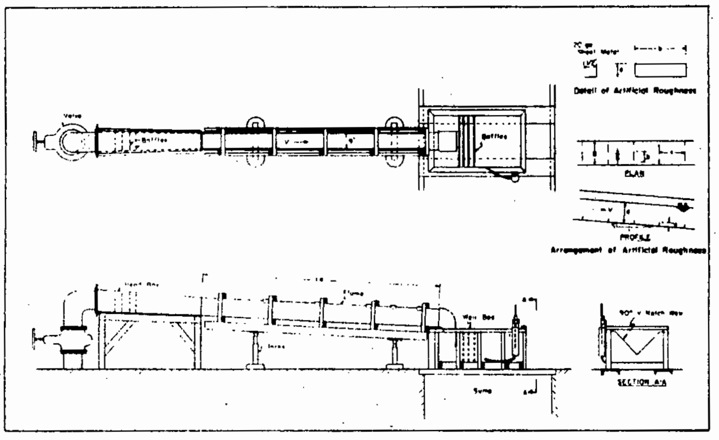

Figure 2.12 : Experimental Equipment

2.6.2 Theoretical analysis

In uniform flow the sum of forces on a block of water of unit length must be equal to zero.

$$\Sigma F = F_1 + \omega \sin\alpha - F_2 - P\tau_o = 0$$

but $F_1 = F_2$

$$\therefore \quad \tau_o = \left[\frac{A}{P}\right] \gamma \sin\alpha = R \gamma \sin\alpha$$

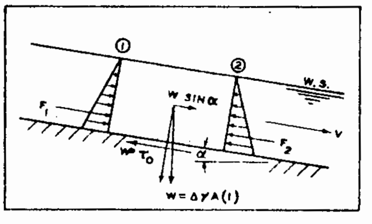

Figure 2.13 : Forces producing flow

The variables which govern the shear stress along the boundary have the following relationship.

$$\tau_o = \phi_1 (\bar{V} , k_s , \beta , R , \rho , \mu , \gamma) .$$

Choosing V , R and ρ as the repeating variables, dimensional analysis yields

$$\frac{\tau_o}{\rho \bar{V}^2} = \phi_2 \left[\frac{R}{k_s} , \beta_k , F_r , R_e \right] ,$$

F_r being the Froude number based on R

$$\therefore \quad R \gamma \sin\alpha = \rho\bar{V}^2 \phi_2 \left[\frac{R}{k_s} , \beta , F_r , R_e \right] ,$$

$$\bar{V} = \sqrt{g} \quad \phi_3 \left[\frac{R}{k_s}, \beta , F_r , R_e \right] \sqrt{RS} .$$

which resembles Chezy's formula for open channels.

$$\bar{V} = C \sqrt{RS} ,$$

$$\therefore \quad \frac{C}{\sqrt{g}} = \phi_3 \left[\frac{R}{k_s} , \beta , F_r , R_e \right] .$$

As the channel used was rectangular and relatively wide compared to depth. R approximates to the flow depth and β can be ignored. As there are no surface waves or surface irregularities the Froude number can be discounted

$$\therefore \quad \frac{C}{\sqrt{g}} = \phi_4 \left[\frac{R}{k_s} , R_e \right] .$$

It was assumed that $k_s = k$. At large values of Reynolds number, R_e does not affect C

$$\frac{C}{\sqrt{g}} = \phi_3 \left[\frac{R}{k} \right] .$$

On the basis of theoretical development and previous research, an equation in logarithmic form was assumed

$$\frac{C}{\sqrt{g}} = A + B \log \left[\frac{R}{k} \right] ,$$

where A and B are parameters to be determined experimentally.

2.6.3 Results

The resistance function $^{C}/\sqrt{g}$, the relative roughness $\frac{R}{k}$ and the Reynolds number were measured to study their effect on flow over large relative roughness. Plotting $^{C}/\sqrt{g}$ against the log of $^{R}/k$ yields the following equation :-

$$\frac{C}{\sqrt{g}} = 1,31 + 4,7 \log \frac{R}{k} . \qquad (2.9)$$

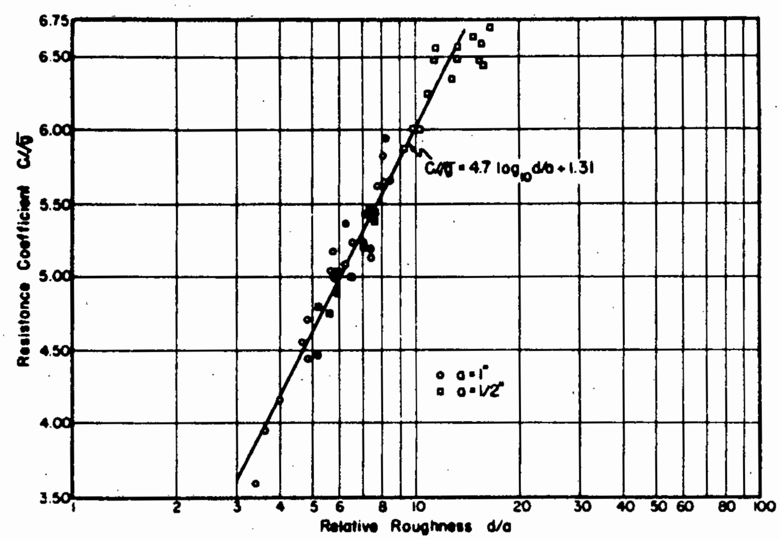

Figure 2.14 : Resistance coefficient versus relative roughness

Plotting $^C/\sqrt{g}$ against the log of Reynolds number for different values of relative roughness yields results very similar to the Moody diagram (see Figure 2.15).

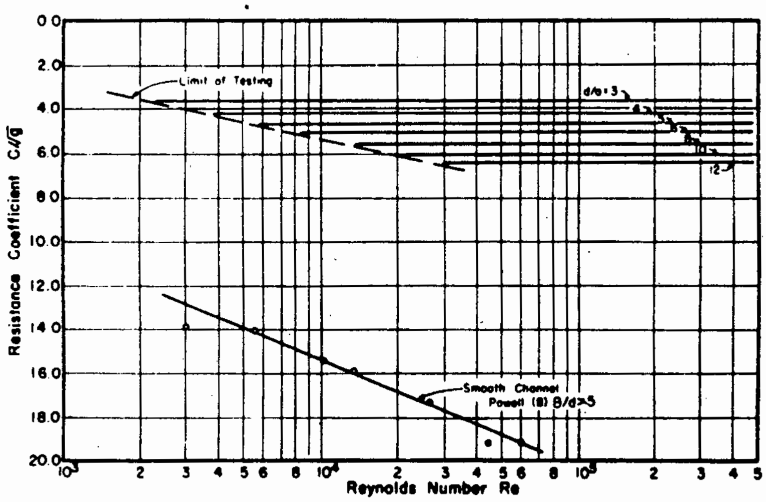

Figure 2.15 : Resistance Coefficient versus Reynolds Number and Relative Roughness

2.6.4 Conclusions

The roughness standard such as exists for pipes may be set up for open channels with rough boundaries. The equation

$$^C/\sqrt{g} \quad = \quad 4,7 \log \left[\frac{R}{k} \right] + 1,31$$

predicts Chezy's coefficient for artificial roughness.

2.7		
Author	:	M.C. Boyer [8]
Title	:	Estimating the Manning coefficient from an average bed roughness in open channels
Date	:	December 1954
Place	:	University of Iowa, Iowa City, Iowa, U.S.A.

2.7.1 Theoretical analysis

(a) Considering the Manning coefficient as a function of bed roughness ;

the velocity distribution is given by

$$V = 2,5\ (g\ R\ S)^{\frac{1}{2}} \quad Ln \left[\frac{y}{y_o} \right] .$$

Assuming $y_n = R$, integrating the velocity distribution with respect to depth and dividing by the depth, the mean velocity is found to be

$$\bar{V} = 2,5\ (g\ R\ S)^{\frac{1}{2}}\ Ln \left[\frac{R}{e y_o} \right] .$$

e is the base of the natural logarithm (2,718 ...).

Combining the above equation with the Manning equation

$$V = \frac{1}{n} R^{2/3} S^{1/2}$$

gives $$\frac{n}{R^{1/6}} = \frac{0,128}{Ln\ (R/y_o) - 1} . \qquad (2.10)$$

The author assumed that for completely developed turbulent flow

$$y_o = \frac{k}{30} . \qquad (2.11)$$

Thus the relationship between $^n/R^{1/6}$ and $^R/k$ can be solved and a curve of the relationship plotted. (See Figure 2.16).

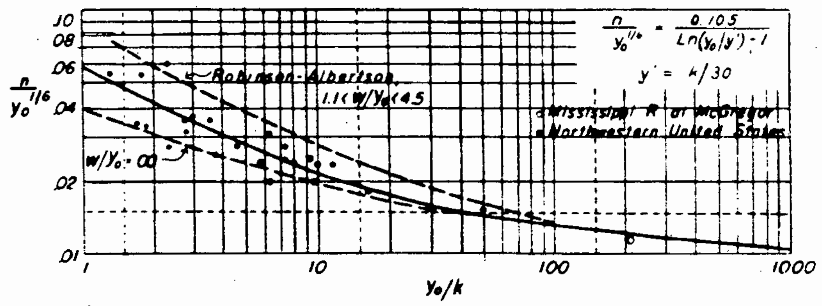

Figure 2.16 : Manning coefficient versus Relative Roughness

(b) The Manning coefficient as a function of the velocity distribution.

The velocity distribution is

$$V = 2,5\ (g\ y\ S)^{\frac{1}{2}}\ \mathrm{Ln}\ \frac{y/_{R}}{y_{o}/_{R}} \quad .$$

Substituting the values of 0,2 and 0,8 in sequence for y/R

gives $\mathrm{Ln}\left[\frac{R}{y_o}\right] = \left[1,61\ \frac{V_{0,2}}{V_{0,8}} - 0,22\right] / \left[\frac{V_{0,2}}{V_{0,8}} - 1\right]$ (2.12)

Combining with the following eqtn.

$$\frac{n}{R^{1/6}} = \frac{0,128}{\mathrm{Ln}(R/_{y_o}) - 1} \quad .$$

gives the the relationship between

$$\frac{n}{R^{1/6}} \quad \text{and} \quad \frac{V_{0,2}}{V_{0,8}} \; ,$$

which may be presented graphically (see Figure 2.17).

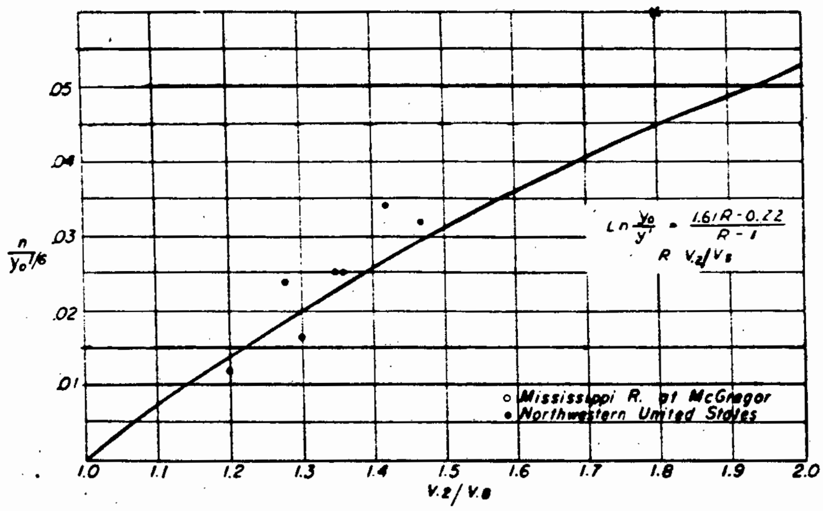

Figure 2.17 : Relation between Manning coefficient and velocity distribution

2.7.2 <u>Results</u>

Robinson and Albertson's results were used as well as results from a United States Geological Survey of streams in the Northwestern United States. These were plotted on both Figures 2.16 and 2.17.

2.7.3 <u>Conclusions</u>

Estimating Manning's "n" for natural channels in terms of roughness height gives results within acceptable limits of accuracy. The method of velocity distribution provides another method of determining "n" but requires further research due to lack of sufficient experimental data.

2.9	Author :	W.W. Sayre and M.L. Albertson [10]
	Title :	Roughness Spacing in Rigid open channels
	Date :	May 1961
	Place :	Colorado State University, Fort Collins, Colorado, U.S.A.

2.9.1 Experimental equipment

Experiments were conducted in an 8 feet. wide by 2 feet. deep rectangular flume which measured 72 feet in length. The water-surface level was controlled by the use of a tailgate. Discharge was measured by the use of an orifice plate. Sheet metal baffles measuring 6 inches wide and 1,5 inches high were used as roughness elements. (See figure 2.20).

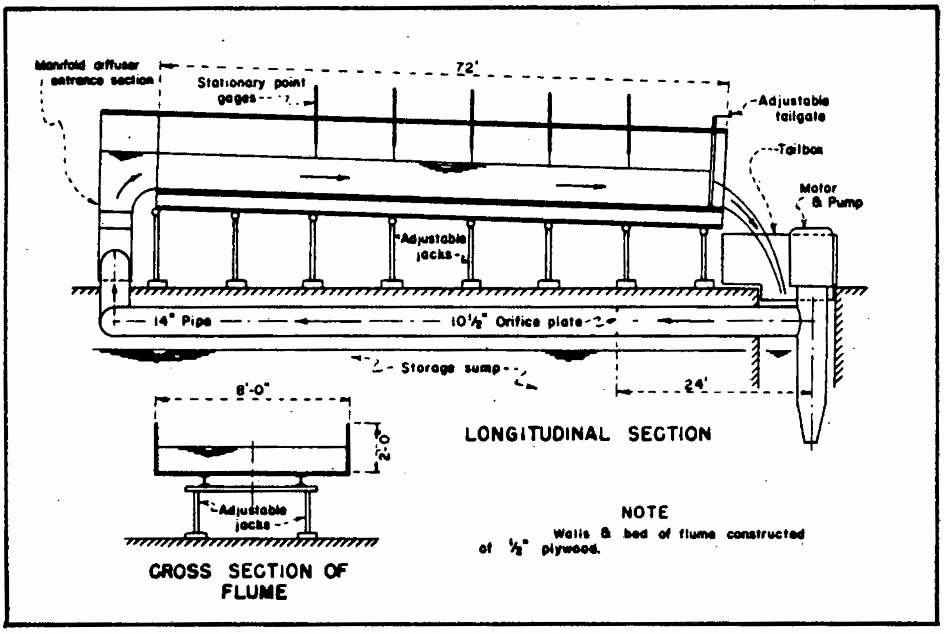

Figure 2.20 : Experimental Equipment

2.9.2 Theoretical analysis

The von Kármán-Prandtl equation for velocity distribution near rough boundaries is :

$$\frac{V}{V_*} = \frac{2,30}{\kappa} \log \frac{y}{k} + C_1 \quad .$$

Obtaining the mean velocity by integrating over the depth

$$\frac{\bar{V}}{V_*} = \frac{2,30}{\kappa} \log \frac{R}{k} + C_2 \quad .$$

Introducing the Chezy coefficient

$$\frac{C}{\sqrt{g}} = \frac{2,30}{\kappa} \log \frac{R}{k} + C_2 \quad . \qquad (2.17)$$

It is assumed that C_2 is the factor dependent on the arrangement and shape of the roughness elements.

$$\frac{C}{\sqrt{g}} = \frac{2,30}{\kappa} \log \frac{R}{\chi} \quad . \qquad (2.18)$$

where χ completely describes the boundary roughness

$$\frac{\chi}{k} = \phi_1 \left\{ \frac{L_s}{k} , \frac{T_s}{k} , \sigma \right\}$$

(where σ is a shape factor of the roughness elements).

Dimensional analysis

$$\phi_2 \ (\bar{V} , R , b , \chi , \beta , \tau_o , \mu , \rho , \gamma) = 0$$

$$\frac{C}{\sqrt{g}} = \phi_3 \left[\frac{R}{\chi} , R_e , F_r \right] \quad .$$

R_e can be eliminated as viscous effects are negligible. The Froude number only is important if surface waves or disturbances occur.

$$\therefore \quad \frac{C}{\sqrt{g}} = \phi_4 \left[\frac{R}{\chi} \right] \quad ,$$

χ/k is assumed to be a function of the combined area of all the roughness element projected perpendicularly to the direction of flow, divided by the area of the bed.

2.9.3 Results

The variation of the Chezy coefficient with the relative roughness $R/_k$ can be seen on Figure 2.21 . The data supports the equation found theoretically :

$$\frac{C}{\sqrt{g}} = 6{,}06 \log \frac{R}{k} + C_2 \quad .$$

Chezy C was then plotted against the relative roughness based on the single parameter which groups all the data about a single curve , described by the equation

$$\frac{C}{\sqrt{g}} = 6{,}06 \log \frac{R}{\chi} \qquad \text{(See Figure 2.22)} \qquad (2.19)$$

$$\therefore \quad \chi = \frac{k}{10^i} \qquad \text{where} \qquad i = C_2/6{,}06$$

2.9.4 Conclusions

The variation of the Chezy resistance function is logarithmic in nature. The equations

$$\frac{C}{\sqrt{g}} = 6{,}06 \log \frac{R}{k} + C_2$$

and

$$\frac{C}{\sqrt{g}} = 6{,}06 \log \frac{R}{\chi}$$

are found to be applicable over the range of roughness types tested.

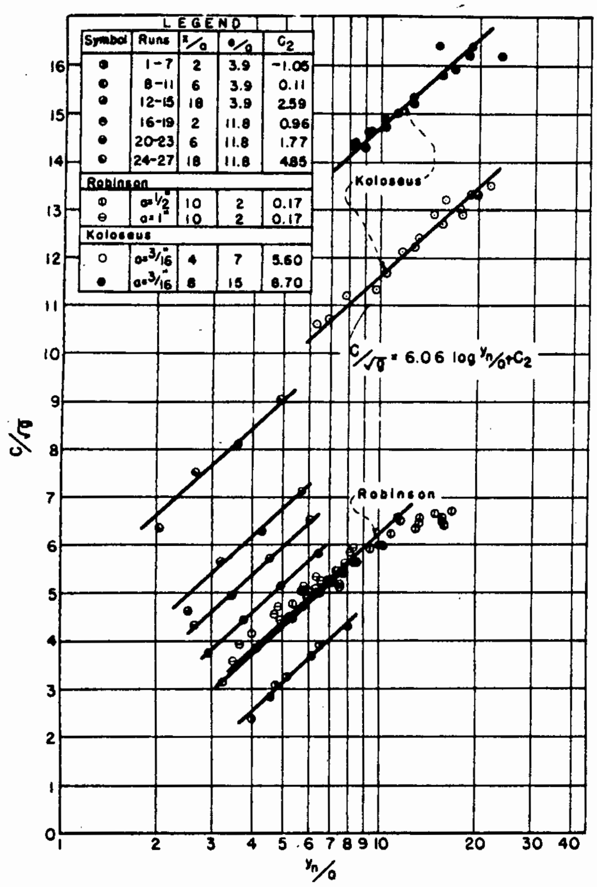

Figure 2.21

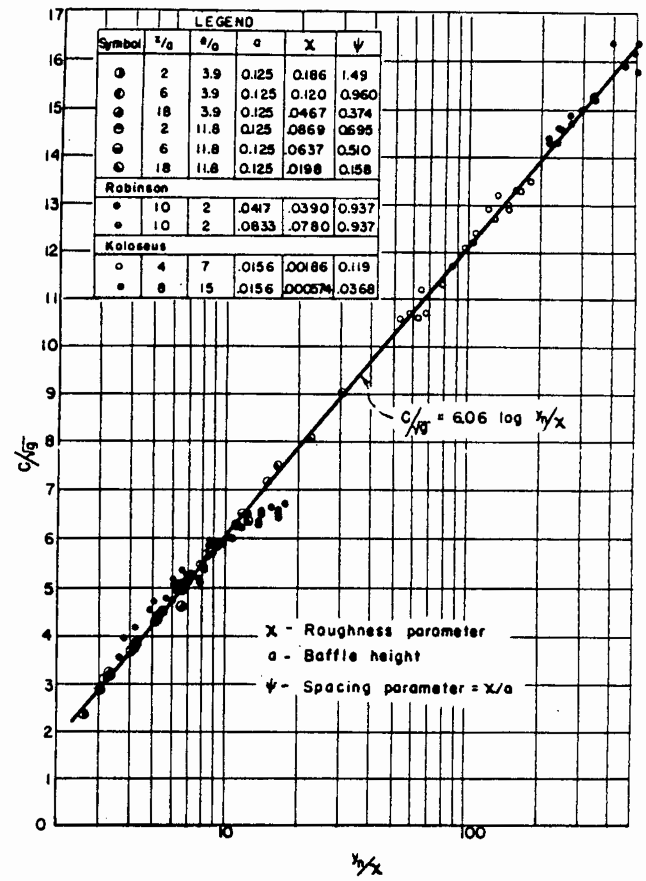

Figure 2.22

2.10		
	Authors:	A.G. Mirajgaoker and K.L.N. Charlu [11]
	Title :	Natural Roughness effects in Rigid open channels
	Date :	September 1963
	Place :	University of Roorkee, Roorkee, India.

2.10.1 Experimental equipment

Experiments were conducted in a 3 ft wide by 28 ft long concrete flume. Flow rate was measured by the use of an orifice plate. The depth was controlled by the use of a tail gate. The natural roughness elements used were small boulders passing through a 3 in sieve and retained on a $2\frac{1}{2}$ in sieve. The roughness spacings can be seen in Figure 2.23.

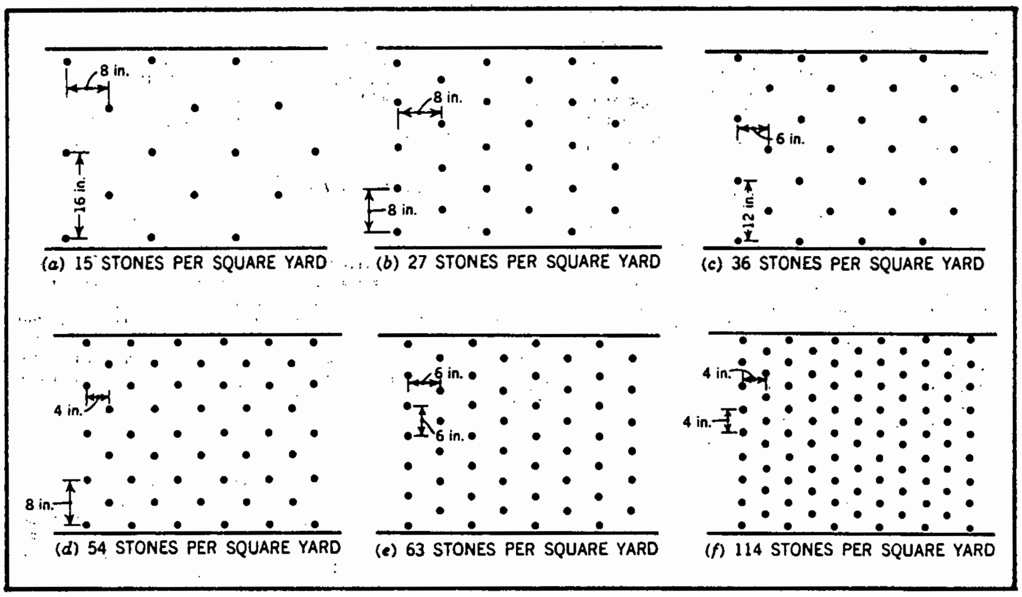

Figure 2.23 : Roughness Patterns tested.

2.10.2 Theoretical analysis

The following variables were chosen in the dimensional analysis

$$\phi_1 (k , \bar{V} , R , g , \tau_o , \rho , \mu , \xi , \chi) = 0$$

(where ξ describes the roughness density)

By dimensional analysis

$$\frac{C}{\sqrt{g}} = \phi_2 \left\{ \frac{R}{k} , \frac{R}{\chi} , \xi R^2 , R_e , F_r \right\} .$$

2.11.3 Results

Plotting $^C/\sqrt{g}$ against the relative roughness $^R/k$. It can be seen that the following relationship exists. (See Figure 2.24).

$$\frac{C}{\sqrt{g}} = 6{,}06 \log \frac{R}{k} + C_2 \quad . \qquad (2.20)$$

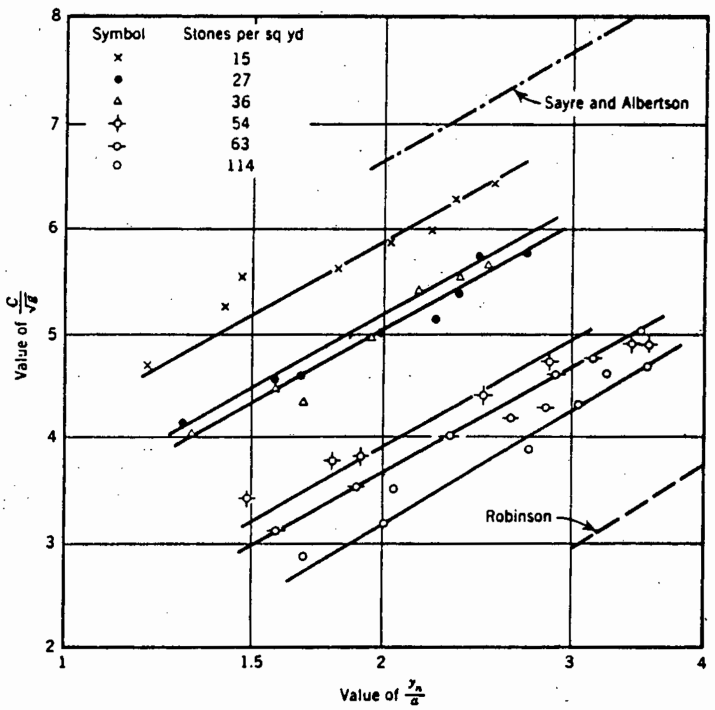

Figure 2.24 : Resistance function versus Relative Roughness

Plotting $^C/\sqrt{g}$ against the roughness density ξR^2 on a log-log scale. The following relationship exists. (See Figure 2.25)

$$\frac{C}{\sqrt{g}} = K\left[\xi R^2\right]^m$$

(where m = 0,25 and K ranges from 5,1 to 1,8).

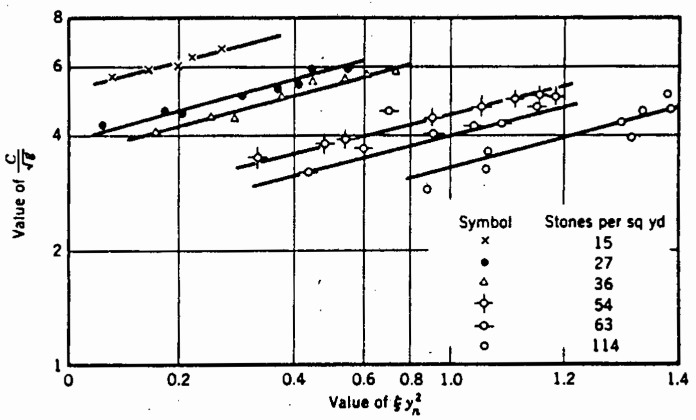

Figure 2.25 : Resistance function versus roughness density

The variation of $\frac{C}{\sqrt{g}}$ with the relative roughness based on the parameter $\frac{R}{\chi}$ can be seen in Figure 2.26 .

$$\frac{C}{\sqrt{g}} = 5{,}28 \log\frac{R}{\chi} + 1{,}72 \qquad (2.21)$$

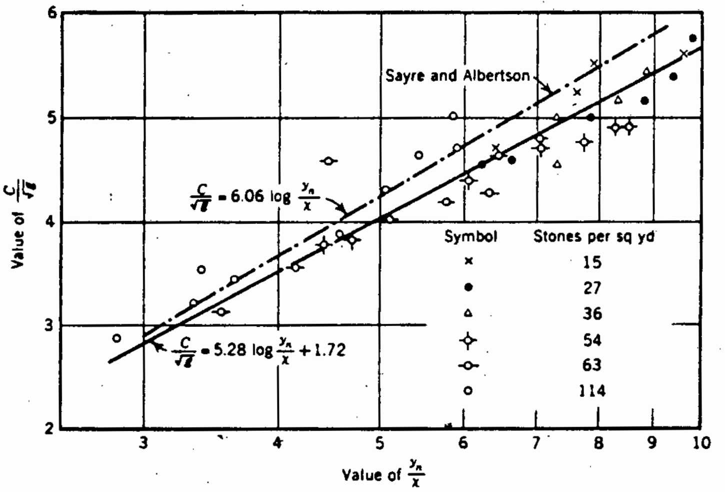

Figure 2.26 : Resistance function versus Relative Roughness $\left[\frac{R}{\chi}\right]$

2.10.4 Conclusions

The Chezy coefficient and relative roughness are related by a logarithmic law. The relationship between the Chezy coefficient and roughness density is a power law. The following equation predicts the Chezy coefficient with a reasonable degree of accuracy :

$$\frac{C}{\sqrt{g}} = 5,28 \log \frac{R}{\chi} + 1,72$$

2.11		
	Author :	M. Bayazit [12]
	Title :	Free Surface flow in a channel of Large relative Roughness
	Date :	July 1975
	Place :	Technical University, Istanbul, Turkey.

2.11.1 Experimental equipment

Experiments were conducted in a tilting flume 9 m long with a 250 mm by 250 mm cross-section. Water depth was adjusted by means of a tailgate. Bottom of the flume was covered by hemispheres of 23 mm diameter, arranged in the most compact configuration. Velocity was measured using a DISA 55D00 anemometer and a conical hot-film probe DISA 55A87.

2.11.2 Theoretical analysis

The velocity distribution for open channel flow in the turbulent zone near a boundary is

$$\frac{V}{V_*} = \frac{1}{0,40} \operatorname{Ln} \frac{y}{k_s} + 8,5 \quad .$$

To determine the theoretical bottom, where V = 0 , various research has found it to be in a range of y_o = (0,15 to 0,27)D, (where D is the diameter of a hemisphere).

Integration of the velocity distribution across the depth leads to the Darcy friction factor.

$$\frac{1}{\sqrt{f}} = \frac{0,35}{0,40} \operatorname{Ln} \frac{R}{k_s} + \frac{1}{\sqrt{8}} \left[8,5 - \frac{1}{0,40}\right]$$

$$\frac{1}{\sqrt{f}} = 0,88 \operatorname{Ln} \frac{R}{k_s} + 2,13 \quad . \qquad (2.22)$$

2.11.3 Results

The theoretical bottom was located at a distance of 0,35D below the tops of the hemispheres. The equation for the Darcy friction factor was found to be :

$$\frac{1}{\sqrt{f}} = 0{,}85 \text{ Ln } \frac{R}{k} + 0{,}74 \quad \text{(see Figure 2.27).}$$

The von Kármán constant was found to be equal to 0,41 and $k_s \simeq 5k$.

Experimental points tend away from the logarithmic equation at small values of $R/_k$. This can be seen more clearly on Figure 2.27, it can be concluded that the logarithmic law breaks down for $R/_k < 3$.

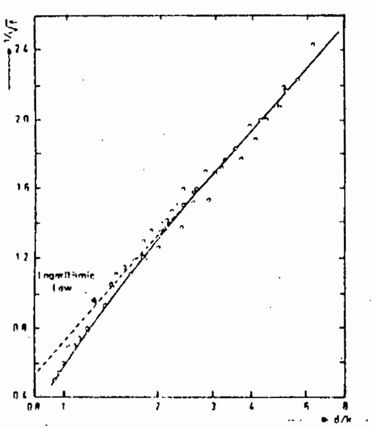

Figure 2.27 : $1/\sqrt{f}$ versus $R/_k$

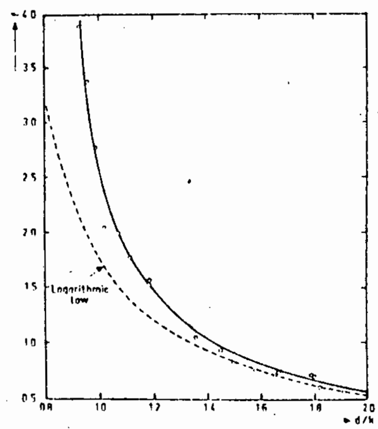

Figure 2.28 : f versus $R/_k$

The velocity profiles do not group around a single curve, but follow different lines for different values of relative roughness. (See Figure 2.29). Velocity distributions at depths ($R/_k > 3$) do obey the velocity distribution equation.

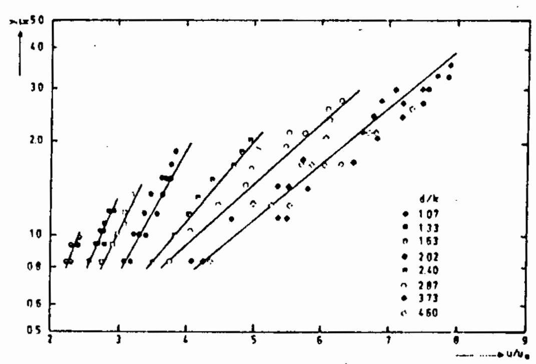

Figure 2.29 : Velocity Profiles at different values of Relative Roughness

2.11.4 Conclusions

There are significant differences in flow structure when relative roughness assumes large values. The theoretical bottom is 0,35D below the tops of the hemispheres and the equivalent roughness size is five times the absolute roughness. Friction factor increases substantially when the relative roughness $R/_k < 3$.

2.12		
Author :	J.C. BATHURST [13]	
Title :	Flow Resistance of Large-scale Roughness	
Date :	December 1978	
Place :	University of East Anglia, Norwich, England.	

2.12.1 Experimental work

Data was gathered during test releases from the Low Green Reservoir on the upper Tees river (Northern England). The releases took the form of a stepped hydrograph with discharges of 3,2 m^3s^{-1} and 6,0 m^3s^{-1} . The normal flow rate of the river is 0,5 m^3s^{-1} .

Data was obtained from three sites. Each section was relatively straight, free of pools, of uniform slope, and a bed composed of boulders with no bedrock or vegetation. The cross-sections are shown in Figure 2.30 .

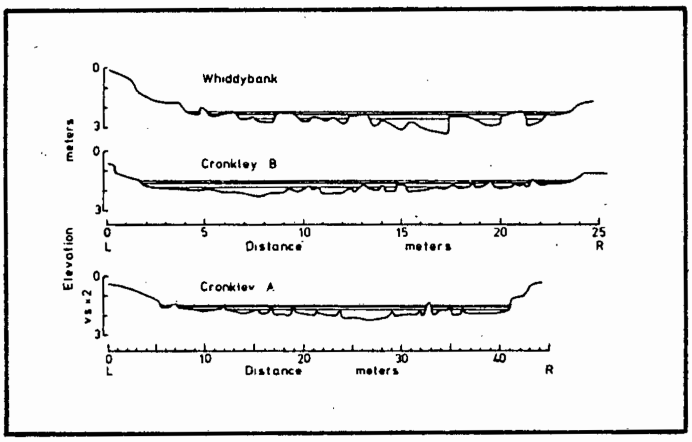

Figure 2.30 : Cross sections of River Tees at test sites

The channel cross-section and water surface slope was obtained by surveying a section of the river. The roughness measurement used was D_{84} which is the size of the median axis in a sample of sediment that is bigger than or equal to 84% of median axes of the sample.

2.12.2 Theoretical analysis

The flow resistance of large-scale roughness cannot be described using the boundary layer theory. The velocity profile is completely disrupted as each roughness element acts individually, producing a total resistance based mainly on the sum of their profile drags.

The profile drag of D_F of an object is :

$$D_F = \frac{1}{2} \rho A_F \bar{V}^2 C_D \quad .$$

The resistive stress on the flow is :

$$\tau_o = \frac{\sum_1^n D_F}{A_{bed}} = \frac{1}{2} \rho C_D \bar{V}^2 \frac{\sum_1^n A_F}{A_{bed}}$$

let $$\lambda_1 = \frac{\sum_1^n A_F}{A_{bed}} \quad \text{(frontal concentration)}$$

and $$\lambda_2 = \frac{\sum_1^n A_B}{A_{bed}} \quad \text{(basal concentration)}$$

$$\therefore \quad \left[\frac{8}{f}\right]^{\frac{1}{2}} = \left[\frac{1}{\frac{1}{2} C_D \lambda_1 \left[\bar{V}/V\right]^2}\right]^{\frac{1}{2}} \quad ,$$

where V is the approach velocity.

2.12.3 Results

The relationship between relative roughness and roughness concentration is found by plotting λ versus $^R/D_{84}$. (See Figure 2.31).

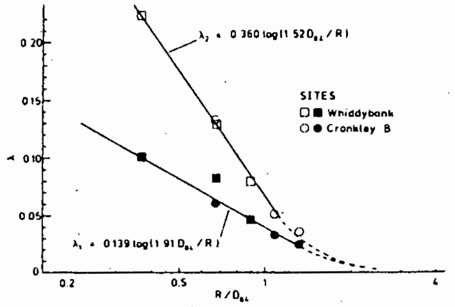

$$\lambda_1 = 0{,}139 \log \left[\frac{1{,}91\ D_{84}}{R} \right]$$

$$\lambda_2 = 0{,}360 \log \left[\frac{1{,}52\ D_{84}}{R} \right] .$$

Figure 2.31 : λ versus R/D_{84}

The theory developed suggests the resistance coefficients depends on the relative roughness, roughness shape, size distribution, spacing and channel geometry.

As the roughness shape and size distribution were approximately constant and there is a relationship between roughness spacing and relative roughness, it is possible to relate the roughness coefficient to channel geometry and relative roughness.

To find the friction coefficient, relative roughness is plotted versus the ratio of $\bar{V}/(gRS)^{1/2}$ to the parameter of channel geometry. (See Figures 2.32 and 2.33). Logarithmic scales are used as a power law is expected.

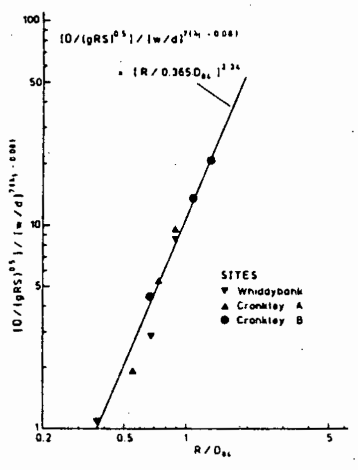

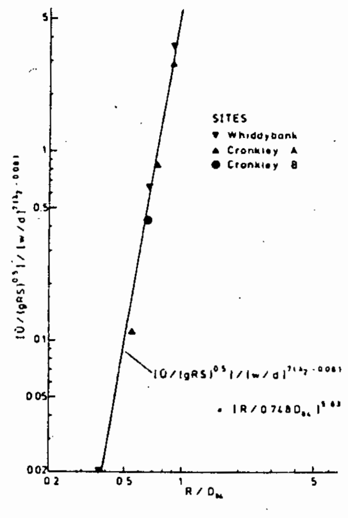

Figures 2.32 : Figure 2.33 :
Ratio of f and channel geometry versus relative roughness

The respective resistance equations are :

$$\left[\frac{8}{f}\right]^{\frac{1}{2}} = \frac{\bar{V}}{(gRS)^{\frac{1}{2}}} = \left[\frac{R}{0,365\ D_{84}}\right]^{2,34} \left[\frac{w}{d}\right]^{7(\lambda_1 - 0,08)} \qquad (2.23)$$

and

$$\left[\frac{8}{f}\right]^{\frac{1}{2}} = \left[\frac{R}{0,748\ D_{84}}\right]^{5,83} \left[\frac{w}{d}\right]^{7(\lambda_2 - 0,08)} \qquad (2.24)$$

2.12.4 Conclusions

The resistance to flow in conditions of large scale roughness depends mainly on the roughness geometry. The resistance equation is limited to the conditions from which it has been derived and further research is required to make it applicable to all conditions for use in general engineering practice.

2.13			
	Author	:	S.M. Thompson and P.L. Campbell [14]
	Title	:	Hydraulics of a large channel paved with boulders
	Date	:	1979
	Place	:	Ministry of Works, Wellington, New Zealand

2.13.1 Experimental works

Tekapo B hydro-electric power station discharges into Lake Pukaki, which was 16 m below the minimum allowable tail water. As the level of the lake was going to rise a temporary channel was only required. The channel was approximately 41 m wide by 308 m long, had flow rates of up to 140 m^3s^{-1} , and a slope of 0,052 . The channel was paved with large natural boulders (see Figure 2.34).

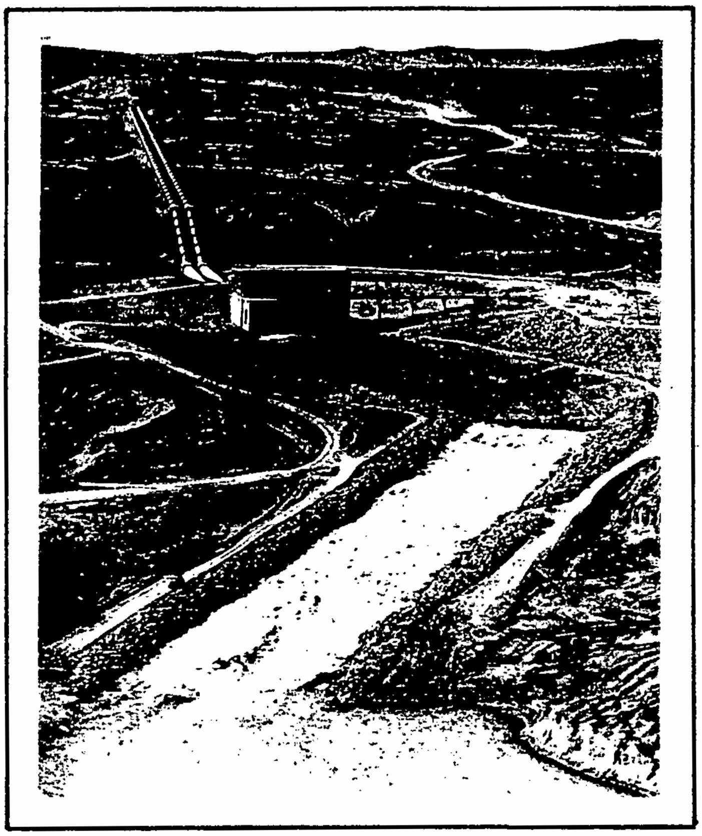

Figure 2.34 : Tekapo B power station discharging 100 m^3/s

2.13.2 Theoretical analysis

Nikuradse equation for resistance of artificially roughened pipes adapted for open channels is :

$$f = \left[2 \log \left[\frac{12\ R}{k_s}\right]\right]^{-2} \quad . \qquad (2.25)$$

O'Loughlin and MacDonald found that the friction factor was much greater than the one predicted from the equation above for shallow flows. They extended Nikuradse equation to :

$$f = \left[\left[1 - 0{,}1 \frac{k_s}{R}\right]\left[2\log \frac{12\ R}{k_s}\right]\right]^{-2} \qquad (2.26)$$

2.13.3 Results

From the data, it was found that k_s = 4,5D (see Table 2.4).

	Q m³/s	R m	W m	S ×1000	D m	f	k_s/R	k_s/D	r m
JUDD & PETERSON (4):									
Blacksmith Fk. R. (11) Utah	3.5	.35	10.9	8.3	.16	.30	1.12	2.5	.08
High Ck. (23) Utah	2.7	.46	4.7	29.4	.22	.66	2.01	4.2	.01
Logan R (30) Utah	25.1	1.28	6.5	41.4	.47	.46	1.58	4.3	.02
Logan R (32) Utah	17.6	.68	14.3	10.1	.17	.16	.59	2.4	.12
Logan R (35) Utah	9.5	.66	11.6	21.1	.34	.71	2.10	4.1	.02
Ashley Ck (61) Utah	36.8	1.27	12.2	17.6	.19	.31	1.17	4.4	.01
Boulder Ck (71) Colorado	6.7	.53	9.5	17.1	.17	.42	1.46	4.6	−.01
Red R (81) N. Mexico	4.0	.38	6.5	13.8	.11	.15	.56	1.9	.10
Red R (82) N. Mexico	4.0	.40	5.3	22.0	.12	.19	.73	2.5	.07
BARNES (1):									
M Fk. Flathead R (.041) Montana	410.6	2.62	55.4	3.7	.14	.096	.26	5.0	.01
Grande Ronde R (0.43) Oregon	130.8	1.62	34.7	5.3	.09	.123	.41	7.4	−.12
Clear Ck (.050) Colorado	39.1	1.06	15.2	13.6	.23	.192	.73	3.4	.08
S. Fk. Clearwater R (.051) Idaho	356.8	2.59	46.2	6.5	.25	.148	.54	5.5	−.11
Rock Ck canal (.060) Montana	3.9	.39	7.6	21.9	.21	.386	1.39	2.6	.08
Merced R (.065) California	55.2	1.27	21.6	12.4	.25	.306	1.14	5.8	−.09
Boundary Ck (.073) Idaho	71.6	1.23	25.5	21.1	.21	.390	1.40	8.2	−.21
Rock Ck (.075) Montana	42.5	1.05	15.0	38.4	.22	.434	1.51	7.2	−.15
Report (8):									
Valetta irrigation canal New Zealand (1)	3.4	.40	5.2	8.1	.07	.095	.26	1.5	.10
(2)	3.4	.44	6.4	9.6	.07	.23	.88	5.5	−.02
(3)	2.8	.25	9.1	9.4	.04	.12	.39	2.5	.03
(4)	2.8	.45	4.9	3.9	.03	.085	.21	3.2	.03
This paper:									
Tekapo B tailwater channel New Zealand	60.0	.79				.94	2.5	4.9	−.03
	82.0	.88				.69	2.1	4.6	−.01
	111.0	1.00	41.0	52.0	.40	.56	1.8	4.5	.00
	125.0	1.04				.49	1.7	4.3	.02
	140.0	1.09				.45	1.6	4.2	.02

Table 2.4 : Field data on flow resistance

By plotting f versus $^{k}s/_{D}$ the results obtained from the field test were compared with data from experiments conducted by O'Loughlin and MacDonald in a flume 93 times smaller than the Tekapo B tailwater channel. (See Figure 2.35).

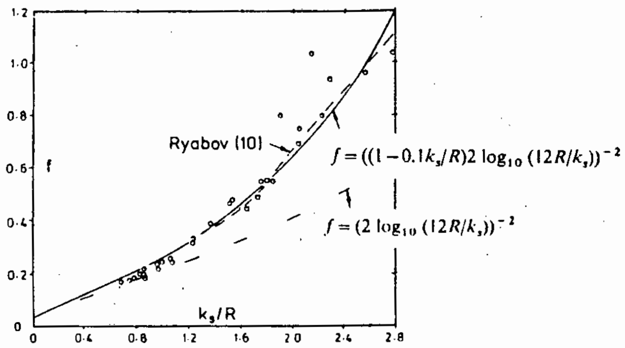

Figure 2.35 : Friction factor versus relative roughness

2.13.4 Conclusions

Laboratory results can be applied to a large channel

$$\text{using} \quad f = \left[\left[1 - 0{,}1\,\frac{k_s}{R}\right] 2\log\left[\frac{12\ R}{k_s}\right]\right]^{-2} \qquad (k_s = 4{,}5D)$$

This predicts the friction factor with reasonable accuracy for shallow flows over large roughness.

2.14

Author :	D.I. Bray [15]
Title :	Estimating average velocity in Gravel-bed rivers
Date :	September 1979
Place :	University of New Brunswick, Frederiction, N.B. Canada

2.14.1 Experimental work

The data was obtained from the study of 67 gravel-bed river reaches in Alberta, Canada. The following features were looked for in each river reach :

(a) relatively high in-bank flows ;

(b) no bed material transport ;

(c) no significant vegetation in the bed ;

(d) no dominant bed features.

2.14.2 Theoretical analysis

Equations used for calculating average velocity were the Manning equation

$$\bar{V} = \frac{1}{n} R^{2/3} S^{1/2} \quad ,$$

where n can be obtained from tables or experience. n can also be calculated from the Cowan method $n = (n_o + n_2)m_c$, the Strickler method $n = a\,D_x^{1/6}$ or the Limerinos method

$$n = \frac{0{,}133\ R^{1/6}}{1{,}16 + 2{,}00 \log\left[\frac{R}{D_{84}}\right]} \qquad (2.27)$$

There are also other ways of calculating the mean velocity, not using Manning's n , for example

the Keulegan equation :-

$$\bar{V} = V_* \left[6{,}25 + 5{,}75 \log\left[\frac{R}{k_s}\right]\right] \qquad (2.28)$$

and the Lacey equation (for this study) :-

$$\bar{V} = 10,8\ R^{2/3}\ S^{1/2} \qquad (2.29)$$

2.14.3 Results

Basic data from each gravel-bed river reach was applied to a specified equation to compute the average velocity. Then for each reach the percent deviation (PDEV) of the computed average velocity from the observed average velocity was calculated from

$$P\,D\,E\,V = \left[\frac{V_c - V_o}{V_o}\right] \times 100$$

V_c = average velocity computed by specified equation

V_o = the observed average velocity

(See Figure 2.36 and Table 2.5).

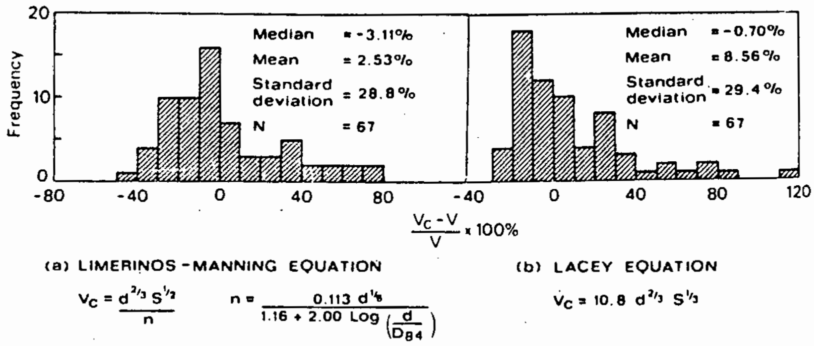

Figure 2.36 : Histogram of percent deviation

Equation (1)	Equation number (2)	Statistics for Distribution of Percent Deviations* Mean (3)	Standard deviation (4)	Minimum value (5)	Median value (6)	Maximum value (7)
Manning's Equation						
n by modified Cowan	2	−3.3	29.6	−50.0	−7.0	−83.2
n by Strickler						
$n = 0.041\ D_{50}^{1/6}$	4	44.9	43.7	−18.6	31.8	181.9
$n = 0.038\ D_{90}^{1/6}$	5	37.5	40.9	−23.1	25.0	159.6
n by Limerinos	6	2.5	28.8	−41.8	−3.1	74.4
Keulegan's Equation						
$k_s = D_{50}$	7	54.2	46.1	−12.7	40.4	195.3
$k_s = D_{65}$	7	47.0	42.7	−17.3	35.2	169.2
$k_s = D_{90}$	7	32.9	38.3	−23.9	23.0	136.4
Lacey's Equation	9	8.6	29.4	−26.6	−0.7	116.1

*Percent deviation = $(V_c - V_o)/V_o \times 100$, in which V_c is the computed average velocity and V_o is the "observed" average velocity.

Note: See text for description of the equations used.

Table 2.5 : Summary of results

2.14.4 Conclusions

The Limerinos equation is the most acceptable expression for determining Mannings n. The Lacey equation, which does not require an explicit determination of bed material size, provides an acceptable way of calculating the average velocity.

2.15			
	Author	:	R. Pyle and P. Novak [16]
	Title	:	Coefficient of friction in conduits with large roughness
	Date	:	1981
	Place	:	Newcastle-Upon-Tyne Laboratory, U.K., and Technical University of Munich, Germany.

2.15.1 Experimental equipment

Experiments were carried out in three different conduits each with a different type of roughness.

(a) single size spheres (16,5 mm diameter) attached to the bed of a 12 m long and 0,3 m wide glass-sided tilting flume ;

(b) single size hemispheres (33 mm diameter) were attached to the top and bottom surfaces of a 5 m long and 0,3 m wide rectangular air tunnel ;

(c) natural river stones of sizes up to 150 mm were used to roughen the bed of a 150 m long by 1 m wide concrete flume.

See Figure 2.37 for different concentrations of spheres used.

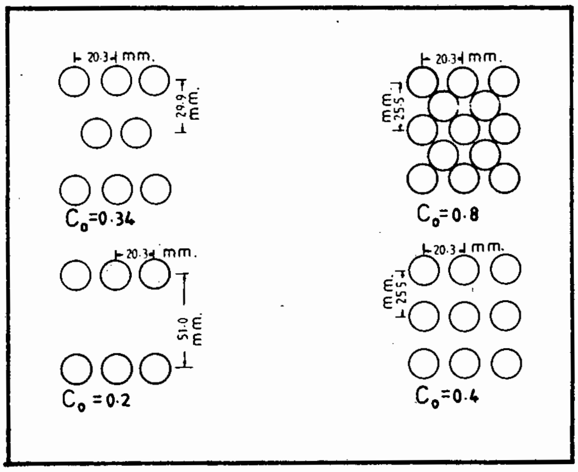

Figure 2.37 : Roughness patterns tested

2.15.2 Theoretical analysis

The friction coefficient in rough turbulent flow is :

$$\frac{1}{\sqrt{f}} = B \log \frac{R}{k} + A$$

where $B = \dfrac{2{,}303}{\kappa \sqrt{8}}$ and A is a constant.

$$\frac{\bar{V}}{V_*} = B' \log \frac{R}{k} + A' \quad ,$$

where $B' = \dfrac{2.303}{\kappa}$ and $A' = \sqrt{8}\, A$

$$\frac{V}{V_*} = B' \log \frac{R}{k} + A'' \quad ,$$

where $A'' = A' + B'$.

If viscous stress is negligible the shear stress caused by a regular pattern of roughness elements can be written as :

$$\tau_o = N_* D_F$$

D_F is the drag on an individual roughness element and N_* is the number of elements per unit area

$$D_F = C_d \rho \frac{\bar{V}^2}{2} A_f$$

$\bar{V}$ is average velocity over area A_f .

For a variable velocity flow field

$$D_F = C_d \int_{A_f} \frac{\rho V^2}{2} \, dA \quad .$$

2.15.3 Results

The full set of experimental lines derived may be seen in Figure 2.38

From Figure 2.38 it can be seen that the slopes of the experimental lines are not constant, but increase with increasing concentration (after a certain limit is reached).

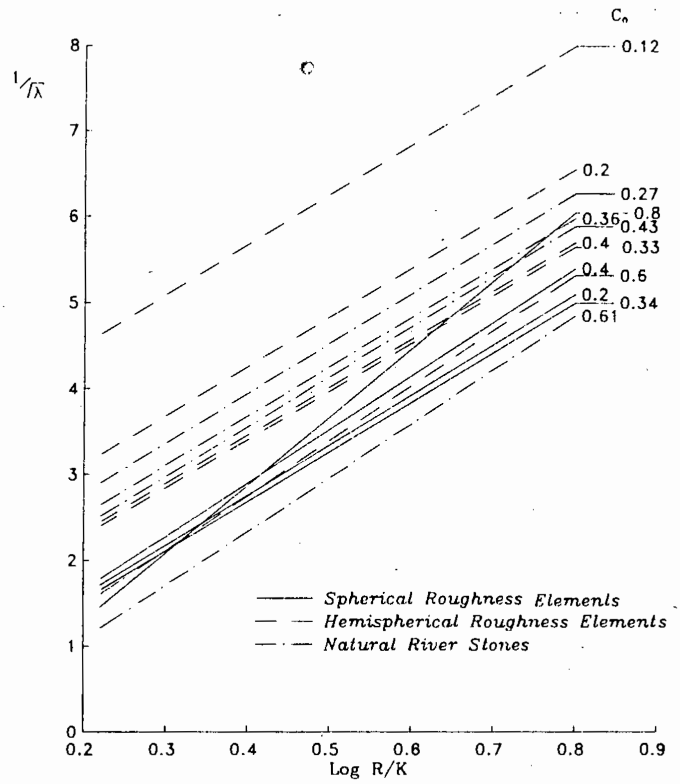

Figure 2.38 : $^1/\sqrt{f}$ versus log $^R/k$ (before datum correction)

The "turbulence constant" associated with each concentration had a constant value of 0,2857 for concentrations up to about 35% , but thereafter, the value decreased to a minimum value of 0,21 (see Figure 2.39).

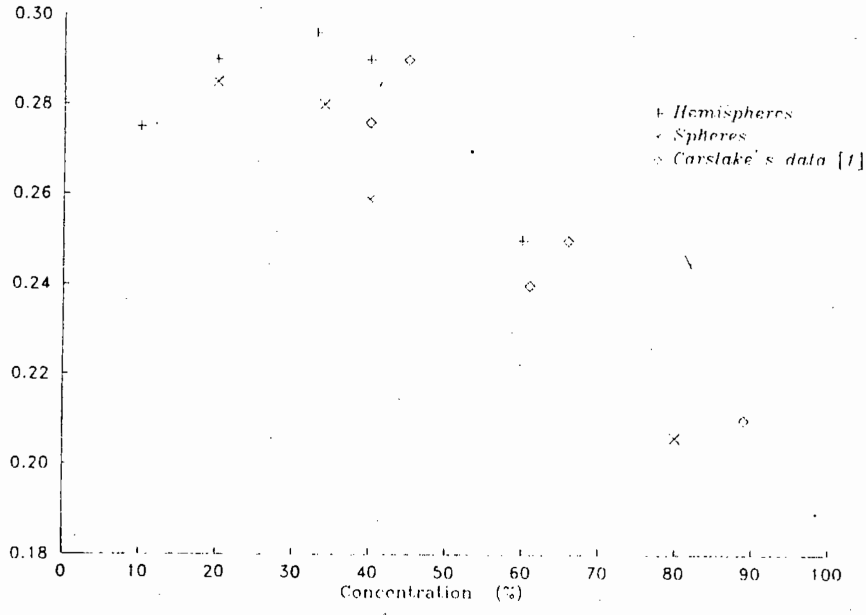

Figure 2.39 : Constant of turbulence versus concentration

If in fact the value of κ were to remain constant, then some parameter in the experiments must have been measured erroneously. Since Nikuradse most researchers have adopted some form of reference datum, the most popular being the geometric mean (ie. the level that would be achieved if the roughness elements were melted to form a new smooth surface). κ was given a constant value of 0,285. The reference datum is then changed for all concentrations greater than 35% so that the slopes of the $1/\sqrt{f}$ versus log R/k lines are constant. (See Figure 2.40).

The adjustment of the datum required to give a κ value of 0,285 gives an indication of the effective element height for any concentration. (See Figure 2.41).

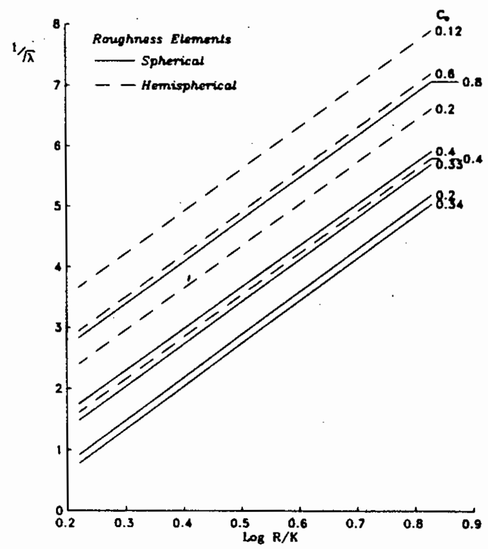

Figure 2.40 : $1/\sqrt{f}$ versus log R/k (after datum correction)

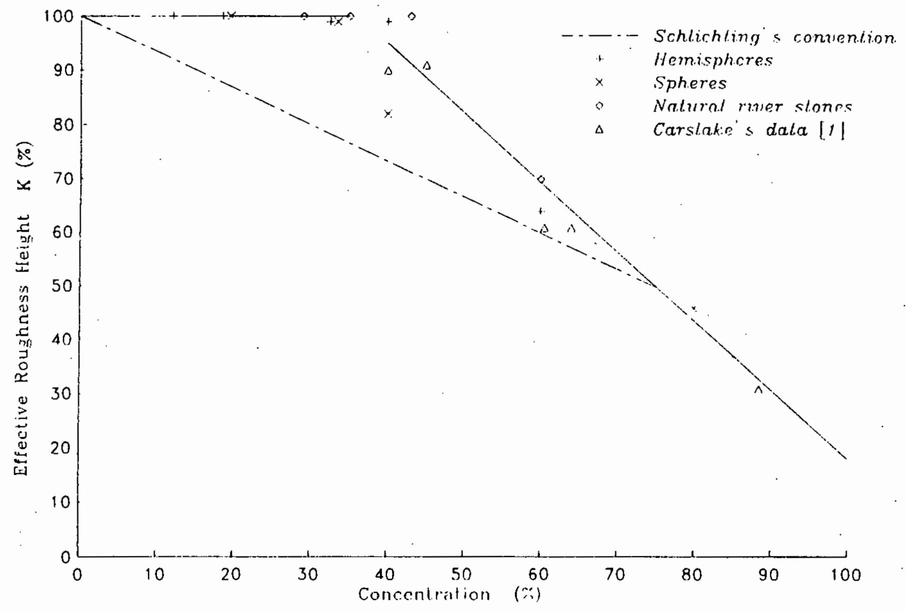

Figure 2.41 : Effective roughness height versus concentration

The friction factor can be calculated from the following equation

$$\frac{1}{\sqrt{f}} = B \log \frac{R}{k} + A \quad , \tag{2.30}$$

where B = 2,86 , k is determined from Figure 2.41, A is determined from Figure 2.40 and R is equal to the hydraulic radius for concentrations of up to 35% thereafter it is reduced by the same value as k is.

2.15.4 Conclusions

The "constant of turbulence" has a value of 0,285 for concentrations up to 35%. Using this value for higher concentrations but adjusting the reference datum gave very consistent results in the plots of $1/\sqrt{f}$ versus log R/k .

2.16		
	Author :	J.C. Bathurst, R. Li and D.B. Simons [17]
	Title :	Resistance equation for Large-scale roughness
	Date :	December 1981
	Place :	Colorado State University, Colorado, U.S.A. and Wallingford, Oxford, U.K.

2.16.1 Experimental equipment

The flume used was 9,54 m long by 1,168 m wide. Five sizes of bed materials were used 0,5 ; 0,75 ; 1,5 ; 2,0 and 2,5 inches. The first three were commercially available gravels, consisting of chips derived by crushing larger cobbles. The 2,0 and 2,5 inch materials were cobbles. Each roughness bed was constructed by smearing masonite boards with fibre glass resin and covering them with the respective material so that no obvious patches of smooth board were visible.

2.16.2 Theoretical analysis

Flow resistance of large scale roughness is related mainly to form drag of the elements. Since the associated resistance processes are different from those for small-scale roughness, it appears a power law is more suitable than a semilogarithmic law for large scale roughness.

In a theoretical based equation for large scale roughness it is necessary to account separately for the processes of fluid mechanics related to Reynolds number and Froude number. The roughness geometry and the channel geometry should also be considered separately.

Channel geometry (Figure 2.42)

Figure 2.42 : Definition diagram for relative roughness area.

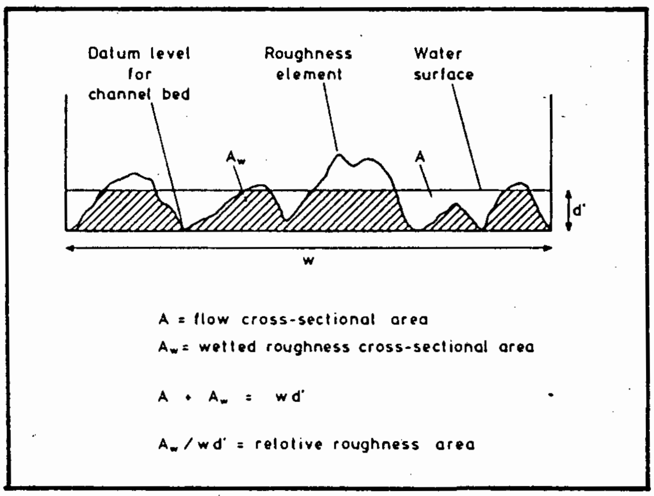

Resistance equation

$$\left[\frac{8}{f}\right]^{\frac{1}{2}} = f_n\,(R_e)\; f_n\,(F_r)\; f_n\left(\frac{\sum_1^n A_F}{A_{bed}}\right) f_n\left(\frac{A_w}{wd'}\right) \; .$$

2.16.3 Results

Drag coefficient is independent of Reynolds number at high values of Reynolds number.

$$b = \left[1{,}175\left[\frac{Y_{50}}{w}\right]^{0{,}557}\left[\frac{d}{S_{50}}\right]\right]^{0{,}648\sigma^{-0{,}134}}$$

b is the relationship between the effective roughness concentration and relative submergence.

$$Y_{50} = \frac{L_{50} + D_{50}}{2} \quad ;$$

L_{50} = long axis

D_{50} = median axis

S_{50} = short axis.

$$\sigma = \log\left[\frac{D_{84}}{D_{50}}\right] \; .$$

The resistance equation is

$$\left[\frac{8}{f}\right]^{\frac{1}{2}} = \left[\frac{0{,}28}{b}F_r\right]^{\log(0{,}755/b)} \left[13{,}434\left[\frac{w}{Y_{50}}\right]^{0{,}492} b^{1{,}205(w/Y_{50})^{0{,}118}}\right] \times \left[\frac{A_\omega}{wd'}\right] \qquad (2.31)$$

Comparing the friction factor given by the resistance equation, and the actual friction factor measured, that is

$$\left[\frac{8}{f}\right]^{\frac{1}{2}} \quad \text{versus} \quad \frac{\bar{V}}{(gRS)^{\frac{1}{2}}}$$

it can be seen there is a good correlation (Figure 2.43).

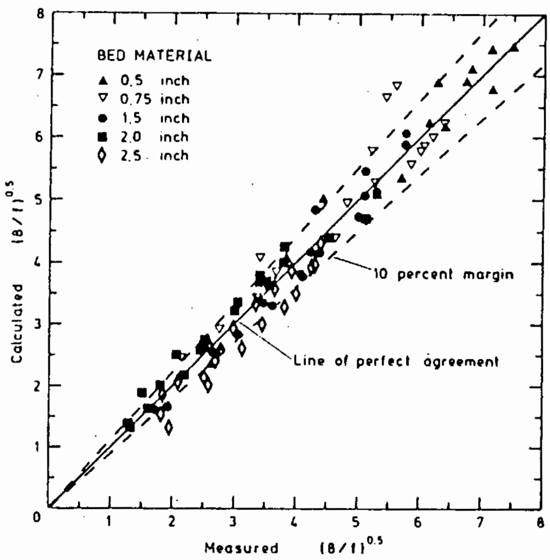

Figure 2.43 : Comparison between observed and calculated f

2.16.4 <u>Conclusions</u>

Flow resistance of large scale roughness depends on the form drag of the elements and their disposition in the channel. Semi-empirical analysis using extensive flume data supports the theory and has allowed the development of a basic resistance equation.

2.17

Author :	J.P. Pansegrouw [18]
Title :	Discrepancy of the Colebrook-White equation in the extreme rough turbulent zone
Date :	November 1984
Place :	Department of Water Affairs, South Africa

2.17.1 Experimental work

Manning's "n" values of 0,072 and 0,106 have been found to exist on the Crocodile River near Brits.

2.17.2 Theoretical analysis

By substituting the Colebrook-White equation for the turbulent zone

$$\frac{1}{\sqrt{f}} = 2 \log \left[\frac{k}{12R} \right]$$

into the Darcy-Weisbach equation

$$V = \sqrt{\frac{8g}{f}} \sqrt{RS} .$$

and then combining it with the Manning equation, the value of k can be described in terms of n and R, as

$$k = \frac{12 R}{\text{antilog} \left[\dfrac{R^{1/6}}{18n} \right]} \tag{2.32}$$

2.17.3 Results

It was found that for high n values ($n > 0,05$), k values became unrealistically large when compared to the hydraulic radius or depth of flow. (See Table 2.6).

	Manning's n obtained by experiment (flow measurement) $s/m^{1/3}$	Flow depth m	Hydraulic radius R m	Absolute roughness derived from Colebrook-White's equation $k = \frac{12R}{\text{antilog}\,(R^{1/6}/18n)}$ m	Remarks
Crocodile river	0.072	2.5	2.3	3,58	Unrealistic high k value ($k >> 2.5$ m. the depth of flow)
Crocodile river tributary	0.106	1,9	1,1	3,87	Unrealistic high k value ($k >> 1.9$ m. the depth of flow)

Table 2.6 : Roughness heights corresponding to measured Manning coefficients

2.17.4 Conclusions

The Colebrook-White equation must not be used in the extreme rough turbulent zone (where $n > 0,05$). Manning's equation may be used with confidence in the extreme rough turbulent zone.

2.18	Author :	A.B. Shahalam and A.R. Mansour [19]
	Title :	New method for the prediction of resistance coefficients for natural streams
	Date :	September 1988
	Place :	Jordan University, Irbid, Jordan.

2.18.1 Experimental work

Measurements were taken at eight sites along the Wadi Elwala. The Wadi Elwala has a length of 35 km extending between the Jordanian Desert and the Dead Sea. A summary of the results are shown on Table 2.7 .

No. of site	R:m	S	V:m/sec	n	$n/R^{1/6}$	$\sqrt{f}$	R/D_{50}
1	0·147	0·0022	0·56	0·023	0·031	0·330	2·3
2	0·107	0·002	0·481	0·021	0·030	0·320	3·0
3	0·107	0·002	0·455	0·022	0·030	0·320	4·1
4	0·105	0·004	0·59	0·024	0·034	0·370	3·1
5	0·175	0·0004	0·13	0·048	0·063	0·680	1·8
6	0·131	0·0035	0·50	0·031	0·043	0·460	2·2
7	0·192	0·0015	0·56	0·068	0·088	0·950	1·2
8	0·234	0·0400	1·38	0·024	0·0303	0·327	2·8

Table 2.7 : Field Data

2.18.2 Theoretical analysis

The relationship which relates flow resistance to roughness size of bed material has got the general form :

$$\frac{1}{\sqrt{f}} = a + b\log\left[\frac{R}{D_X}\right]$$

(summarized in Table 2.8)

2.19.3 Results

Plotting the friction factor $^{1}/\sqrt{f}$ versus relative roughness $^{R}/D_{50}$. and converting D_{84} to D_{50} using the following relationship. D_{84} = 2,5 D_{50} , leads to Figure 2.44.

Equation	Lengths in ft	Lengths in m	Non-dimensional units
Leopold			$\frac{1}{\sqrt{f}} = 1{\cdot}0 + 2{\cdot}0 \log \frac{R}{D_{84}}$
Limerinos	$\frac{n}{R^{1/6}} = \frac{0{\cdot}0926}{a + b \log(R/D)}$	$\frac{n}{R^{1/6}} = \frac{0{\cdot}113}{a + b \log(R/D)}$	$\frac{1}{\sqrt{f}} = 0{\cdot}35 + 2{\cdot}0 \log \frac{R}{D_{50}}$
Simons		$n = 0{\cdot}04 D_{50}^{1/6}$ $n = 0{\cdot}038 D_{90}^{1/6}$	
Bray		$n = 0{\cdot}0593 D_{50}^{0{\cdot}179}$ $n = 0{\cdot}0561 D_{65}^{0{\cdot}176}$ $n = 0{\cdot}0495 D_{90}^{0{\cdot}160}$	$\frac{1}{\sqrt{f}} = 0{\cdot}248 + 2{\cdot}36 \log \frac{R}{D_{50}}$ $\frac{1}{\sqrt{f}} = 0{\cdot}608 + 2{\cdot}28 \log \frac{R}{D_{65}}$ $\frac{1}{\sqrt{f}} = 1{\cdot}26 + 2{\cdot}16 \log \frac{R}{D_{90}}$
Hey			$\frac{1}{\sqrt{f}} = 2{\cdot}03 \log \left(\frac{11{\cdot}75R}{3{\cdot}5D_{84}}\right)$
Griffiths			$\frac{1}{\sqrt{f}} = 0{\cdot}76 + 1{\cdot}98 \log_{10} \frac{R}{D_{50}}$

Table 2.8 : Summary of friction equations

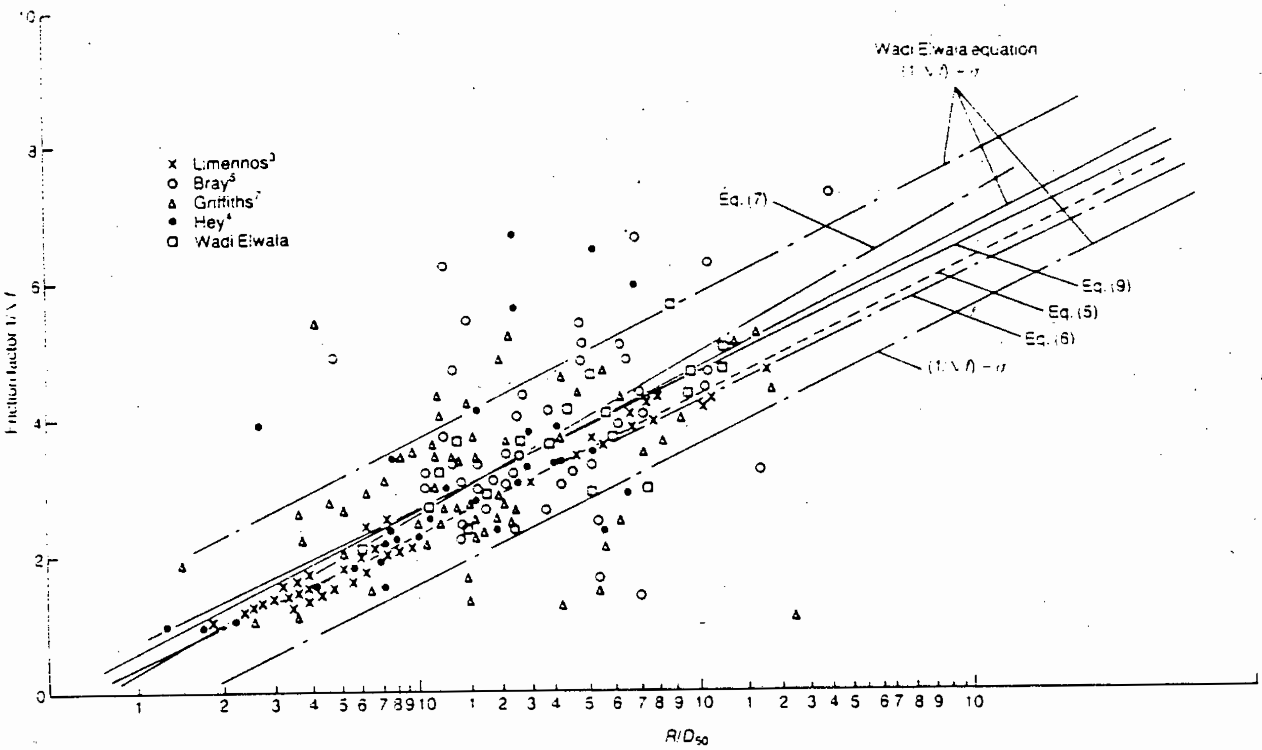

Figure 2.44 : $1/\sqrt{f}$ versus R/D_{50}

Wadi Elwala equation $1/\sqrt{f} = 0{,}55 + 2{,}09 \text{ Log } (R/D_{50})$

The relationship yields a correlation coefficient of 0,87 and a standard deviation of 0,97 .

Checking the equation for the Wadi Elwala data (see Figure 2.45)

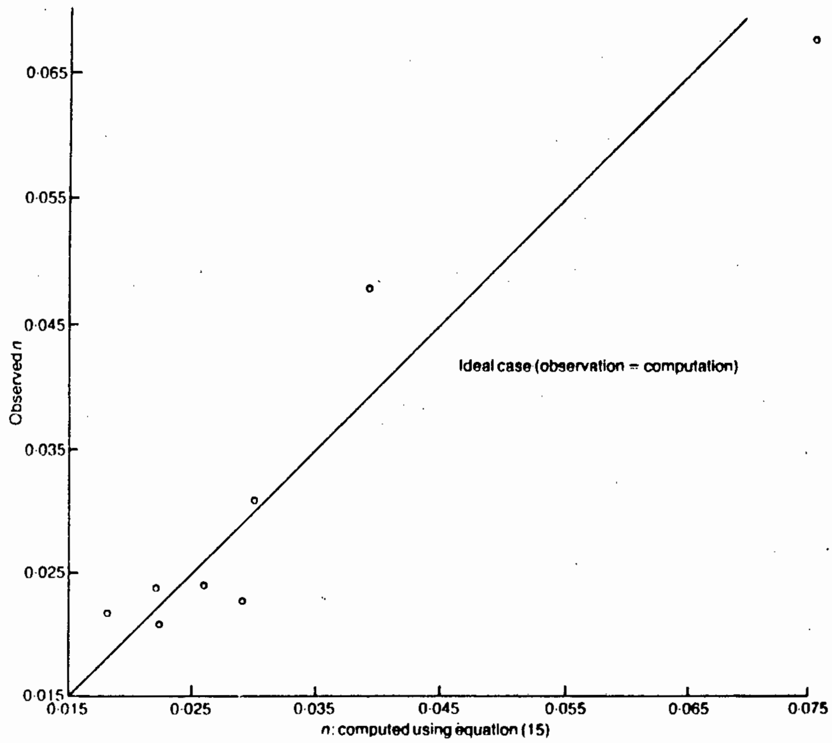

Figure 2.45 : Comparison of observed to calculated n values

The ratio of the velocities measured at depths of 0,2 and 0,8 was given the symbol x

$$x = \frac{V_{0.2}}{V_{0.8}} .$$

The relationship between $n/R^{1/6}$ and x can be determined from Figure 2.46 .

$$\frac{n}{R^{1/6}} = \frac{x - 1}{6,78\ (x + 0,95)} \qquad (2.34)$$

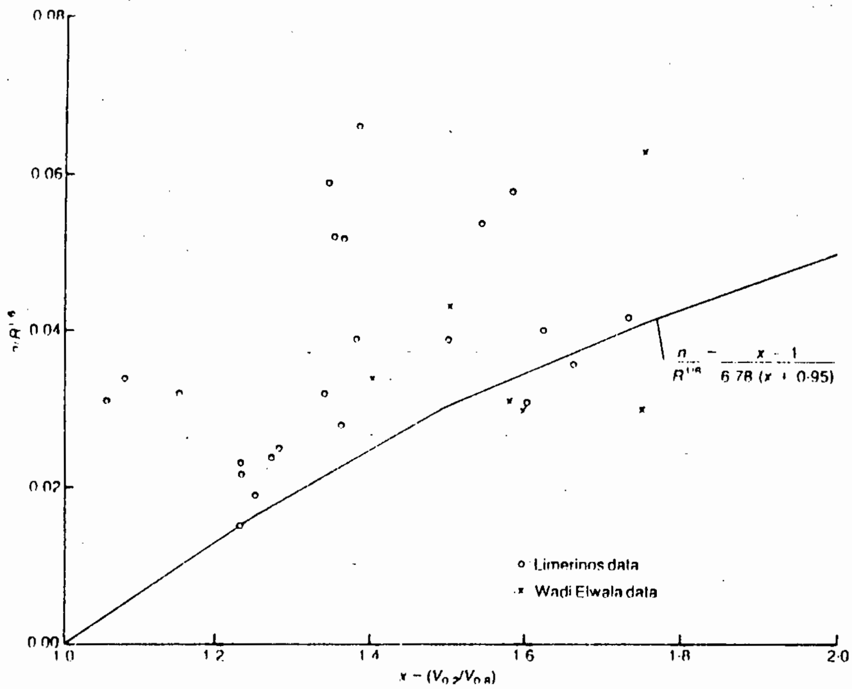

Figure 2.46 : Relationship between the velocity ratio and Manning's n

2.18.4 Conclusions

The basic resistance coefficient for a straight uniform natural stream which does not meander, and without vegetation and obstructions can be successfully estimated from bed-particle sizes. A velocity ratio method can also predict friction factors but must be used with caution.

CHAPTER 3

THEORETICAL ANALYSIS

3.1 Development of Uniform flow formulae

Uniform flow is considered to have the following features :

(i) the depth, water area, velocity and discharge at every section of the channel are constant ;

(ii) the energy line, water surface and channel bottom are all parallel, that is, their slopes are equal.

It is possible to relate the friction factor f to the Reynolds number R_e to yield a standard diagram for open channel flow, using Reynolds number

$$R_e = \frac{\bar{V}R}{\nu} .$$

and Darcy-Weisbach friction factor

$$f = \frac{8gRS}{\bar{V}^2} .$$

The friction factor for a smooth channel is

$$\frac{1}{\sqrt{f}} = 2\log \frac{R_e \sqrt{f}}{0,627} .$$

and the friction factor for a rough channel is

$$\frac{1}{\sqrt{f}} = 2\log \frac{14,8R}{k}$$

and the transition law is

$$\frac{1}{\sqrt{f}} = -2\log\left[\frac{k}{14,8R} + \frac{0,627}{R_e\sqrt{f}}\right] .$$

(All these formulae have been modified from pipe flow to open channel flow using $R = {}^{D}/_{4}$, except in the Reynolds number).

When considering the validity of these logarithmic formulas it is important to remember that their derivation, though logical, is somewhat artificial and lacks a sound analytical base. The presence of a free surface and the influence of channel shape are not accounted for. Because of the additional variables the f versus R_e diagram (Figure 3.1) is not of such utility as is the case in pipe flow, where the diameter or hydraulic radius is constant for a given pipe. In open channel flow as the depth increases so does the relative roughness $R/_k$ therefore the friction factor decreases.

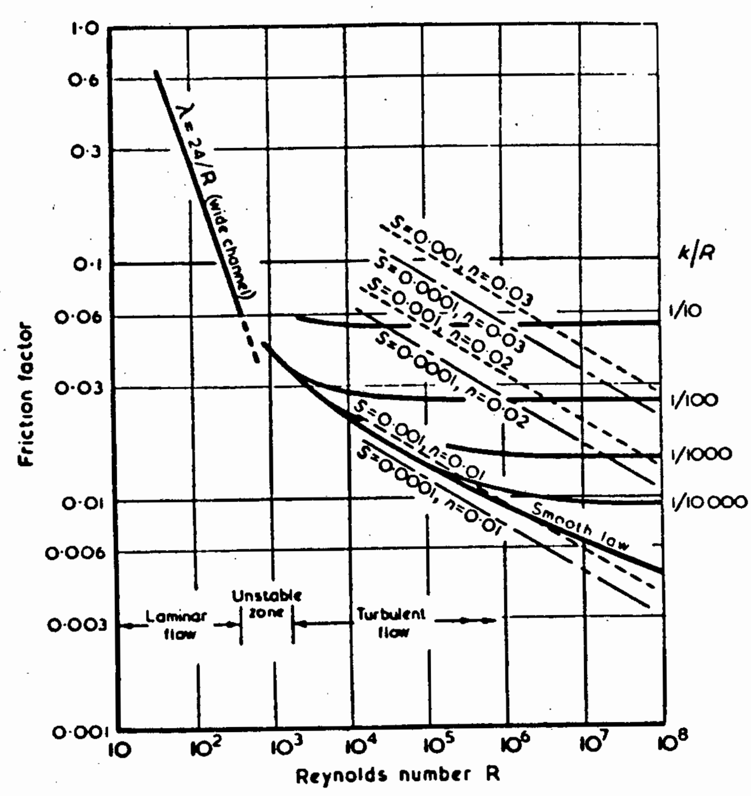

Figure 3.1 : f versus R_e (for open channel flow)

3.1.1 The Chézy formula

One of the first uniform-flow formulae was developed by the French engineer Antoine Chézy which is usually expressed as follows

$$V = C\sqrt{RS} \quad .$$

The Chézy formula can be derived from two assumptions. The first is the force resisting the flow per unit area of channel bed is proportional to the square of the velocity. This force is equal to αV^2 where α is a constant of proportionality. The surface of contact of the flow with the stream bed is equal to the product of the wetted perimeter and the length of the channel reach or PL . The total force resisting flow is then equal to $\alpha \bar{V}^2$ PL. (figure 3.2).

The second assumption is the effective component of the gravity force causing flow must be equal to the total force of resistance. The effective gravity-force component is parallel to the channel bottom and equal to $\omega AL\sin\theta = \omega ALs$ (figure 3.2).

Assuming $\quad \omega ALs = \alpha \bar{V}^2 PL$

$$\therefore \quad \bar{V} = \sqrt{\left[\frac{\omega}{\alpha}\right]\left[\frac{A}{P}\right] S}$$

$$\therefore \quad \bar{V} = C\sqrt{RS}$$

where $C = \sqrt{\frac{\omega}{\alpha}}$

and is known as the Chèzy coefficient. It is treated as a pure number but has the dimensions $L^{\frac{1}{2}}T^{-1}$, or $(\text{acceleration})^{\frac{1}{2}}$

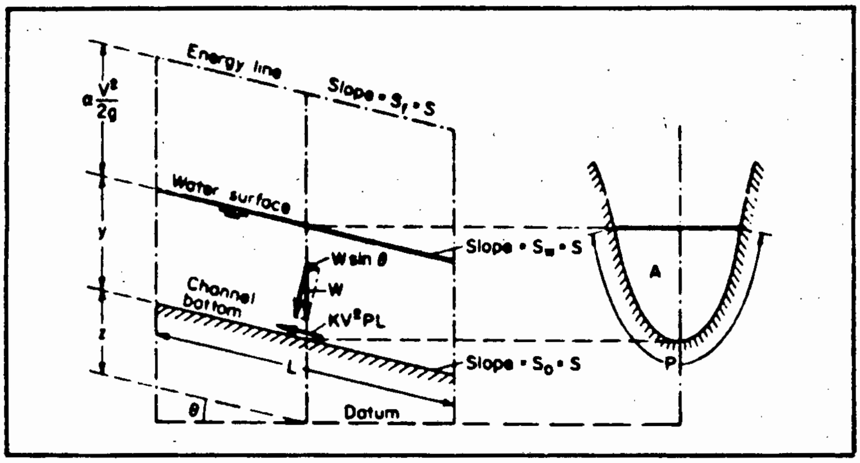

Figure 3.2 : Derivation of the Chézy formula

We can obtain a direct relationship between C and f as

$$\bar{V} = \left[\frac{8g}{f}\right]^{\frac{1}{2}}\left[RS\right]^{\frac{1}{2}} .$$

Therefore $\quad C = \sqrt{\frac{8g}{f}} .$

3.1.2 <u>The Manning formula</u>

Robert Manning, an Irish engineer, presented a formula in 1889, which was later modified to its present well-known form

$$V = \frac{1}{n} R^{2/3} S^{1/2} .$$

From Figure 3.2

$$\tau pL = \omega ALsin\alpha$$

$$\tau = \omega Rs$$

The shear stress may be related to the mean speed $\bar{V}$, by an equation of the form .

$$\tau = \frac{1}{8} f \rho \bar{V}^2 ,$$

(although some authors use the factor of $^1/_2$). The Darcy-Weisbach equation can be obtained from these two relationships.

$$\bar{V}^2 = \frac{8g\ RS}{f} .$$

The main source of information on f is the Moody diagram (Figure 3.1) where f is plotted against the Reynolds number. As channels are generally large conduits and frequently rougher than pipes, the Reynolds numbers are relatively high and it may be assumed that all channels operate in the fully developed rough turbulent zone. In this zone f depends on relative roughness only.

$$f = \phi \left\{ \frac{R}{k} \right\} .$$

If a plot of log f versus log $R/_k$ is drawn, (Figure 3.3) a reasonably straight line may be drawn giving a power law of the form

$$f \propto \left[\frac{k}{R} \right]^{1/3}$$

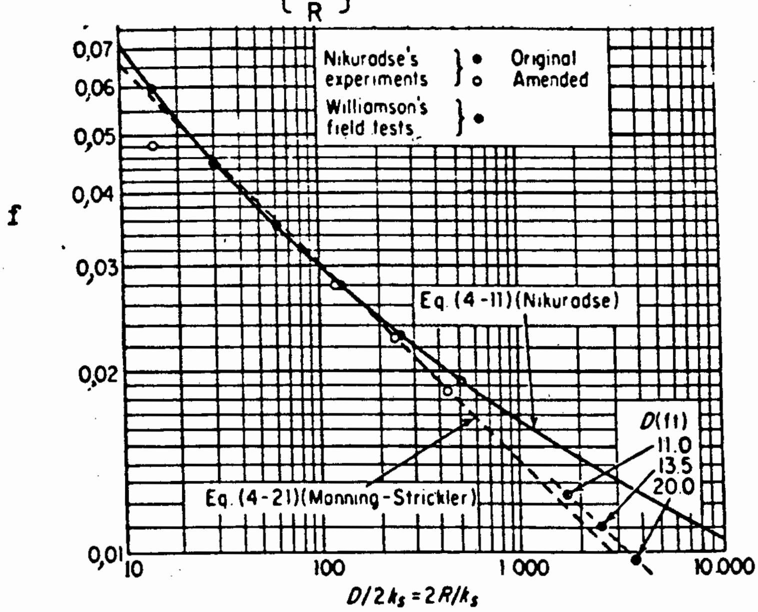

Figure 3.3 : Log f versus Log R/ks

Combining the Darcy-Weisbach equation with $f \propto \left[\frac{k}{R} \right]^{1/3}$

$$\bar{V}^2 \propto 8g \left\{ \frac{R}{k} \right\}^{1/3} RS$$

$$\bar{V} \propto \frac{\sqrt{8g}}{k^{1/6}} R^{2/3} S^{1/2}$$

$\sqrt{g}/k^{1/6}$ is absorbed into a constant n , called Manning's n .

$$V = \frac{1}{n} R^{2/3} S^{1/2}$$

Manning's n is considered as a constrant, independent at depth variation with the dimensions $TL^{-1/3}$. Relating n to the Chézy's coefficient

$$C = \frac{R^{1/6}}{n}$$

3.2 Roughness Description (See Figure 4.1)

For the purpose of this study the following roughness parameters have been considered and defined.

i Roughness size k
The physical height of a roughness element measured from a defined reference datum.

ii Longitudinal spacing L_S
The distance between individual roughness elements in the direction of flow.

iii Transverse spacing T_s

The distance between elements perpendicular to the direction of flow.

iv Concentration C_o

$$C_o = N_* \frac{A_p}{A_B}$$

A_p = plan area of an element
A_B = total bed area
N_* = number of elements in bed area A_B

v Element shape σ

Defining the shape is a very complex problem except where the elements have a standard geometrical shape. In this study only hemispheres have been used.

3.3 Dimensional Analysis

The following variables were chosen in the dimensional analysis of the problem:

$\bar{V}$	the mean velocity	LT^{-1}
R	the hydraulic radius	L
ρ	the mass density of the fluid	$M L^{-3}$
μ	the dynamic viscosity	$M L^{-1} T^{-1}$
k_s	the equivalent roughness size	L

Considering the wall shear stress (τ_o) as dependent on all the factors listed above.

The gravitational constant "g" has not been used in the dimensional analysis as it does not influence the wall shear stress. If g were introduced the Froude number becomes related to the friction factor.

The Froude number was not significant in the experiments done as there were no appreciable surface waves or disturbances, thus the assumption must be valid.

$$\tau_o = \phi \{ \bar{V} , R , \rho , \mu , k_s \} \qquad M L^{-1} T^{-2}$$

by dimensional analysis (Appendix II)

$$f = \phi \left\{ \left[\frac{k_s}{R} \right] , \left[\frac{\rho V R}{\mu} \right] \right\}$$

or

$$f = \phi \{\text{relative roughness, Reynolds Number}\}.$$

For large values of Reynolds Number the laminar sub-layer is destroyed so that the viscous effects are negligible and therefore the Reynolds number can be omitted in the analysis. For the purpose of this thesis the region of interest is the right hand side of Figure 3.1 .

$$f = \phi \left\{ \frac{k_s}{R} \right\}$$

The equivalent roughness size (k_s) is dependent on absolute roughness size (k), the longitudinal spacing (L_s), transverse spacing (T_s), the concentration (C_o) and the element shape (σ). Traditionally k_s has only been related to k by $k_s = \alpha k$, where α is an arbitary constant which makes k_s predict the correct friction factor for a certain type of roughness

$$k_s = \phi \{ k , L_s , T_s , C_o , \sigma \}$$

$$\frac{k_s}{k} = \alpha = \phi \left\{ \frac{L_s}{k} , \frac{T_s}{k} , C_o , \sigma \right\}$$

3.4 Velocity distribution

The shearing stress at any point in a turbulent flow moving over a solid surface is

$$\tau = \rho L_m^2 \left[\frac{dV}{dy} \right]^2$$

L_m is the mixing length

$\frac{dV}{dy}$ is the velocity gradient

Assuming that the mixing length is proportional to y and that the shear stress is constant, across a thin layer adjacent to the wall

$$\therefore \qquad dV = \frac{1}{\kappa} \sqrt{\frac{\tau_o}{\rho}} \frac{dy}{y}$$

κ is the constant of proportionality between L_m and y , and κ has been determined experimentally to be approximately equal to 0,40.

Integrating with respect to y

$$V = \frac{1}{\kappa} V_* \text{Ln} \frac{y}{y_o}$$

This is known as the Prandtl-von Kàrmàn universal-velocity-distribution law.

When the surface is rough, the constant y_o is found to depend on the equivalent roughness height

$$y_o = mk_s$$

$$V = \frac{2,30}{\kappa} V_* \log \frac{y}{mk_s} \quad .$$

The expression for mean velocity is obtained by integrating with respect to depth and dividing by the depth

$$\bar{V} = \frac{\int_0^{y_n} V \, dy}{y_n}$$

this results in the expression. (Appendix D).

$$\frac{\bar{V}}{V_*} = \frac{2,30}{\kappa} \left\{ \log \frac{y_n}{k_s} + \log 2,718 \; m \right\}$$

If m is assumed to equal $^1/_{30}$ and κ equal to 0,4 then :-

$$\frac{1}{\sqrt{f}} = 2,03 \log \frac{y_n}{k_s} + 2,12$$

3.5 Theoretical Bottom Location

Most researchers have adopted some form of reference datum convention. The most popular of these is the geometric mean, ie. the level that would be achieved if the roughness elements were melted down to form a new smooth surface.

A second convention used is a datum shift which will give κ a constant value ie. $^1/\sqrt{f}$ versus log $^R/k_s$ graph always has a constant slope.

3.6 Types of Rough Surface Flow

Morris [9] assumed that the loss of energy in turbulent flow over a rough surface is largely due to the formation of wakes behind each roughness element. The frequency of such vortices in the direction of flow will determine the character of their turbulence and the energy dissipation, therefore making the longitudinal spacing of the roughness elements an important dimension. Under this concept, there must exist three basic types of flow. They are isolated-roughness flow, wake-interference flow, and quasi-smooth flow (Figure 3.4).

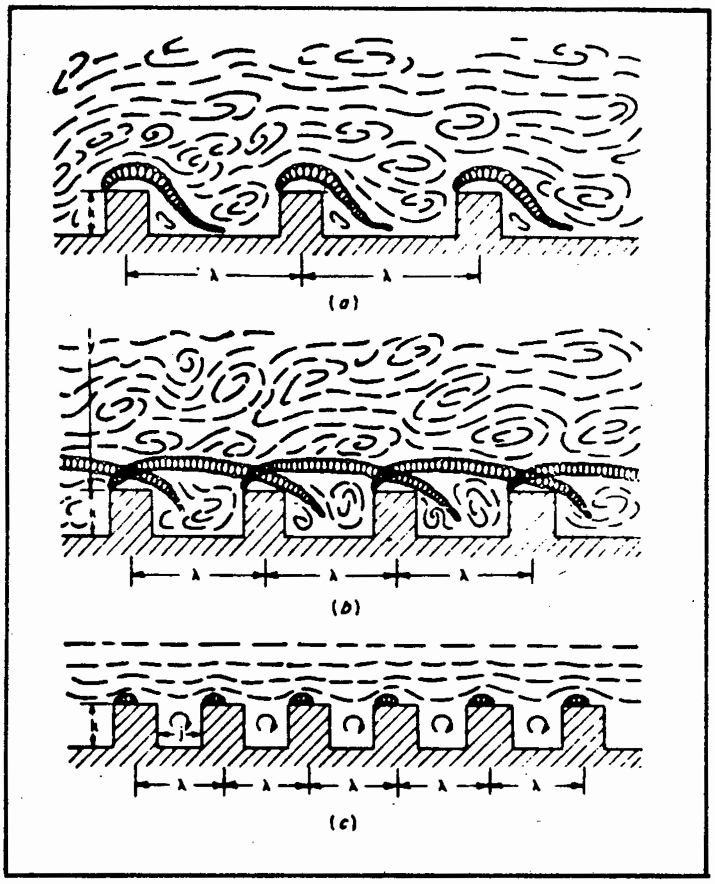

Figure 3.4 : Three types of rough-surface Flow
(a) isolated-roughness flow; (b) wake-interference flow
(c) quasi-smooth flow

3.6.1 Isolated-roughness flow

Isolated-roughness flow prevails when the roughness elements are so far apart that the wake or vortex at each element are completely developed and dissipated before the next element is reached. The apparent roughness would result from form drag on each element plus the friction drag along the smooth surface between the roughness elements. In such a flow condition, the ratio of k/L_s (roughness index) may be taken as a significant parameter influencing flow.

3.6.2 Wake-Interference flow

Wake-interference flow results when the roughness elements are placed close enough together that the wake at each element will interfere with those developed at the following element, resulting in intense and complex vorticity and turbulence mixing. The relative roughness spacing $\left[{}^{L}s/_{R}\right]$ becomes an important parameter.

3.6.3 Quasi-smooth flow

Quasi-smooth flow occurs when the roughness elements are so close together that the flow skims the crests of the elements. In such flow the roughness index $\left[{}^{k}/L_{s}\right]$ becomes significant again.

3.7 Von Karman's constant

Von Kàrman's turbulence constant has been found not to be a true constant in the extreme rough turbulent zone.

The velocity distribution equation is

$$\frac{V}{V_*} = \frac{1}{\kappa} \operatorname{Ln} \frac{y}{y_o}$$

if κ was a true constant the velocity distribution would always have a constant gradient in the fully developed turbulent zone, in a semi logarithmic plot.

For large relative roughness Bayazit found κ decreased with increasing relative roughness (see Figure 2.29). Bayazit also found that with increased relative roughness the turbulence intensity outside the separation zone decreased thus decreasing the mixing length. ($L_m = \kappa y$)

Morris found that for wake-interference flow there are two distinct zones, the wall region and the central region, which have two different velocity distributions (see Figure 2.18). In the central region, normal turbulence characterized by κ will prevail. In the wall region a new parameter has to be introduced, which is not a constant but dependent on the wall Reynolds number. The net effect would be to decrease the κ value in the friction factor equation.

$$\frac{1}{\sqrt{f}} = \frac{0,813}{\kappa}\left\{\log \frac{y_n}{k_s} - \log 2,718\ m\right\}$$

CHAPTER 4

4. EXPERIMENTAL APPARATUS

4.1 Initial Assumptions

The objective of this thesis was to develop an equation to predict the Darcy-Weisbach friction factor for flow over large relative roughnesses and to also check the effect of roughness geometry on f. The traditional Colebrook-White formula does not account for roughness geometry and also can not predict large values of Manning's n (n > 0,05).

Hemispheres were selected as the roughness shape to be tested as they were the best geometric shape to simulate natural boulder roughness. Natural roughness was not selected in order to reduce the number of uncertainties in the results.

The height of the roughness above the flume bed, k , is equal to half the diameter of the hemispheres. The symbols describing the roughness geometry are given in Chapter 3.2 . (See Figure 4.1).

$$T' = \frac{T_d}{T_s} = \text{dimensionless offset parameter.}$$

It was decided to keep $T' = 1/2$ for all patterns tested. L_s and T_s were the parameters that were varied in order to investigate the effect of roughness geometry on the friction factor. This enabled five patterns to be tested for both the large and the small hemispheres and one combination of the two.

The flume used was assumed to be very wide as the perspex walls resistance to flow is very small compared to the bed covered in hemispheres. The slope of the flume was set at 1/1000 and all experiments were conducted at this slope. This ensured streaming flow occurred during all tests.

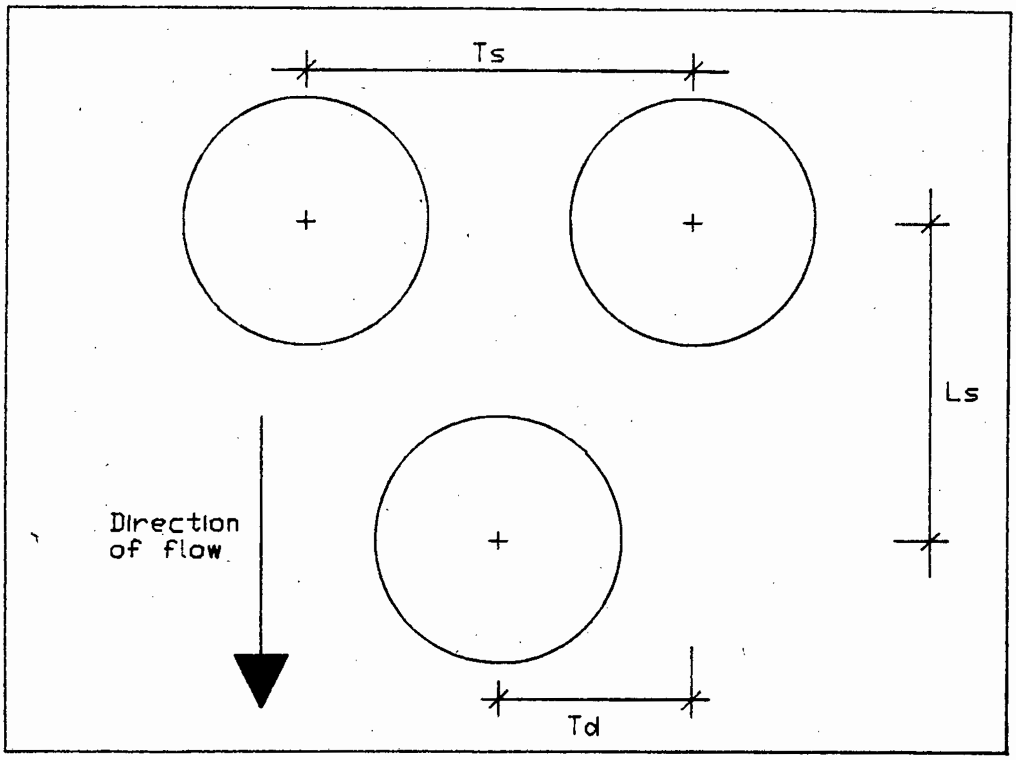

Figure 4.1 : Roughness geometry.

In order to manufacture the hemispheres a number of options were considered. Van Gysen [20] had milled a wooden mould identical to the pattern he choose to represent, then poured resin into the mould and placed a fibreglass sheet on top of the mould, the end result being a panel of his desired pattern. (See plate 4.1 and 4.2).
The limitations to this procedure is that each time a new geometric pattern is needed so is a new mould, also a large quantity of resin would be required.

The method decided on was to cast the hemispheres individually in a large wooden mould. They were made of resin and had a brass screw protruding out of the bottom of each hemisphere. A base plate was then designed for the flume. Brass was used, as steel would rust and marine-grade-aluminium would react through electrolysis with the existing brass bed of the flume. An array of holes was then designed and a thread tapped into each hole in the brass plate. The hemispheres could thus be screwed into the holes and create the desired geometric patterns.

plate 4.1 : test pattern 12 (Van Gysen)

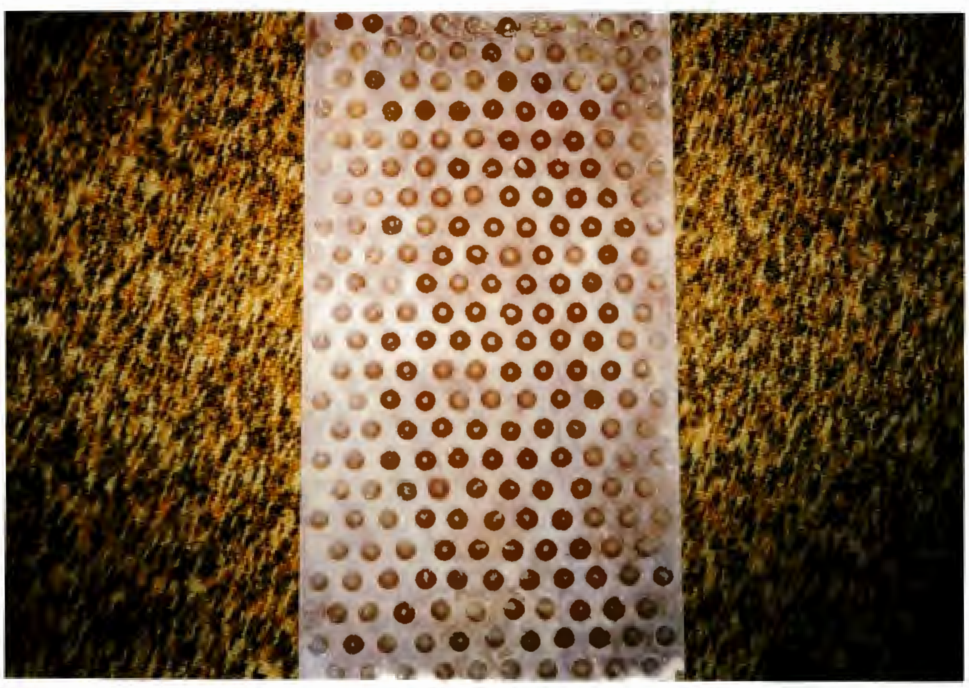

plate 4.2 : test pattern 12 b (Van Gysen)

The plate was then covered with rubber so that the hemisphere made a perfect fit when screwed into the plate. Binding tape was used to cover the holes not in use.

A more detailed explanation of the experimental apparatus used is given in the following sections.

4.2 EQUIPMENT USED

4.2.1 Flume

The flume used is situated in the Civil Engineering laboratory at the University of Cape Town. The flume is 310 mm wide and approximately 6 m long. This channel has a brass bed and perspex sides. There is also a rail above the sides to accommodate gauges which could slide up and down the flume. (See figure 4.2 and plate 4.3).

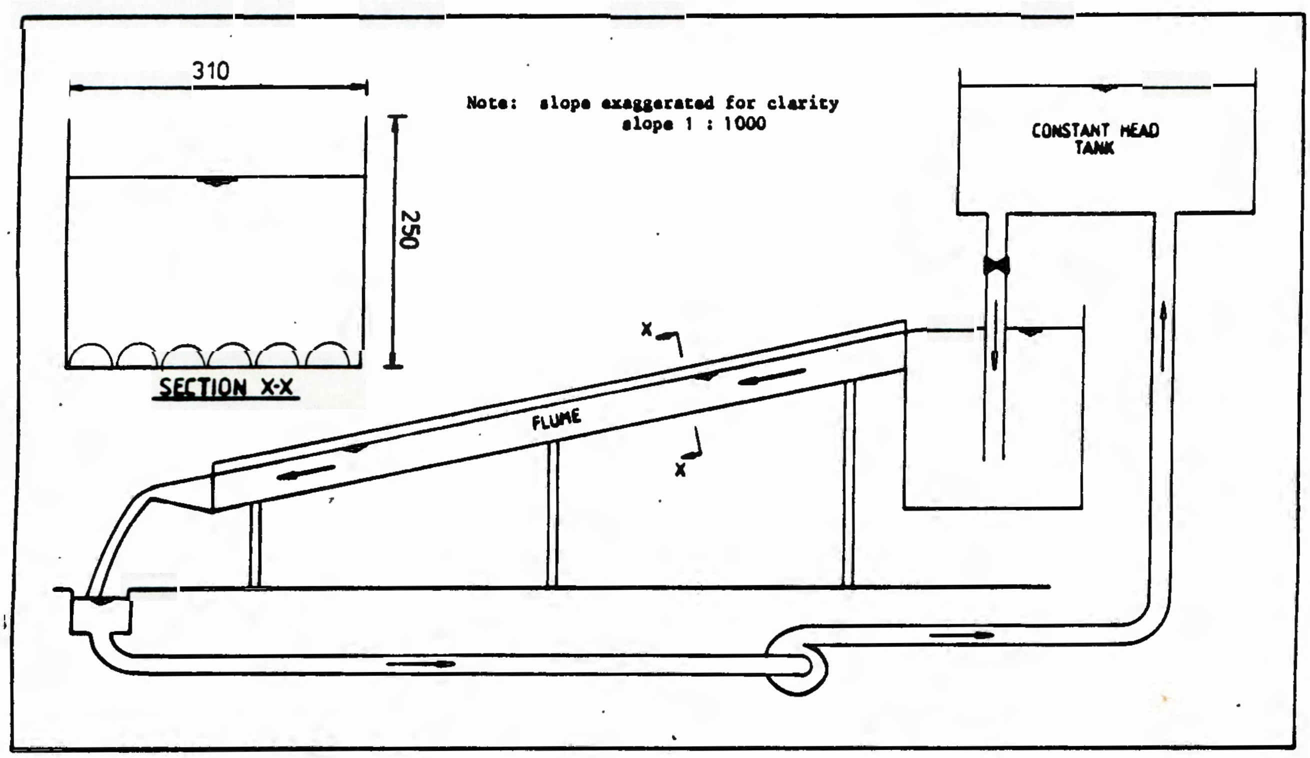

figure 4.2 : general layout of flume, and recirculating system

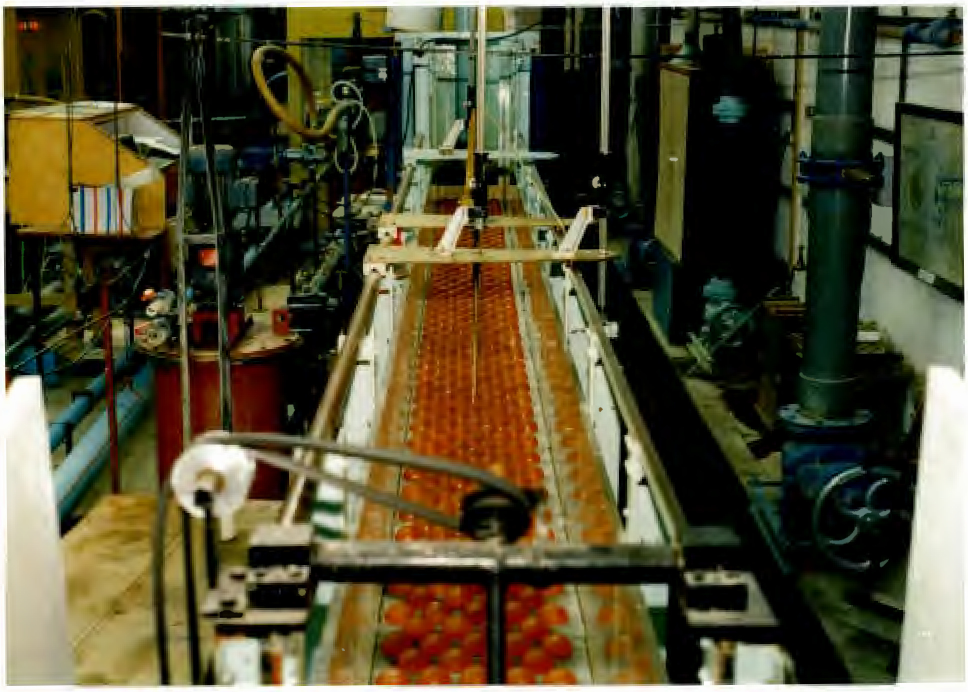

plate 4.3 : flume and gauges

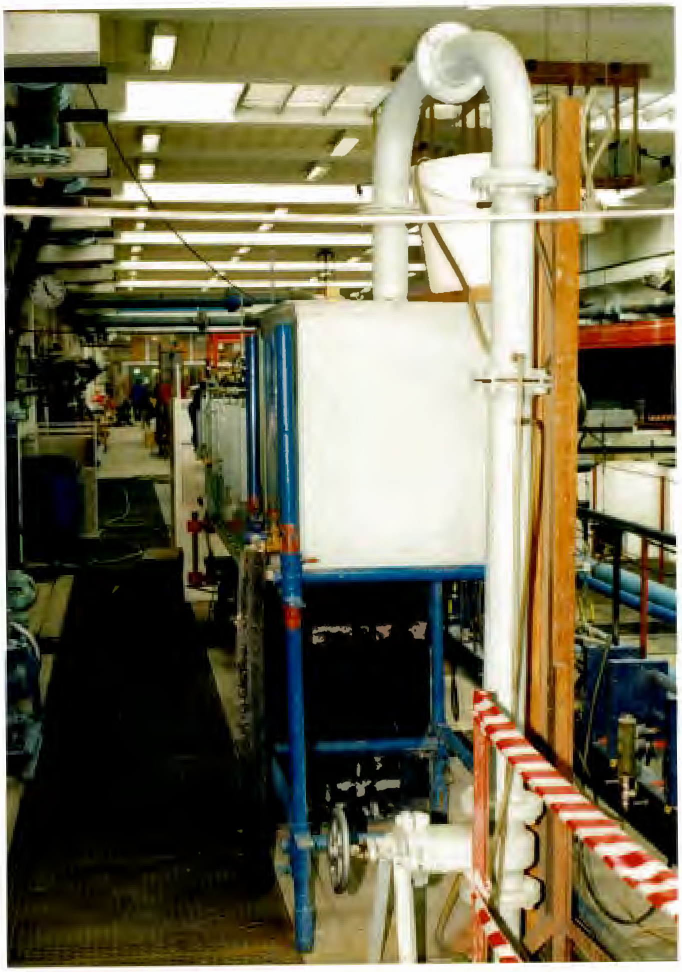

plate 4.4 : inlet valve and tank

The inlet system consists of a valve and a tank. The water is supplied to the tank via a constant head tank above the laboratory. The inlet valve controlled the flow rate. (See plate 4.4)

The outlet system consists of an electrically controlled gate. The water then flows via a channel back to a holding tank and then gets pumped up to the constant head tank. The flume slope could be changed using a jacking device but the slope of the flume was kept at 1/1000 for all experiments done. (See plates 4.5 and 4.6)

4.2.2 Gauges

Two micrometre point gauges were used, and they were placed a measured distance apart on the guide rails of the flume. They measured to 1/10 of a millimetre. (See plate 4.7).

A Pitot cylinder apparatus was also used in an attempt to measure the velocity distribution. A cylinder was used as it could be placed between the hemispheres without too much interference. It was always placed in the centre of the distance between hemispheres in the direction of flow. (See plate 4.8 and figure 4.3).

Flow measurement was done using two manometers connected to an orifice plate situated in the pipe leading into the inlet tank.

4.2.3 Brass plates

Twelve brass plates 4 mm thick and of dimension 308 x 500 mm were cut from a large sheet. An array of holes was then designed to accommodate the large and small hemispheres (see Figure 4.4). The pattern on each plate was the same.

Using the milling machine in the civil engineering workshop a master plate was drilled. The milling machine was used as it is extremely accurate in positioning itself at a co-ordinate on the brass plate (the x-y datum lines were taken along a corner of the brass plate). The holes drilled were 3,2 mm in diameter. Three plates were then clamped

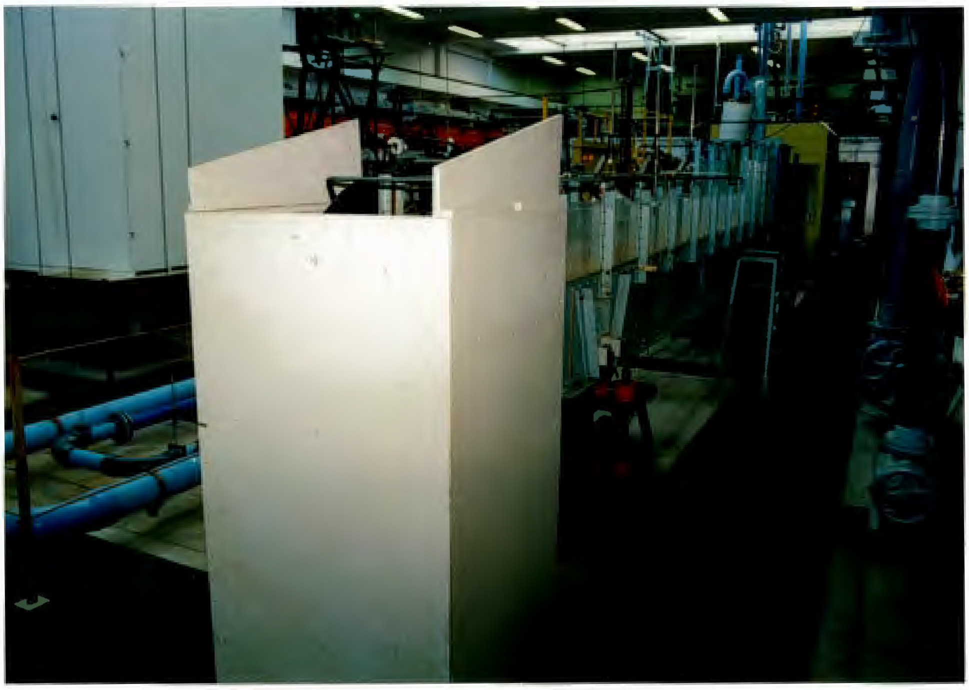

plate 4.5 : jacking device and outlet gate

plate 4.6 : adjustable outlet gate

plate 4.7 : micrometre point gauge

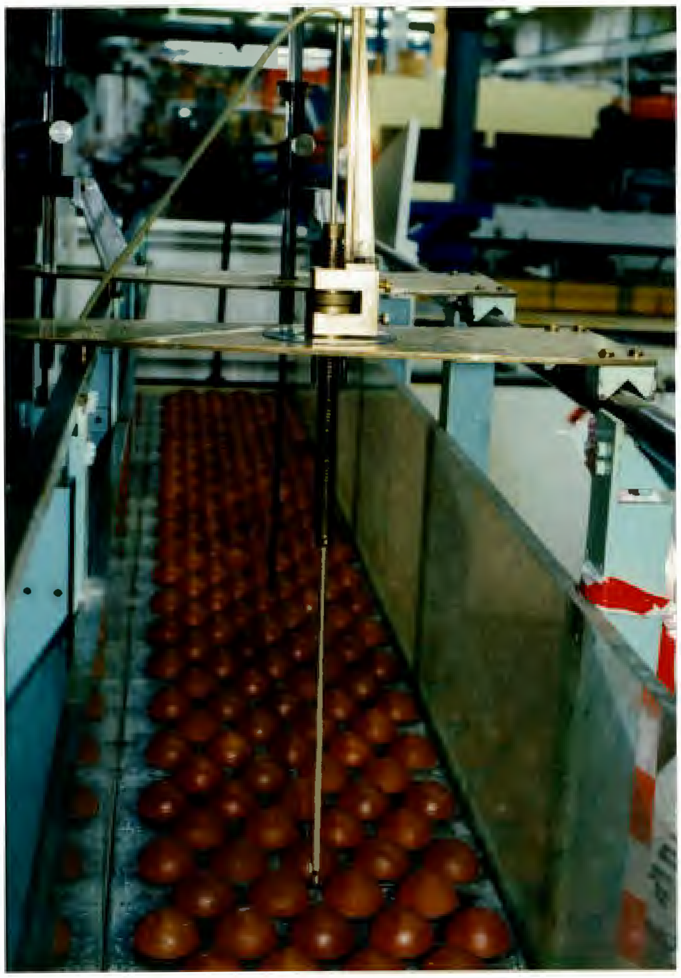

plate 4.8 : Pitot cylinder

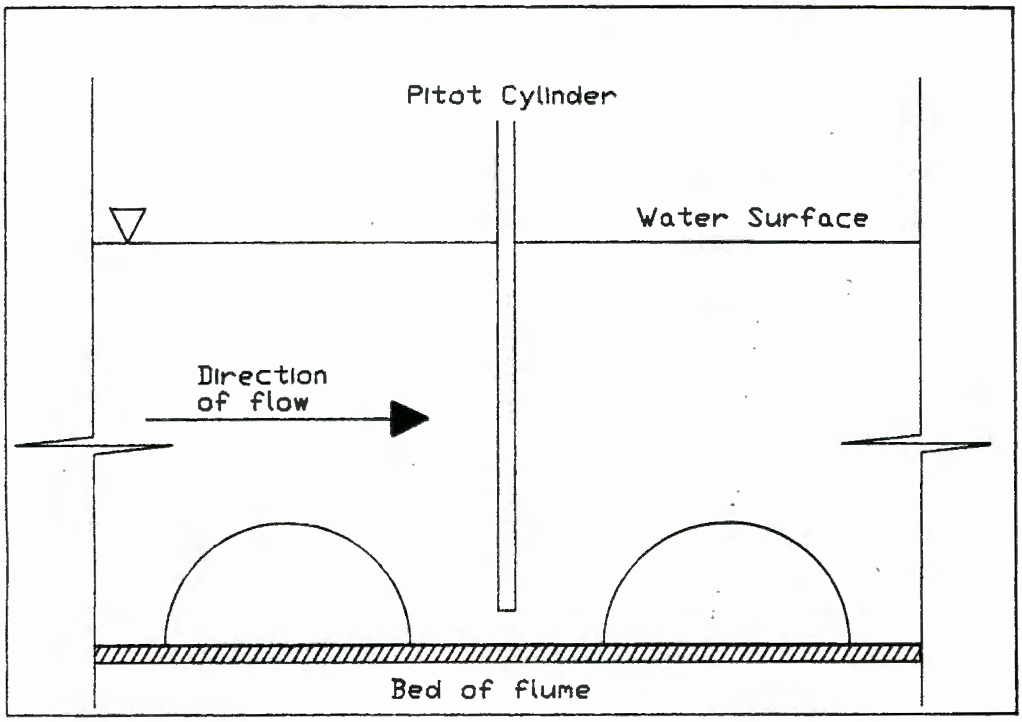

figure 4.3 : position of Pitot cylinder

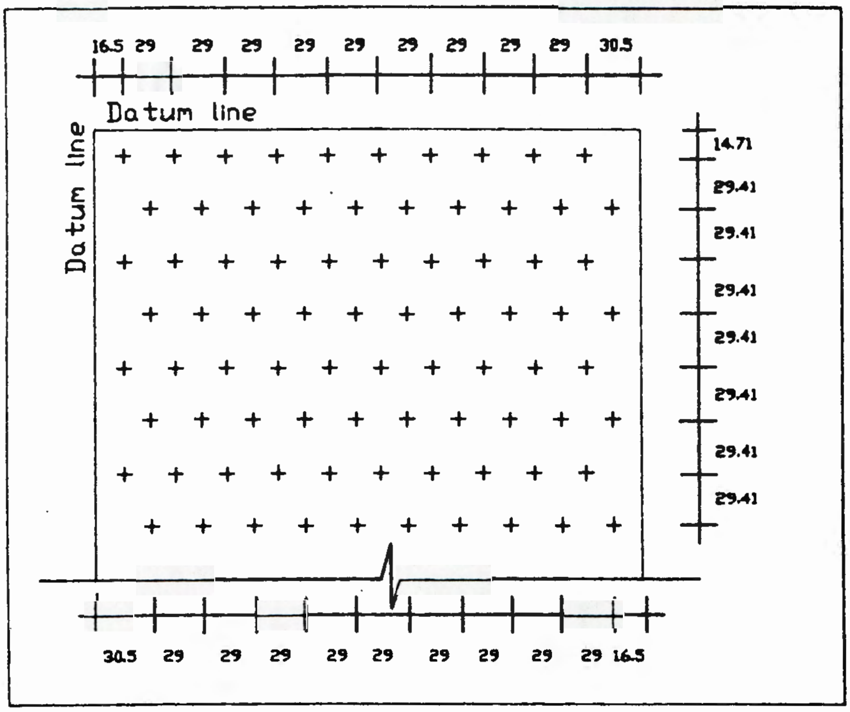

Figure 4.4 : Pattern of holes in Brass Plate

together at a time, squared off at the datum corner, and clamped onto the table of a drilling machine. In this way pilot holes were drilled through all the plates.

Each hole was then countersunk on both sides using a bevelling bit on the drilling machine. Using a 4 mm tapping drill bit, a thread was then tapped through each hole. (See plate 4.9).

A sheet of 1,5 mm gum rubber was then cut into twelve 308 x 500 mm pieces. Holes of diameter 9 mm were then punched out of each piece of rubber in their corresponding positions on the brass plates.

Double-sided tape was then stuck onto the surface of the brass plates and the pieces of rubber were then stuck to the brass plates. The rubber then acted as a large washer, letting the hemispheres make a perfect fit onto the brass plate. (See plate 4.10).

plate 4.9 : brass plate with tapped holes

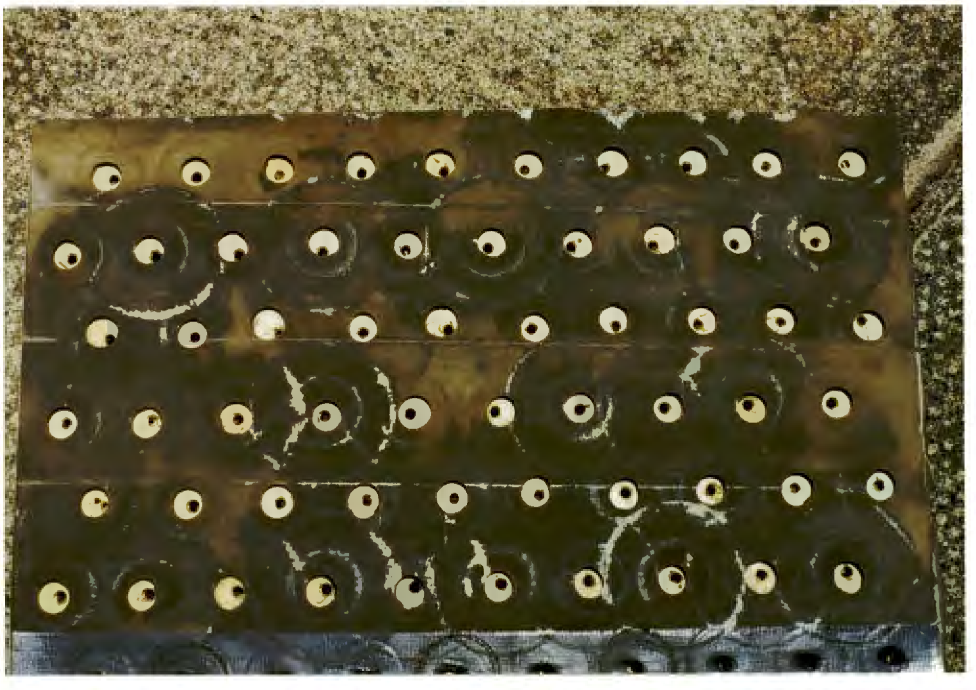

plate 4.10 : brass plate with rubber

4.2.4 Hemispheres

Two sizes of hemispheres were made, 50 mm and 25 mm in diameter. Four wooden moulds were milled out of Jelutong wood. This wood was chosen as it has a very smooth grain. Four sheets of hardboard were then cut to the same dimensions as the wooden moulds. Holes of 3,2 mm diameter were then drilled at points corresponding to the centres of the hemispheres in the moulding. (See plates 4.11 and 4.12).

Brass screws (with cheese heads and diameter 4 mm) were then screwed into the holes in the hardboard. It was important that these screws were perpendicular to the hardboard. For the 25 mm diameter hemispheres 12 mm long screws were used, and for the 50 mm diameter hemispheres 22 mm long screws were used. A wax-based releasing agent (dubbin) was then applied to all the hemispherically shaped holes in the wooden mould.

Resin was poured into the moulds, then the hardboard was placed on top of the mould. The brass screws set in the resin with a small section of the thread protruding from the bottom of the hemisphere. Both sizes of hemispheres were manufactured using this process.

The hemispheres were then screwed into the brass plate in the desired pattern, and binding tape was used to cover the holes in the plate not occupied by a hemisphere. The plates were then placed in the flume, with the edges where the plates connect sealed with binding tape. (See plates 4.13 and 4.14).

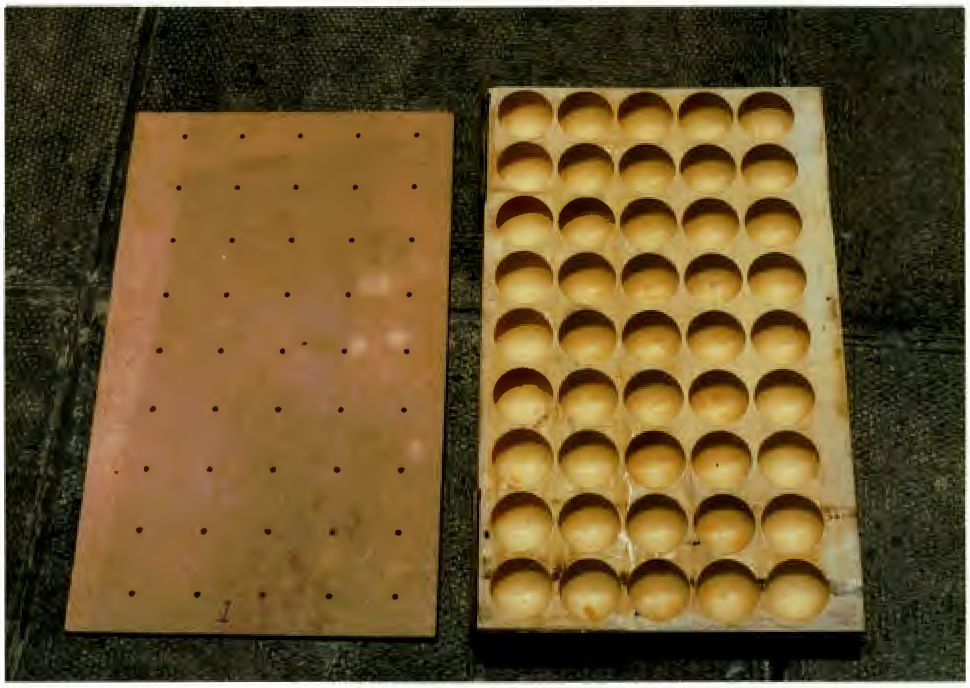

plate 4.11 : wooden mould for Ø 50mm. hemispheres

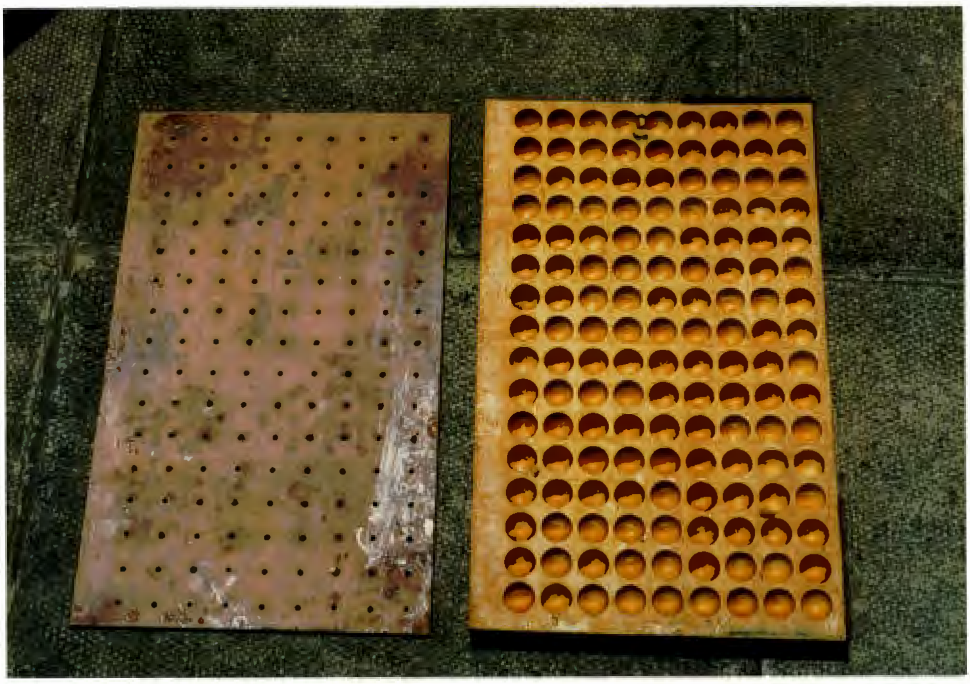

plate 4.12 : wooden mould for Ø 25mm. hemispheres

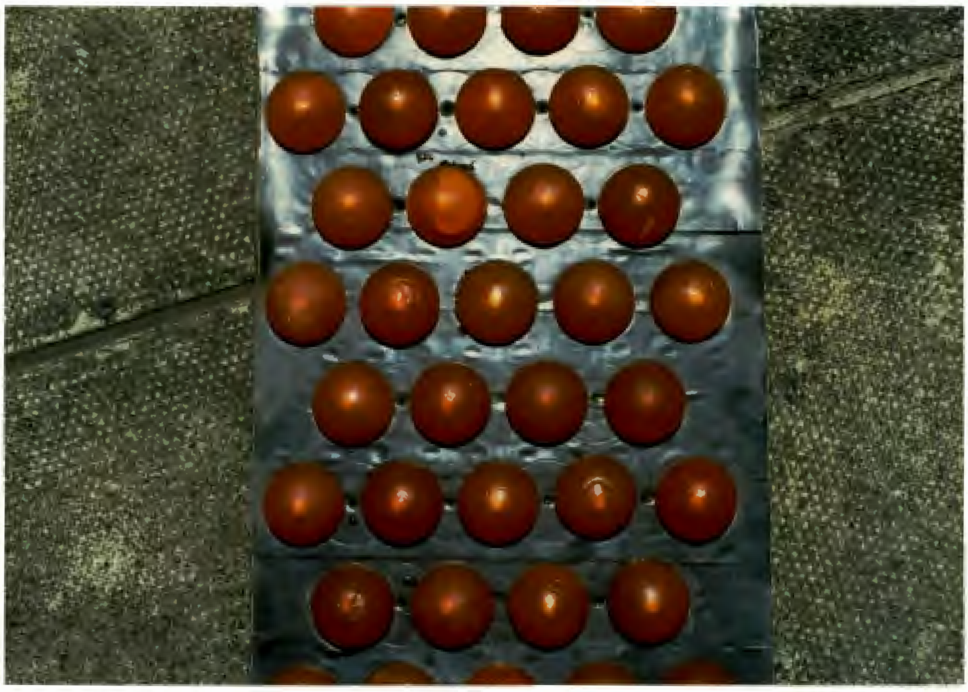

plate 4.13 : test pattern 1

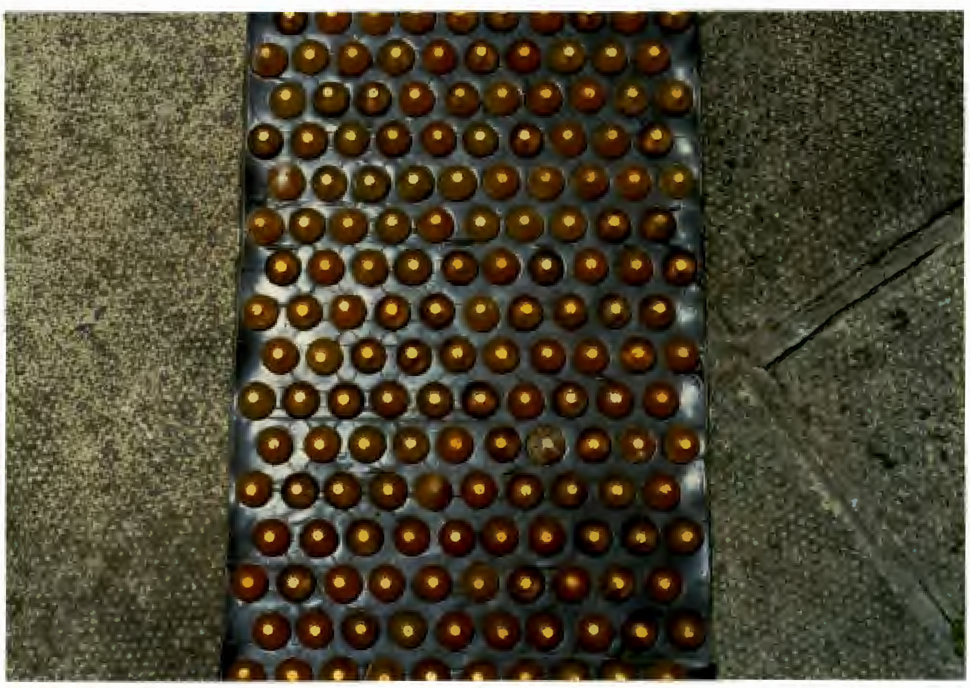

plate 4.14 : test pattern 11

CHAPTER 5

5. EXPERIMENTAL PROCEDURE

The following experimental procedure was used. Five patterns of both the ϕ 50 mm and ϕ 25 mm hemispheres were tested plus one pattern of a combination of the two sizes. The use of two other test pattern results made by Van Gysen were also used. These hemispheres were ϕ 40 mm and ϕ 16,6 mm. The geometric configuration of each pattern tested can be seen in Figures 5.5 to 5.17.

A worksheet was made to record the experimental data. (See Figure 5.1). The worksheet parameters are :

d1 = distance between the micrometer point gauges
d2 = distance to the top of stationary water on the downstream side
d3 = distance to the top of stationary water on the upstream side
d4 = distance to the bottom of the flume on the downstream side
d5 = distance to the bottom of the flume on the upstream side
d6 = distance to the top of the water level on the downstream side
d7 = distance to the top of the water level on the upstream side
h1 = measured height on the right hand manometer, connected to orifice plate
h2 = measured height on the left hand manometer, connected to orifice plate
k = radius of the hemisphere
L_s , T_s and T′ are defined in Chapter 4.1 .
da = distance from the flume bed, the point velocity is measured
db = measured height on the manometer when the pitot cylinder is pointing in the direction of flow
dc = measured height on the manometer when the pitot cylinder is pointing at 40^0 to the direction of flow.

LARGE SCALE ROUGHNESS WORKSHEET

SHEET No. [310 × 6000 FLUME] DATE :

SLOPE mm		TEST NUMBER	DEPTH mm		ORIFICE PLATE mm		VELOCITY DISTRIBUTION mm (except da in inchs)									
d 1			d 6	d 7	h 1	h 2	TEST NUMBER									
d 2		1					STEP	d a	d b	d c	d a	d b	d c	d a	d b	d c
d 3		2					I									
d 4		3					II									
d 5		4					III									
ROUGHNESS GEOMETRY mm		5					IV									
K	1 2	6					V									
Ls	1 2	7					VI									
Ts	1 2	8					VII									
T'	1 2	9					VIII									
Shape	1 2	10					IX									

Figure 5.1

5.1 Setting the slope

The readings for d1, d4 and d5 were taken and then water was allowed to enter the channel. The outflow gate was then closed, and the flume was filled with water. The readings for d2 and d3 were taken (see Figure 5.2)

The formula for the slope is :

$$\frac{\Delta y}{\Delta x} = \frac{d2 + d5 - d4 - d3}{d1}$$

The slope was changed until a slope of 1/1000 was obtained. This slope was used for all experiments.

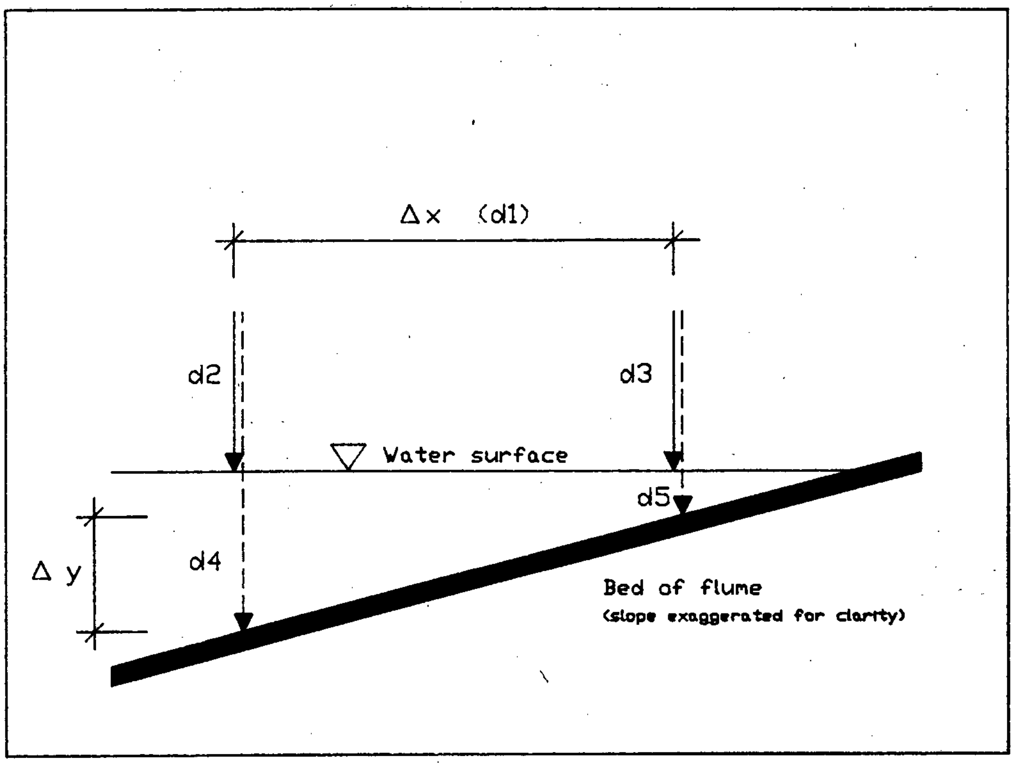

Figure 5.2 : Setting the slope

5.2 <u>Obtaining uniflow flow</u>

The inlet valve was opened until a relatively low flow rate was obtained. The tail gate was opened and then adjusted to achieve uniform depth. (See figure 5.3)

when d6 - d4 = d7 - d5

uniform flow has been achieved.

Readings were them taken for d6, d7, h1 and h2 . This process was then repeated each time increasing the flow rate until the maximum flow rate was achieved.

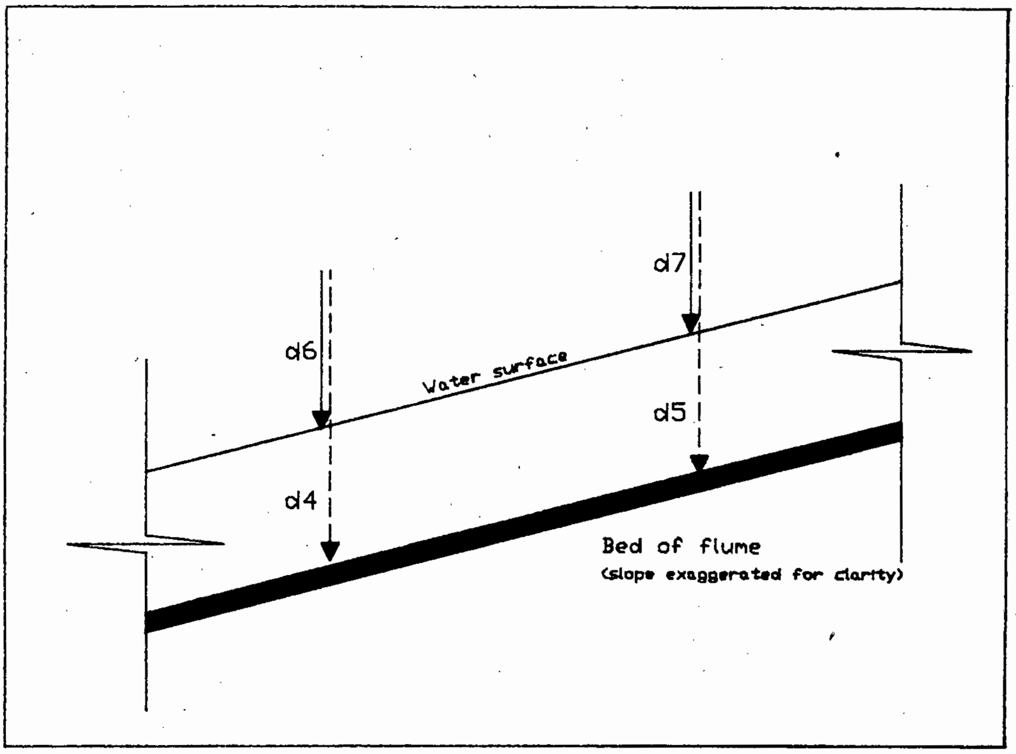

Figure 5.3 : Uniform flow.

5.3 <u>The velocity distribution</u>

The Pitot cylinder apparatus (as described in Chapter 4.2.2) was used. The Pitot tube was placed in the direction of flow and the hydrostatic head was measured as was the depth from the bottom. The Pitot tube was then rotated by 40^0 and the hydrostatic head was measured again. (See Figure 5.4)

da = measurement of distance from the bottom. The formula for the point velocity is $V = \sqrt{\Delta H \times 2g}$ where $\Delta H = db - dc$.

The readings obtained using this method were not too reliable, this is because of the high intensity of turbulence of flow over large relative roughness, and the choice of 40^0 to read the local static pressure is only an estimate.

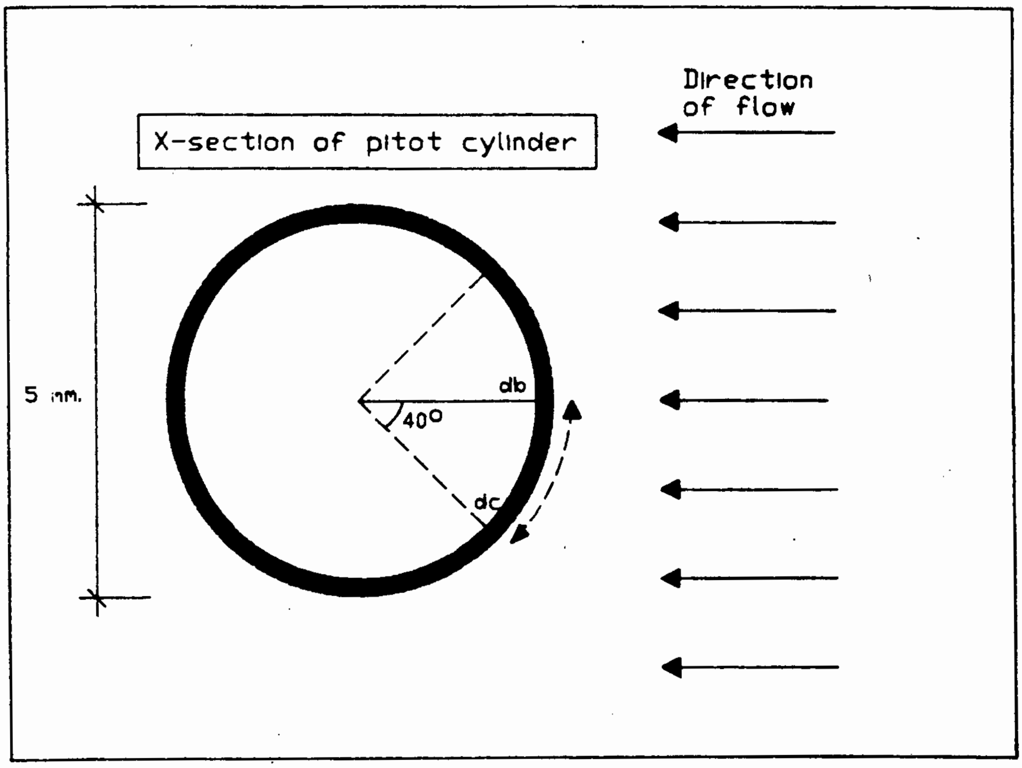

Figure 5.4 : Cross-section of Pitot cylinder.

5.4 <u>The roughness patterns tested</u>

After every set of test runs a different roughness pattern was tested. The roughness patterns and sizes tested can be seen in Figures 5.5 to 5.17, which are drawn to a scale of approximately 1 in 4.

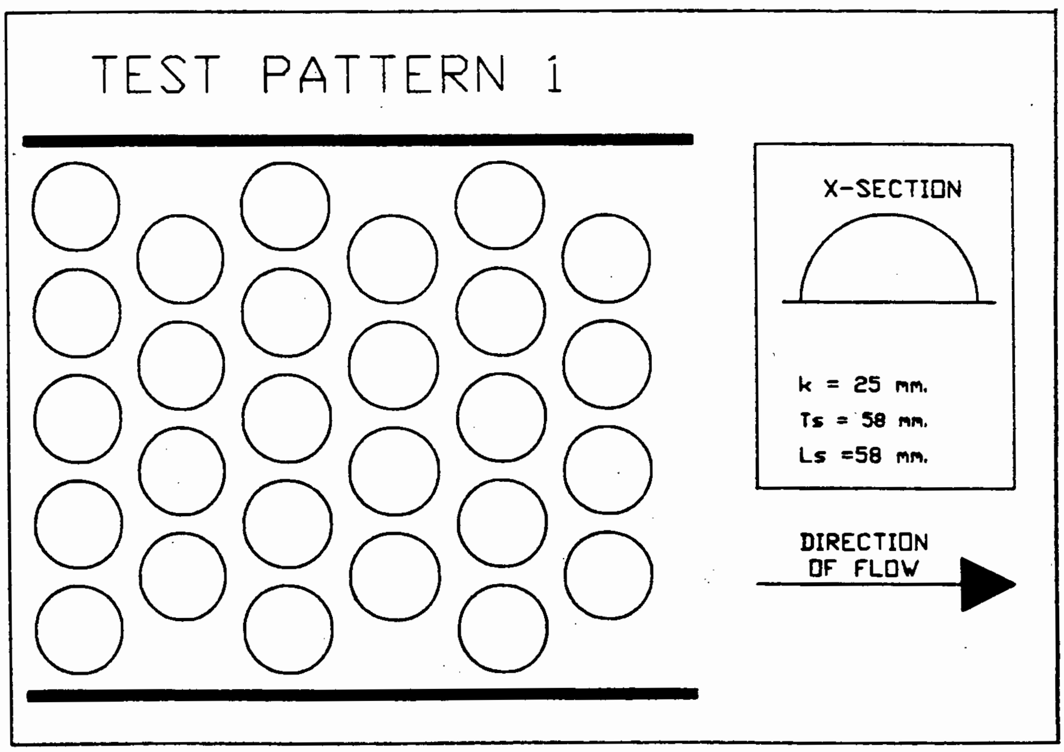

figure 5.5

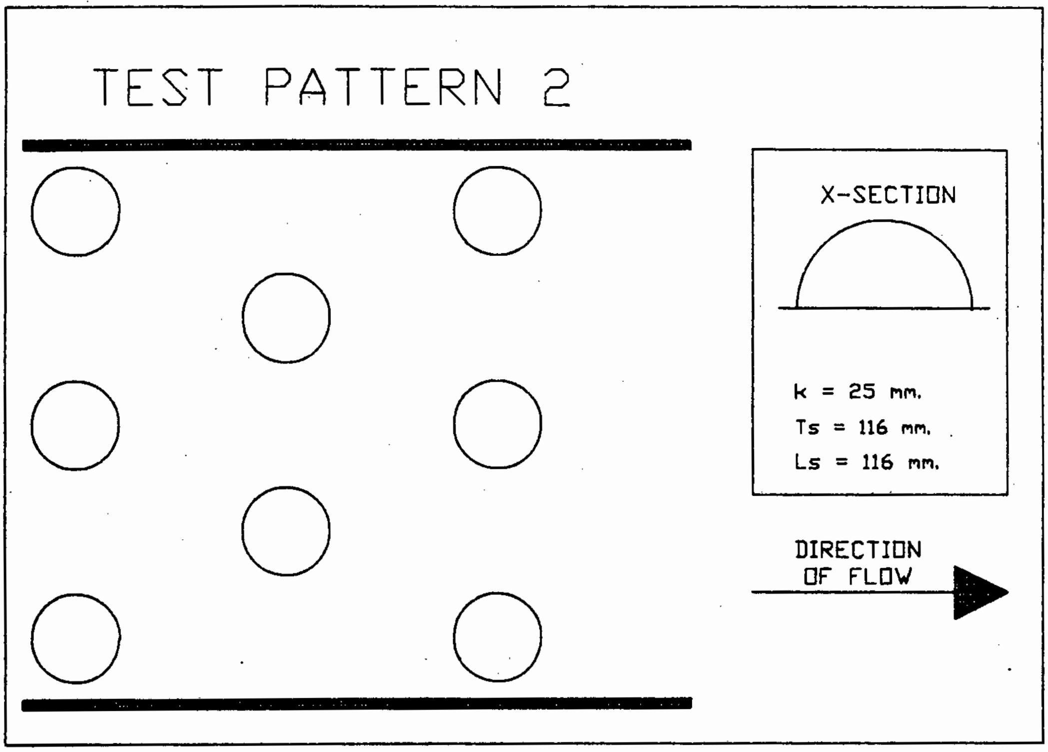

figure 5.6

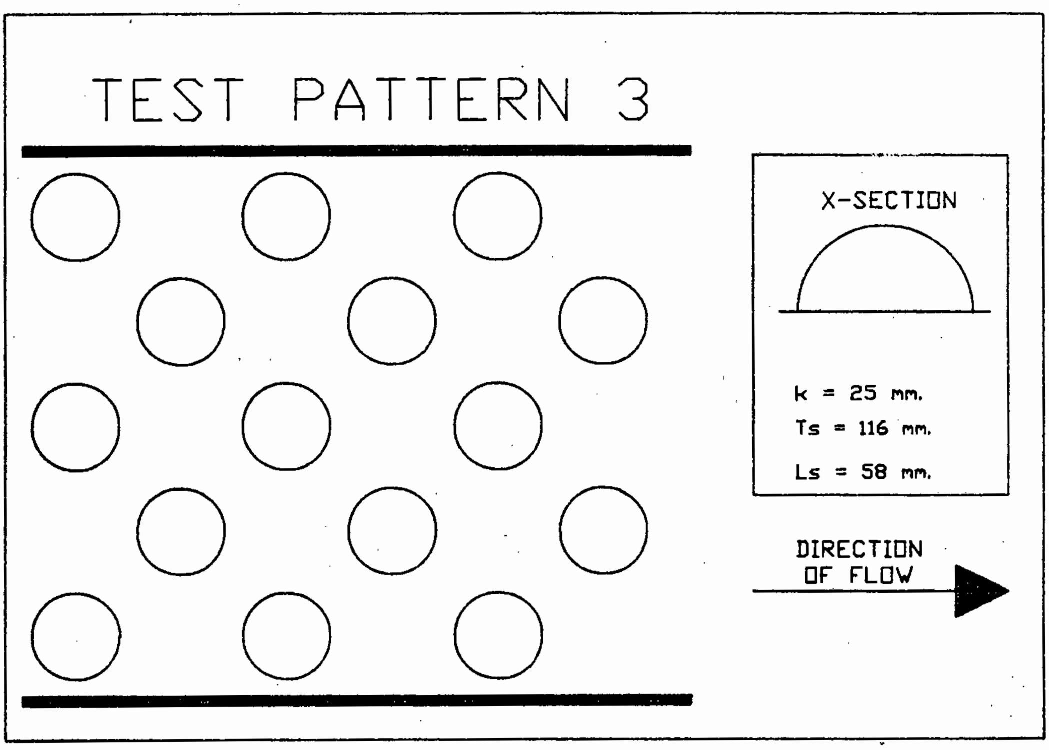

figure 5.7

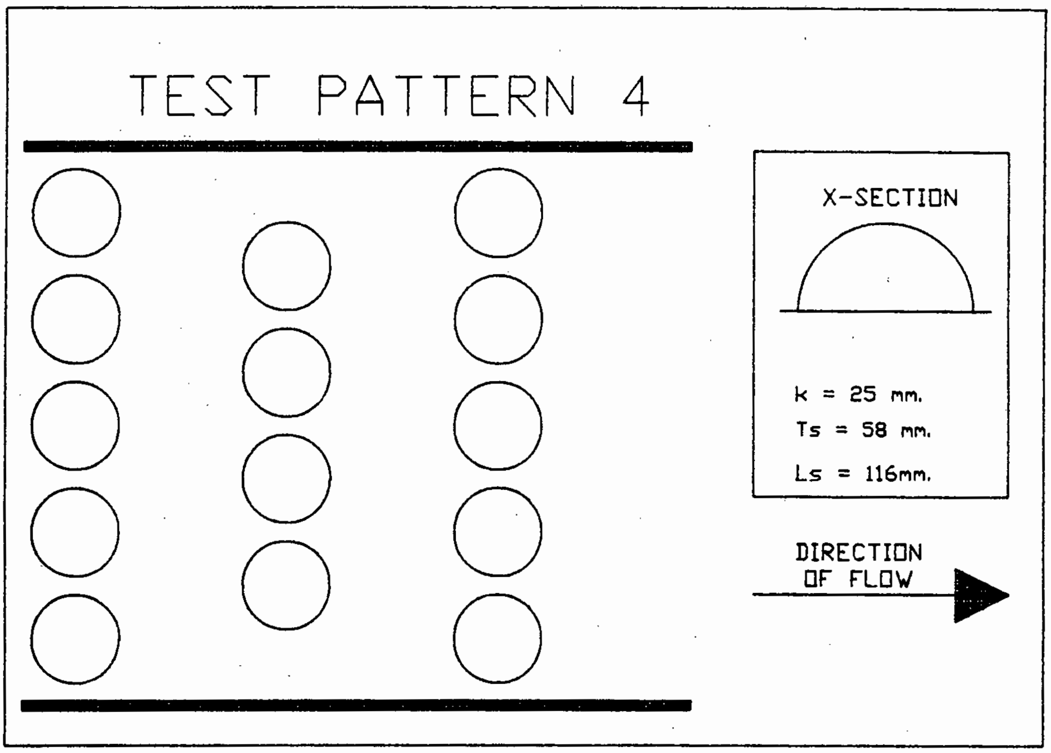

figure 5.8

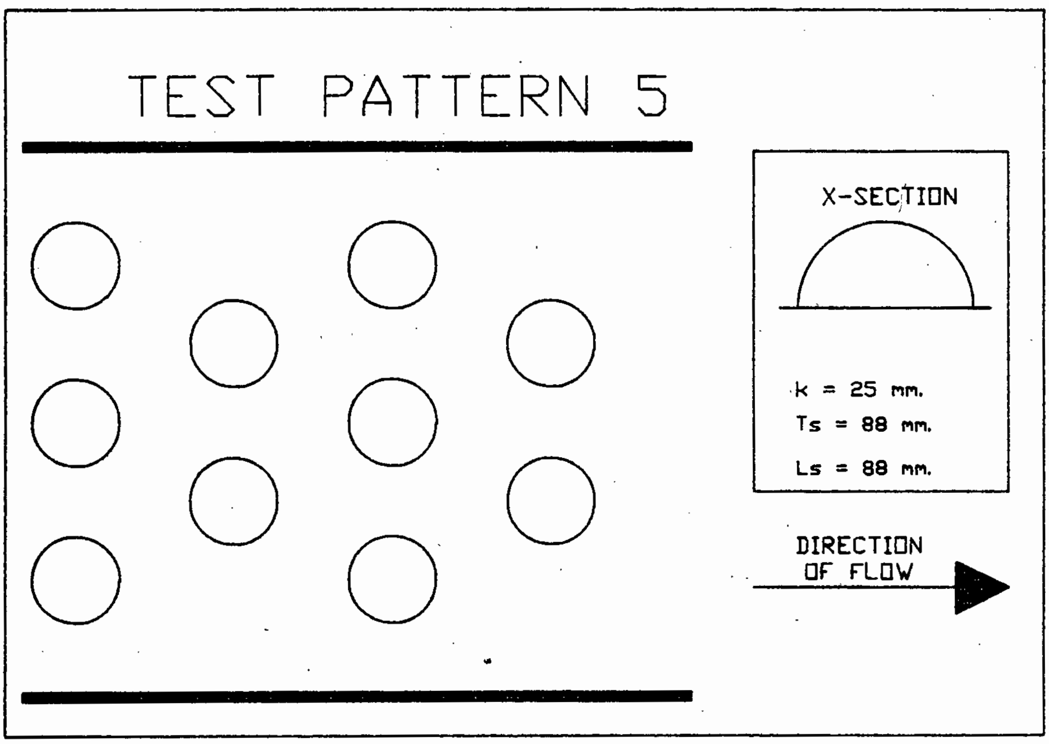

figure 5.9

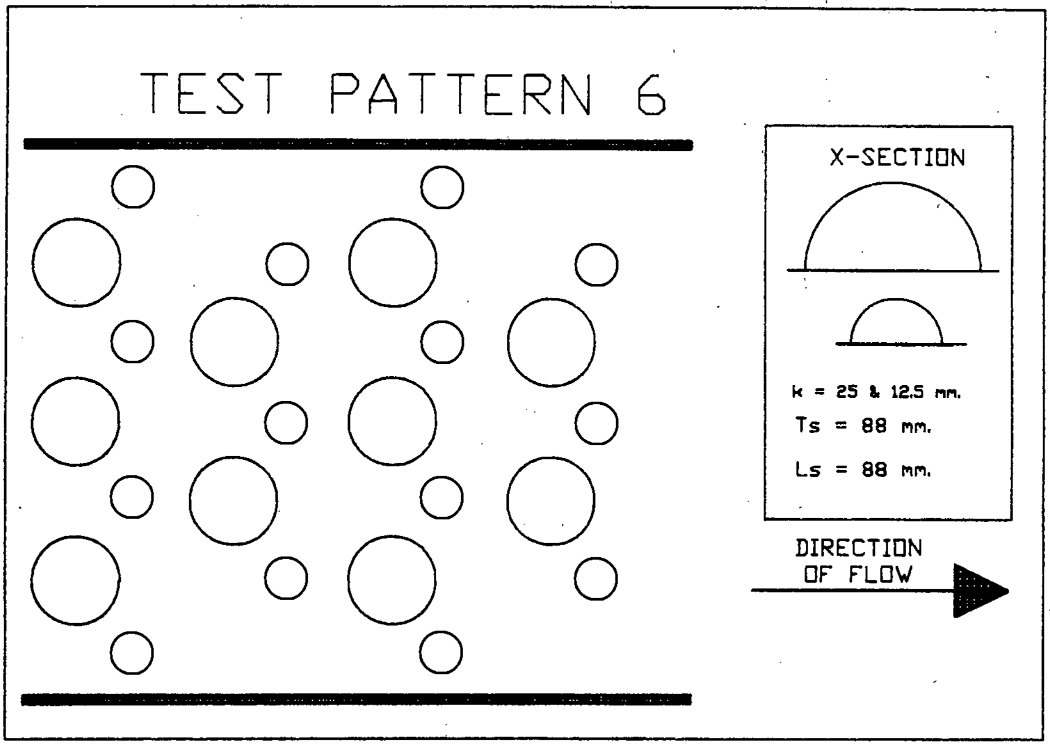

figure 5.10

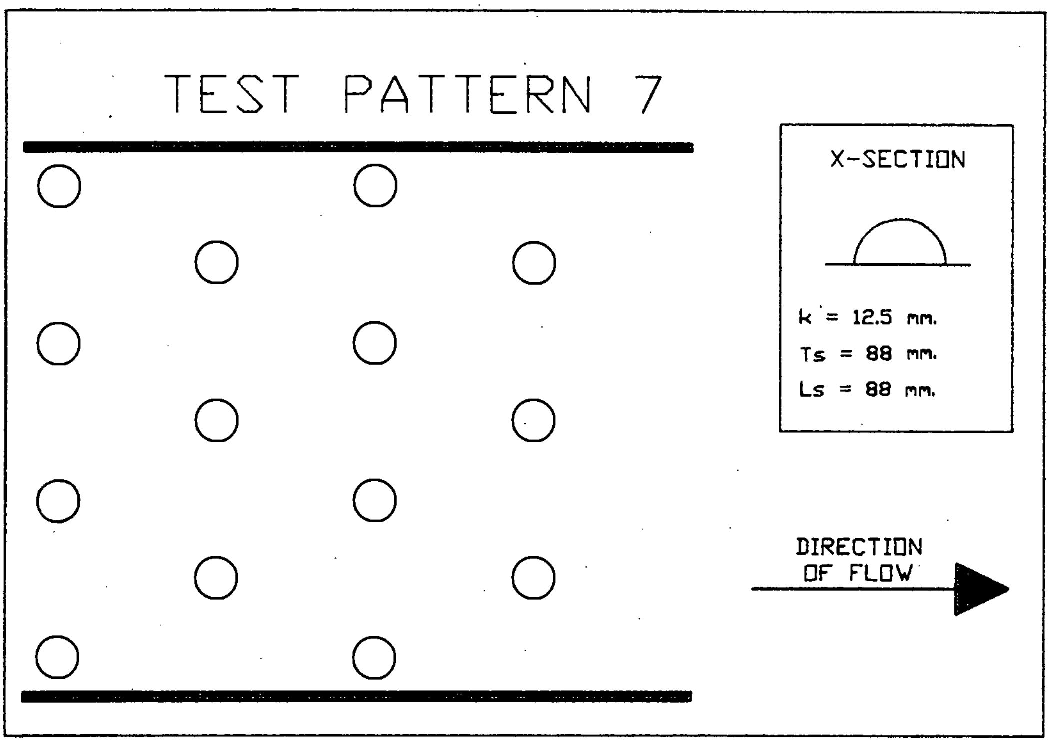

figure 5.11

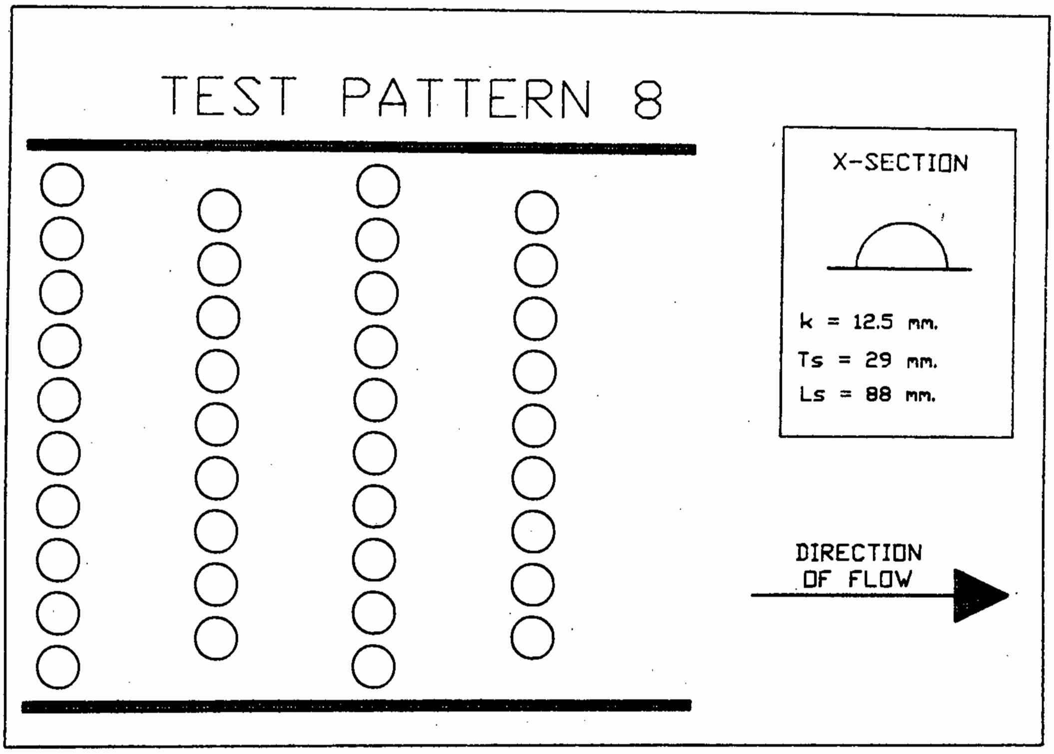

figure 5.12

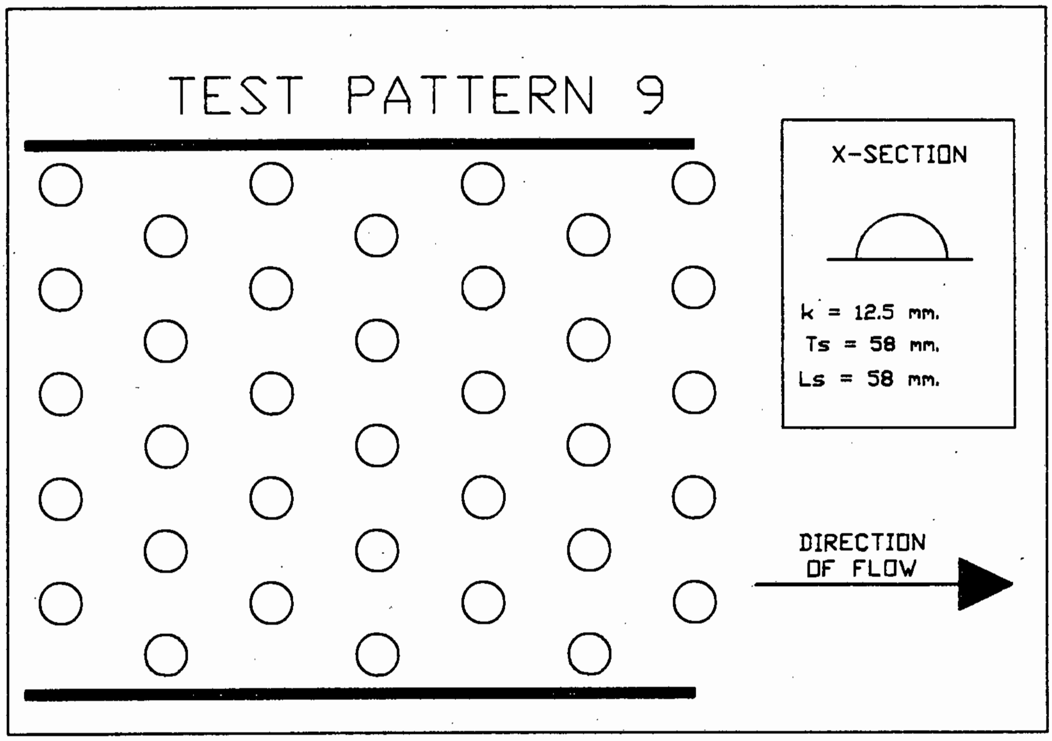

figure 5.13

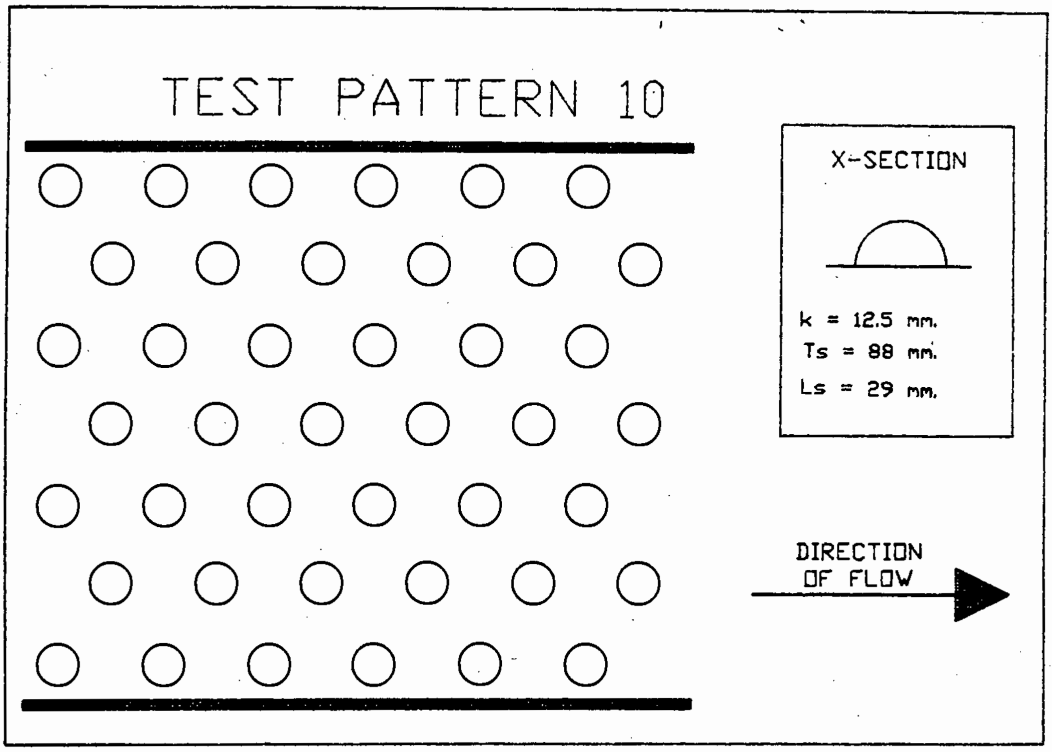

figure 5.14

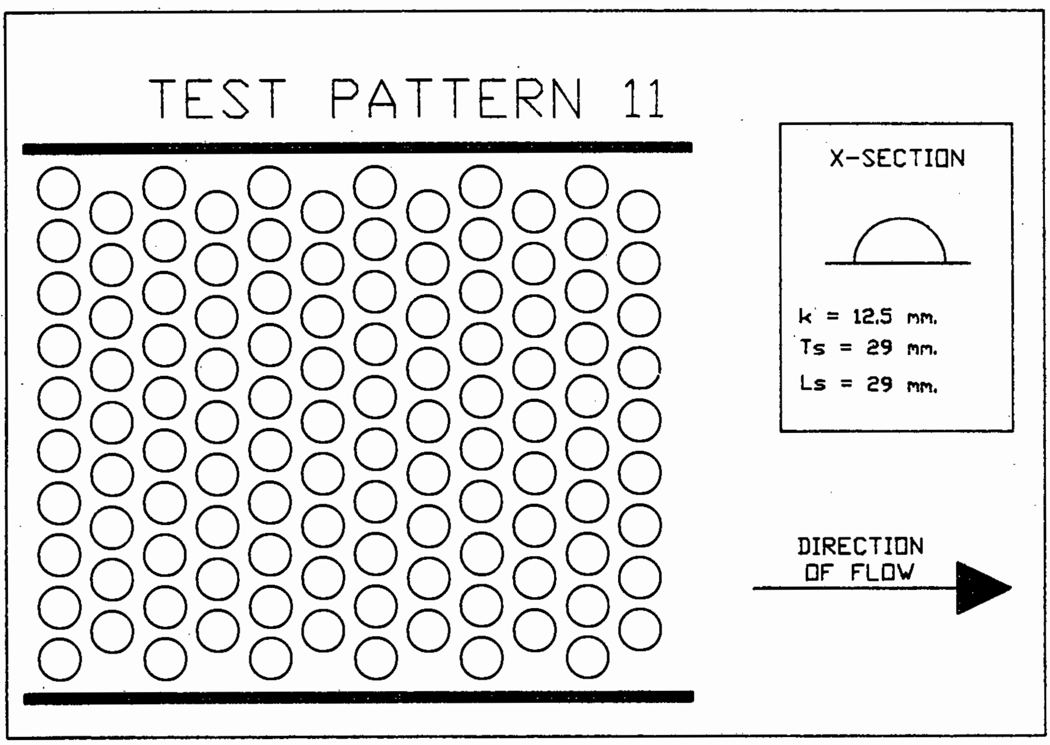

figure 5.15

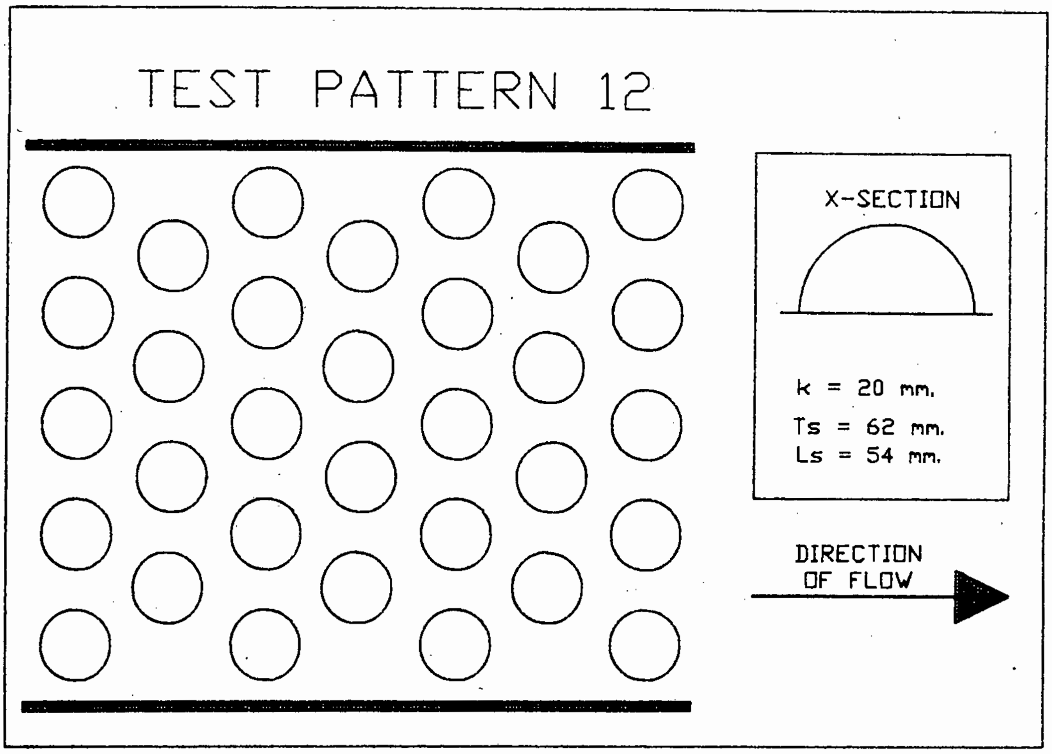

figure 5.16

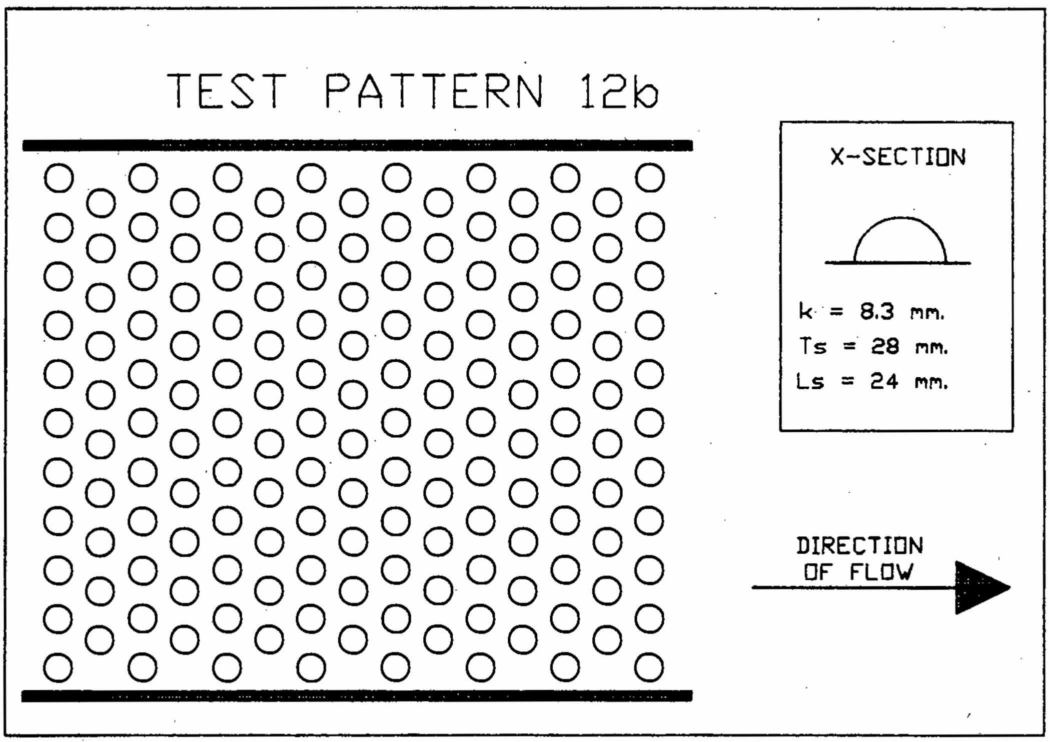

figure 5.17

CHAPTER 6

ANALYSIS OF EXPERIMENTAL RESULTS

6.1 INTRODUCTION

This chapter deals with the technique used to analyse the experimental data. Lotus 1-2-3 (Version 2) was used to process the data and display it in worksheet form. (Appendix E). Trends were looked for using Lotus graphics and its statistics package. The trends which were found were plotted using Lotus print graph.

6.2 CALCULATION OF PARAMETERS IN WORKSHEET (Appendix IV)

6.2.1 Geometric mean

The geometric mean is the height the bed of the flume would be raised if the roughness elements were melted down to form a smooth surface.

6.2.2 Hydraulic radius (R and R′)

The hydraulic radius R was set equal to the depth of flow (for reasons explained in Chapter 4.1). R′ is the hydraulic radius which has included a datum shift. R′ is equal to R minus the geometric mean.

6.2.3 Flow parameters

The flow rate Q was calculated from the readings on the manometer connected to the orifice plate.

The mean velocity V was calculated by dividing the flow rate by the cross-sectional area.

The shear velocity V_* was calculated from the formula

$$V_* = \sqrt{gRS} \quad .$$

The mean boundary shear stress τ_o was calculated from :-

$$\tau_o = \rho g R S \quad .$$

6.2.4 Friction coefficients

i) Chézy's coefficient

$$C = \frac{\bar{V}}{\sqrt{RS}} \quad ;$$

ii) Manning's coefficient

$$n = \frac{R^{2/3}\, S^{1/2}}{\bar{V}}$$

n' is the Manning coefficient corrected for the effects of the flume walls (developed by H.A. Einstein). In order to break the friction distribution up, two assumptions are necessary. The cross sectional area can be divided into units that correspond to units of wetted perimeter. The friction formula will be applicable to the units.

The hydraulic radius of the walls is

$$R_w = \left[n_w \frac{\bar{V}}{S^{\frac{1}{2}}} \right]^{3/2}$$

(n_w = 0,01 for the perspex walls).

The area with reference to the wall is

$$A_w = 2d\, R_w$$

The area with reference to the bed is

$$A_b = d(b - 2R_w) \quad ,$$

and the corresponding hydraulic radius is

$$R_b = \frac{A_b}{b} = d\left[1 - \frac{2R_w}{b}\right]$$

n′ value of the bed can be determined

$$n' = \frac{S^{1/2} R_b^{2/3}}{\bar{V}} .$$

For the 310 mm wide flume used :-

$$n' = \frac{0{,}0316\ (R' - 1{,}147R'\ \bar{V}^{3/2})^{2/3}}{\bar{V}} .$$

iii) Darcy-Weisbach friction coefficient

$$f = \frac{8gRS}{\bar{V}^2} \qquad \text{(U.S.A. practice)} .$$

6.2.5 Equivalent roughness size k_s

k_s is the roughness height that would correctly predict the Darcy-Weisbach friction factor from the Colebrook-White equation

$$k_s = \frac{R'}{10\left[\frac{1/\sqrt{f} - 2{,}12}{2}\right]} .$$

6.2.6 Dimensionless numbers

i) Relative roughness k/R'

ii) Reynolds number R_e ; $R_e = \frac{\rho \bar{V} R'}{\mu}$

Reynolds number is the ratio of inertial forces to viscous forces ;

iii) wall Reynolds number R_{ew}

$$R_{ew} = \rho \frac{V_* k}{\mu} \quad ;$$

iv) Froude number F_r

$$F_r = \frac{V}{\sqrt{gR'}} \quad .$$

Froude number is the ratio of inertial forces to gravity forces.

6.3 RELATIONSHIP BETWEEN FRICTION FACTOR f AND RELATIVE ROUGHNESS

In order to establish if the relationship between f and R′/k was a power law or a semi-log relationship graphs were plotted of both :

$$\frac{1}{\sqrt{f}} \quad \text{versus } \log \frac{R'}{k}$$

and $\log f$ versus $\log R'/k$

(an example of these is given in figures 6.1 and 6.2).

A linear regression was performed to find the best fit equation for the data available and the correlation coefficient was found to establish how well the data fitted the equation.

The equations found were of the form :

$$\frac{1}{\sqrt{f}} = A + B \log \frac{R'}{k} \qquad (6.1)$$

and

$$f = A' \left[\frac{R'}{k} \right]^{B'} \qquad (6.2)$$

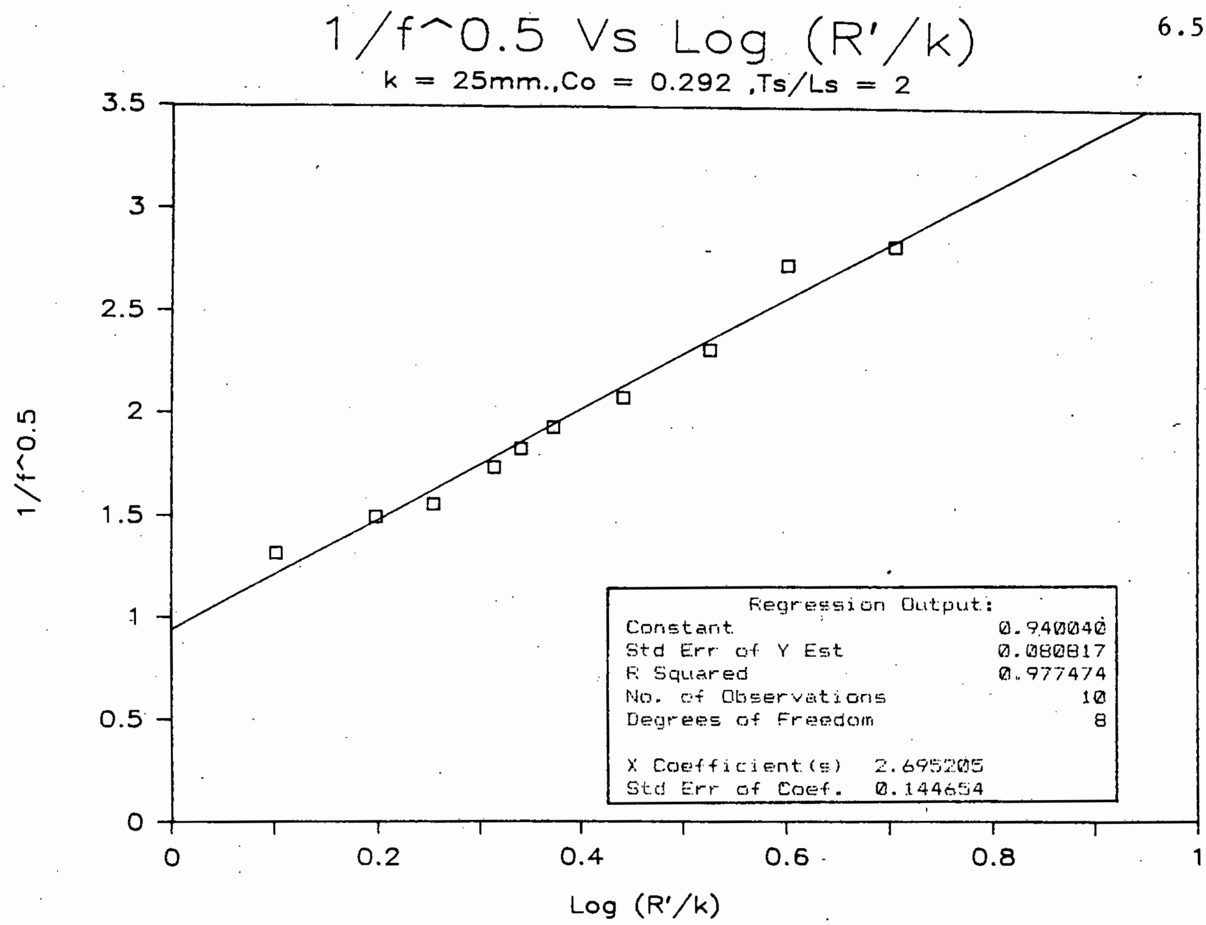

figure 6.1

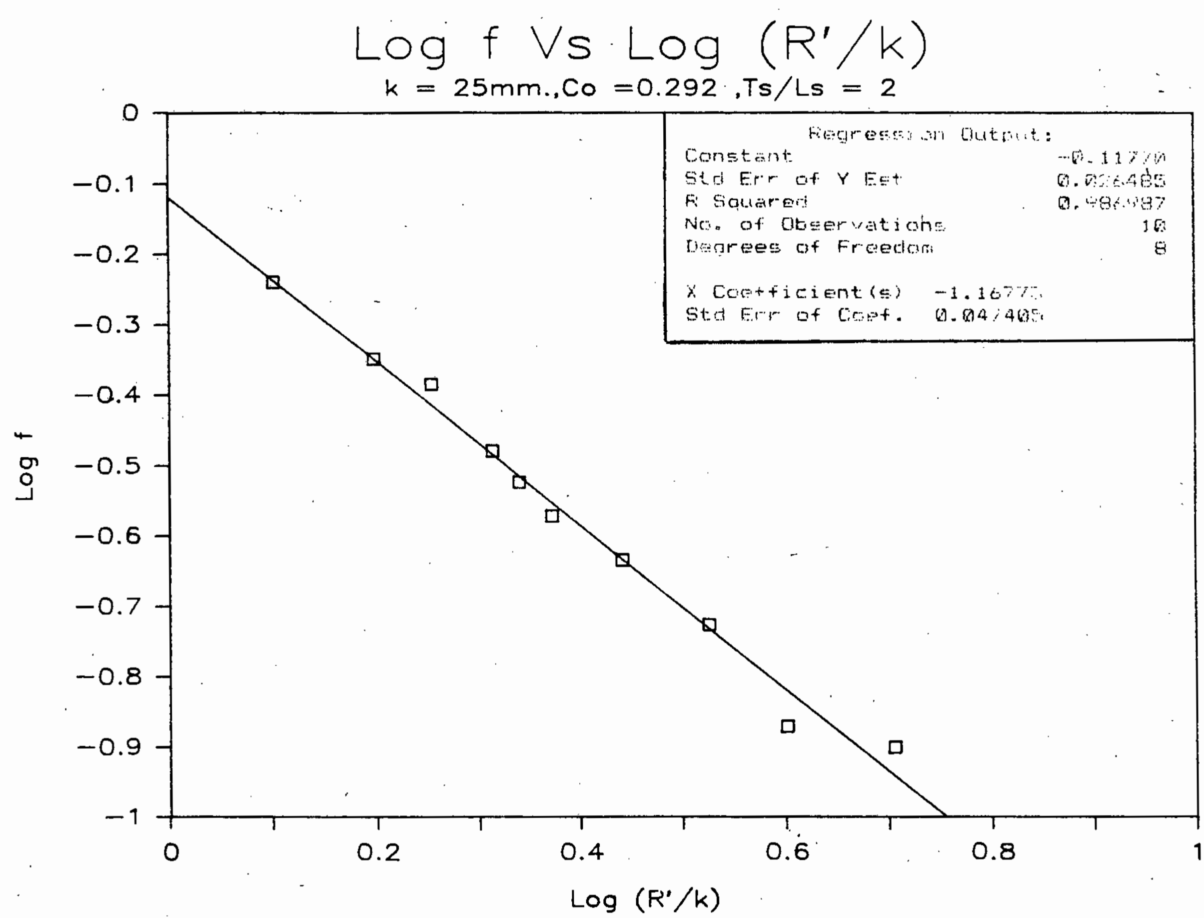

figure 6.2

The first equation is a development of the classical friction equation used for pipe flow (used by Colebrook-White). The second equation is the relationship which is used in the development of the Manning equation.

Both equations were found to fit the data with correlation coefficients close to one (see Figures 6.1 and 6.2). To choose which equation would be suitable for general application of solving the friction factor, comparison between the A and B values was made for roughness patterns which were geometrically similar. It was found that A and B were the same if the roughness pattern was geometrically similar but to a different scale, where A′ and B′ were not. It was decided to try and find how A and B varied with roughness geometry (i.e. adopt the semi-log relationship).

All the A and B values were obtained from the plots of $1/\sqrt{f}$ versus log R'/k . (See Appendix F). A summary of these values can be seen in Table 6.1 . A summary of A and B values for natural roughness was extracted from the literature and recorded in Table 6.2 .

It was attempted to establish a relationship between A and a dimensionless number describing roughness geometry. After plotting A against the dimensionless numbers in Tables 6.1 and 6.2, a trend was found to exist between A and k^2/T_sL_s . k^2/T_sL_s is a function describing roughness concentration (see Figures 6.3 and 6.4) The equation describing the relationship between A and k^2/T_sL_s was found using a program called "Curvefit" which fits 25 different equations to the data and yields the best fit curve. The curve was found to be shifted hyperbola, with a correlation coefficient of 0,93.

$$A = 0,67 + \frac{0,04}{\left[\frac{k^2}{T_sL_s}\right]} \qquad (6.3)$$

Roughness shape: Hemispheres

$1/\sqrt{f} = A + B\log R'/K$

Pattern No.	k (mm)	T_s/L_s	k/T_s	k/L_s	$\frac{k^2}{T_s L_s}$	A	B	κ	Correlation Coefficient
1	25	1	0,43	0,43	0,185	0,73	1,73	47	0,92
2	25	1	0,22	0,22	0,048	1,50	2,20	0,41	0,97
3	25	2	0,22	0,43	0,095	0,94	2,70	0,30	0,99
4	25	1/2	0,43	0,22	0,095	1,07	1,57	0,57	0,93
5	25	1	0,28	0,28	0,078	1,18	2,29	0,36	0,97
6	25 & 12,5	1	0,28	0,28	0,078	1,36	1,95	0,42	0,95
7	12,5	1	0,14	0,14	0,020	2,60	1,60	0,51	0,94
8	12,5	1/3	0,43	0,14	0,060	1,18	1,65	0,49	0,94
9	12,5	1	0,22	0,22	0,048	1,68	1,94	0,42	0,94
10	12,5	3	0,14	0,43	0,060	0,90	2,85	0,29	0,95
11	12,5	1	0,43	0,43	0,185	1,14	1,94	0,42	0,95
12	20	1,15	0,32	0,37	0,118	1,29	1,85	0,44	0,99
12b	8,3	1,17	0,30	0,35	0,105	1,43	1,97	0,41	0,96
Bayazit	23	0,87	0,58	0,05	0,290	0,74	1,96	0,41	0,99

TABLE 6.1 : A and B values related to Roughness Geometry.

Roughness shape: Natural Boulders

$1/\sqrt{f} = A + B\log R'/K$

Pattern No.	k (mm)	T_s/L_s	k/T_s	k/L_s	$\frac{k^2}{T_s L_s}$	A	B	κ
a	70	2	0,17	0,34	0,058	1,46	1,98	0,41
b	70	1	0,34	0,34	0,115	1,19	1,98	0,41
c	70	2	0,23	0,46	0,106	1,15	2,14	0,38
d	70	2	0,34	0,69	0,235	0,78	1,98	0,41
e	70	1	0,46	0,46	0,212	0,70	1,98	0,41
f	70	1	0,69	0,69	0,476	0,48	2,14	0,38
g	150	1	0,74	0,74	0,548	0,60	2,85	0,29
h	150	1	0,68	0,68	0,462	0,65	2,85	0,29
i	150	1	0,58	0,58	0,336	0,80	2,85	0,29
j	10	1	0,14	0,14	0,020	2,65	2,14	0,38
k	10	1	0,29	0,29	0,084	1,35	2,14	0,38

a - f A.G. Mirajgalker and K.L.N. Charlu [12] (See Figure 2.24).
g - i R. Pyle and P. Novak [17]
j - k K.G. Ranga Raju, G. Webel and M. Schatzman

TABLE 6.2 : A and B values related to roughness geometry.

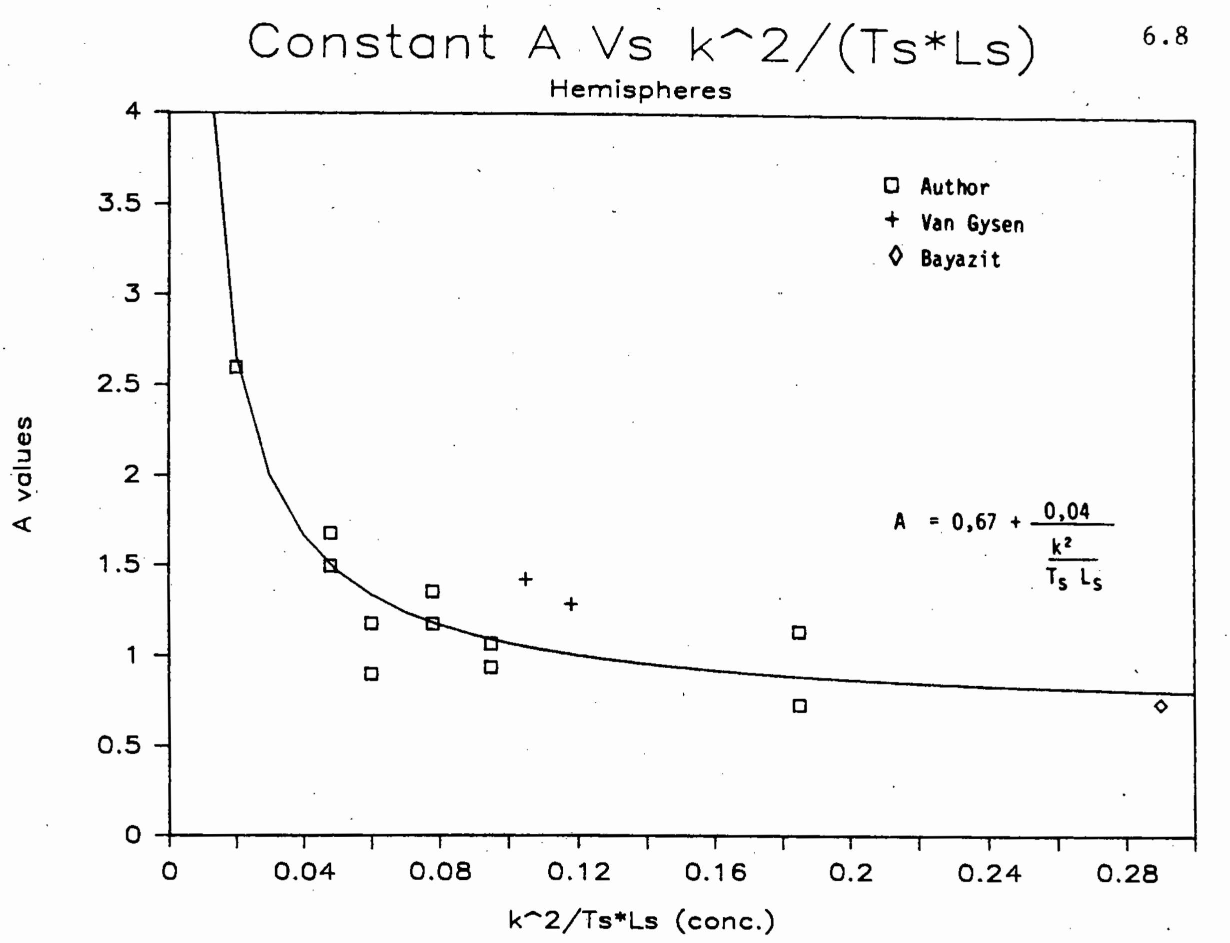

figure 6.3

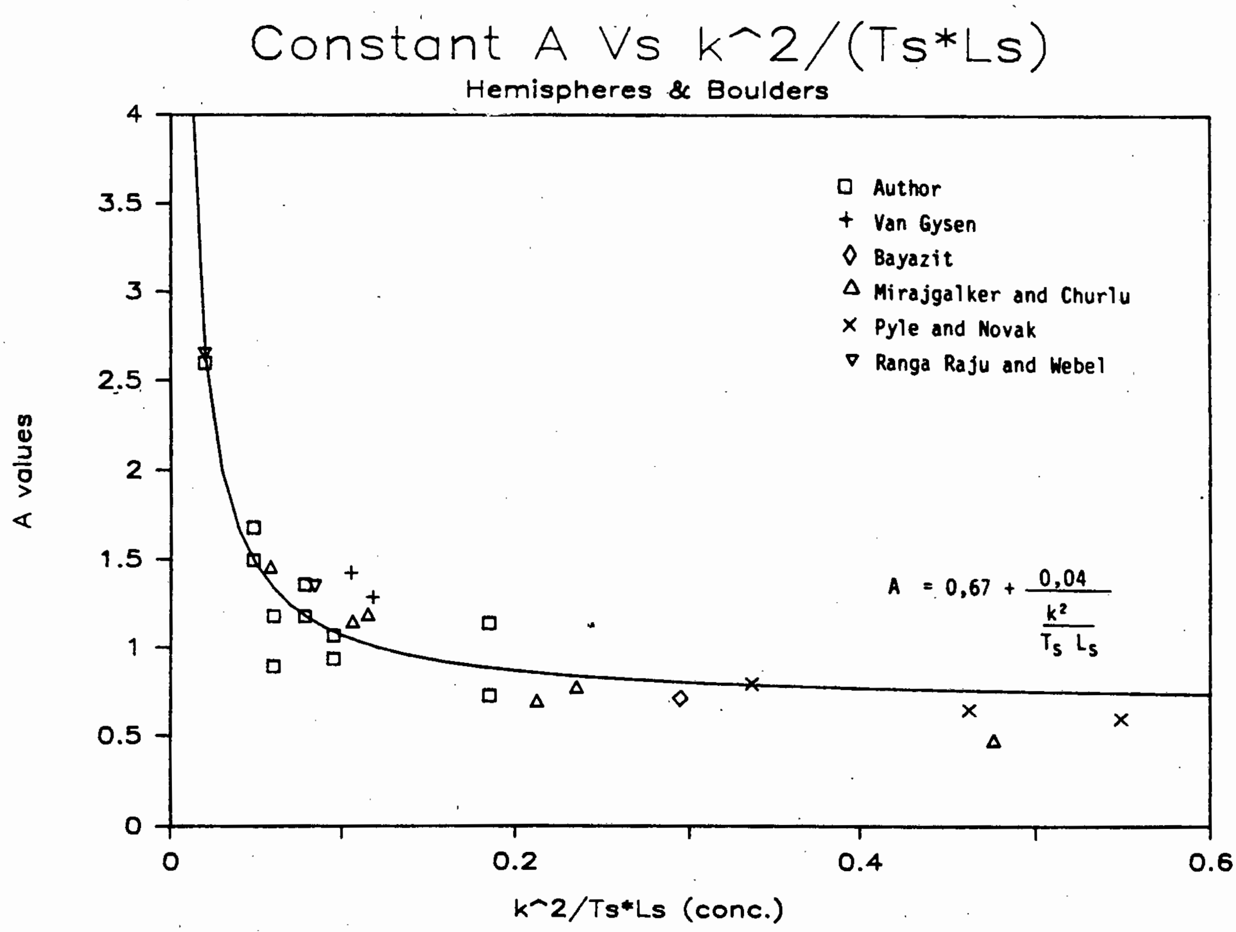

figure 6.4

B is equal to $^{0,813}/\kappa$, but von Kármán's constant was found not to be a true constant. Therefore B cannot be a constant. (See Figures 6.5 and 6.6). In order to make B a constant value it had to be multiplied by $\left[\frac{L_s}{T_s}\right]^{0,25}$ (see Figures 6.7 and 6.8) Therefore the friction equation is

$$\frac{1}{\sqrt{f}} = \left\{0,67 + \frac{0,04}{\left[\frac{k^2}{T_s L_s}\right]}\right\} + 2\left[\frac{T_s}{L_s}\right]^{0,25} \log \frac{R'}{k} \quad . \tag{6.4}$$

A comparison between observed and calculated f values can be seen in Figure 6.9 . This gives a good indication of how accurately the formula can predict the friction factor. The correlation coefficient between calculated and observed values is 0,94 .

6.4 RELATIONSHIP BETWEEN MANNING'S n AND RELATIVE ROUGHNESS

Manning's "n" can also be calculated in terms relative roughness, A , B and the hydraulic radius. (See Figure 6.10).

$$n' = \frac{R^{1/6}}{\sqrt{8g}\,\{A + B\log R'/k\}} \quad . \tag{6.5}$$

As the hydraulic radius increases (or the relative roughness $^{k}/R'$ decreases). Manning's n′ can be seen to tend to a constant. Therefore for a channel of large depth of flow compared to roughness height to have a constant n value is quite acceptable. However Manning's n must be used with caution in a channel of large relative roughness, as the n value changes by a large amount as the relative roughness changes.

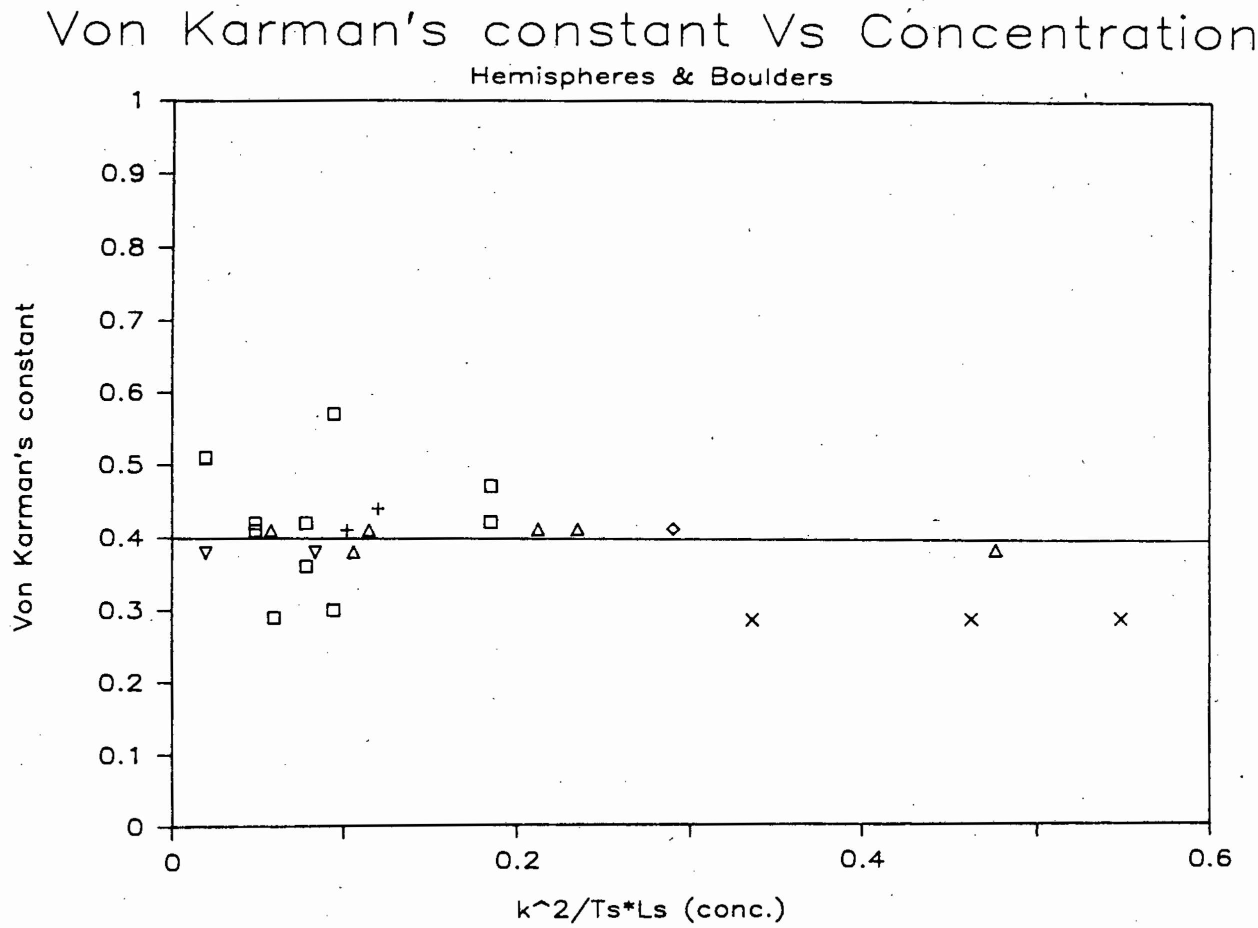

figure 6.5

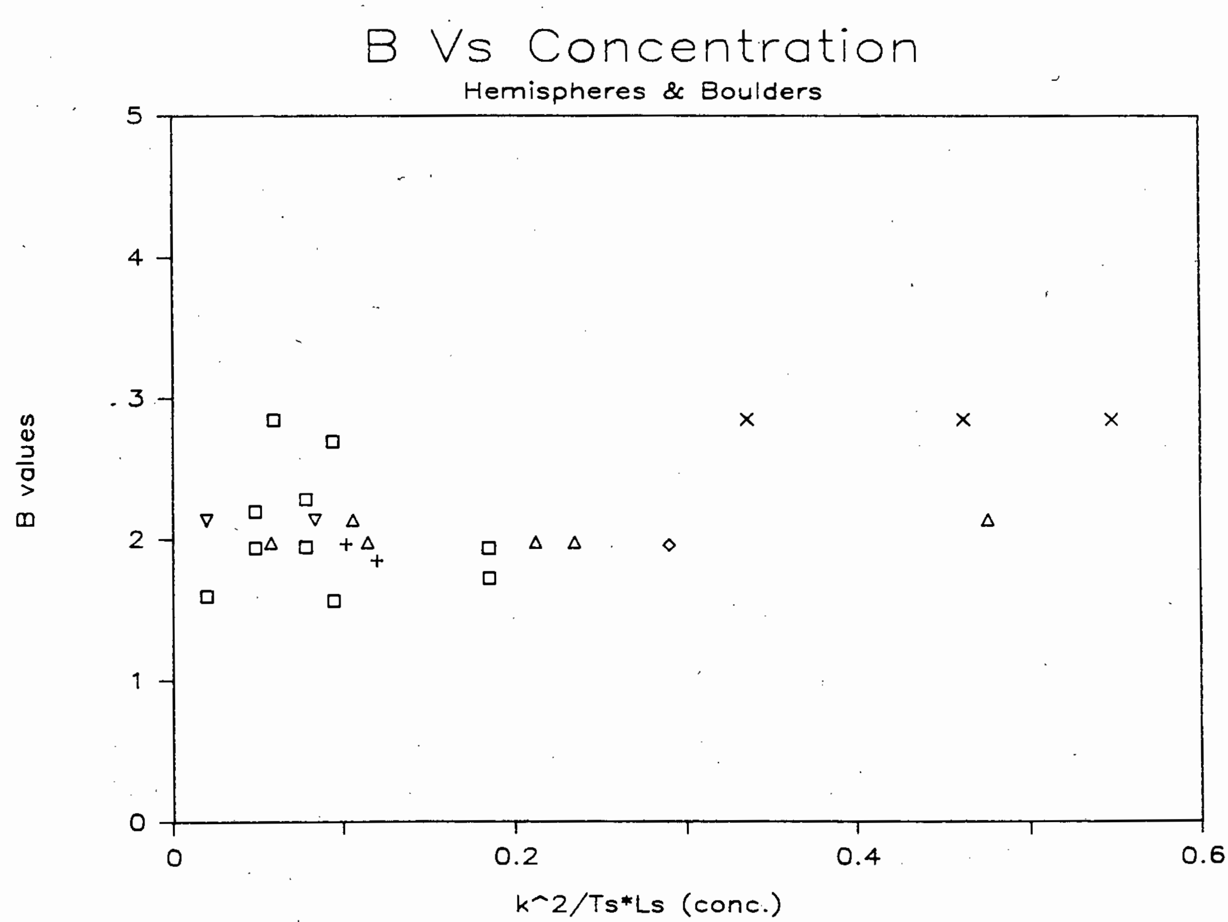

figure 6.6

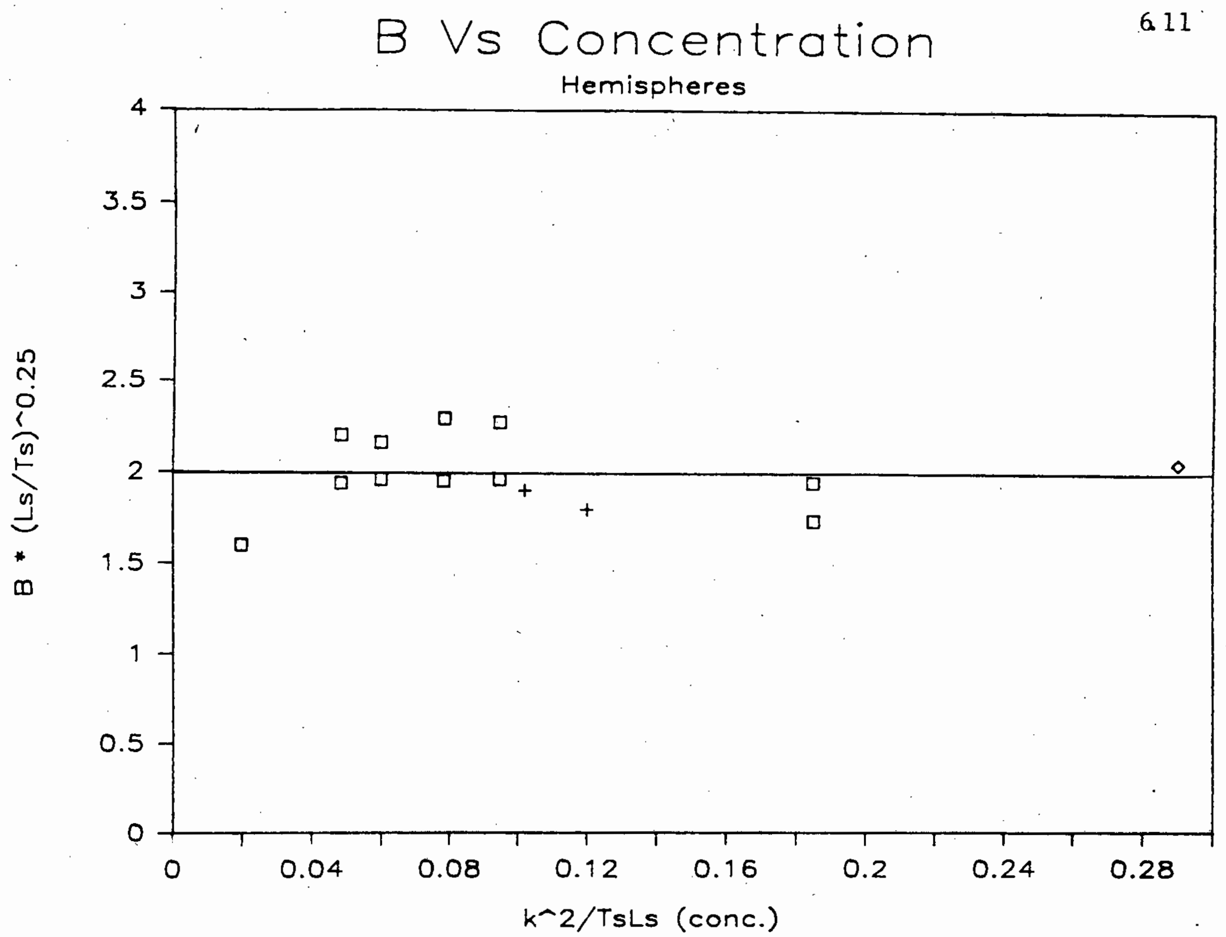

figure 6.7

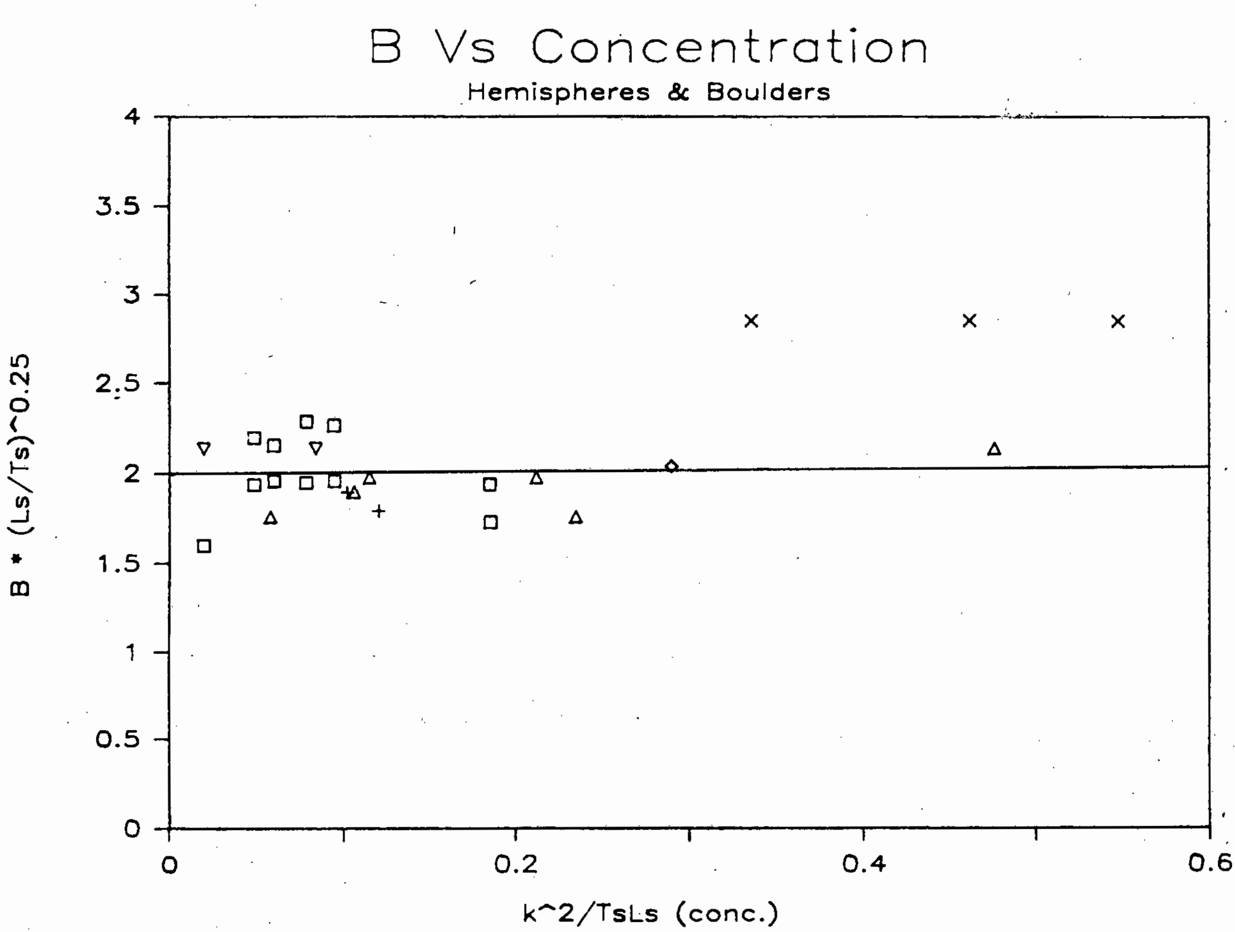

figure 6.8

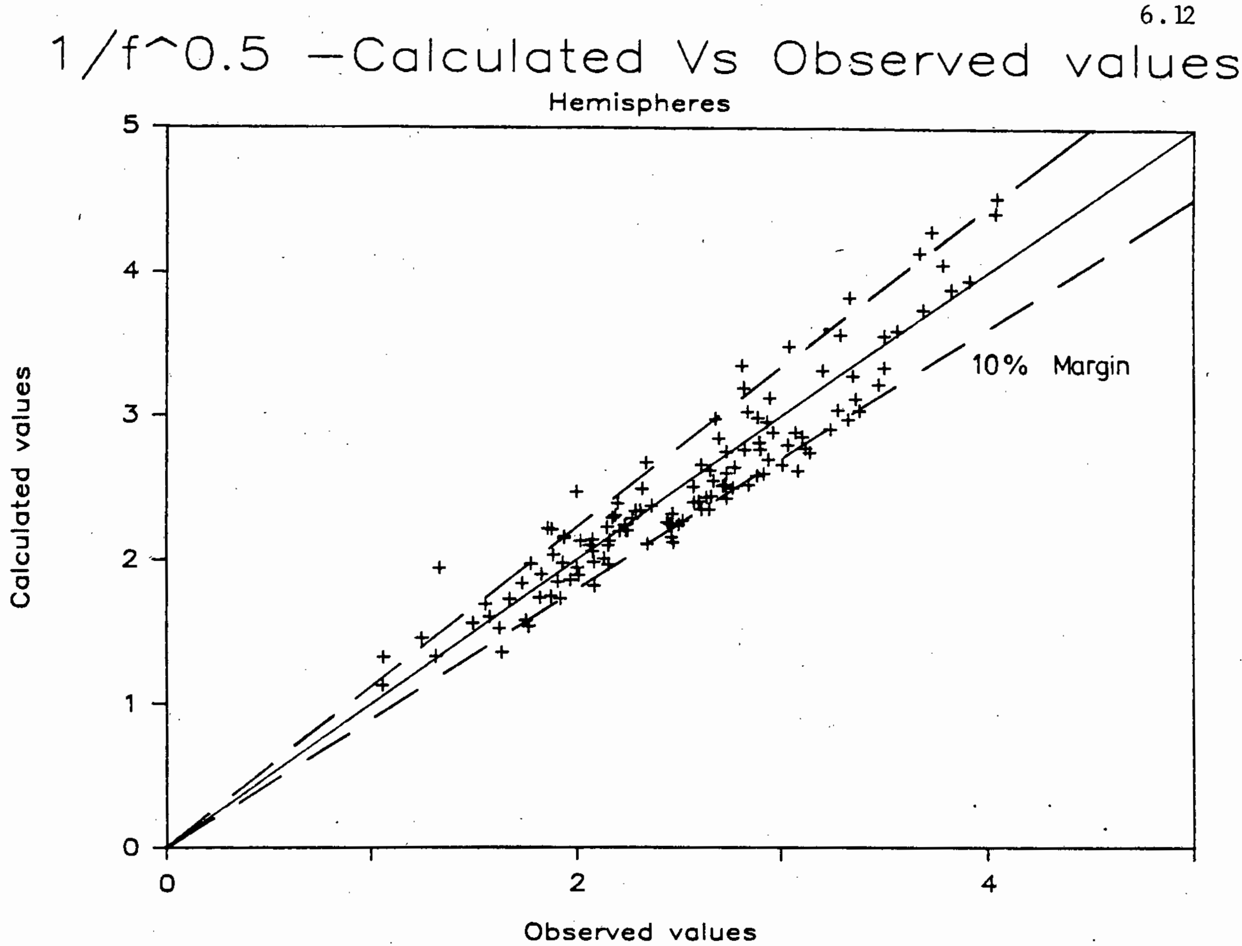

figure 6.9

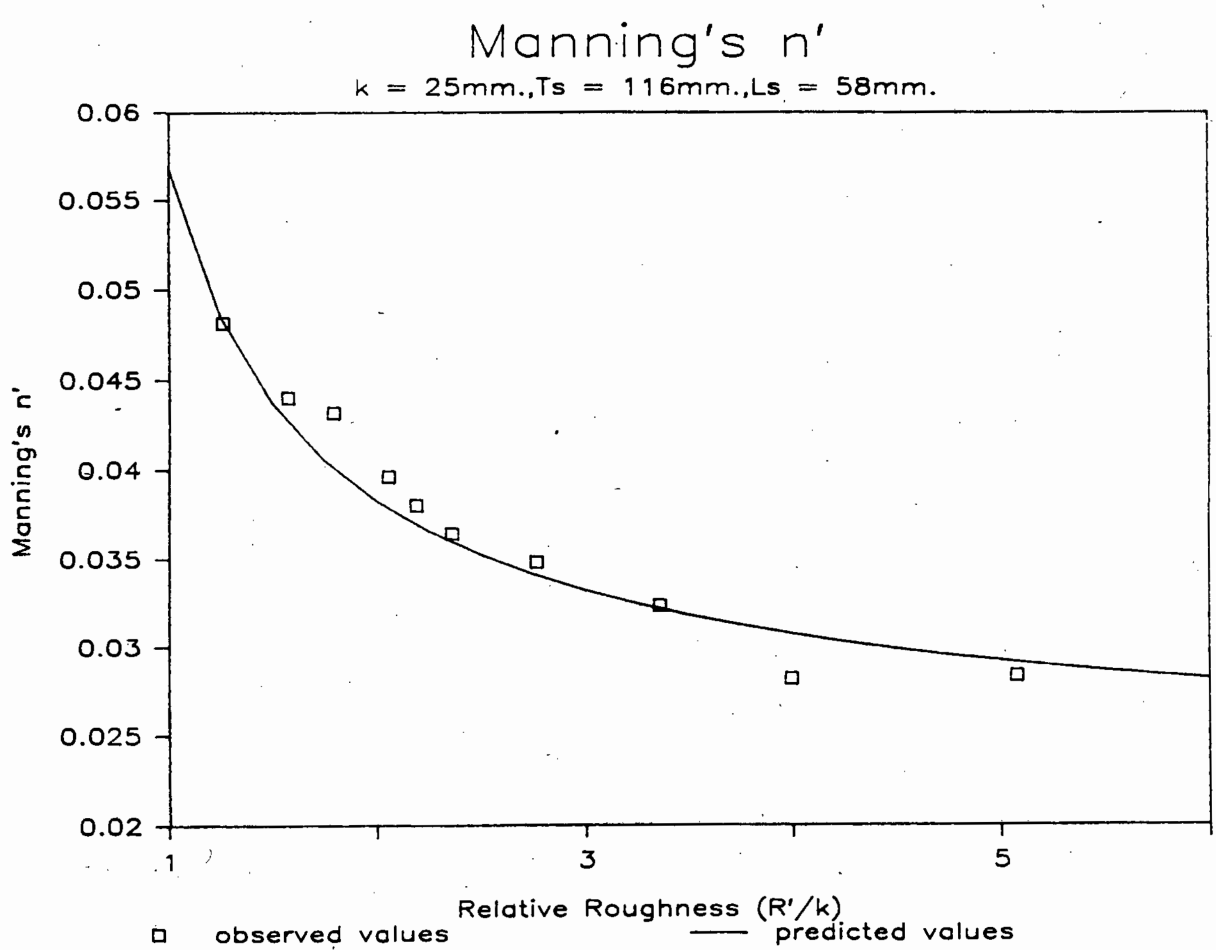

figure 6.10

CHAPTER 7

CONCLUSIONS

From the analysis of the experimental data and other studies the following conclusions were made :

1. The variation of the Darcy-Weisbach friction factor with respect to relative roughness is logarithmic. The equation can be written in the form :

$$\frac{1}{\sqrt{f}} = A + B\log\frac{R}{k}$$

where $A = 0{,}67 + 0{,}04/\left[\frac{k^2}{L_s T_s}\right]$

$$B = 2\left[\frac{T_s}{L_s}\right]^{0{,}25} .$$

(The equation yielded a correlation coefficient of 0,94).

2. Von Karman's constant of turbulence was found not to be a true constant, but was found to vary with the dimensionless number L_s/T_s .

3. Manning's n was found not to be a true constant. n varied considerably as depth of flow changed, up to a value of relative roughness of approximately ten $\left[R/k < 10\right]$. As the depth of flow increased n tended to a constant value. The equation to predict the correct n value is :

$$n = \frac{R^{1/6}}{\sqrt{8g}\,\{A + B\log R/k\}}$$

Therefore for small relative roughness it is quite satisfactory to have a constant n , but not for large relative roughness.

4. The general resistance diagram (or Moody diagram), where the friction factor is plotted against the Reynolds number, was found not to be very useful in the plotting of results from open channel flow as the relative roughness $\left[{}^{R}/k\right]$ is not constant as in pipe flow.

LIST OF REFERENCES

1. SCHLICHTING, H. Experimental investigation of the roughness problem, Proc. ASCE, Nov 1937, 16-31.

2. COLEBROOK, C.F. and WHITE, C.M. Experiments with fluid friction on roughened pipes, Proc. of Royal Society, London, 1937, 367-381.

3. COLEBROOK, C.F. Turbulent flow in pipes with particular reference to the transition region between smooth and rough pipe laws, J. Inst. C.E., London, 1938-39, 133-157.

4. MOODY, L.F. Friction factors for pipe flow, Trans. ASME, 1944, 671-684.

5. POWELL, R.W. Flow in a channel of definite roughness, Trans. ASCE., 1946, 531-566.

6. POWELL, R.W. Resistance to flow in rough channels, Trans. American Geophysical Union, Vol 31, Aug 1950, 575-582.

7. ROBINSON, A.R. and ALBERTSON, M.L. Artificial roughness standard for open channels, Trans. American Geophysical Union, Vol 33, Dec 1952, 881-888.

8. BOYER, M.C. Estimating the Manning coefficient from an average bed roughness in open channels, Trans. American Geophysical Union, Vol 35, Dec 1954, 957-961.

9. MORRIS, H.M. Flow in rough conduits, Trans. ASCE, Vol 120, 1955, 373-410.

10. SAYRE, W.W. and ALBERTSON, M.L. Roughness spacing in rigid open channels, Jnl. Hyd. Div. Proc. ASCE, Vol 87, May 1961, 121-150.

11. MIRAJGAOKER, A.G. and CHARLU, K.L.N. Natural roughness effects in rigid open channels, Jnl. Hyd. Div. Proc. ASCE, Vol 89, Sept 1963, 29-44.

12. BAYAZIT, M. Free surface flow in a channel of large relative roughness, Journal of Hydraulic Research, Vol 14, 1976, 115-126.

13. BATHURST, J.C. Flow resistance of large-scale roughness, Jnl. Hyd.Div. Proc. ASCE, Vol 104, Dec 1978, 1587-1603.

14. THOMPSON, S.M. and CAMPBELL, P.L. Hydraulics of a large channel paved with boulders, Jnl. Hyd. Res., Vol 17, 1979, 341-354.

15. BRAY, D.I. Estimating average velocity in gravel-bed rivers, Jnl. Hyd. Div. Proc. ASCE, Sept 1979, 1103-1122.

16. PYLE, R. and NOVAK, P. Coefficient of friction in conduits with large roughness, Jnl. Hyd. Res. Vol 19, 1981, 119-140.

17. BATHURST, J.C., LI, R. and SIMONS, D.B. Resistance equation for large-scale roughness, Jnl. Hyd. Div. Proc. ASCE, Vol 107, Dec 1981, 1593-1613.

18. PANSEGROUW, J.P. Discrepancy of the Colebrook-White equation in the extreme rough turbulent zone, The Civil Engineer in South Africa, Sept 1985, 489-492.

19. SHAHALAM, A.B. and MANSOUR, A.R. New method for the prediction of resistance coefficients for natural streams, Proc. Instn. Civ. Engrs., Part 2, 1988, 517-531.

20. VAN GYSEN, J.A. Large scale channel roughness, B.Sc thesis, U.C.T., 1986 (unpublished work).

21. WILSON, A. An investigation of roughness effects in open channel flow, B.Sc thesis, U.C.T., 1988 (unpublished work).

BIBLIOGRAPHY

1. BATHURST, J.C. Flow resistance of large-scale roughness, Jnl. Hyd. Div. Proc. ASCE, Vol 104, Dec 1978, 1587-1603.

2. BATHURST, J.C., LI, R., and SIMONS, D.B. Resistance equation for large-scale roughness roughness, Jnl. Hyd. Div. Proc. ASCE, Vol 107, Dec 1981, 1593-1613.

3. BAYAZIT, M. Free surface flow in a channel of large relative roughness. Journal of Hydraulic Research, Vol 14, 1976, 115-126.

4. BIERY, P.F. and DELLEUR, J.W. Discussion on roughness spacing in rigid open channels, Jnl. Hyd. Div. Proc. ASCE, Vol 87, 1961, 231-238.

5. BOYER, M.C. Estimating the Manning coefficient from an average bed roughness in open channels, Trans. American Geophysical Union, Vol 35, Dec 1954, 957-961.

6. BRAY, D.I. Estimating average velocity in gravel-bed rivers, Jnl. Hyd. Div. Proc. ASCE, Vol 105, Sept 1979, 1130-1122.

7. BRETTING, A.E. A set of practical hydraulic formulae based on recent experimental research, Proc. 2nd General Meeting, I.A.H.R. Stockholm, 1948, 399-415.

8. CHOW, V.T. Open channel hydraulics, McGraw-Hill, New York, 1959.

9. COLEBROOK, C.F. and WHITE, C.M. Experiments with fluid friction on roughened pipes, Proc. of Royal Society, London, 1937, 367-381.

10. COLEBROOK, C.F. Turbulent flow in pipes with particular reference to the transition region between smooth and rough pipe laws, J. Inst. C.E., London, 1938-1939, 133-157.

11. EINSTEIN, H.A. and BANKS, R.B. Flow resistance of composite roughness, Trans. American Geophysical Union, Vol 31, 1950, 603-610.

12. FLAMER, G.H. Free surface, velocity gradient flow past hemisphere, Jnl. Hyd. Div. Proc. ASCE, Vol 96, July 1970, 1485-1502.

13. GHOSH, S.N. and ROY, N. Boundary shear distribution in open channel flow, Jnl. Hyd. Div. Proc. ASCE, Vol 96, April 1970, 967-994.

14. HENDERSON, F.M. Open channel flow, Macmillan, New York, 1966.

15. HEY, R.D. Bar form resistance in gravel-bed rivers, Jnl. of Hydraulic Eng. ASCE, Vol 114, Dec 1988, 1498-1508.

16. Hydraulic Engineering, CIV 403F course notes, University of Cape Town, 1987.

17. LELIAVSKY, S. River and canal hydraulics, Chapman and Hall, 1965.

18. LOMAX, W.R. and SAUL, A.J. Laboratory work in hydraulics, Granada, London, 1979.

19. MIRAJGAOKER, A.G. and CHARLU, K.L.N. Natural roughness effects in rigid open channels, Jnl. Hyd. Div. Proc. ASCE, Vol 89, Sept 1963, 29-44.

20. MOODY, L.F. Friction factors for pipe flow, Trans. ASME, New Jersey, 1944, 671-684.

21. MORRIS, H.M. Flow in rough conduits, Trans. ASCE, Vol 120, 1955, 373-410.

22. MOTAYED, A.K. and KRISHNAMURTHY, M. Composite roughness of natural channels, Jnl. Hyd. Div. Proc. ASCE, Vol 106, Jan 1980, 1111-1116.

23. NEIL, C.R. Discussion on natural roughness effects in rigid open channels, Jnl. Hyd. Div. Proc. ASCE, Vol 90, 1964, 359.

24. NOVAK, P. and CABELKA, J. Models in hydraulic engineering, Pitman, advanced publishing.

25. POWELL, R.W. Flow in a channel of definite roughness, Trans. ASCE, 1946, 531-566.

26. POWELL, R.W. Resistance to flow in rough channels, Trans. American Geophysical Union, Vol 31, Aug 1950, 575-582.

27. PANSEGROUW, J.P. Discrepancy of the Colebook-White equation in the extreme rough turbulent zone, The Civil Engineer in South Africa, Sept 1985, 489-492.

28. PANSEGROUW, J.P. Comparison of conventional composite roughness formulae for channels, The Civil Engineer in South Africa, July 1986, 272-273.

29. PYLE, R. and NOVAK, P. Coefficient of friction in conduits with large roughness, Jnl. Hyd. Res., Vol 19, 1981, 119-140.

30. RANGA RAJU, K.G., WEBEL, G. and SCHATZMAN, M. Discussion on coefficient of friction in conduits with large roughness, Jnl. Hyd. Res., Vol 19, 1981, 359-362.

31. REYNOLDS, A.J. Turbulent flows in engineering, John Wiley and Sons, 1974.

32. ROBINSON, A.R, and ALBERTSON, M.L. Artificial roughness standard for open channels, Trans. American Geophysical Union, Vol 33, Dec 1952, 881-888.

33. ROUSE, H. Fluid mechanics for hydraulic engineers, McGraw-Hill, New York and London, 1938.

34. ROUSE, H. Critical analysis of open-channel resistance, Jnl. Hyd. Div. Proc. ASCE, Vol 91, July 1965, 1-25.

35. SAYRE, W.W. and ALBERTSON, M.L. Roughness spacing in rigid open channels, Jnl. Hyd. Div. Proc. ASCE, Vol 87, May 1961, 121-150.

36. SCHLICHTING, H. Experimental investigation of the roughness problem, Proc. ASCE, No. 1937, 16-31.

37. SHAHALAM, A.B. and MANSOUR, A.R. New method for the resistance coefficients for natural streams, Proc. Instn. Civ. Engrs. Part 2, 1988, 517-531.

38. Task force on friction factors in open channels, Jnl. Hyd. Div. Proc. ASCE, March 1963, 97-143.

39. THOMPSON, S.M. and CAMPBELL, P.L. Hydraulics of a large channel paved with boulders, Jnl. Hyd. Res. Vol 17, 1979, 341-354.

40. THORN, R.B. River engineering and water conservation works, Butterworths, London, 1966.

41. UNDERHILL, L.G. Introstat, third edition, Juta & Co., 1981.

42. VAN GYSEN, J.A. Large scale channel roughness, B.Sc Thesis, U.C.T., 1986, (unpublished work).

43. WEBBER, N.B. Fluid mechanics for civil engineers, E. and F.N. Spon Ltd., London, 1965.

44. WILSON, A. An investigation of roughness effects in open channel flow, B.Sc Thesis, U.C.T., 1988, (unpublished work).

APPENDIX A

Open Channel flow formulae

Equation name	Mean velocity (ms^{-1})	Applicable friction factor	Dimensions
Darcy-Weisbach	$\bar{V} = \sqrt{\frac{8g\,Rs}{f}}$	$\frac{1}{\sqrt{f}} = A + B\log\left[\frac{R}{k_s}\right]$	-
Chèzy	$\bar{V} = C\sqrt{RS}$	$C = \frac{1}{\sqrt{8g}}\left\{A + B\log\left[\frac{R}{k_s}\right]\right\}$	$\frac{\sqrt{L}}{T}$
Manning	$\bar{V} = \frac{1}{n}R^{2/3}S^{1/2}$	$n = \frac{R^{1/6}}{\sqrt{8g}\left\{A+B\log\left[R/ks\right]\right\}}$	$\frac{T}{L^{1/3}}$

It is assumed at high Reynolds numbers the friction factor becomes independent of viscous forces.

APPENDIX B

Friction Factors for Large Scale Roughness

Investigator/s (year)	Experimental Work (measurements converted to metric and approximated)	Roughness Geometry	Applicable Formula $1/\sqrt{f} = A + B \log R/k_s \; [k_s = \alpha k]$
H. Schlichting (1937)	Closed Flume width = 1,7 m length = 64 m	Spheres Spherical segments Cones Short angles Long angles (at different densities)	$A = 1,74$; $B = 2$; $0,118 \lesssim \alpha \lesssim 11,90$ eqn. (2.3); table 2.2
C.F. Colebrook and C.M. White (1937-39)	Pipe diameter 53,5 mm length 6m (air used)	Two sizes of Sand Grains (at different densities)	$A = 2,34$; $B = 2$; $\alpha = 1$ eqn. (2.4)
L.F. Moody (1944)	(used Colebrook-White results)	-	Graphical solution of the Colebrook-White equation figure 2.7
R.W. Powell (1950)	Flume length = 15 m width = 0,2 m	Square Strips (at different densities)	$A = 0$; $B = 2,62$; α is dependant on Roughness spacing $0,140 \lesssim \alpha \lesssim 0,753$ eqn. (2.7)
A.R. Robinson and M.L. Albertson (1952)	Flume length = 4 m width = 0,23 mm	Sheet metal angles	$A = 0,46$; $B = 1,66$; $\alpha = 1$ equn. (2.9)

M.C. Boyer (1954)	Rivers in Northwestern U.S.A.	Natural Roughness	A = 2,11 ; B = 2,03 ; α = 1 eqn. (2.10)
H.M. Morris (1955)	-	-	Wake-Interference Flow: $A = 1,75 + 0,35 \left[\frac{C\,L_s}{R}\right]\left[2,5-\psi\right];$ $B = 2\ ;\ k_s = L_s$ $\psi = 1,00 + \frac{R_e\sqrt{f}}{155000 \times \frac{2R}{L_s}}$ Isolated-Roughness Flow: see equation 2.15 Quazi-smooth Flow: see equation 2.16
W.W. Sayre and M.L. Albertson (1961)	Flume length = 22 m width = 2,4 m	Sheet metal angles	A = 0 ; B = 2,14 ; $K_s = \chi$ χ is dependant on Roughness Geometry eqn. (2.19)
A.G. Mirajgoaker & K.L.N. Charlu (1963)	Flume length = 8,5 m width = 0,9 m	Selected boulders	A = 0,61 ; B = 1,87 ; $K_s = \chi$ χ is dependant on Roughness Geometry eqn. (2.21)
M. Bayazit (1975)	Flume length = 9 m width = 0,25 m	Hemispheres (one concentration)	A = 2,13 ; B = 1,96 ; α = 5 eqn. (2.22)

J.C. Bathurst (1978)	Upper Tees River (Northern England)	Natural Roughness	See equation 2.23
S.M. Thompson P.L. Campbell (1979)	Open Channel and length = 308 m width = 41 m	Paved with loose boulders	$A = 2{,}16\left[1 - \frac{0{,}1\ k_s}{R}\right]$; $\alpha = 4{,}5$ $B = 2\left[1 - \frac{0{,}1\ k_s}{R}\right]$ eqn. (2.26)
D.I. Bray (1979)	Gravel-bed rivers in Alberta, Canada	Natural Roughness	A = 1,16 ; B = 2 ; $k_s = D_{84}$ eqn. (2.27)
R. Pyle and P. Novak (1981)	i) Flume length = 12 m width = 0,3 m ii) Rectangular Air Tunnel length = 5 m width = 0,3 m iii) Flume length = 150 m width = 1 m	i) Spheres ii) Hemispheres iii) Natural river boulders	A is a function Roughness Concentration figure 2.40 B = 2,86 R = is measured to a reference datum, so that κ is equal to 0,286 α is a function Roughness Concentration figure 2.41
J.C. Bathurst, R. Li, & D. Simons (1981)	Flume length = 9,54 m width = 1,168 m	Gravel and boulders	See equation 2.31
A.B. Shahalam & A.R. Mansour (1988)	Wadi Elwala River Jordan	Natural Roughness	A = 0,55 ; B = 2,09 ; $k_s = D_{50}$ figure 2.44

APPENDIX C

Dimensional Analysis

$$\tau_o = \phi \{ \bar{V} , R , \rho , \mu , k_s \}$$

or

$$\tau_o = \Sigma \, \bar{V}^a \, R^b \, \rho^c \, \mu^d \, k_s{}^e$$

equating the dimensions on both sides

$$ML^{-1}T^{-2} = (LT^{-1})^a \, L^b \, (ML^{-3})^c \, (ML^{-1}T^{-1})^d \, L^e$$

$$\underline{M}| \quad 1 = c + d$$

$$\underline{L}| \quad -1 = a + b - 3c - d + e$$

$$\underline{T}| \quad 2 = a + d$$

$$a = 2 - d$$

$$b = -d - 3$$

$$c = 1 - d$$

$$\tau_o = \Sigma \, \bar{V}^2 \, \bar{V}^{-d} \, R^{-d} \, R^{-e} \, \rho \, \rho^{-d} \, \mu^d \, k_s{}^e$$

$$\tau_o = \Sigma \, \rho \bar{V}^2 \left[\frac{\rho \bar{V} R}{\mu} \right]^{-d} \left[\frac{k_s}{R} \right]^{-e}$$

$$f = \frac{\tau_o}{{}^1/_8 \, \rho \, \bar{V}^2} = \phi \left\{ \left[\frac{\rho \bar{V} R}{\mu} \right] ; \left[\frac{k_s}{R} \right] \right\}$$

APPENDIX D

Integration of the velocity distribution over the flow depth in order to determine the mean velocity

$$\bar{V} = \frac{\int_o^{y_n} V\,dy}{y_n} \qquad \left\{ V = \frac{2,30}{\kappa} V_* \log \frac{y}{m\,k_s} \right\}$$

$$\bar{V} = \frac{2,30}{\kappa} V_* \left\{ \int_o^{y_n} \log \frac{y}{m\,k_s}\,dy \right\} / yn$$

as $$\log \frac{y}{m\,k_s} = \frac{\mathrm{Ln}\ {}^{y}/m\,k_s}{\mathrm{Ln}\ 10}$$

$$\int_o^{y_n} \frac{\mathrm{Ln}\ {}^{y}/m\,k_s}{\mathrm{Ln}\ 10}\,dy = \frac{[y \ln \frac{y}{m\,k_s} - y + c]_o^{y_n}}{\mathrm{Ln}\ 10} = \frac{y_n\ \mathrm{Ln} \left\{ {}^{y_n}/m\,k_s \right\} - y_n}{\mathrm{Ln}\ 10}$$

$$\bar{V} = \frac{2,30}{\kappa} V_* \left\{ \log \frac{y_n}{m\,k_s} - \frac{1}{\mathrm{Ln} 10} \right\}$$

$$\frac{\bar{V}}{V_*} = \frac{2,30}{\kappa} \left\{ \log \frac{y_n}{m\,k_s} - \log 2,718 \right\}$$

$$\frac{\bar{V}}{V_*} = \frac{2,30}{\kappa} \left\{ \log \frac{y_n}{k_s} - \log 2,718m \right\}$$

From the Darcy-Weisbach equation

$$\frac{\bar{V}}{V_*} = \sqrt{\frac{8}{f}}$$

$$\therefore \qquad \frac{1}{\sqrt{f}} = \frac{0,813}{\kappa}\left\{\log\frac{y_n}{k_s} - \log 2,718\ m\right\}$$

assume $\kappa = 0,4$ and $m = \frac{1}{30}$

$$\therefore \qquad \frac{1}{\sqrt{f}} = 2,03\ \log\frac{y_n}{k_s} + 2,12$$

Can be written in the general form :

$$\frac{1}{\sqrt{f}} = A + B\ \log\left[\frac{R}{k_s}\right] \quad .$$

APPENDIX E

LARGE SCALE ROUGHNESS WORKSHEET
(CALCULATIONS)

TEST No. 1 SLOPE= 0.001

ROUGHNESS GEOMETRY
(Hemispheres)

k= 25 mm.
Ls= 58 mm.
Ts= 58 mm.
Conc.= 0.583940

k^2/Ts*Ls=0.185790
Ts/Ls= 1
G. mean= 9.732337

Run	R mm.	R' mm.	Q 1/s	v m/s	v* m/s	To N/m^2
1	43.05	33.31766	0.558	0.054025	0.018078	0.326846
2	51.55	41.81766	0.789	0.060863	0.020254	0.410231
3	94.25	84.51766	2.846	0.108623	0.028794	0.829118
4	114.85	105.1176	5.976	0.183388	0.032112	1.031204
5	125.25	115.5176	6.412	0.179053	0.033663	1.133228
6	126.2	116.4676	6.428	0.178036	0.033801	1.142547
7	138.8	129.0676	8.813	0.220264	0.035583	1.266153
8	165.4	155.6676	10.677	0.221252	0.039078	1.527099
9	219.45	209.7176	16.255	0.250028	0.045357	2.057330
10	225.9	216.1676	17.081	0.254894	0.046050	2.120604

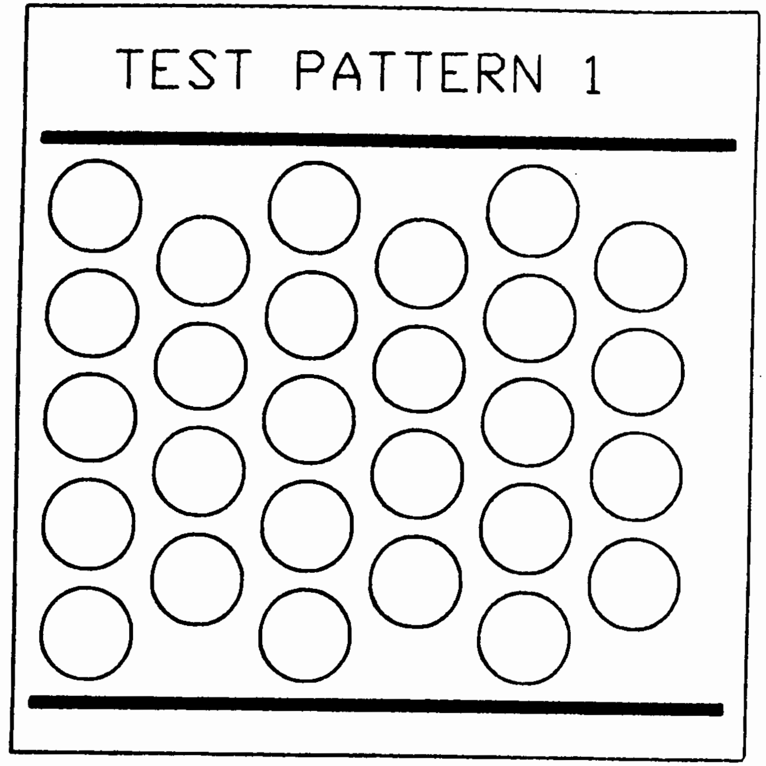

Run -	C m^0.5/s	n m^-0.33/s	n' m^-0.33/s	1/f^0.5 -	Log f -	R'/k -	LogR'/k -	ks mm	LogRe -	LogRew -	LogFr -
1	9.359673	0.060605	0.059972	1.056528	-0.04776	1.332706	0.124734	73.18301	3.255272	2.655111	-0.78174
2	9.411864	0.062595	0.061824	1.062419	-0.05259	1.672706	0.223419	91.23255	3.405715	2.704454	-0.82867
3	11.81549	0.056065	0.054477	1.333744	-0.25014	3.380706	0.529007	134.9197	3.962873	2.857248	-0.88269
4	17.88691	0.038406	0.036035	2.019090	-0.61031	4.204706	0.623735	76.23076	4.285048	2.904612	-0.74997
5	16.65939	0.041889	0.039395	1.880527	-0.54855	4.620706	0.664708	98.26176	4.315631	2.925098	-0.80133
6	16.49704	0.042359	0.039859	1.862201	-0.54005	4.658706	0.668265	101.1823	4.316714	2.926877	-0.80736
7	19.38812	0.036665	0.033680	2.188549	-0.68031	5.162706	0.712877	77.00919	4.453762	2.949183	-0.75954
8	17.73331	0.041359	0.037969	2.001752	-0.60282	6.226706	0.794258	115.1653	4.537087	2.989873	-0.83897
9	17.26524	0.044643	0.040235	1.948916	-0.57958	8.388706	0.923694	164.8833	4.719625	3.054592	-0.91531
10	17.33666	0.044684	0.040141	1.956978	-0.58317	8.646706	0.936850	168.3842	4.741151	3.061169	-0.92009

LARGE SCALE ROUGHNESS WORKSHEET
(CALCULATIONS)

TEST No. 2 SLOPE= 0.001

ROUGHNESS GEOMETRY
(Hemispheres)

k=	25 mm.	k^2/Ts*Ls=	0.046447
Ls=	116 mm.	Ts/Ls=	1
Ts=	116 mm.	G. mean=	2.433084
Conc.=	0.145985		

Run	R mm.	R' mm.	Q l/s	v m/s	v* m/s	To N/m^2
1	30.5	28.06691	0.644	0.074016	0.016593	0.275336
2	45.95	43.51691	1.643	0.121791	0.020661	0.426900
3	58.35	55.91691	2.537	0.146357	0.023421	0.548544
4	68.2	65.76691	3.349	0.164265	0.025400	0.645173
5	80.5	78.06691	4.394	0.181564	0.027673	0.765836
6	86	83.56691	5.599	0.216129	0.028632	0.819791
7	93.3	90.86691	6.314	0.224149	0.029856	0.891404
8	98.15	95.71691	6.713	0.226238	0.030642	0.938982
9	108	105.5669	8.139	0.248703	0.032180	1.035611
10	126.05	123.6169	11.181	0.291770	0.034823	1.212681

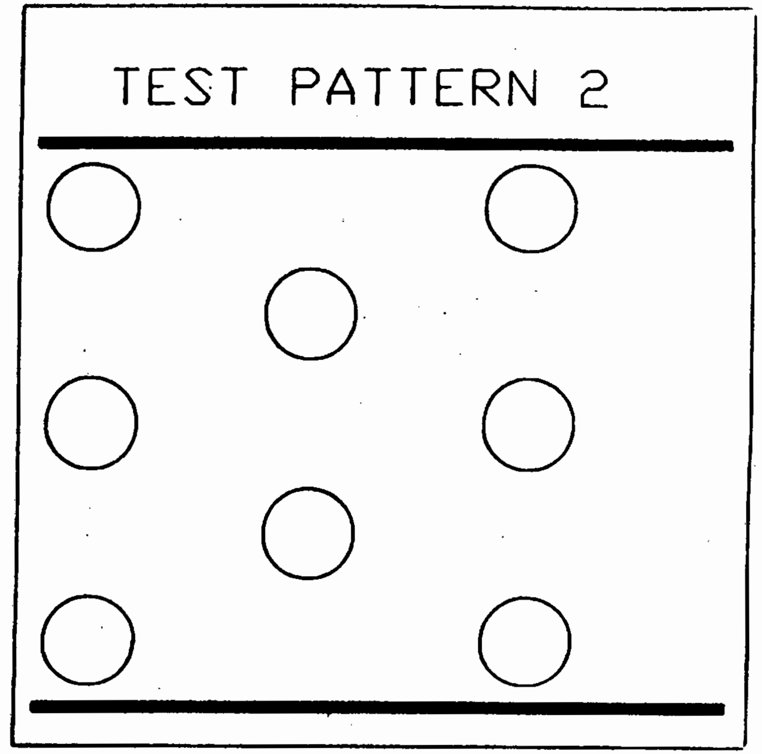

Run -	C m^0.5/s	n m^-0.33/s	n' m^-0.33/s	1/f^0.5 -	Log f -	R'/k -	LogR'/k -	ks mm	LogRe -	LogRew -	LogFr -
1	13.97114	0.039457	0.038815	1.577076	-0.39570	1.122676	0.050254	33.85763	3.317524	2.617871	-0.57053
2	18.46242	0.032122	0.031044	2.084055	-0.63781	1.740676	0.240718	29.28400	3.724275	2.713103	-0.54470
3	19.57239	0.031594	0.030202	2.209349	-0.68852	2.236676	0.349603	32.57379	3.912958	2.767546	-0.57379
4	20.25546	0.031365	0.029723	2.286455	-0.71832	2.630676	0.420067	35.05740	4.033553	2.802778	-0.59413
5	20.54933	0.031813	0.029878	2.319627	-0.73083	3.122676	0.494527	40.05466	4.151498	2.840008	-0.62510
6	23.64270	0.027966	0.025753	2.668810	-0.85263	3.342676	0.524094	28.68330	4.256748	2.854791	-0.57898
7	23.51441	0.028514	0.026129	2.654328	-0.84790	3.634676	0.560465	31.71329	4.308942	2.872977	-0.59953
8	23.12447	0.029247	0.026767	2.610311	-0.83338	3.828676	0.583048	35.14250	4.335554	2.884268	-0.61809
9	24.20569	0.028400	0.025618	2.732361	-0.87307	4.222676	0.625587	33.67807	4.419209	2.905538	-0.61951
10	26.24231	0.026894	0.023528	2.962256	-0.94324	4.944676	0.694137	30.26563	4.557118	2.939813	-0.61870

LARGE SCALE ROUGHNESS WORKSHEET
(CALCULATIONS)

TEST No. 3 SLOPE= 0.001

ROUGHNESS GEOMETRY
(Hemispheres)

k= 25 mm.
Ls= 58 mm.
Ts= 116 mm.
Conc.= 0.291970

k^2/Ts*Ls=0.092895
Ts/Ls= 2
G. mean= 4.866168

Run	R mm.	R' mm.	Q 1/s	v m/s	v* m/s	To N/m^2
1	36.5	31.63383	0.644	0.065670	0.017616	0.310327
2	44.35	39.48383	1.019	0.083251	0.019680	0.387336
3	49.8	44.93383	1.289	0.092537	0.020995	0.440800
4	56.4	51.53383	1.765	0.110481	0.022484	0.505546
5	59.7	54.83383	2.039	0.119951	0.023193	0.537919
6	63.95	59.08383	2.411	0.131633	0.024075	0.579612
7	74.1	69.23383	3.285	0.153057	0.026061	0.679183
8	88.9	84.03383	4.887	0.187597	0.028711	0.824371
9	104.85	99.98383	7.488	0.241587	0.031318	0.980841
10	131.85	126.9838	11.088	0.281671	0.035294	1.245711

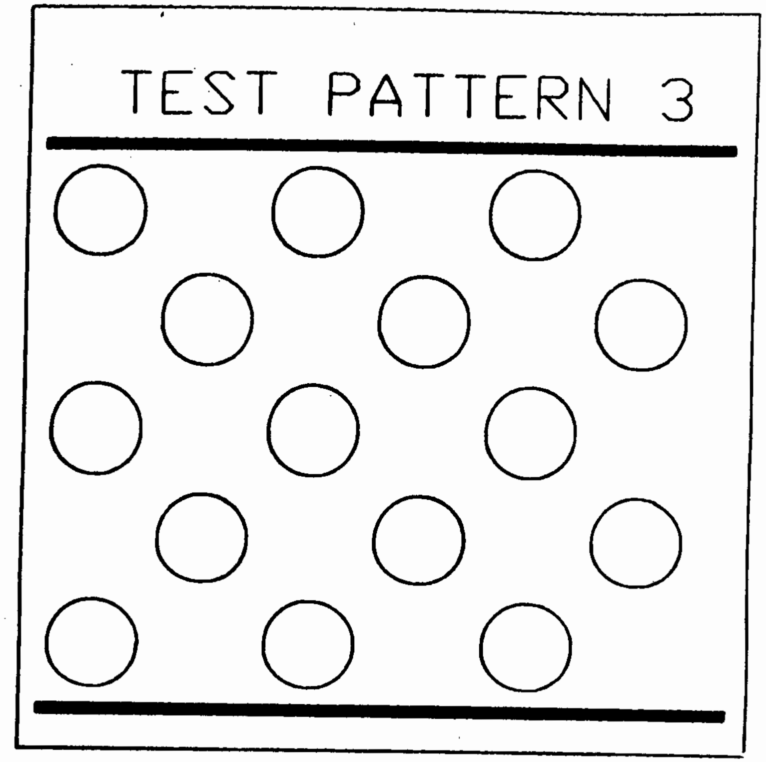

Run -	C m^0.5/s	n m^-0.33/s	n' m^-0.33/s	1/f^0.5 -	Log f -	R'/k -	LogR'/k -	ks mm	LogRe -	LogRew -	LogFr -
1	11.67606	0.048163	0.047503	1.318004	-0.23983	1.265353	0.102211	51.42205	3.317524	2.643850	-0.67444
2	13.24901	0.044043	0.043195	1.495560	-0.34960	1.579353	0.198479	52.31652	3.516812	2.691984	-0.66769
3	13.80482	0.043190	0.042221	1.558301	-0.38530	1.797353	0.254633	55.38888	3.618891	2.720061	-0.67792
4	15.39020	0.039636	0.038484	1.737260	-0.47972	2.061353	0.314152	51.69664	3.755383	2.749820	-0.66047
5	16.19879	0.038049	0.036801	1.828534	-0.52420	2.193353	0.341108	49.52008	3.818055	2.763298	-0.65171
6	17.12507	0.036442	0.035070	1.933094	-0.57250	2.363353	0.373528	47.30657	3.890835	2.779508	-0.64377
7	18.39484	0.034835	0.033194	2.076426	-0.63463	2.769353	0.442378	47.00076	4.025173	2.813933	-0.64713
8	20.46441	0.032339	0.030273	2.310042	-0.72723	3.361353	0.526514	43.59464	4.197680	2.856001	-0.64289
9	24.16069	0.028197	0.025554	2.727281	-0.87145	3.999353	0.601989	32.08403	4.383004	2.893739	-0.60852
10	24.99590	0.028362	0.025000	2.821560	-0.90097	5.079353	0.705808	36.55679	4.553491	2.945648	-0.64567

LARGE SCALE ROUGHNESS WORKSHEET
(CALCULATIONS)

TEST No. 4 SLOPE= 0.001

ROUGHNESS GEOMETRY
(Hemispheres)

k= 25 mm.
Ls= 116 mm.
Ts= 58 mm.
Conc.= 0.291970

k^2/Ts*Ls=0.092895
Ts/Ls= 0.5
G. mean= 4.866168

Run	R mm.	R' mm.	Q l/s	v m/s	v* m/s	To N/m^2
1	46.2	41.33383	0.911	0.071096	0.020136	0.405484
2	50.3	45.43383	1.367	0.097057	0.021111	0.445705
3	64.85	59.98383	2.137	0.114923	0.024257	0.588441
4	75.7	70.83383	3.124	0.142268	0.026360	0.694879
5	88.85	83.98383	3.758	0.144344	0.028703	0.823881
6	105.1	100.2338	5.691	0.183152	0.031357	0.983293
7	113.8	108.9338	6.062	0.179511	0.032690	1.068640
8	120.15	115.2838	7.611	0.212966	0.033629	1.130934
9	134.6	129.7338	9.216	0.229154	0.035674	1.272688
10	154.15	149.2838	11.022	0.238169	0.038268	1.464474

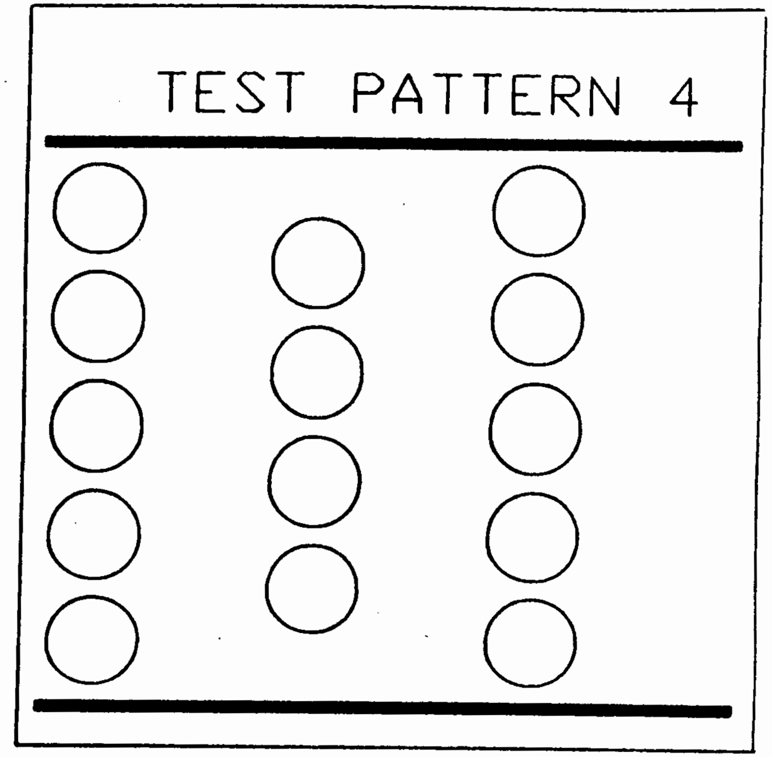

Run -	C m^0.5/s	n m^-0.33/s	n' m^-0.33/s	1/f^0.5 -	Log f -	R'/k -	LogR'/k -	ks mm	LogRe -	LogRew -	LogFr -
1	11.05855	0.053171	0.052355	1.248299	-0.19263	1.653353	0.218365	72.80413	3.468156	2.701927	-0.75612
2	14.39918	0.041484	0.040486	1.625392	-0.42191	1.817353	0.259439	51.84215	3.644406	2.722464	-0.66202
3	14.83855	0.042163	0.040865	1.674989	-0.44802	2.399353	0.380094	64.64568	3.838442	2.782791	-0.70929
4	16.90395	0.038052	0.036445	1.908133	-0.56121	2.833353	0.452300	58.36789	4.003349	2.818894	-0.68880
5	15.75076	0.042013	0.040201	1.777960	-0.49984	3.359353	0.526255	80.39249	4.083595	2.855872	-0.75646
6	18.29386	0.037255	0.034960	2.065027	-0.62985	4.009353	0.603074	68.94462	4.263826	2.894281	-0.72987
7	17.19927	0.040180	0.037778	1.941469	-0.57626	4.357353	0.639222	86.38294	4.291254	2.912355	-0.77474
8	19.83478	0.035171	0.032450	2.238968	-0.70009	4.611353	0.663828	64.90591	4.390080	2.924658	-0.72512
9	20.11874	0.035364	0.032307	2.271022	-0.71244	5.189353	0.715113	70.39504	4.473180	2.950301	-0.74459
10	19.49303	0.037363	0.033937	2.200391	-0.68500	5.971353	0.776072	87.86517	4.550898	2.980780	-0.78879

LARGE SCALE ROUGHNESS WORKSHEET
(CALCULATIONS)

TEST No. 5 SLOPE= 0.001

ROUGHNESS GEOMETRY
(Hemispheres)

k= 25 mm.
Ls= 88 mm.
Ts= 88 mm.
Conc.= 0.253664

k^2/Ts*Ls=0.080707
Ts/Ls= 1
G. mean= 4.227735

Run	R mm.	R' mm.	Q l/s	v m/s	v* m/s	To N/m^2
1	45.45	41.22226	1.116	0.087331	0.020109	0.404390
2	52.1	47.87226	1.705	0.114889	0.021670	0.469626
3	61.1	56.87226	2.368	0.134313	0.023620	0.557916
4	73	68.77226	3.254	0.152630	0.025974	0.674655
5	79.05	74.82226	3.84	0.165553	0.027092	0.734006
6	91.1	86.87226	5.43	0.201630	0.029192	0.852216
7	100.45	96.22226	6.866	0.230179	0.030723	0.943940
8	110.95	106.7222	8.049	0.243290	0.032356	1.046945
9	120.3	116.0722	9.328	0.259237	0.033744	1.138668
10	132.45	128.2222	10.898	0.274171	0.035466	1.257860

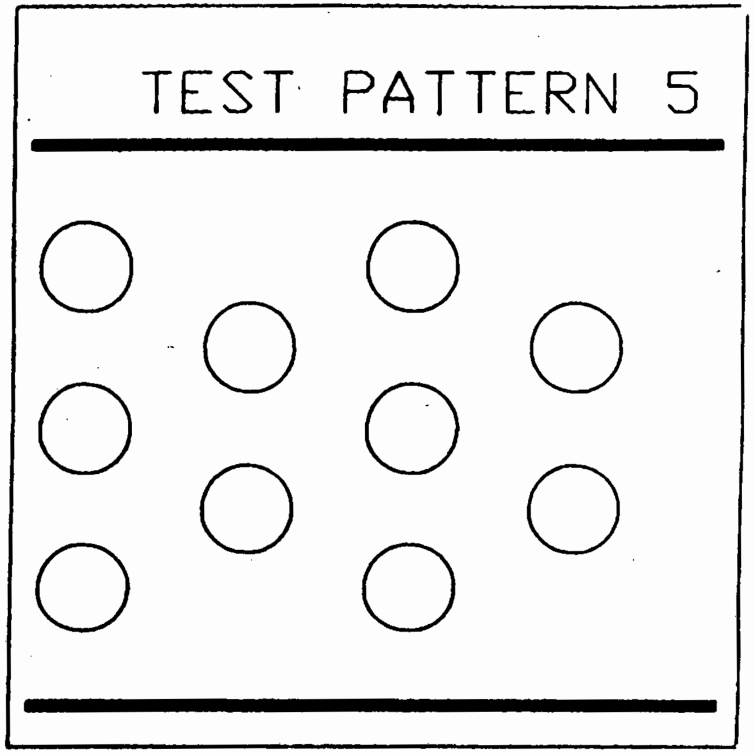

Run -	C m^0.5/s	n m^-0.33/s	n' m^-0.33/s	1/f^0.5 -	Log f -	R'/k -	LogR'/k -	ks mm	LogRe -	LogRew -	LogFr -
1	13.60206	0.043209	0.042317	1.535413	-0.37245	1.648890	0.217191	52.17053	3.556302	2.701340	-0.66563
2	16.60491	0.036288	0.035171	1.874378	-0.54571	1.914890	0.282143	41.01047	3.740362	2.733816	-0.61147
3	17.81021	0.034818	0.033468	2.010433	-0.60657	2.274890	0.356960	41.65659	3.883020	2.771224	-0.61845
4	18.40500	0.034777	0.033146	2.077573	-0.63511	2.750890	0.439473	46.62583	4.021055	2.812481	-0.64543
5	19.13917	0.033916	0.032120	2.160447	-0.66908	2.992890	0.476090	46.11125	4.092969	2.830789	-0.64676
6	21.63298	0.030762	0.028571	2.441950	-0.77547	3.474890	0.540941	38.71735	4.243438	2.863215	-0.62599
7	23.46544	0.028847	0.026336	2.648800	-0.84609	3.848890	0.585335	33.79678	4.345342	2.885412	-0.61287
8	23.55036	0.029244	0.026474	2.658386	-0.84923	4.268890	0.630315	37.07332	4.414380	2.907902	-0.63379
9	24.06213	0.029025	0.025996	2.716155	-0.86790	4.642890	0.666788	37.72685	4.478426	2.926138	-0.64269
10	24.21251	0.029327	0.025992	2.733131	-0.87332	5.128890	0.710023	40.86936	4.545985	2.947756	-0.66161

LARGE SCALE ROUGHNESS WORKSHEET
(CALCULATIONS)

TEST No. 6 SLOPE= 0.001

ROUGHNESS GEOMETRY
(Hemispheres)

k= 25 mm.
Ls= 88 & 88 mm.
Ts= 88 & 88 mm.
Conc.= 0.31708

k^2/Ts*Ls=0.080707
Ts/Ls= 1
G. mean= 4.227735

Run	R mm.	R' mm.	Q 1/s	v m/s	v* m/s	To N/m^2
1	42.3	38.07226	1.116	0.094557	0.019325	0.373488
2	51.85	47.62226	1.705	0.115492	0.021614	0.467174
3	59.4	55.17226	2.185	0.127752	0.023264	0.541239
4	69.6	65.37226	3.057	0.150848	0.025323	0.641301
5	76.8	72.57226	3.617	0.160774	0.026682	0.711933
6	86.2	81.97226	4.534	0.178423	0.028357	0.804147
7	92.6	88.37226	5.691	0.207735	0.029443	0.866931
8	101.05	96.82226	6.774	0.225687	0.030819	0.949826
9	119.15	114.9222	10.696	0.300230	0.033576	1.127387
10	150.4	146.1722	16.239	0.358370	0.037867	1.433949

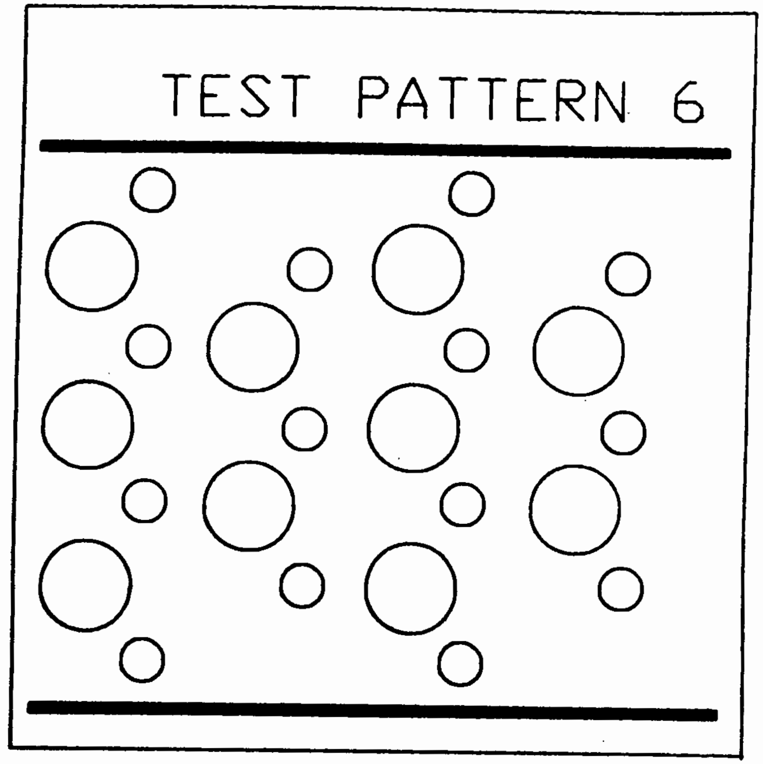

Run -	C m^0.5/s	n m^-0.33/s	n' m^-0.33/s	1/f^0.5 -	Log f -	R'/k -	LogR'/k -	ks mm	LogRe -	LogRew -	LogFr -
1	15.32461	0.037847	0.036971	1.729855	-0.47601	1.522890	0.182668	38.51950	3.556302	2.684078	-0.59658
2	16.73584	0.035973	0.034857	1.889157	-0.55253	1.904890	0.279870	40.10803	3.740362	2.732679	-0.60692
3	17.19921	0.035873	0.034581	1.941462	-0.57625	2.206890	0.343780	43.75115	3.848089	2.764634	-0.62702
4	18.65707	0.034018	0.032450	2.106027	-0.64692	2.614890	0.417453	42.89236	3.993933	2.801471	-0.62852
5	18.87255	0.034220	0.032486	2.130351	-0.65690	2.902890	0.462830	46.30147	4.066986	2.824159	-0.64622
6	19.70695	0.033444	0.031462	2.224538	-0.69447	3.278890	0.515726	46.92428	4.165119	2.850607	-0.65388
7	22.09799	0.030201	0.027951	2.494442	-0.79394	3.534890	0.548375	37.07617	4.263826	2.866932	-0.62047
8	22.93615	0.029543	0.027047	2.589054	-0.82628	3.872890	0.588035	36.42907	4.339483	2.886762	-0.62413
9	28.00615	0.024896	0.021640	3.161359	-0.99974	4.596890	0.662464	22.37300	4.537859	2.923976	-0.57461
10	29.64149	0.024485	0.020266	3.345959	-1.04904	5.846890	0.766924	23.00834	4.719197	2.976207	-0.60220

LARGE SCALE ROUGHNESS WORKSHEET
(CALCULATIONS)

TEST No. 7 SLOPE= 0.001

ROUGHNESS GEOMETRY
(Hemispheres)

k= 12.5 mm.
Ls= 88 mm.
Ts= 88 mm.
Conc.= 0.063416

k^2/Ts*Ls=0.020176
Ts/Ls= 1
G. mean= 0.528466

Run	R mm.	R' mm.	Q l/s	v m/s	v* m/s	To N/m^2
1	18.45	17.92153	0.558	0.100437	0.013259	0.175810
2	21.7	21.17153	0.789	0.120216	0.014411	0.207692
3	27.1	26.57153	1.206	0.146409	0.016145	0.260666
4	35.45	34.92153	1.986	0.183452	0.018508	0.342560
5	47.9	47.37153	2.988	0.203470	0.021557	0.464714
6	54.8	54.27153	4.299	0.255525	0.023073	0.532403
7	68.5	67.97153	5.655	0.268376	0.025822	0.666800
8	80.9	80.37153	7.39	0.296606	0.028079	0.788444
9	93.8	93.27153	9.994	0.345643	0.030248	0.914993
10	105.7	105.1715	11.987	0.367663	0.032120	1.031732

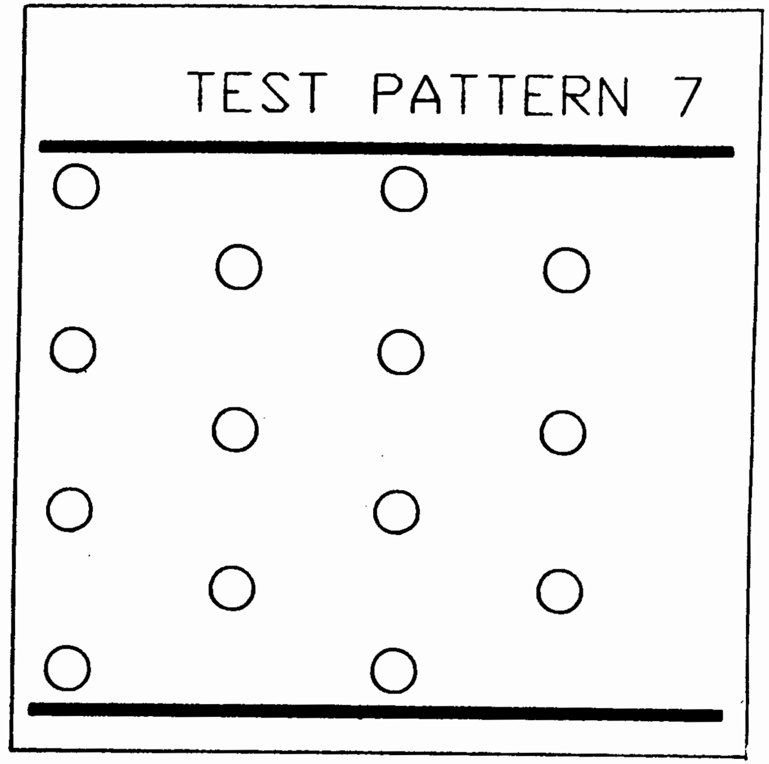

Run -	C m^0.5/s	n m^-0.33/s	n' m^-0.33/s	1/f^0.5 -	Log f -	R'/k -	LogR'/k -	ks mm	LogRe -	LogRew -	LogFr -
1	23.72519	0.021561	0.021015	2.678121	-0.85566	1.433722	0.156465	6.085754	3.255272	2.219432	-0.24314
2	26.12683	0.020130	0.019467	2.949221	-0.93941	1.693722	0.228842	5.261889	3.405715	2.255620	-0.23745
3	28.40276	0.019232	0.018384	3.206130	-1.01196	2.125722	0.327506	4.913051	3.589985	2.304952	-0.25051
4	31.04399	0.018416	0.017278	3.504274	-1.08919	2.793722	0.446183	4.580955	3.806617	2.364291	-0.27123
5	29.56260	0.020347	0.018877	3.337054	-1.04672	3.789722	0.578607	7.533389	3.984018	2.430503	-0.35868
6	34.68547	0.017739	0.015928	3.915327	-1.18553	4.341722	0.637662	4.435149	4.142005	2.460030	-0.31880
7	32.55219	0.019624	0.017464	3.674521	-1.13040	5.437722	0.735417	7.329362	4.261070	2.508908	-0.39525
8	33.08486	0.019855	0.017306	3.734649	-1.14449	6.429722	0.808192	8.086813	4.377282	2.545295	-0.42459
9	35.78936	0.018816	0.015752	4.039935	-1.21274	7.461722	0.872839	6.603605	4.508377	2.577619	-0.42278
10	35.85101	0.019163	0.015726	4.046895	-1.21424	8.413722	0.924988	7.386698	4.587348	2.603693	-0.44811

LARGE SCALE ROUGHNESS WORKSHEET
(CALCULATIONS)

TEST No. 8 SLOPE= 0.001

ROUGHNESS GEOMETRY
(Hemispheres)

k= 12.5 mm.
Ls= 88 mm.
Ts= 29 mm.
Conc.= 0.192434

k^2/Ts*Ls=0.061226
Ts/Ls= 0.329545
G. mean= 1.603623

Run	R mm.	R' mm.	Q l/s	v m/s	v* m/s	To N/m^2
1	37.55	35.94637	1.116	0.100149	0.018778	0.352633
2	44.8	43.19637	1.511	0.112838	0.020585	0.423756
3	51.1	49.49637	2.137	0.139273	0.022035	0.485559
4	54.9	53.29637	2.324	0.140661	0.022865	0.522837
5	62.1	60.49637	3.057	0.163006	0.024361	0.593469
6	67.75	66.14637	3.893	0.189852	0.025473	0.648895
7	131.2	129.5963	10.54	0.262353	0.035655	1.271340
8	136.55	134.9463	12.065	0.288406	0.036384	1.323823
9	140.3	138.6963	13.34	0.310262	0.036886	1.360611
10	146.45	144.8463	14.724	0.327911	0.037695	1.420942

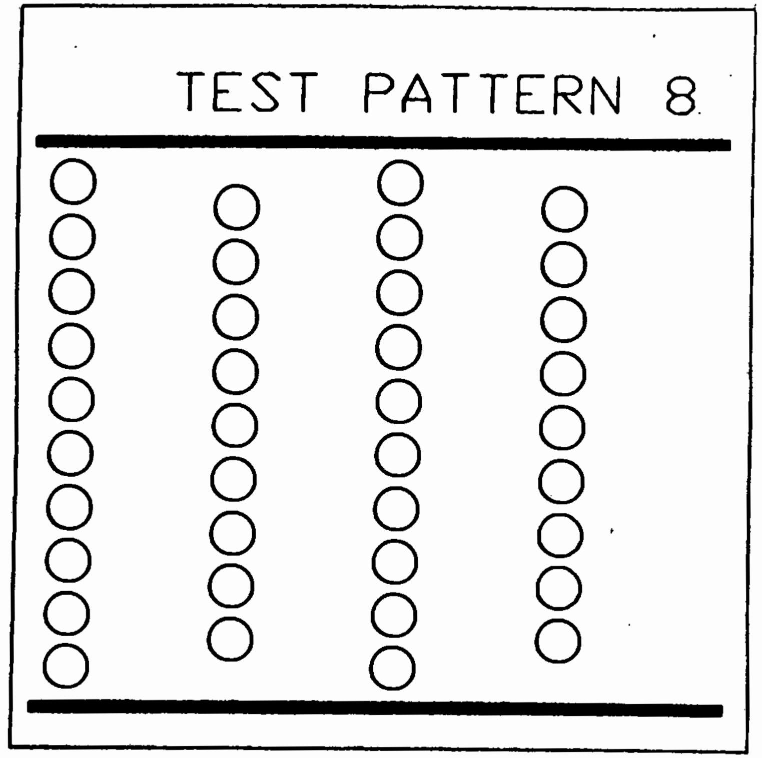

Run -	C m^0.5/s	n m^-0.33/s	n' m^-0.33/s	1/f^0.5 -	Log f -	R'/k -	LogR'/k -	ks mm	LogRe -	LogRew -	LogFr -
1	16.70397	0.034391	0.033525	1.885559	-0.55088	2.875710	0.458745	30.40011	3.556302	2.370572	-0.54667
2	17.16847	0.034501	0.033466	1.937993	-0.57470	3.455710	0.538537	34.39145	3.687902	2.410468	-0.57466
3	19.79624	0.030608	0.029355	2.234617	-0.69840	3.959710	0.597663	28.00687	3.838442	2.440031	-0.54237
4	19.26761	0.031838	0.030515	2.174945	-0.67489	4.263710	0.629787	32.30166	3.874874	2.456093	-0.57018
5	20.95751	0.029895	0.028348	2.365702	-0.74792	4.839710	0.684819	29.43593	3.993933	2.483609	-0.56119
6	23.34337	0.027242	0.025470	2.635021	-0.84156	5.291710	0.723596	23.60453	4.098922	2.502997	-0.53375
7	23.04568	0.030867	0.027586	2.601417	-0.83042	10.36771	1.015682	48.07108	4.531478	2.649040	-0.68537
8	24.82697	0.028846	0.025300	2.802491	-0.89508	10.79571	1.033251	39.71142	4.590165	2.657825	-0.66182
9	26.34489	0.027309	0.023550	2.973835	-0.94663	11.09571	1.045155	33.50790	4.633794	2.663777	-0.64200
10	27.24599	0.026597	0.022608	3.075552	-0.97584	11.58771	1.063997	31.12657	4.676664	2.673198	-0.63682

LARGE SCALE ROUGHNESS WORKSHEET
(CALCULATIONS)

TEST No. 9 SLOPE= 0.001

ROUGHNESS GEOMETRY
(Hemispheres)

k= 12.5 mm.
Ls= 58 mm.
Ts= 58 mm.
Conc.= 0.145985

k^2/Ts*Ls=0.046447
Ts/Ls= 1
G. mean= 1.216542

Run	R mm.	R' mm.	Q l/s	v m/s	v* m/s	To N/m^2
1	30	28.78345	0.911	0.102097	0.016803	0.282365
2	37.55	36.33345	1.643	0.145871	0,018879	0.356431
3	44.8	43.58345	2.278	0.168604	0.020677	0.427553
4	55.2	53.98345	3.157	0.188647	0.023012	0.529577
5	63.05	61.83345	4.101	0.213946	0.024628	0.606586
6	70.6	69.38345	4.58	0.212935	0.026089	0.680651
7	81.85	80.63345	6.697	0.267918	0.028124	0.791014
8	92.05	90.83345	8.265	0.293518	0.029850	0.891076
9	104.85	103.6334	10.149	0.315908	0.031884	1.016644
10	140.9	139.6834	16.175	0.373540	0.037017	1.370294

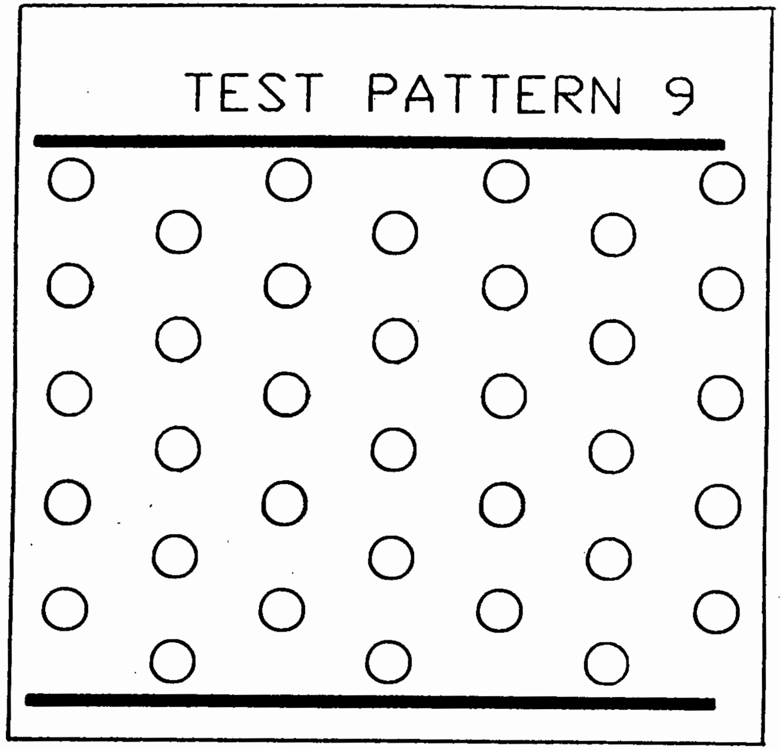

Run -	C m^0.5/s	n m^-0.33/s	n' m^-0.33/s	1/f^0.5 -	Log f -	R'/k -	LogR'/k -	ks mm	LogRe -	LogRew -	LogFr -
1	19.03015	0.029089	0.028336	2.148140	-0.66412	2.302676	0.362232	17.99171	3.468156	2.322315	-0.44179
2	24.20002	0.023780	0.022738	2.731720	-0.87287	2.906676	0.463396	11.59969	3.724275	2.372897	-0.38800
3	25.53933	0.023227	0.021963	2.882902	-0.91966	3.486676	0.542411	11.69150	3.866192	2.412405	-0.40412
4	25.67567	0.023943	0.022400	2.898293	-0.92428	4.318676	0.635350	14.22702	4.007912	2.458874	-0.44827
5	27.20775	0.023111	0.021311	3.071236	-0.97462	4.946676	0.694313	13.35381	4.121528	2.488356	-0.45258
6	25.56347	0.025075	0.023135	2.885628	-0.92048	5.550676	0.744345	18.55418	4.169503	2.513372	-0.50467
7	29.83634	0.022029	0.019610	3.367954	-1.05473	6.450676	0.809605	12.37479	4.334518	2.546002	-0.47018
8	30.79728	0.021769	0.019019	3.476425	-1.08226	7.266676	0.861335	12.30362	4.425881	2.571867	-0.48227
9	31.03212	0.022085	0.018959	3.502934	-1.08886	8.290676	0.918589	13.61546	4.515061	2.600494	-0.50760
10	31.60567	0.022790	0.018599	3.567677	-1.10477	11.17467	1.048234	17.03358	4.717482	2.665317	-0.56447

LARGE SCALE ROUGHNESS WORKSHEET
(CALCULATIONS)

TEST No. 10 SLOPE= 0.001

ROUGHNESS GEOMETRY
(Hemispheres)

k= 12.5 mm.
Ls= 29 mm.
Ts= 88 mm.
Conc.= 0.192434

k^2/Ts*Ls=0.061226
Ts/Ls= 3.034482
G. mean= 1.603623

Run	R mm.	R' mm.	Q l/s	v m/s	v* m/s	To N/m^2
1	41.9	40.29637	1.643	0.131525	0.019882	0.395307
2	48.4	46.79637	32.368	2.231217	0.021425	0.459072
3	56.75	55.14637	3.19	0.186600	0.023259	0.540985
4	65.45	63.84637	3.946	0.199369	0.025026	0.626332
5	74.5	72.89637	4.801	0.212453	0.026741	0.715113
6	83.55	81.94637	6.198	0.243983	0.028353	0.803893
7	89.95	88.34637	7.515	0.274396	0.029439	0.866677
8	104.35	102.7463	10.56	0.331539	0.031748	1.007941
9	117.75	116.1463	13.152	0.365278	0.033754	1.139395
10	136.75	135.1463	16.335	0.389899	0.036411	1.325785

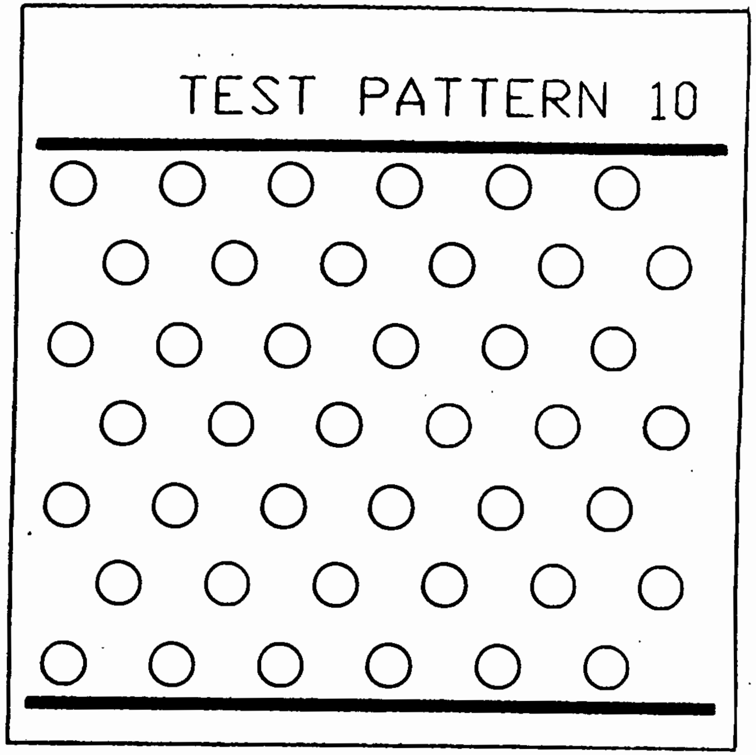

Run -	C m^0.5/s	n m^-0.33/s	n' m^-0.33/s	1/f^0.5 -	Log f -	R'/k -	LogR'/k -	ks mm	LogRe -	LogRew -	LogFr -
1	20.71938	0.028259	0.027196	2.338823	-0.73799	3.223710	0.508355	20.22341	3.724275	2.395377	-0.47792
2	326.1638	0.001840	ERR	36.81767	-3.13211	3.743710	0.573302	1.4E-16	5.018754	2.427850	0.686660
3	25.12774	0.024552	0.022996	2.836442	-0.90554	4.411710	0.644606	15.60614	4.012428	2.463503	-0.46227
4	24.95117	0.025337	0.023562	2.816511	-0.89942	5.107710	0.708226	18.48760	4.104795	2.495312	-0.49714
5	24.88347	0.025973	0.023971	2.808869	-0.89706	5.831710	0.765795	21.29467	4.189970	2.524097	-0.52711
6	26.95226	0.024452	0.022125	3.042396	-0.96643	6.555710	0.816619	18.29497	4.300889	2.549509	-0.51783
7	29.19336	0.022859	0.020256	3.295373	-1.03580	7.067710	0.849278	14.74014	4.384567	2.565838	-0.49947
8	32.70788	0.020923	0.017731	3.692095	-1.13454	8.219710	0.914856	10.85721	4.532302	2.598627	-0.48289
9	33.89390	0.020608	0.016949	3.825974	-1.16548	9.291710	0.968095	10.52006	4.627630	2.625247	-0.49405
10	33.53905	0.021358	0.017156	3.785919	-1.15634	10.81171	1.033894	12.81872	4.721757	2.658146	-0.53152

LARGE SCALE ROUGHNESS WORKSHEET
(CALCULATIONS)

TEST No. 11 SLOPE= 0.001

ROUGHNESS GEOMETRY
(Hemispheres)

k= 12.5 mm.
Ls= 29 mm.
Ts= 29 mm.
Conc.= 0.583940

k^2/Ts*Ls=0.185790
Ts/Ls= 1
G. mean= 4.866168

Run	R mm.	R' mm.	Q l/s	v m/s	v* m/s	To N/m^2
1	47.15	42.28383	1.511	0.115273	0.020366	0.414804
2	56.75	51.88383	2.537	0.157734	0.022560	0.508980
3	65.16	60.29383	3.157	0.168904	0.024320	0.591482
4	76.4	71.53383	4.275	0.192780	0.026490	0.701746
5	85.25	80.38383	5.468	0.219431	0.028081	0.788565
6	94.85	89.98383	6.835	0.245026	0.029710	0.882741
7	105.45	100.5838	8.138	0.260992	0.031412	0.986727
8	118.45	113.5838	10.087	0.286473	0.033380	1.114257
9	141.7	136.8338	12.881	0.303664	0.036637	1.342339
10	154.75	149.8838	16.524	0.355630	0.038345	1.470360

TEST PATTERN 11

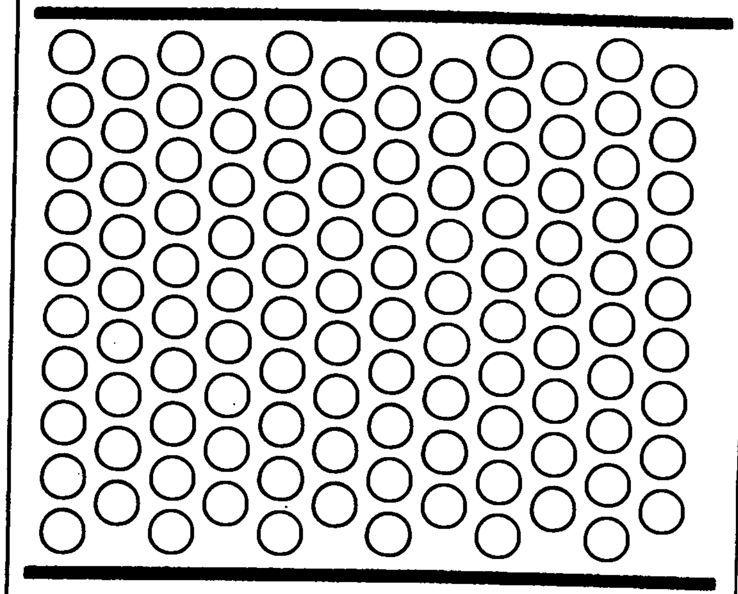

Run –	C m^0.5/s	n m^-0.33/s	n' m^-0.33/s	1/f^0.5 –	Log f –	R'/k –	LogR'/k –	ks mm	LogRe –	LogRew –	LogFr –
1	17.72724	0.033295	0.032264	2.001067	-0.60252	3.382706	0.529264	31.30693	3.687902	2.405831	-0.55611
2	21.89831	0.027888	0.026514	2.471901	-0.78606	4.150706	0.618122	22.33989	3.912958	2.450260	-0.50877
3	21.75221	0.028787	0.027216	2.455410	-0.78024	4.823506	0.683362	26.45865	4.007912	2.482880	-0.54430
4	22.79329	0.028266	0.026384	2.572928	-0.82085	5.722706	0.757601	27.41872	4.139574	2.520000	-0.56111
5	24.47449	0.026841	0.024668	2.762703	-0.88266	6.430706	0.808258	24.76378	4.246466	2.545328	-0.55553
6	25.83033	0.025915	0.023433	2.915752	-0.92950	7.198706	0.857254	23.24279	4.343376	2.569826	-0.55662
7	26.02338	0.026205	0.023441	2.937543	-0.93596	8.046706	0.905618	25.33708	4.419155	2.594008	-0.57756
8	26.87977	0.025889	0.022739	3.034212	-0.96409	9.086706	0.958406	25.59823	4.512400	2.620402	-0.58990
9	25.95957	0.027652	0.023971	2.930340	-0.93383	10.94670	1.039283	34.75545	4.618587	2.660841	-0.64546
10	29.04833	0.025089	0.020818	3.279003	-1.03148	11.99070	1.078844	25.48315	4.726753	2.680621	-0.61642

LARGE SCALE ROUGHNESS WORKSHEET
(CALCULATIONS)

TEST No. 12 SLOPE= 0.001

ROUGHNESS GEOMETRY
(Hemispheres)

k= 20 mm.
Ls= 54 mm.
Ts= 62 mm.
Conc.= 0.375507

k^2/Ts*Ls=0.119474
Ts/Ls= 1.148148
G. mean= 5.006770

Run	R mm.	R' mm.	Q l/s	v m/s	v* m/s	To N/m^2
1	34.5	29.49322	0.721	0.078858	0.017009	0.289328
2	42.7	37.69322	1.116	0.095507	0.019229	0.369770
3	50	44.99322	1.511	0.108331	0.021009	0.441383
4	54.4	49.39322	1.99	0.129964	0.022012	0.484547
5	63.1	58.09322	2.621	0.145539	0.023872	0.569894
6	73.3	68.29322	3.636	0.171745	0.025883	0.669956
7	91.3	86.29322	5.434	0.203133	0.029095	0.846536
8	111	105.9932	7.708	0.234585	0.032245	1.039793
9	128	122.9932	10.396	0.272661	0.034735	1.206563
10	155	149.9932	14.607	0.314143	0.038359	1.471433

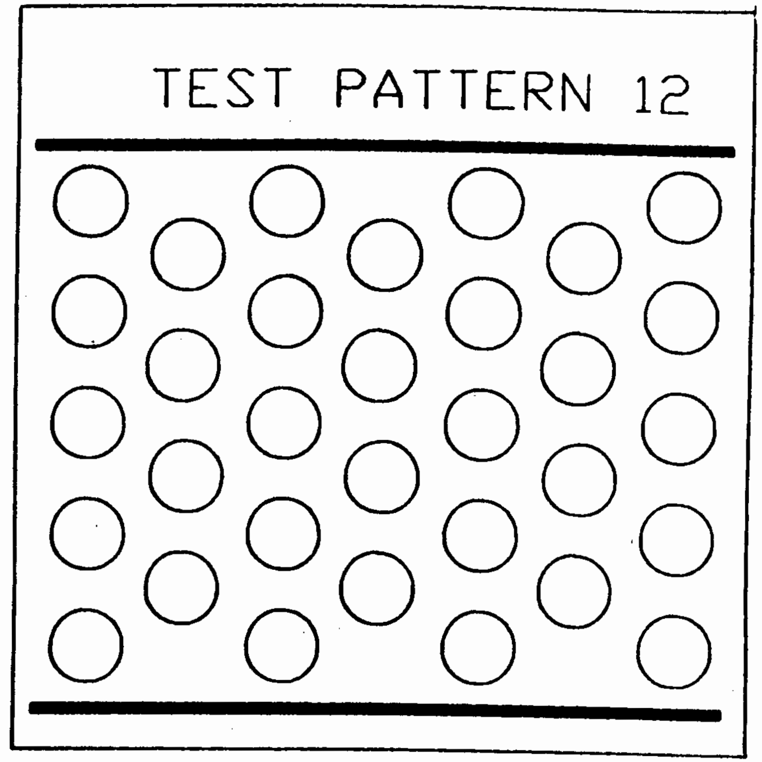

Run -	C m^0.5/s	n m^-0.33/s	n' m^-0.33/s	1/f^0.5 -	Log f -	R'/k -	LogR'/k -	ks mm	LogRe -	LogRew -	LogFr -
1	14.52078	0.038278	0.037596	1.639119	-0.42922	1.474661	0.168692	33.12551	3.366573	2.531725	-0.56454
2	15.55634	0.037221	0.036347	1.756014	-0.48905	1.884661	0.275233	37.00465	3.556302	2.584996	-0.58789
3	16.15035	0.036926	0.035883	1.823066	-0.52160	2.249661	0.352117	40.88969	3.687902	2.623438	-0.61006
4	18.49227	0.032755	0.031545	2.087424	-0.63922	2.469661	0.392637	33.10969	3.807491	2.643698	-0.57151
5	19.09488	0.032590	0.031167	2.155447	-0.66707	2.904661	0.463095	36.00820	3.927105	2.678927	-0.59281
6	20.78240	0.030762	0.029041	2.345936	-0.74063	3.414661	0.533347	33.99456	4.069262	2.714053	-0.59116
7	21.86718	0.030399	0.028209	2.468387	-0.78482	4.314661	0.634946	37.30636	4.243757	2.764852	-0.61986
8	22.78572	0.030190	0.027485	2.572073	-0.82056	5.299661	0.724248	40.66694	4.395580	2.809503	-0.64664
9	24.58571	0.028683	0.025448	2.775257	-0.88660	6.149661	0.788851	37.34672	4.525504	2.841805	-0.64592
10	25.65026	0.028417	0.024430	2.895425	-0.92342	7.499661	0.875041	39.66057	4.673199	2.884900	-0.67061

LARGE SCALE ROUGHNESS WORKSHEET
(CALCULATIONS)

TEST No. 12b SLOPE= 0.001

ROUGHNESS GEOMETRY
(Hemispheres)

k= 8.3 mm.
Ls= 24 mm.
Ts= 28 mm.
Conc.= 0.322204

k^2/Ts*Ls=0.102514
Ts/Ls= 1.166666
G. mean= 1.782863

Run	R mm.	R' mm.	Q l/s	v m/s	v* m/s	To N/m^2
1	30	28.21713	1.014	0.115921	0.016637	0.276810
2	33	31.21713	1.197	0.123691	0.017499	0.306240
3	39	37.21713	1.62	0.140413	0.019107	0.365100
4	44	42.21713	2.141	0.163593	0.020350	0.414150
5	49	47.21713	2.749	0.187807	0.021522	0.463200
6	58	56.21713	3.614	0.207375	0.023483	0.551490
7	67	65.21713	4.694	0.232177	0.025293	0.639780
8	72	70.21713	5.379	0.247113	0.026245	0.688830
9	77	75.21713	6.066	0.260150	0.027163	0.737880
10	100	98.21713	8.959	0.294246	0.031040	0.963510

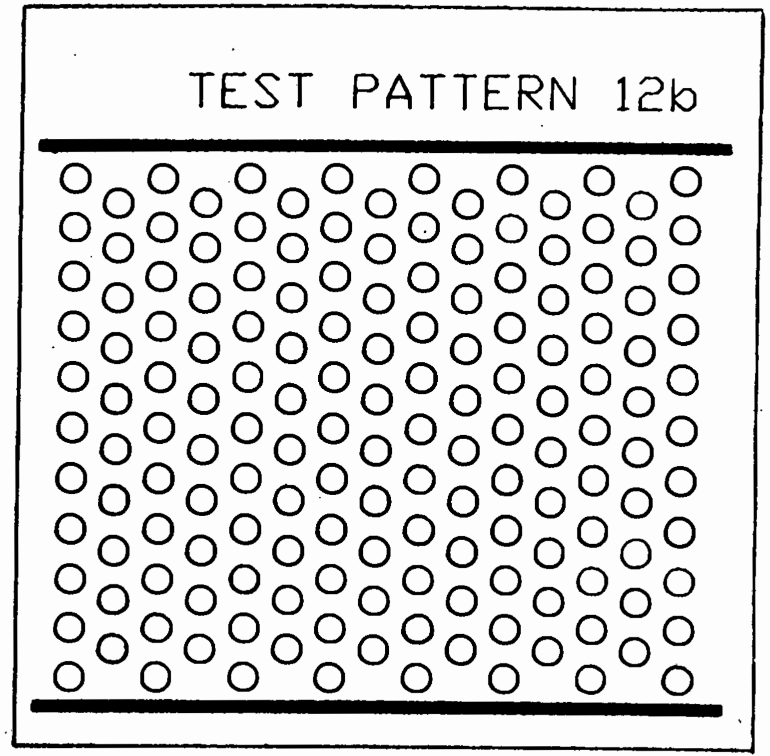

Run -	C m^0.5/s	n m^-0.33/s	n' m^-0.33/s	1/f^0.5 -	Log f -	R'/k -	LogR'/k -	ks mm	LogRe -	LogRew -	LogFr -
1	21.82261	0.025283	0.024494	2.463357	-0.78305	3.399654	0.531434	12.26971	3.514676	2.140169	-0.37801
2	22.13822	0.025346	0.024475	2.498983	-0.79552	3.761100	0.575314	13.02870	3.586732	2.162109	-0.39372
3	23.01647	0.025104	0.024063	2.598121	-0.82931	4.483992	0.651664	13.85742	3.718153	2.200284	-0.41500
4	25.17803	0.023436	0.022216	2.842119	-0.90728	5.086401	0.706410	11.86940	3.839254	2.227656	-0.40339
5	27.33150	0.021996	0.020588	3.085205	-0.97856	5.688811	0.755021	10.03452	3.947813	2.251962	-0.39205
6	27.65816	0.022377	0.020714	3.122078	-0.98888	6.773148	0.830790	11.45062	4.066626	2.289846	-0.42477
7	28.75006	0.022067	0.020120	3.245333	-1.02251	7.857486	0.895283	11.52643	4.180181	2.322093	-0.44021
8	29.49002	0.021780	0.019667	3.328861	-1.04459	8.459895	0.927365	11.27229	4.239339	2.338134	-0.44521
9	29.99615	0.021659	0.019386	3.385992	-1.05937	9.062305	0.957238	11.30629	4.291540	2.353070	-0.45276
10	29.69046	0.022877	0.019976	3.351486	-1.05047	11.83338	1.073109	15.36187	4.460897	2.411006	-0.51514

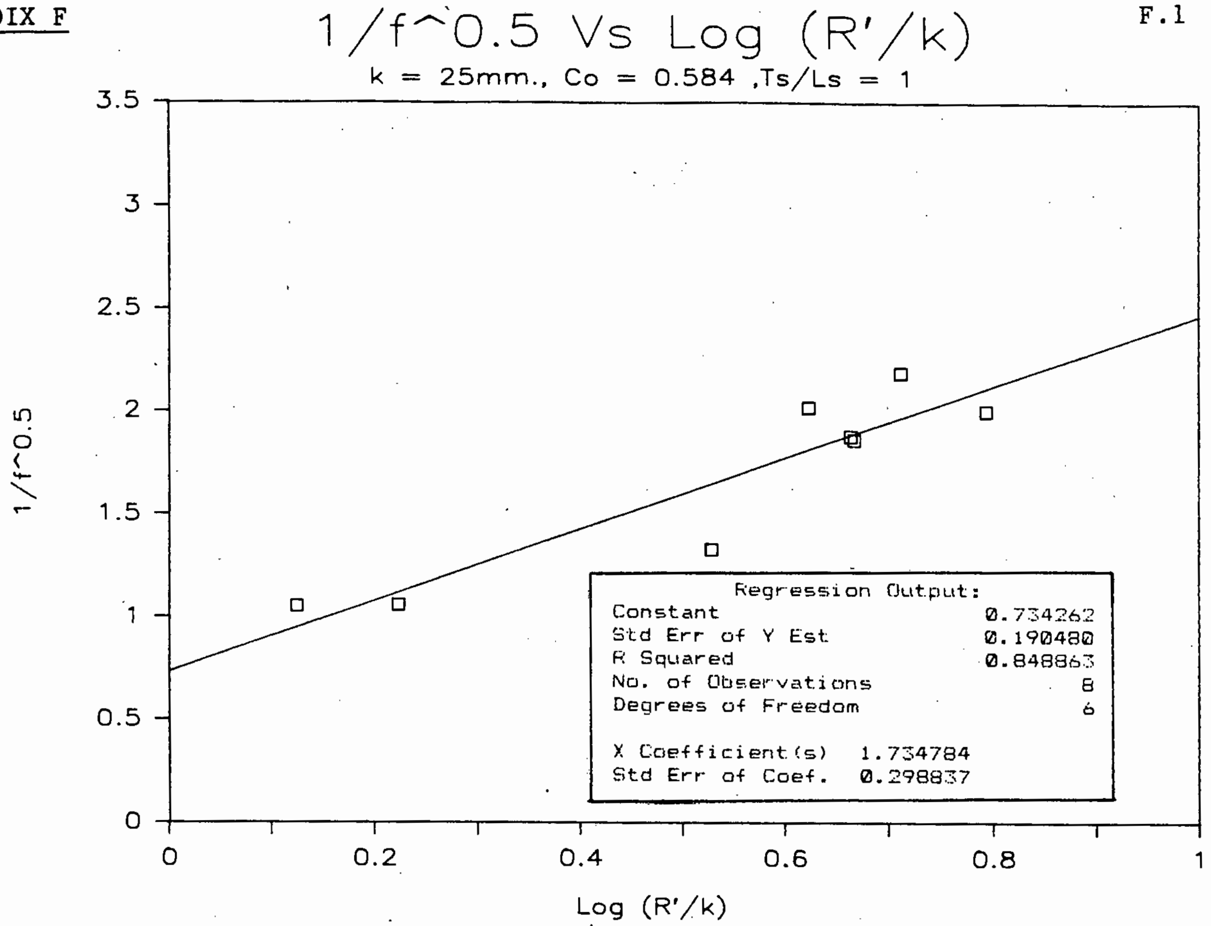
1/f^0.5 Vs Log (R'/k)
k = 25mm., Co = 0.584 ,Ts/Ls = 1
1/f^0.5
Log (R'/k)
Regression Output:
Constant 0.734262
Std Err of Y Est 0.190480
R Squared 0.848863
No. of Observations 8
Degrees of Freedom 6
X Coefficient(s) 1.734784
Std Err of Coef. 0.298837

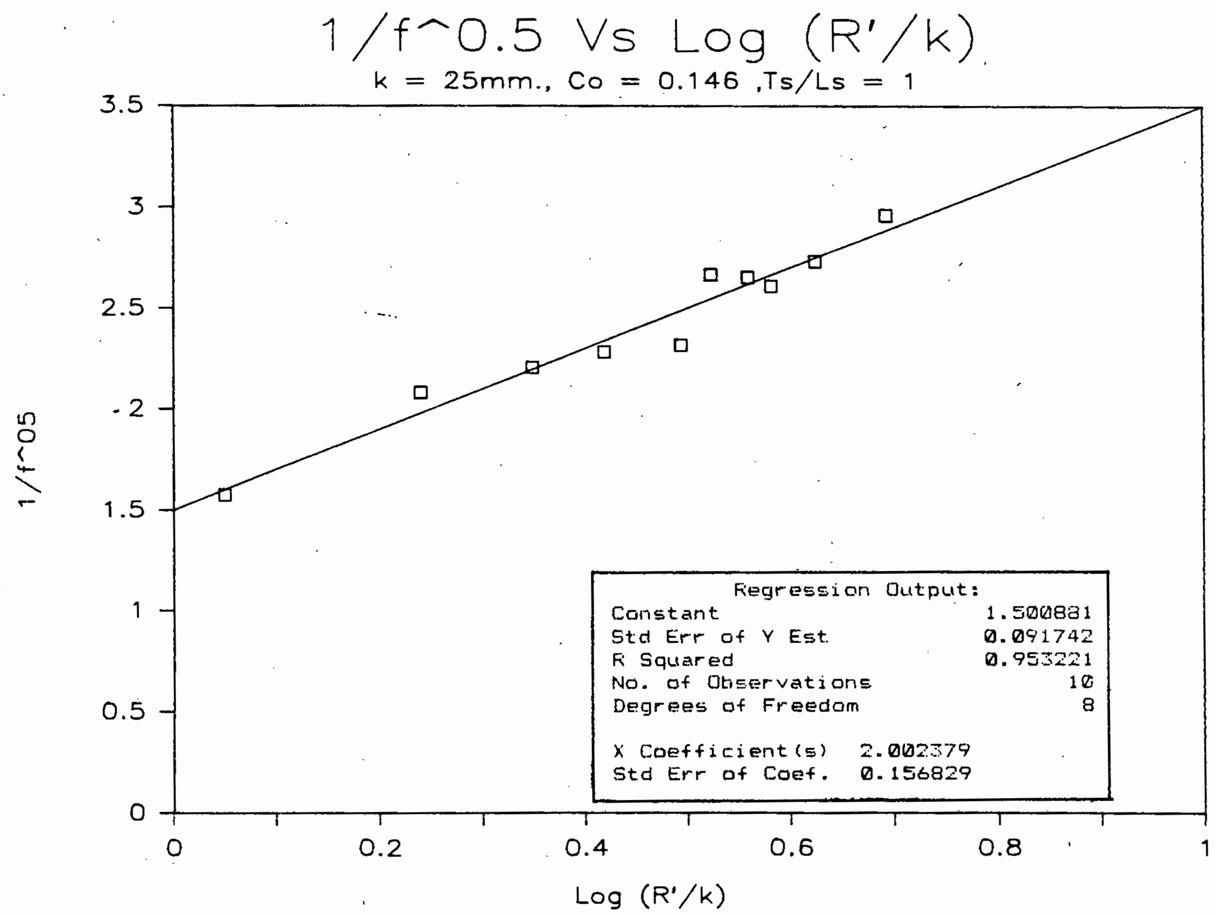
1/f^0.5 Vs Log (R'/k)
k = 25mm., Co = 0.146 ,Ts/Ls = 1
1/f^05
Log (R'/k)
Regression Output:
Constant 1.500881
Std Err of Y Est 0.091742
R Squared 0.953221
No. of Observations 10
Degrees of Freedom 8
X Coefficient(s) 2.002379
Std Err of Coef. 0.156829

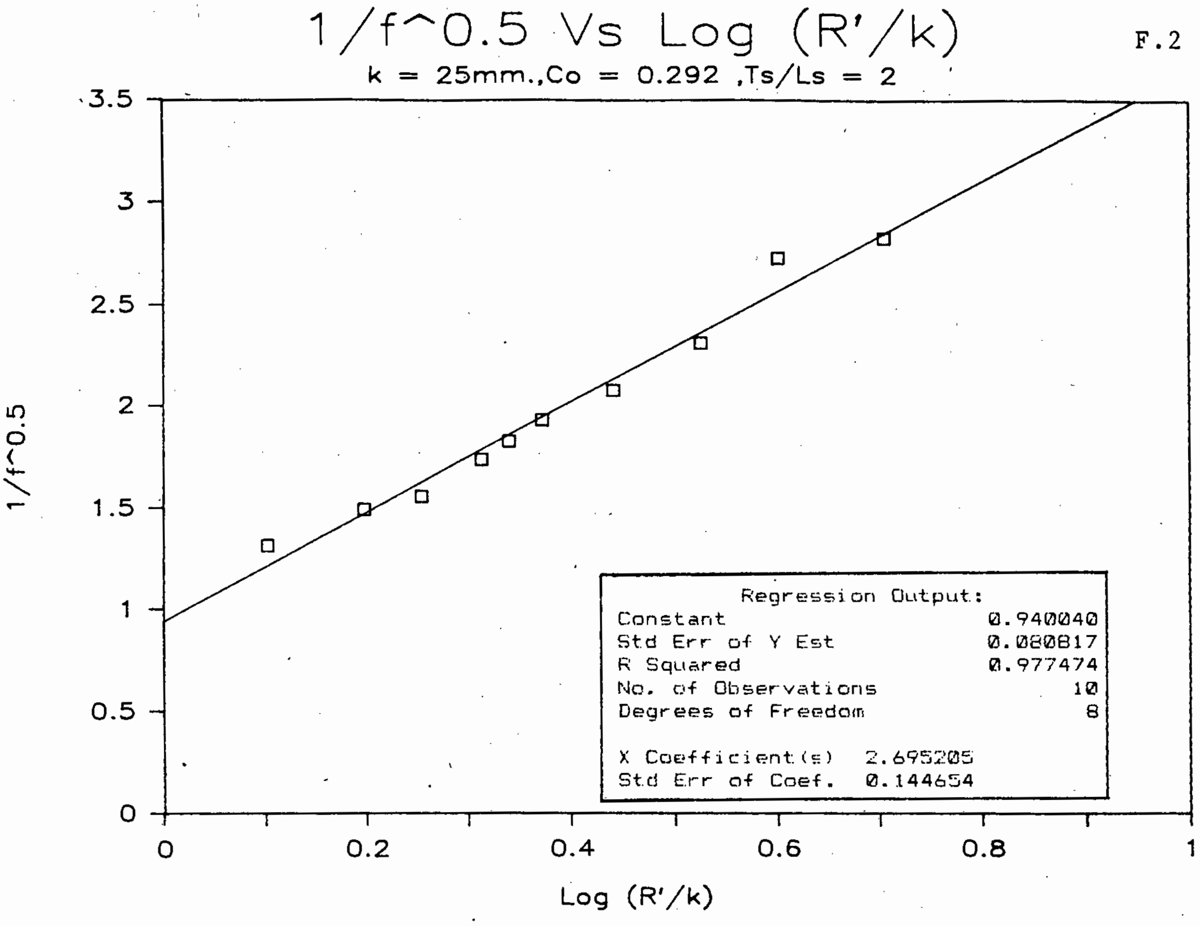
1/f^0.5 Vs Log (R'/k)
k = 25mm.,Co = 0.292 ,Ts/Ls = 2
1/f^0.5
Log (R'/k)
Regression Output:
Constant 0.940040
Std Err of Y Est 0.080817
R Squared 0.977474
No. of Observations 10
Degrees of Freedom 8
X Coefficient(s) 2.695205
Std Err of Coef. 0.144654

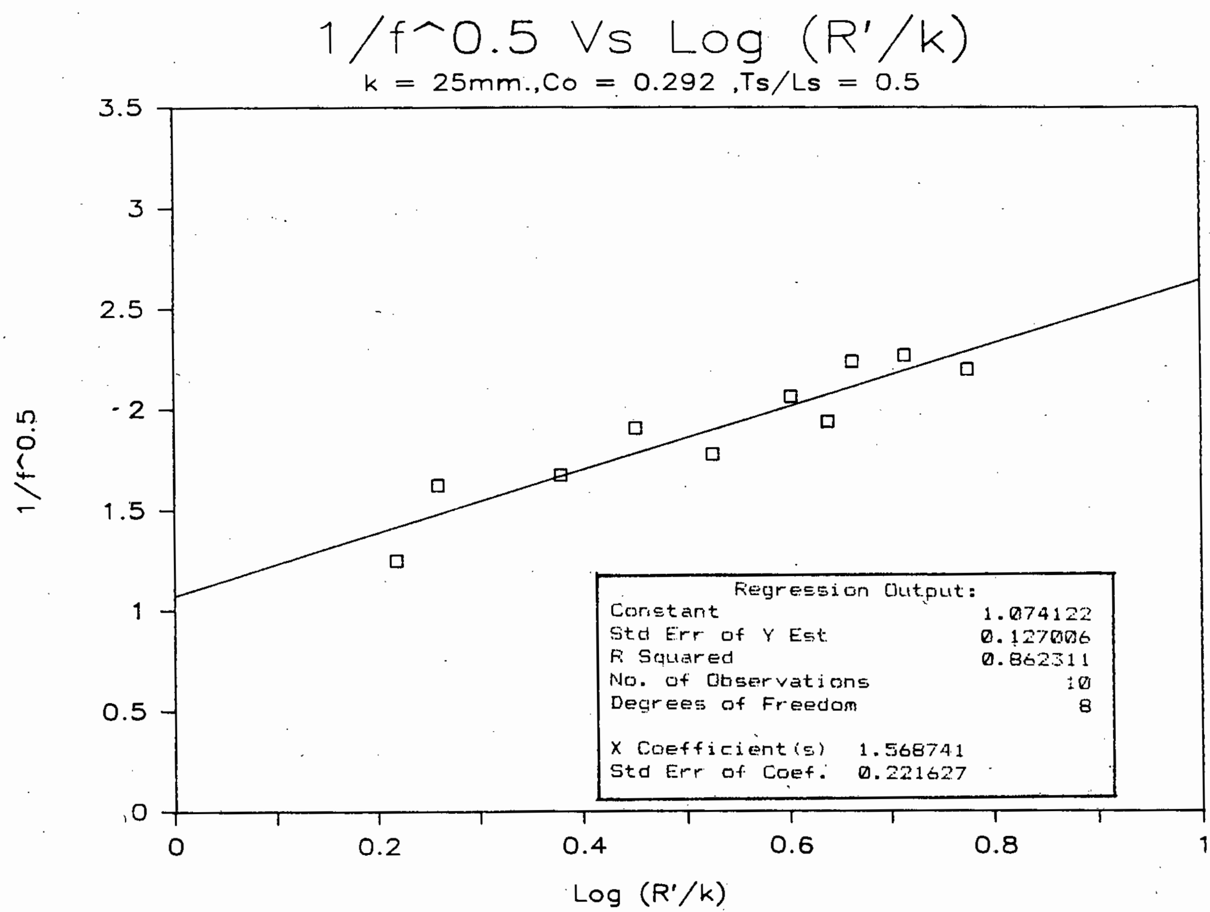
1/f^0.5 Vs Log (R'/k)
k = 25mm.,Co = 0.292 ,Ts/Ls = 0.5
1/f^0.5
Log (R'/k)
Regression Output:
Constant 1.074122
Std Err of Y Est 0.127006
R Squared 0.862311
No. of Observations 10
Degrees of Freedom 8
X Coefficient(s) 1.568741
Std Err of Coef. 0.221627

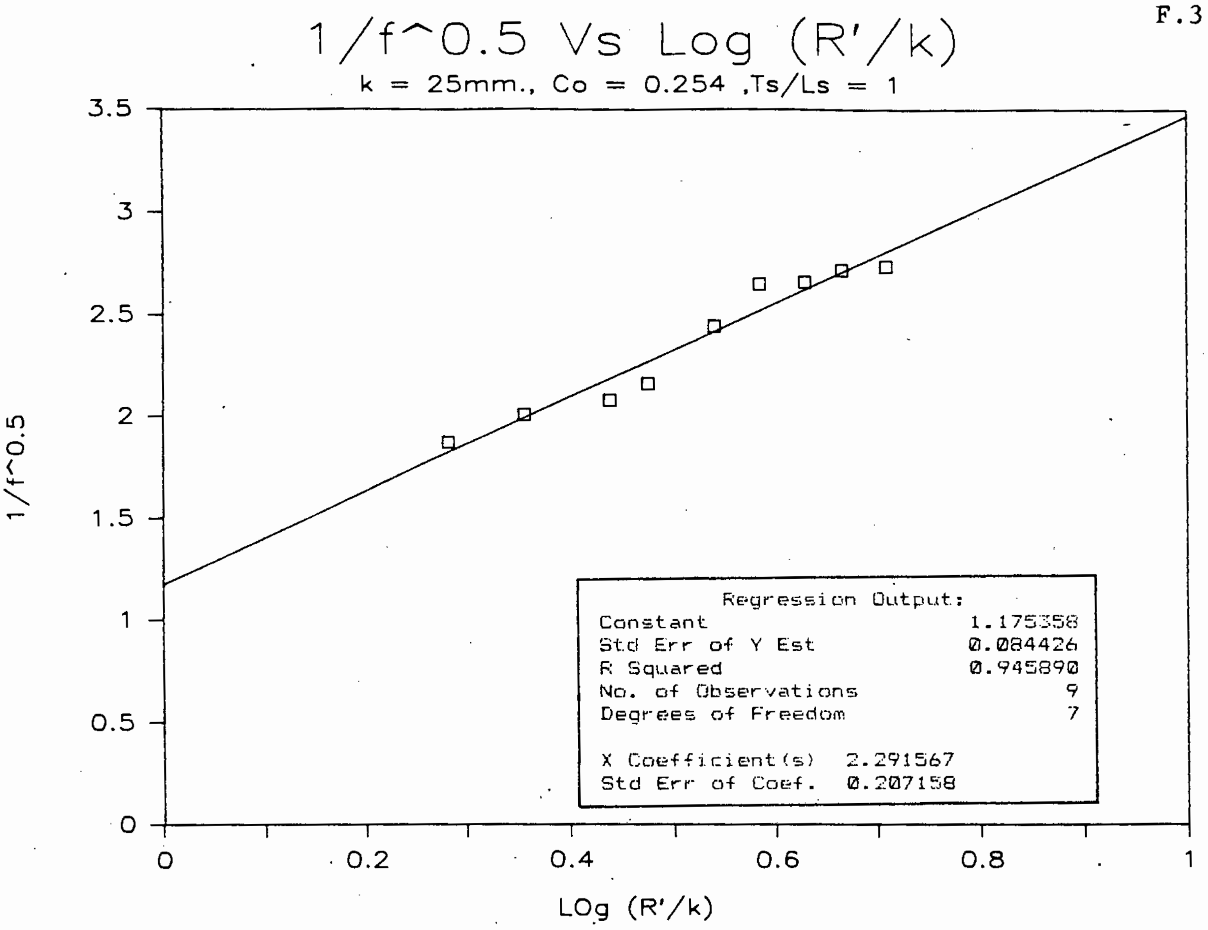
1/f^0.5 Vs Log (R'/k)
k = 25mm., Co = 0.254 ,Ts/Ls = 1
1/f^0.5
LOg (R'/k)
Regression Output:
Constant 1.175358
Std Err of Y Est 0.084426
R Squared 0.945890
No. of Observations 9
Degrees of Freedom 7
X Coefficient(s) 2.291567
Std Err of Coef. 0.207158

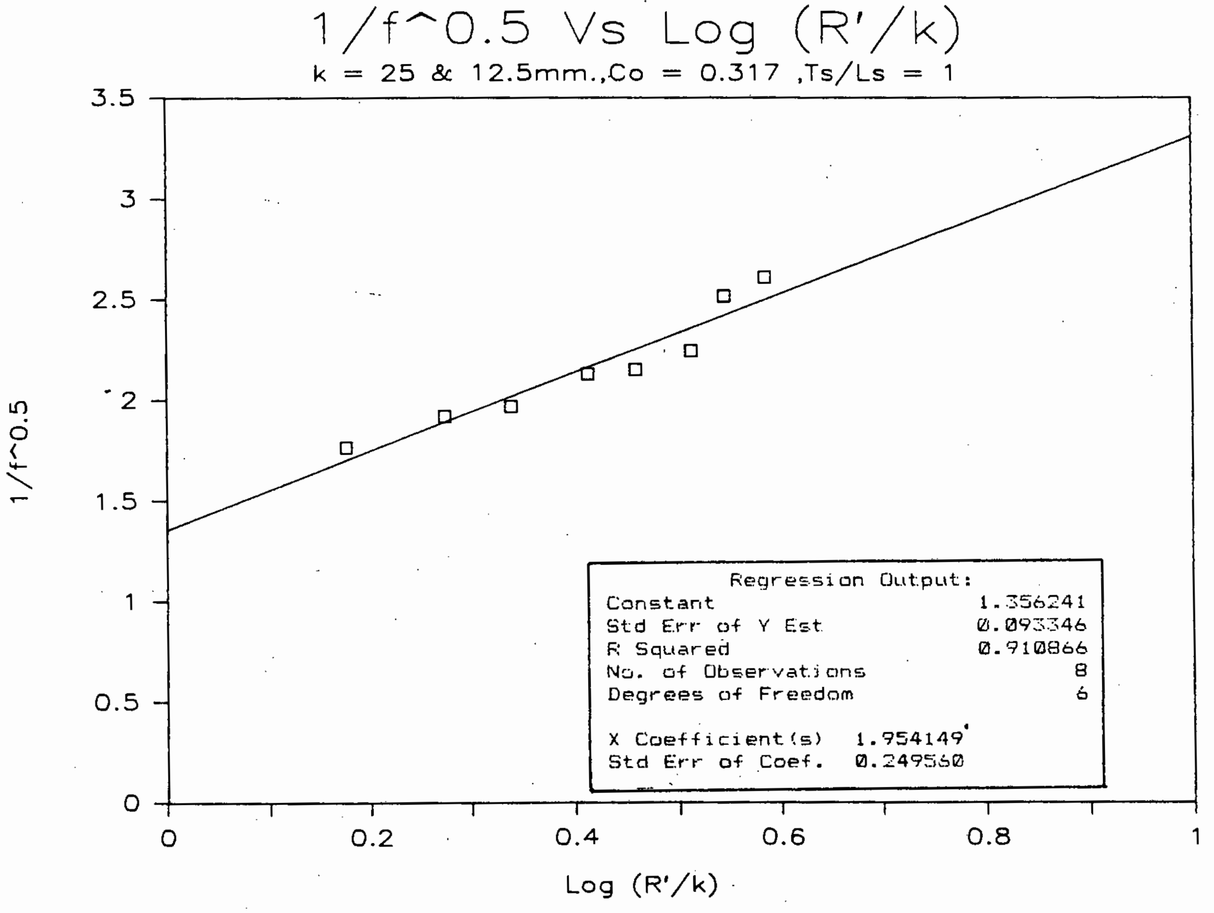
1/f^0.5 Vs Log (R'/k)
k = 25 & 12.5mm.,Co = 0.317 ,Ts/Ls = 1
1/f^0.5
Log (R'/k)
Regression Output:
Constant 1.356241
Std Err of Y Est 0.093346
R Squared 0.910866
No. of Observations 8
Degrees of Freedom 6
X Coefficient(s) 1.954149
Std Err of Coef. 0.249560

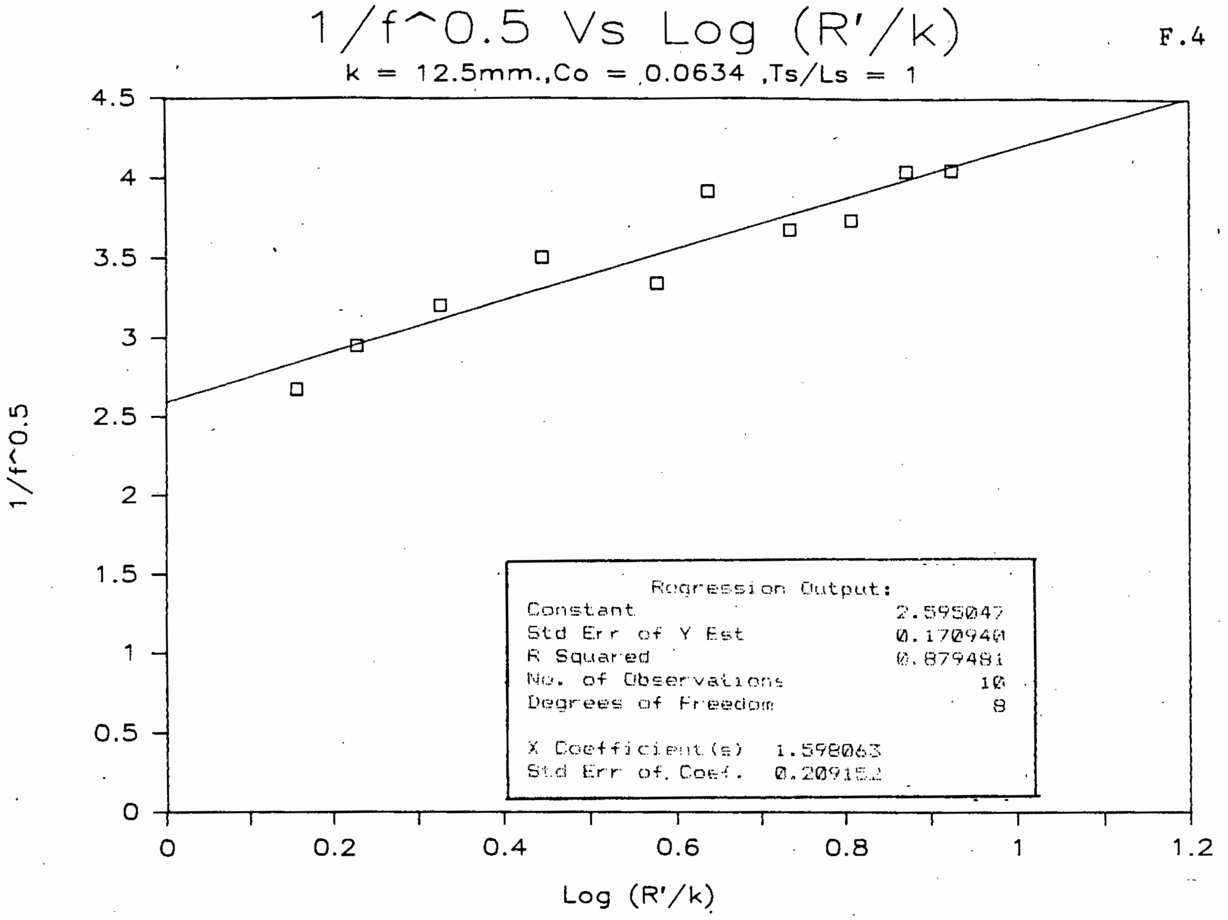
1/f^0.5 Vs Log (R'/k)
k = 12.5mm.,Co = 0.0634 ,Ts/Ls = 1
1/f^0.5
Log (R'/k)
Regression Output:
Constant 2.595047
Std Err of Y Est 0.170940
R Squared 0.879481
No. of Observations 10
Degrees of Freedom 8
X Coefficient(s) 1.598063
Std Err of Coef. 0.209152

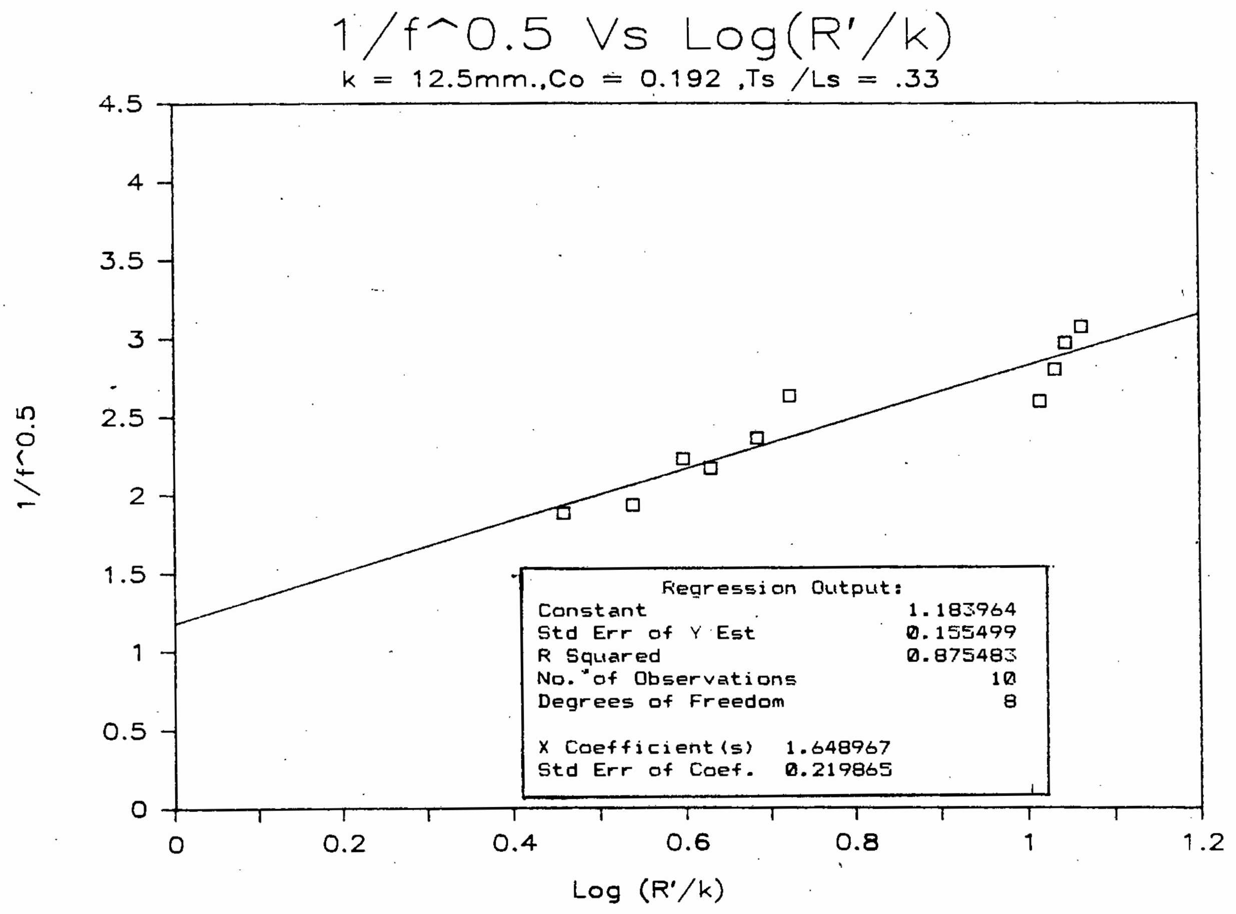
1/f^0.5 Vs Log(R'/k)
k = 12.5mm.,Co = 0.192 ,Ts /Ls = .33
1/f^0.5
Log (R'/k)
Regression Output:
Constant 1.183964
Std Err of Y Est 0.155499
R Squared 0.875483
No. of Observations 10
Degrees of Freedom 8
X Coefficient(s) 1.648967
Std Err of Coef. 0.219865

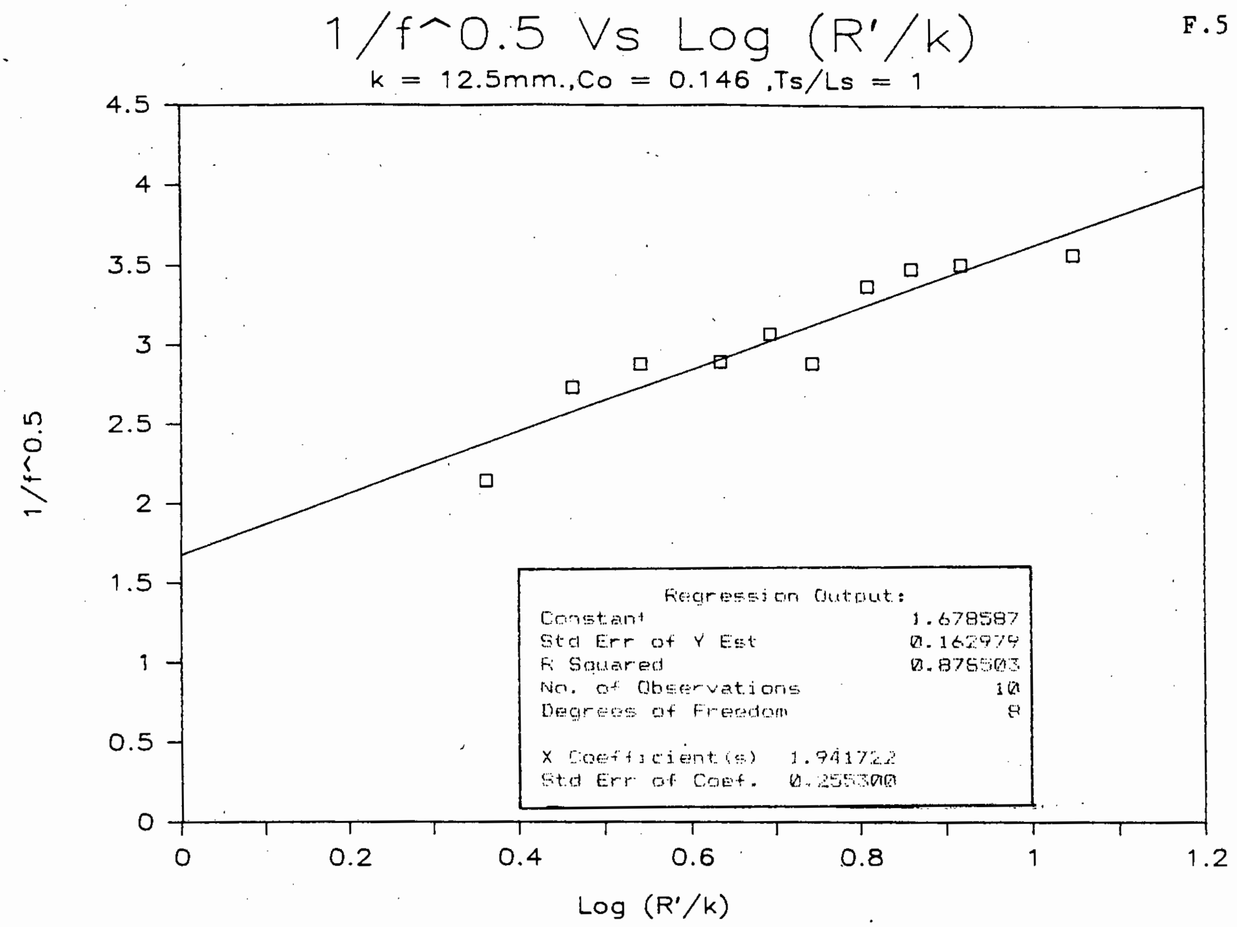
1/f^0.5 Vs Log (R'/k)
k = 12.5mm.,Co = 0.146 ,Ts/Ls = 1
1/f^0.5
Log (R'/k)
Regression Output:
Constant 1.678587
Std Err of Y Est 0.162979
R Squared 0.876503
No. of Observations 10
Degrees of Freedom 8
X Coefficient(s) 1.941722
Std Err of Coef. 0.255300

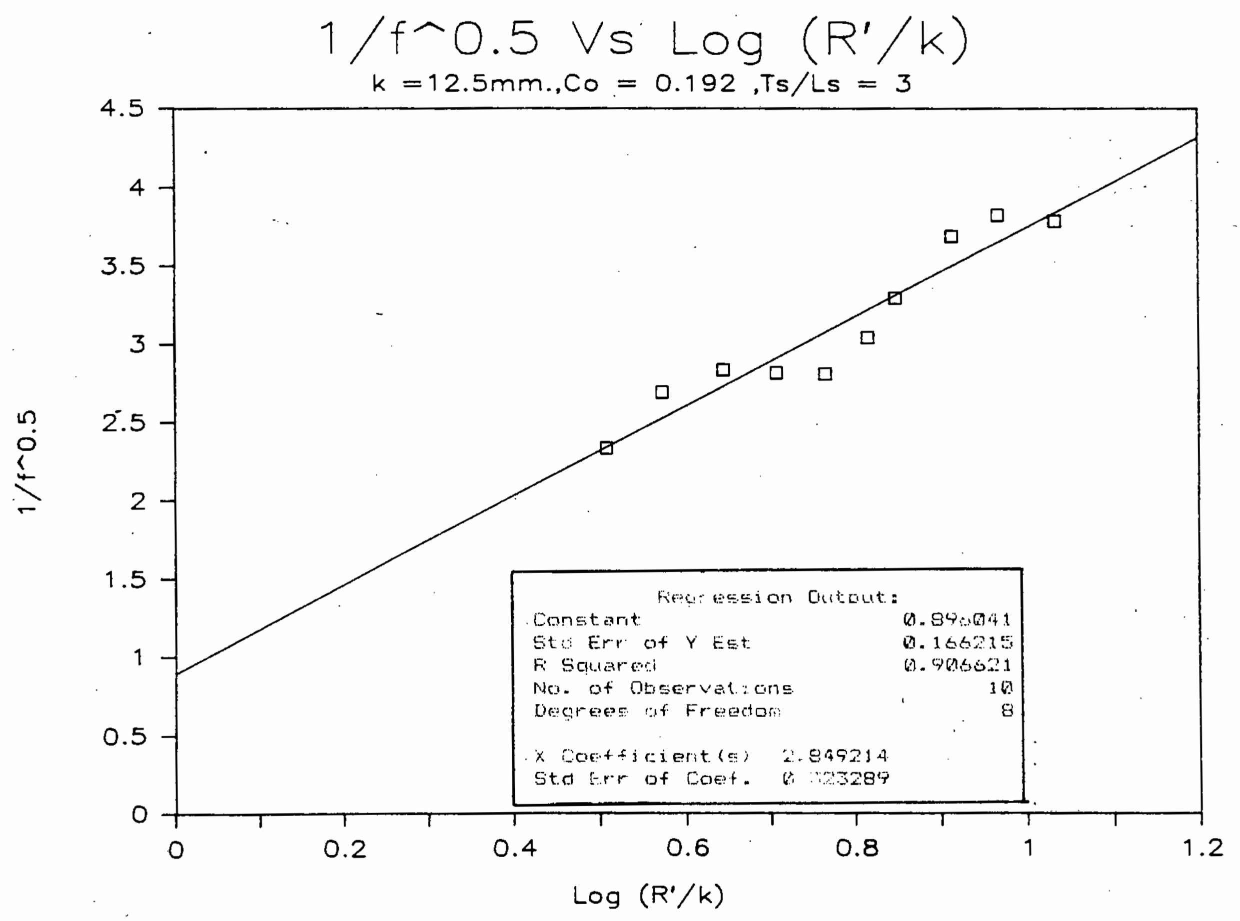
1/f^0.5 Vs Log (R'/k)
k =12.5mm.,Co = 0.192 ,Ts/Ls = 3
1/f^0.5
Log (R'/k)
Regression Output:
Constant 0.896041
Std Err of Y Est 0.166215
R Squared 0.906621
No. of Observations 10
Degrees of Freedom 8
X Coefficient(s) 2.849214
Std Err of Coef.

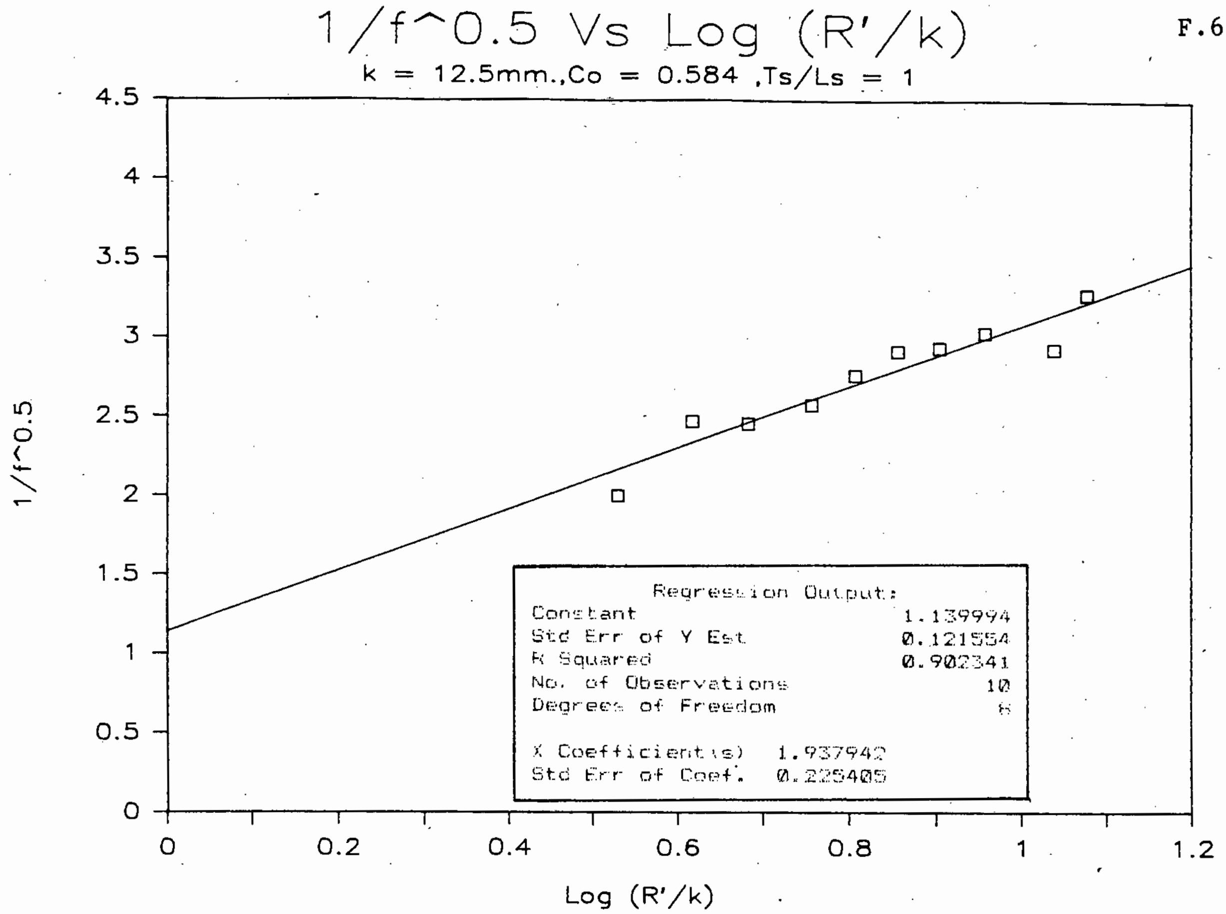
1/f^0.5 Vs Log (R'/k)
k = 12.5mm.,Co = 0.584 ,Ts/Ls = 1
1/f^0.5
Log (R'/k)
Regression Output:
Constant 1.139994
Std Err of Y Est 0.121554
R Squared 0.902341
No. of Observations 10
Degrees of Freedom 8
X Coefficient(s) 1.937942
Std Err of Coef. 0.225405

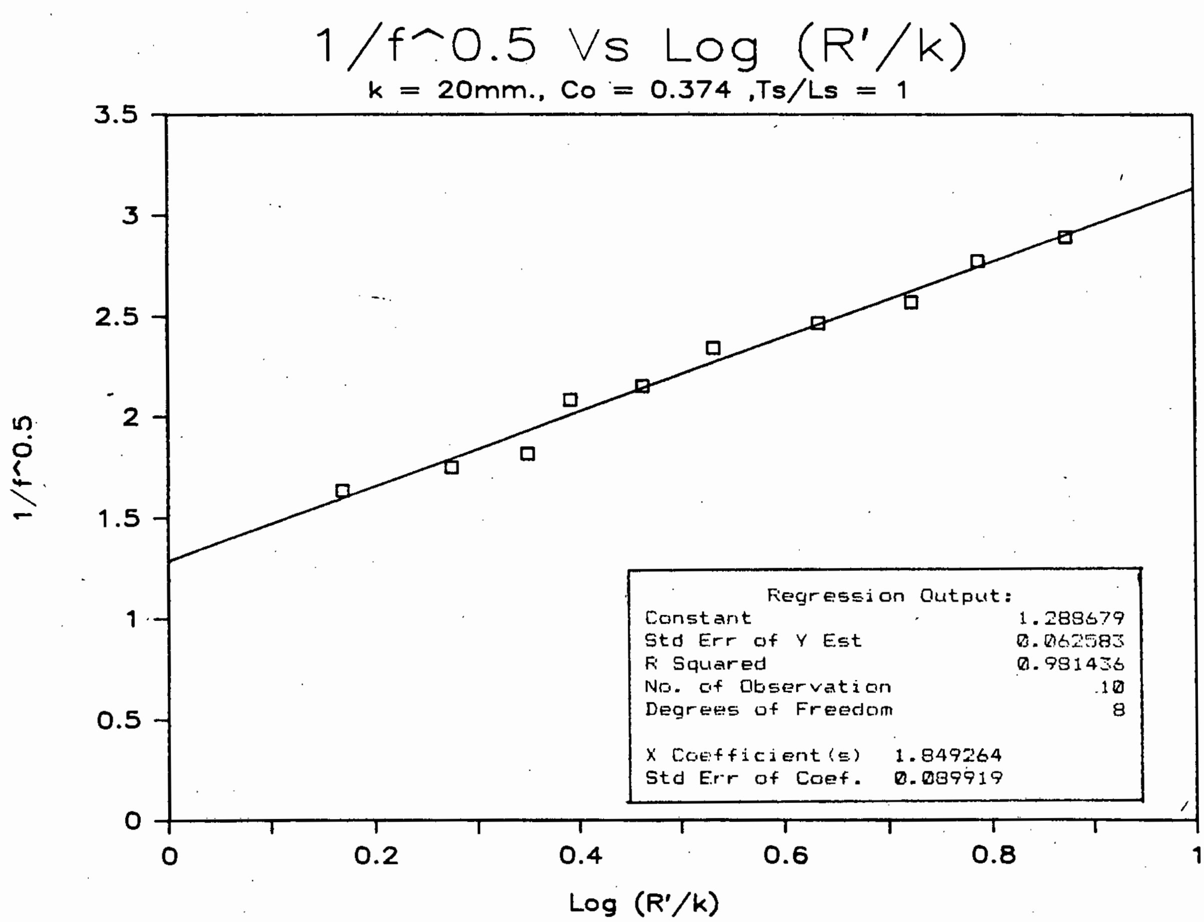
1/f^0.5 Vs Log (R'/k)
k = 20mm., Co = 0.374 ,Ts/Ls = 1
1/f^0.5
Log (R'/k)
Regression Output:
Constant 1.288679
Std Err of Y Est 0.062583
R Squared 0.981436
No. of Observation 10
Degrees of Freedom 8
X Coefficient(s) 1.849264
Std Err of Coef. 0.089919

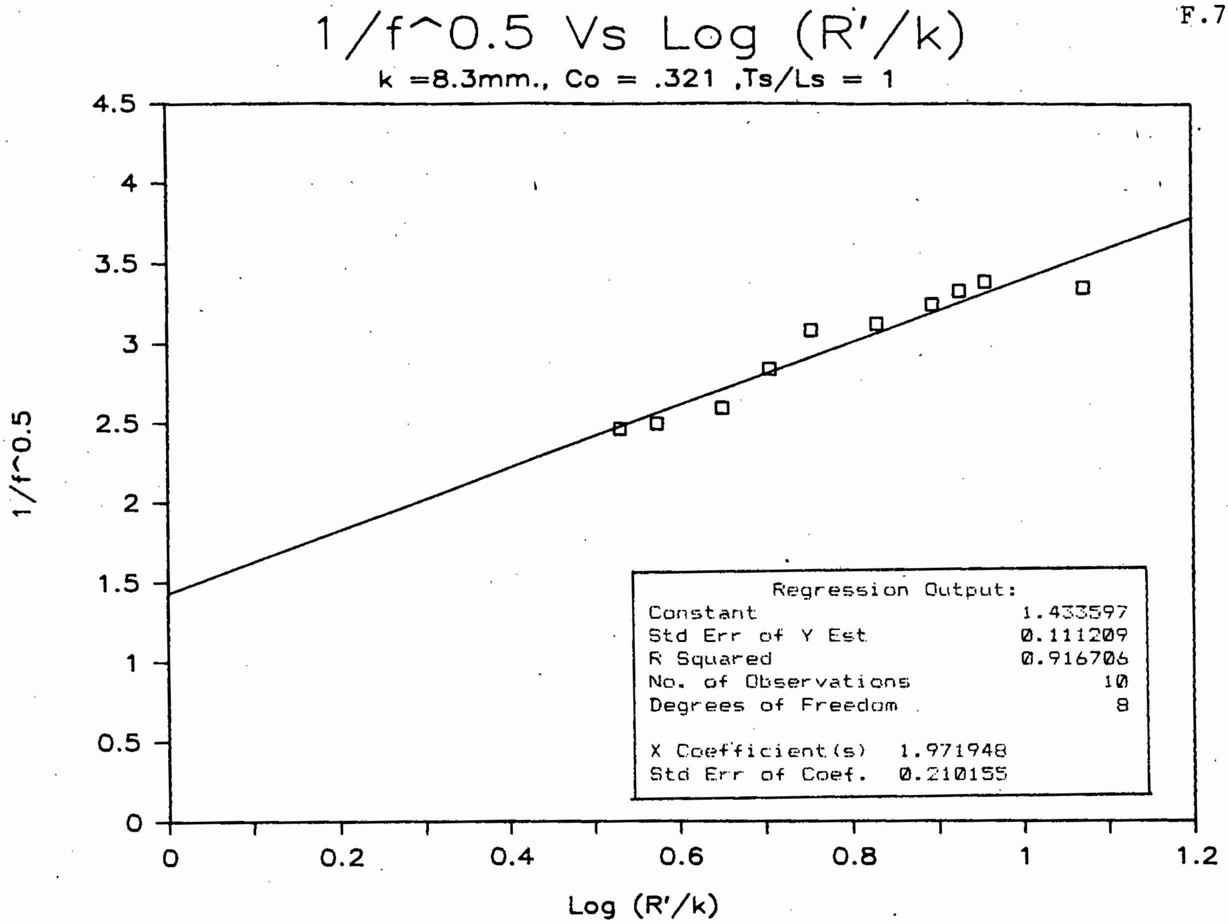
1/f^0.5 Vs Log (R'/k)
k =8.3mm., Co = .321 ,Ts/Ls = 1
1/f^0.5
Log (R'/k)
Regression Output:
Constant 1.433597
Std Err of Y Est 0.111209
R Squared 0.916706
No. of Observations 10
Degrees of Freedom 8
X Coefficient(s) 1.971948
Std Err of Coef. 0.210155

APPENDIX G

Examinations written by the author to complete the requirements of the degree.

Examination		Credit Rating
CIV 509F	Structural Loading	3
CIV 516F	Coastal Hydraulics	5
CIV 592Z	Project Management in Civil Engineering	3
CIV 536S	Coastal Engineering Practice	5
CIV 525S	Contract Law	3
CIV 543S	Airport Design	3
CIV 522	Introduction to Finite Elements	3
Thesis	"Friction Equation for uniform flow in Channels of Large Relative Roughness"	20
	TOTAL	45
	Credits required for degree	40

UNIVERSITY OF CAPE TOWN

DEPARTMENT OF CIVIL ENGINEERING

CIV 509F - STRUCTURAL LOADING

Time : 3 hours — Date: 18 June 1988

Answers should be concise, but must show understanding of the subject. Approximately equal marks will be awarded for each question.

1.(a) List the probability functions best suited to each of the following loads : dead, imposed office floor, wind, flood, earthquake.

(b) Explain how the overall probability of failure of a structural element is derived from the probability functions of load effect and of resistance.

2.(a) For imposed loading on floors of buildings, describe the relationship between load intensity and floor area.

(b) For multi-storey buildings, describe the relationship between floor loading magnitude and the number of storeys.

3. List the most likely combinations of loads on a steel railway bridge according to BS 5400. Discuss the relevance of each combination.

4. Explain the need for specifying three different types of road bridge traffic loadings : NA, NB and NC in TMH 7, instead of just one single loading system.

5. Describe the procedure for obtaining the displacement spectrum for a flexible tower from records of the wind gust velocity.

6. Describe one example of a restraint action responsible for structural failure, that was discussed in the seminars in this course - other than the one that you might have submitted as a project.

7. Discuss how each relevant property of a structural system can contribute to minimize earthquake damage.

8. Discuss the major factors influencing the pressure distribution inside a tall circular grain silo filled from the top and emptied at the bottom.

9. Sliding formwork is used to construct a tall concrete chimney. Discuss all the factors likely to affect the loading on the formwork and on the concrete just below the formwork.

[4 PAGES]

UNIVERSITY OF CAPE TOWN

DEPARTMENT OF CIVIL ENGINEERING

M.Sc. in CIVIL ENGINEERING

CIV 516F : COASTAL HYDRAULICS

UNIVERSITY EXAMINATION : JULY 1988

ALL question may be attempted. TIME: 4 hours +

(OPEN BOOK EXAMINATION)

Constants

Sea water density = 1025 kg/m^3

Sea water weight = 10 kN/m^3

QUESTION 1

The standard alignment chart is attached and a new blank line has been inserted at the bottom of the page. This line is to be used for determining values of U_{max} , the maximum horizontal orbital velocity at the water surface, according to the Airy theory. If $U^*_{max} = \frac{U_{max}}{\pi H/T}$ is to be the dimensionless form of the variable on this line, mark off the correct positions of the U^*_{max} values given in the following list.

U^*_{max} = 1,01 2 6
1,10 3
1,40 4

Note that H is the local wave height throughout. Suggest a small change in the line label which would permit the scale to be used for maximum horizontal surface acceleration values. Use the new line to solve the following problem.

A swell of 10 second period with a deep water wave height H_o = 1,59 m approaches a beach with the wave crests parallel to the shore. Plot the value of u_{max} at the water surface for the following selected water depths.

65 m ; 34,4 m ; 15,9 m ; 6,8 m ; 2,86 m .

Use these calculations to estimate the water depth when the U_{max} value first reaches 1,5 m/s and check that the wave has not broken.

QUESTION 2

A sea platform consists of a square concrete slab positioned horizontally on four cylindrical vertical piles, each placed at a corner, the slab side being parallel to the local wave crest. The pile diameter is 1 m, the total pile height above sea bed is 6,4 m, and the slab dimensions are sides of 5 m with a thickness of 200 mm. The local wave characteristics are height 2 m, length 100 m, and period 12 s, the local water depth being 8 m.

(a) Considering the central 1 m high slice of any pile, calculate the horizontal forces per metre due to velocity and acceleration and by plotting these throughout one wave period or otherwise, identify the maximum force and the timing of its occurrence. Check that the velocity and acceleration distributions over the height of the pile are reasonably constant and thus estimate the total force on one pile.

Take C_D = 1,2 and C_M = 2,0 .

QUESTION 2 (continued)

(b) Estimate the maximum vertical force on the slab due to wave action.

Take $C_D = 1,0$ and $C_M = 1,8$.

QUESTION 3

In a study of wave penetration into a bay, the 10 m, 9 m and 8 m sea bed contours are approximated by three straight lines with contained angles of 12 degrees as shown on the attached page. An incoming wave orthogonal, 10 second period, impinges on the 10 m contour at an angle of 50 degrees as shown. With the usual approximations obtain by trial the angle at whch the emerging orthogonal cuts the 8 m contour. Take the step lines on the 9,5 m and 8,5 m lines.

[1 diagram attached]

QUESTION 4

A train of waves is approaching a shore line, of regular bed slope 1 in 80, the wave crests being essentially parallel to the shore. Two aerial still photographs are taken 8 seconds apart. On the first photograph, two successive crests are identified as being 247 m apart. A comparison between the two photographs indicates that the trough between the two crests has advanced forward a distance of 153 m. Further, stereo photographs taken at the same time as the first exposure indicate that the wave height in the vicinity of the trough is close to 3 m. Retrace the history of this wave as it came in from deep water, and further trace the progress of the wave as it moves towards the beach, including the following calculations:

(i) the wave length and celerity in deep water ;

(ii) the wave length, celerity and height for water depths at 20 m intervals from deep to the 10 m depth, and at 1 m intervals inshore from this to a depth of 3 m ;

(iii) the depth of water in which the wave breaks, the type of breaker, and the wave height at breaking. Set up and down may be ignored ;

(iv) the energy flow in W/m in two water depths outside the breakers, and one depth in the breaker zone (depths at your choice) and compare.

QUESTION 5

(a) A storm at sea generates waves with a period range of 6 to 12 seconds. The resulting swell travels towards a harbour 400 km away. Estimate the time interval between the arrival of the shortest and longest waves, assuming deep water throughout.

(b) A refraction diagram is constructed for a bay, and the spacing between a particular pair of adjacent orthogonals doubles in travelling from deep water to the 10 m depth zone, the wave period being 7 seconds. Estimate the percentage change in wave height occurring between these two zones on the assumption that no breaking waves are present in-between.

(c) In a zero damage design calculation for the armour protection of a rubble mound breakwater, 3 tonne and 5 tonne dolosse are specified for the trunk and head respectively, the slope of the breakwater face being cot α = 2. Estimate the block masses and block heights if tetrapods had been used in the same design. If the design wave height was 3 m, and a storm causes damage of the order 20 - 30 per cent to the tetrapod scheme, estimate the storm wave height (concrete density 2245 kg/m^3).

(d) An incoming swell has crests parallel to a straight beach with a deep water wave height of 2 m. Estimate the horizontal force (per metre along the beach) acting on the beach inside the refraction zone, due to the dynamic action of the waves.

(e) In an area where the sea bed is horizontal, and the water depth is 3 m, a wave has a period of 7 s, a wave length of 38 m, and a wave height of 1,5 m. Estimate the drift velocity at bed level, and indicate the direction. Compare this velocity with the maximum orbital velocity at the same level, and indicate the influence on bed drift of a strong onshore wind.

(f) A coastal model is to be constructed to explore wave action in a sea area 1 km offshore by 2 km along shore. The laboratory area available is 20 m wide and of considerable length. Suggest a linear scale suitable for this and calculate the wave period of the model paddles to duplicate a 12 second wave in nature. Discuss which of the following characteristics are accurately modelled in the laboratory:

(i) wave refraction pattern ;
(ii) wave heights before breaking ;
(iii) wave heights after breaking ;
(iv) settlement of fine sands.

* * * * * * * * * *

UNIVERSITY OF CAPE TOWN

DEPARTMENT OF CIVIL ENGINEERING

CIV 592F POSTGRADUATE EXAMINATION

PROJECT MANAGEMENT IN CIVIL ENGINEERING

15 JUNE 1988 TOTAL MARK 100

NOTE

* The examination is three (3) hours
* Attempt all questions
* All writing to be in ink or ballpoint pen

1. Refer to Annexure A . Complete and hand in with the answer book.

2. Discuss the functions of a Project Manager. [20]

3. Describe the different types of information required by a Project Manager to plan a project. [20]

4. Discuss the problems which may arise when a Project Manager underestimates the cost of a Contract in his motivation to the Client for acceptance. [10]

5. Indicate , with comment , the cost items which may be affected in a contractor's claim as also the reasons for a claim . [10]

Name............................ 15 June 1988

ATTEMPT ALL THE FOLLOWING QUESTIONS WITH SHORT PRECISE ANSWERS

TOTAL MARK 40

a) What is the purpose of organising. [1]

....

....

b) Give four reasons why organisational charts are useful. [2]

1)..

2)..

3)..

4)..

c) For what reason are people motivated. [1]

....

....

d) Name two reasons why a Client would be motivated to undertake a project. [1]

1)......................................

2)......................................

e) Time and cost is interrelated but can be in conflict ,is this true or false ? [1]

True / false (circle the correct reply)

d) Indicate which of the following are procedural constraints : [3]

availability of local funding	yes/no
tendering	yes/no
detail design	yes/no
conditions of contract	yes/no
contractural incentives	yes/no
arbitration	yes/no

e) Give ten benefits of good planning : [5]

1).......................

2).......................

3).......................

4).......................

5).......................

6).......................

7).......................

8).......................

9).......................

10).......................

f) Indicate which of the following can assist with project control . [3]

personal commitment	yes/no
programme coordination	yes/no
review meetings	yes/no
project reports	yes/no
management support	yes/no
communication	yes/no

g) List six project management monitoring actions which should be excercised during construction. [3]

1)...........................

2)...........................

3)...........................

4)...........................

5)...........................

6)...........................

h) Indicate four normal reactions to which a person may resort if faced with a risk situation . [2]

1)..........................

2)..........................

3)..........................

4)..........................

i) Give three types of critical path charts for programming a project . [3]

1)..........................

2)..........................

3)..........................

j) Give eight reasons for providing a client with an estimate for a project . [4]

1)..........................

2)..........................

3)..........................

4)..........................

5)..........................

6)..........................

7)..........................

8)..........................

k) What should be considered when compiling a Schedule of Quantities for a project . [3]

1)..

2)..

3)..

4)..

5)..

6)..

l) Is the cummulative monthly payments made to a contractor a straight line , if not what shape is it ? [2]

....

....

m) Who takes the risk in a fixed priced contract. [1]

....

n) On which cost elements in a contract are the inflation index values applied. [2]

1).............................

2).............................

3).............................

4).............................

o) What is the normal maximum percentage variation of a payment item that can be accepted before a Contractor may request a revision of the pay item rate , and for what reason. [2]

....

....

....

p) What are statutory increases. [1]

....

UNIVERSITY OF CAPE TOWN

DEPARTMENT OF CIVIL ENGINEERING

UNIVERSITY EXAMINATION : 29 OCTOBER 1988

CIV 536 - COASTAL ENGINEERING PRACTICE

Time Allowed: 3 hours

Answer ALL Questions

There is a potential of 158 marks

SECTION 1 is to be handed in at the end of the first hour - CLOSED BOOK

SECTION 2 is "OPEN BOOK"

Name: ....

QUESTION 1

Briefly explain, in words and by means of annotated sketches, the meaning of the following terms:

1.1 Cope level [2]

1.2 Pendant fender [2]

1.3 Tidal prism [2]

1.4 Seiche [2]

1.5 Clinometer [2]

1.6 Show on a sketch plan of Hout Bay where you would expect to observe the effects of wave diffraction and refraction. Clearly indicate the physical cause of each effect and the form of the wave orthogonals and crests. [2]

1.7 Explain, by means of a sketch, the basic physical elements of airborne (single channel) linescan apparatus that could be used for remote sensing of the ground. [2]

1.8 Explain by means of a sketch how a dredger may be positioned using sextant resection. [2]

1.9 Explain the principle of subtense ranging using a sextant. Indicate the practical distance limit.
[2]

1.10 Explain by means of a sketch the principle of echo sounding for seabed profiling.
[2]

1.11 Give a sketch of the components and the arrangement that is used for tide recording at Granger Bay.
[2]

1.12 Explain the term "tidal residual". What is the cause of tidal residuals?
(2)

1.13 Explain the principle of the "Wave rider" accelerometer buoy. [2]

1.14 Show by means of simple sketches how field measurements of the following may be graphically presented in reports :

wind speed and direction [2]

Radioactive tracers [2]

Beach profiles [2]

1.15(a) Give a typical section of a rubble mound breakwater (annotate). [2]

1.15(b) Show the sequence of how this would be constructed in an exposed situation. [2]

1.16 Comment very briefly (with a simple sketch) on the adequacy or inadequacy of the following :

position of the slipway at Granger Bay [2]

boat "access" situation at harbour entrance in Hout Bay [2]

boat "access" situation at Kalk Bay harbour entrance [2]

a boat ramp at 1:6 [2]

a boat ramp at 1:15 [2]

1.17 Explain what you would look for in an aerial photograph of the coast to discern the direction of littoral drift. [2]

Total for SECTION 1 = 48 marks.

SECTION 2 - OPEN BOOK

2.1 Assuming that you are a Consulting Engineer specialising in coastal matters, reporting to the local authority responsible for the coast, write advisory notes to the responsible Committee on the following :

(a) It is September and the beach has steepened and eroded sufficiently for an adjacent parking area to appear to be in danger of being totally eroded.

Outline your proposed method of investigation, your preliminary advice as to what the Council should instruct you or Contractors to do, what alternatives measures are likely to be appropriate after completing the investigation. Give a staged breakdown of costs with time/construction expense justification. Assume the total beach length is 1 km and that the situation is as occurs at Fish Hoek.

[15]

(b) It is proposed that the harbour at Granger Bay be improved. Write a memorandum to the responsible Committee outlining the problems that occur at present and the approach you would take to improve the situation. Provide an approximate cost for the investigation and the development of a new construction plan. Give a breakdown of the work required. (Give sketch plans as needed).

[15]

(c) Describe the present situation and outline the approach you would take to investigate the cause of the tilt on the breakwater at Hermanus. Indicate two possible alternative causes, and how you would remedy the situation for each case. (In a sketch show the type of construction).

[10]

(d) Briefly explain how you would determine the directions of nett littoral drift and how you would estimate the littoral drift quantity at Hout Bay beach.

[10]

(e) Hout Bay harbour is to be extended to provide for an additional 500 floating berths for small craft. Present a breakwater and mooring layout, and show in plan details of boat ramps, harbour control <u>and other infrastructure requirements</u> that should be considered at a preliminary stage. State all assumptions.

[60]

Total for SECTION 2 = 110 marks

UNIVERSITY OF CAPE TOWN

DEPARTMENT OF CIVIL ENGINEERING

UNIVERSITY EXAMINATION - NOVEMBER 1988

COURSE CIV 525S - CONTRACT LAW

OPEN BOOK EXAMINATION

Time : 150 Minutes

PLEASE ANSWER ALL QUESTIONS, BEARING IN MIND THE NUMBER OF QUESTIONS, IT IS SUGGESTED THAT YOUR ANSWERS BE KEPT AS BRIEF AS POSSIBLE.

TOTAL NUMBER OF MARKS : 100 MARKS

External Examiner

10/11/88

Internal Examiner

External Examiner

QUESTION 1

"It must be conceded that the phraseology of Clause 54 (of the Standard Engineering Contract) is capable of bearing the construction placed upon it by the Court a quo. But in my opinion it is also open to a different interpretation". (Per Van Heerden JA in Melmoth Town Board v Marius Mostert (Pty) Limited 1984 (3) 718 at 728 F).

Comment on the above statement and deal with the powers of the engineer in terms of the said Clause 54.

10 Marks

QUESTION 2

You are a director of a construction company.

The construction company applies to an insurance company for the issue of a performance bond and the insurance company requires you to sign a suretyship for the obligations of the construction company in respect of that contract. However, in terms of the suretyship you bind yourself "as surety and co-principal debtor in solidum for the due and faithful performance by the construction company to the insurance company of all and whatsoever obligations undertaken by it on behalf of the construction company in connection with any matter whatsoever".

Shortly afterwards you resign from the construction company, and a year later you receive a letter from the insurance company advising you that in connection with another project carried out by the construction company after you had left its employ, the construction company was indebted to the insurance company, who are now looking to you for payment in terms of the suretyship signed by you.

You are very alarmed because you had not envisaged that you would be liable for obligations which were incurred after you had left the employ of the construction company. You decide to take legal advice.

What are you likely to be told?

10 Marks

QUESTION 3

You are a director of a construction company.

In terms of the construction contract, certain work was to be sub-contracted to a sub-contractor nominated by the architect.

The architect obtained a tender for this work from the sub-contractor and instructed your firm to accept the work. You sent an order on your standard printed form which contained on its reverse side printed conditions which included a clause reading as follows :-

"Payment of the amount due in terms of this order will only be effected after we (the main contractor) have received payment from the employer".

The sub-contractor wrote back to you thanking you for the order and the work was carried out.

The employer became insolvent before having paid for all the work.

The sub-contractor calls on you to obtain payment for all the work done by him.

What would you reply?

10 Marks

QUESTION 4

You are a director of a construction firm.

You contract with a development company (X Developers (Pty) Limited) to build houses on separate erven which are owned separately by individual owners who are clients of the development company, and with whom the the development company had entered into agreements for the building of these houses.

As the work progressed from time to time, each of the owners paid X Developers (Pty) Limited the amount required from them.

Unfortunately, X Developers (Pty) Limited find fault with your work and advise that they are not prepared to pay you any further sums until you have completed what they regard as the remedial work.

You dispute that in fact any remedial work is necessary, but you are not prepared to continue work until the amount due to you in terms of your contract with X Developers (Pty) Limited has been paid.

The individual owners need their accommodation urgently and decide to contract with another firm to build for them and finish off the work.

You do not want to give up possession of the building sites and the work thereon until you have been paid in full, and the individual owners institute action against your firm for an order claiming possession of the various sites. Your Board asks you for an outline of what your rights are in this matter.

Draw a short memorandum setting out your rights.

10 Marks

QUESTION 5

You are a director of a construction company.

It appears that your firm has failed to comply fully with performance of work undertaken in terms of the contract, but you wish to claim for the work which you have done.

You decide to take legal advice on your rights, and the attorney whom you consult says "Ah, this is a B K tooling case", and proceeds to give you certain advice.

On the basis that he knows what he is talking about, write a short memorandum for your managing director setting out what your rights are.

10 Marks

QUESTION 6

You are a director of a construction company.

Your firm has entered into a contract to build certain road works, and the contract is in terms of the General Conditions of Contract of 1982 as issued by the South African Institution of Civil Engineers.

Times are difficult - interest rates are rising - and your managing director advises you that it looks like it may be necessary to enter into an arrangement with the company's creditors.

He asks you to prepare a short memorandum for the Board setting out the rights of the employer under your contract, should your company decide to follow this course.

Prepare the memorandum.

10 Marks

QUESTION 7

You are a director of a construction company.

In terms of the contract your company has undertaken to pay your employer R10 000,00 a day for every day by which delivery of the completed works is delayed.

Due to internal disputes in the construction company, delivery of the completed works is delayed for a period of 3 months and your company's accountants make provision for the sum of R90 000,00 as being due by your company to the employer.

The managing director asks you to write a short memorandum for the Board setting out whether this is a liability, whether it can be reduced, and whether there would be any defence to a claim.

Write it.

10 Marks

QUESTION 8

In what circumstances may an extension of time be granted in terms of the General Conditions of Contract 1982.

10 Marks

QUESTION 9

You are a director of a construction company.

It is clear that a dispute is arising between the employer and your company, and the Board intends discussing whether the matter should go to arbitration or litigation.

You are asked to prepare a short memorandum discussing the relative merits of these methods of dispute settlement.

10 Marks

QUESTION 10

You are in practise as a consultant engineer.

You are appointed as the engineer in regard to a particular contract entered into in accordance with the General Conditions of Contract 1982.

One of the nominated sub-contractors complains bitterly to you that the main contractor has not paid him for work already done by such sub-contractor, for which you know the employer has already paid the contractor, and the nominated sub-contractor advises you that he is still working under the sub-contract and he would like you to protect him insofar as regards payment in the future.

What could you do?

Would your answer be any different if the sub-contractor was not a nominated sub-contractor?

10 Marks

UNIVERSITY OF CAPE TOWN

DEPARTMENT OF CIVIL ENGINEERING

CIV 543S AIRPORT DESIGN

POSTGRADUATE EXAMINATION

9 November,1988 Total Mark 100

NOTE

* Examination time 3 hours
* Attempt all questions
* All writing to be in ink or ballpoint

1 Refer to Annexure A . Complete and hand in with the answer book . [30]

2 Discuss fully all aspects which affect the determination of a runway length . [20]

3 Discuss the environmental impact a new airport could have on the status quo . [20]

4 Discuss fully the various aspects to be considered in the design of the terminal building relating to the passenger activities and the physical facilities . [20]

5 Provide a specification for both rigid and flexible pavements , with regard to the design layers and the surface treatment [10]

Annexure A

Name :....................   Civ 543S   Airport Design

a) On what date did Orville Wright make his first flight

.... (1)

b) For what reason did the Corps of Engineers decide to establish a design method for airport pavements during the last war.

....

.... (1)

c) Give four factors that influence a passenger to choose air travel as a travel mode

....

....

....

.... (2)

d) Which aircraft has steadily increased its seat/kilometres since its introduction to commercial aviation

.... (1)

e) What nature of demand variation affects a passenger airline in arranging its flight schedules

....

.... (2)

f) What is the "standard busy rate "

.... (1)

Annexure A

g) Give eight factors which influence choosing air cargo as a means of transport

....

....

....

....

....

....

....

.... (4)

h) Indicate what is meant by the following terms :

Turboprop ....

Turbojet ....

Turbofan .... (3)

i) What is the most important function governing an aircraft's turning radius

.... (1)

j) What percentage of the load is normally assumed on the nose gear

.... (1)

k) Name six factors which have a bearing on the runway length

....

....

....

....

....

.... (3)

Annexure A

l) Define the following :

VFR ....

IFR .... (2)

m) Give four points of information which the Air Traffic Control gives to a pilot for his landing

....

....

....

.... (2)

n) Give four points which are likely to cause strained relationships between airport administration and the residents of local neighbourhoods

....

....

....

.... (2)

o) Name the four different runway configurations

....

....

....

.... (2)

p) What is the accepted deceleration for a landing aircraft

.... (1)

q) On approaching the runway what are the most important visual aspects to a pilot

....

....

....

.... (2)

UNIVERSITY OF CAPE TOWN

FRD/UCT CENTRE FOR RESEARCH IN COMPUTATIONAL AND APPLIED MECHANICS

UNIVERSITY EXAMINATION : 11 MAY 1989

END 522Z : AN INTRODUCTION INTO FINITE ELEMENTS

PAPER 1

ANSWER ALL QUESTIONS

HAND IN : 12.00 am , 15 MAY 1989

TOTAL 60 MARKS

Question 1

The structure shown below consists of two horizontal beams rigidly fixed at the ends. The bottom beam is supported by three cables which can only take axial forces. A uniformly distributed load of w kN/m is applied on the bottom beam.

Calculate by hand the vertical displacement at the centre of the bottom beam when w = 25kN/m. Use the Euler-Bernoulli beam element. Show all your calculations, including the element stiffness matrices and the assembled global stiffness matrix and load vector. (Do not formulate the problem by minimimizing the potential energy, but start with the equilibrium equations $\mathbf{Ku} = \mathbf{f}$.) Determine the bending moment distribution in the beam and the forces in the cables.

[20marks]

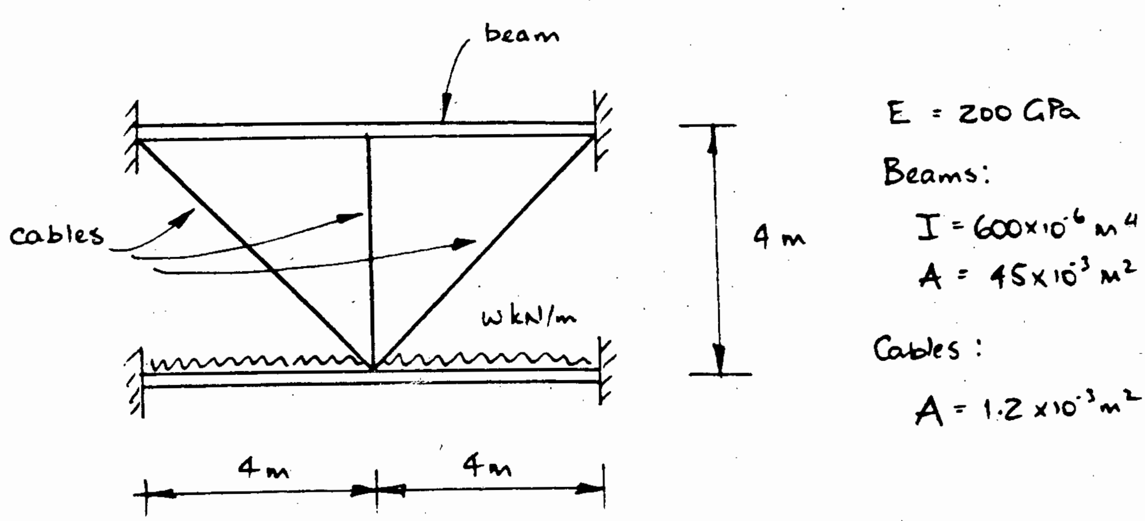

Question 2

The structure shown in Figure 2(a) consists of a girder supported vertically at points A,B and C, and horizontally at A. The girder is a H section with the details given in Figure 2(b). A uniformly distributed load of 5 kN/m is applied between B and C. The support at B consists of a column which can be considered as infinitely stiff. A load of 300 kN is applied at B by a solid column which covers the full width of the H section's flange.

This is a rather special structure in that this particular H section has to be used. The designer wants you to perform a finite element analysis to determine the maximum stresses in the H section at support B. He is concerned that plastic yielding may occur in the section. He wants the results to within 10% accuracy.

Your answer should be presented in the form of a report. State all your assumptions clearly, including justifications. Do not perform a 3-D analysis. Include your final computer printouts with your report.

[40marks]

END 522Z - AN INTRODUCTION INTO FINITE ELEMENTS

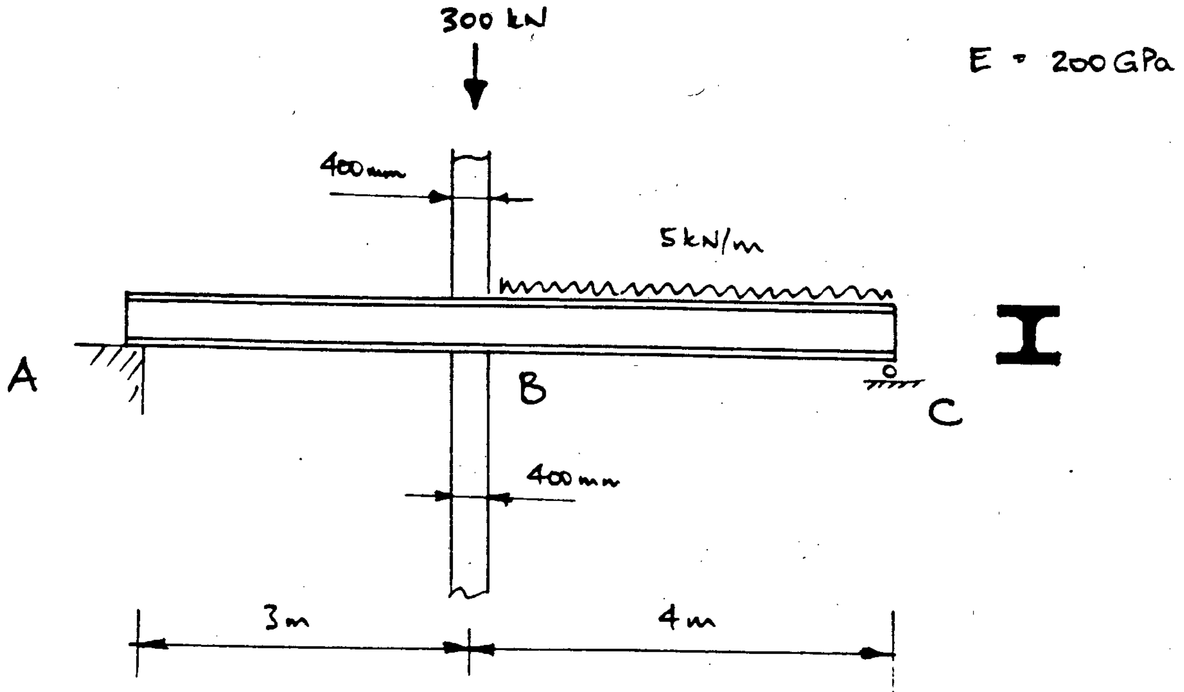

Figure 2(a)

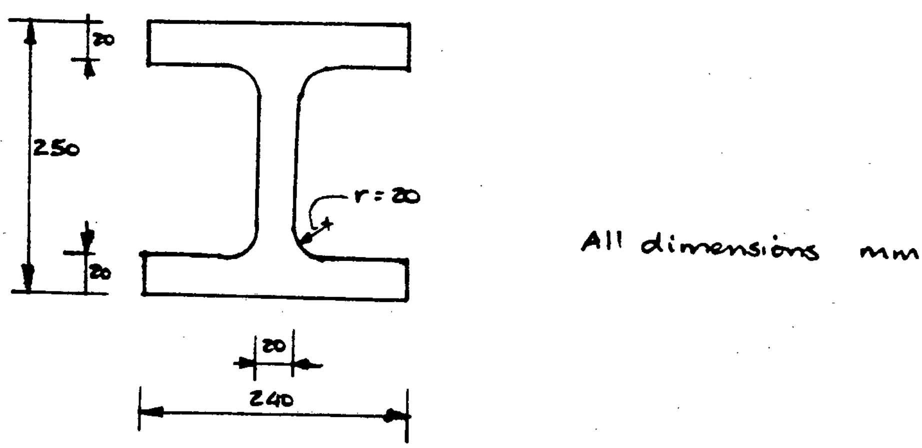

Figure 2(b)

UNIVERSITY OF CAPE TOWN

FRD/UCT CENTRE FOR RESEARCH IN COMPUTATIONAL AND APPLIED MECHANICS

UNIVERSITY EXAMINATION : 12 MAY 1989

END 522Z : AN INTRODUCTION INTO FINITE ELEMENTS

PAPER 2

ANSWER ALL QUESTIONS

Time : 1 Hour

TOTAL 40 MARKS

Question 1

Discuss the problems associated with each of the following finite element meshes. Suggest ways to improve or correct the models.

[16 marks]

(a)

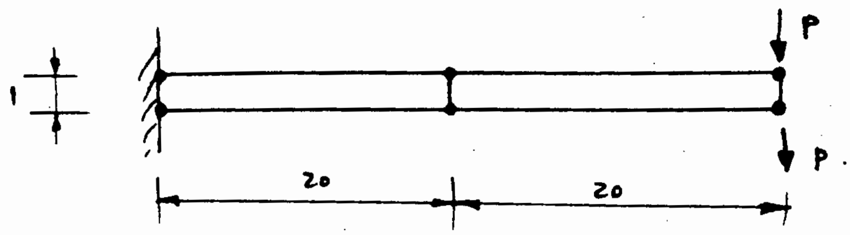

(b)

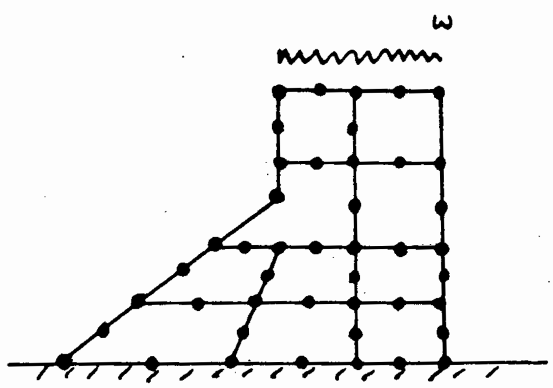

(c)

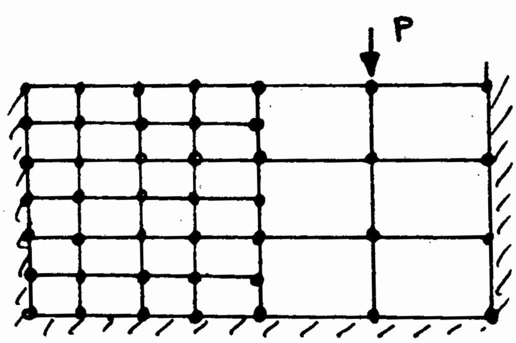

(d)

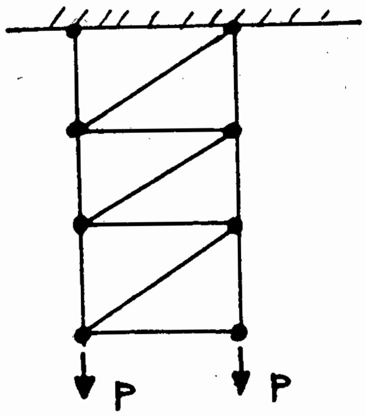

(e)

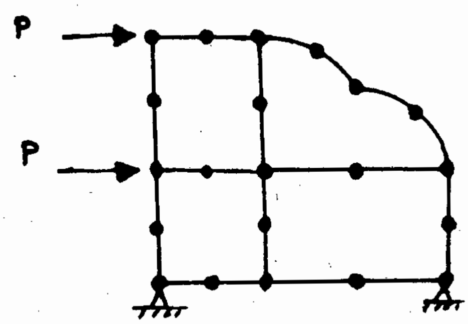

(f)

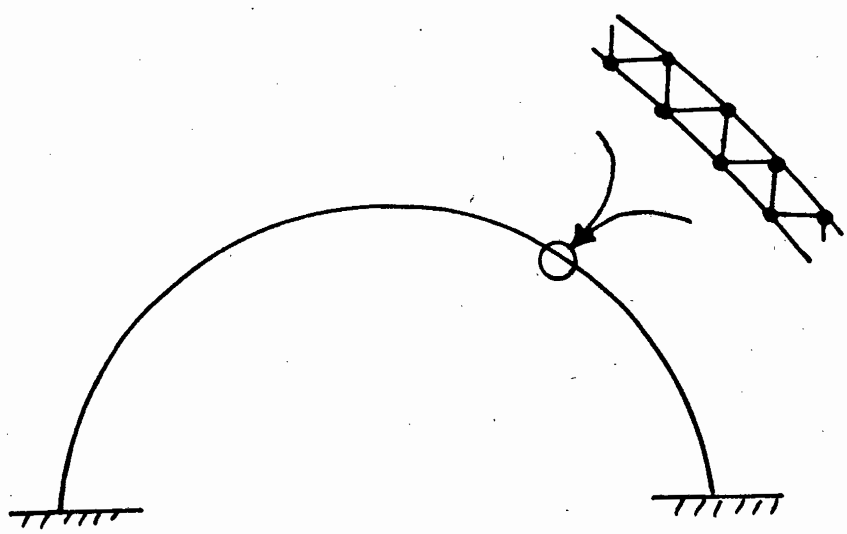

Question 2

Show how symmetric and/or antisymmetric loading can be used for each of the following structures. The objective is to model only part of the structure in each case. Clearly illustrate the boundary conditions that must be used.

[12 marks]

(a)

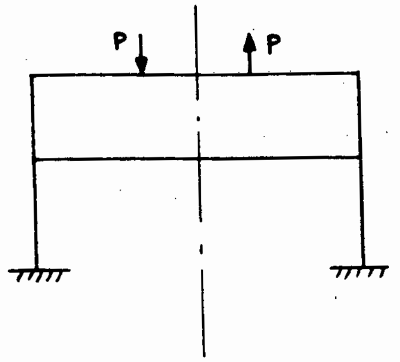

(b)

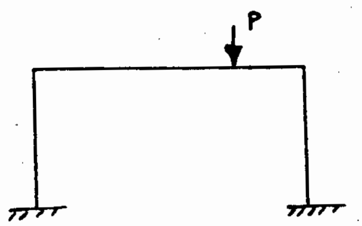

(c)

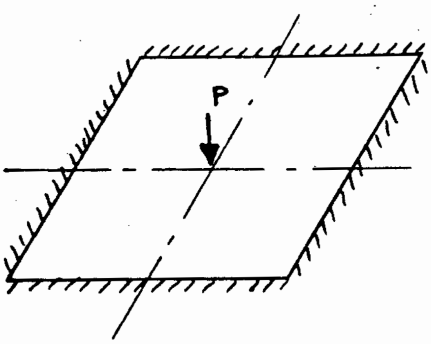

(d)

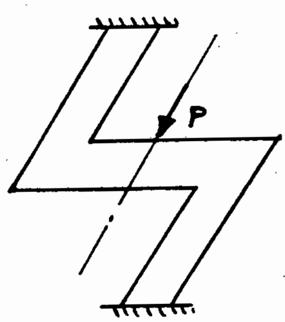

Question 3

Consider the three-node quadratic isoparametric truss element shown in Figure 3(a) below. Show that if node 2 is specified to be at the quarter point, as shown in Figure 3(b), the stress has a singularity of $\frac{1}{\sqrt{x}}$ at node 1. (Stress is given by $\sigma = DBu$)

[12 marks]

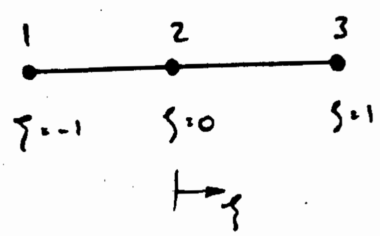

3(a)

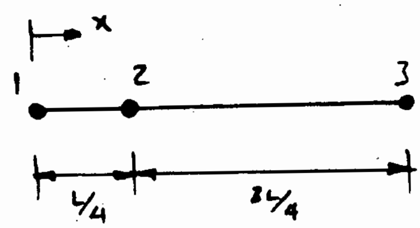

3(b)